

# ***The DIII-D Five-Year Program Plan***

1999 - 2003

by  
***PROJECT STAFF***



**AUGUST 1998**

**THE DIII-D FIVE-YEAR PROGRAM PLAN  
1999-2003**

**by  
PROJECT STAFF**

**ABRIDGED VERSION**

This is an abridged version of the DIII-D Five-Year Technical Proposal. Not included are sections which include resumes, past publications and GA management structure.

Work prepared under  
Contract Nos. DE-AC03-89ER51114, W-31-109-ENG-38, W-7405-ENG-36,  
W-7405-ENG-48, DE-AC05-96OR22464, DE-AC02-76CH03073, DE-AC04-94AL85000,  
and Grant Nos. DE-FG02-89ER53297, DE-FG02-86ER53223, DE-FG03-89ER51116,  
DE-FG03-86ER53266, DE-FG03-86ER53225, DE-FG03-95ER54294, DE-FG05-  
96ER64373, and DE-FG03-97ER54415 for the U.S. Department of Energy

**GA PROJECT 3466  
AUGUST 1998**

## DISCLAIMER

This report was prepared as an account of work sponsored by an agency of the United States Government. Neither the United States Government nor any agency thereof, nor any of their employees, makes any warranty, express or implied, or assumes any legal liability or responsibility for the accuracy, completeness, or usefulness of any information, apparatus, product, or process disclosed, or represents that its use would not infringe privately owned rights. Reference herein to any specific commercial product, process, or service by trade name, trademark, manufacturer, or otherwise, does not necessarily constitute or imply its endorsement, recommendation, or favoring by the United States Government or any agency thereof. The views and opinions of authors expressed herein do not necessarily state or reflect those of the United States Government or any agency thereof.

## TABLE OF CONTENTS

<b>1.0 THE DIII-D FIVE-YEAR PROGRAM SUMMARY .....</b>	<b>1-1</b>
1.0.1. The DIII-D National Program Overview and Mission .....	1-1
1.0.2. The Proposed DIII-D Five-Year Program Plan.....	1-2
1.0.3. Leadership .....	1-3
1.1. Tokamak Research Using the DIII-D National Facility .....	1-5
1.1.1. Science Research .....	1-9
1.1.2. DIII-D Facility Operations .....	1-14
1.2. Upgrade DIII-D Components and Systems to Achieve Program Objectives .....	1-19
1.2.1. ECH Upgrade .....	1-20
1.2.2. Divertor Upgrade .....	1-21
1.2.3. Magnet Pulse Length Upgrade.....	1-22
1.2.4. Upgrade Contingency Options .....	1-23
<b>2. TECHNICAL DISCUSSION: THE DIII-D FIVE-YEAR PROGRAM PLAN .....</b>	<b>2.1-1</b>
2.1. The DIII-D Five-Year Program Plan .....	2.1-1
2.1.1. The DIII-D Mission .....	2.1-1
2.1.2. The DIII-D Program .....	2.1-3
2.1.3. National Leadership .....	2.1-8
2.1.4. Benefits of DIII-D Research .....	2.1-8
2.1.5. The DIII-D National Team .....	2.1-10
2.2. The DIII-D Advanced Tokamak Program .....	2.2-1
2.2.1. The Plan .....	2.2-1
2.2.2. What is an Advanced Tokamak? .....	2.2-6
2.2.3. The Science, the Tools, and the Integration .....	2.2-6
2.3. Fusion Energy Science in DIII-D .....	2.3-1
2.3.1. Confinement Science and Transport Barrier Control .....	2.3-2
2.3.2. Stability Science .....	2.3-20
2.3.3. Boundary Science .....	2.3-35
2.3.4. Physics of Current Drive and Heating .....	2.3-62
2.4. Pathways to the Future.....	2.4-1
2.4.1. The Path to ITER.....	2.4-1
2.4.2. The Path to an Optimized Superconducting Tokamak Power System .....	2.4-7
2.4.3. The Path to a Compact Ignition Experiment .....	2.4-13
2.4.4. The Path to the Spherical Tokamak Pilot Plant .....	2.4-15
2.4.5. Research Implications for DIII-D from a Look at Future Tokamak Possibilities .....	2.4-18

2.5.	The DIII-D National Fusion Facility — Status and Upgrades .....	2.5-1
2.5.1.	Electron Cyclotron Heating and Current Drive Systems Upgrade .....	2.5-14
2.5.2.	Divertor System Upgrades .....	2.5-16
2.5.3.	Magnet Pulse Length Upgrade (Baseline) .....	2.5-21
2.5.4.	Improvements to the DIII-D Tokamak (Completed as Part of Tokamak Research) .....	2.5-23
2.5.5.	Diagnostic Systems (Tokamak Research).....	2.5-28
2.5.6.	Control, Data Acquisition and Analysis Systems (Tokamak Research) .....	2.5-39
2.5.7.	Fast Wave ICRF Systems (Option) .....	2.5-45
2.5.8.	Neutral Beam Heating Systems .....	2.5-47
2.5.9.	Other Upgrade Options .....	2.5-50
2.6.	The DIII-D National Fusion Program .....	2.6-1
2.6.1.	National Leadership Role .....	2.6-2
2.6.2.	Collaborations and Outreach .....	2.6-3
2.6.3.	The DIII-D National Team .....	2.6-20
2.6.4.	DIII-D National Program Governance .....	2.6-34
<b>3.</b>	<b>OTHER PERTINENT INFORMATION .....</b>	<b>3-1</b>
3.1.	Development Process of the DIII-D Five-Year National Program Plan .....	3-1
3.2.	History and Accomplishments of the DIII-D Program.....	3-5
3.2.1.	Origin of the Program .....	3-5
3.2.2.	Accomplishments of the 1993 Five-Year DIII-D Plan and Context for the 1998 Five-Year Plan .....	3-6
3.2.3.	DIII-D Scientific Progress and Accomplishments .....	3-12
3.2.4.	DIII-D Operations and Facility Improvements.....	3-17
3.2.5.	Transition to a National Program .....	3-20

## LIST OF FIGURES

1-1.	The DIII-D program plan progresses from short pulse AT physics, through optimization, to 10 s operation .....	1-3
1-2.	DIII-D Advanced Tokamak research plan will integrate the upgraded heating and divertor to optimize performance .....	1-5
1-3.	Implementation of the proposed DIII-D research requires the plasma control tools defined in the facility upgrades .....	1-7
1-4.	Pursuit of the key research thrusts requires the diagnostic upgrades included in the DIII-D Plan .....	1-7
1-5.	Recent technical developments of 110 GHz gyrotrons and a high-power diamond window (upper right) motivate an accelerated ECH program .....	1-19
1-6.	We plan to implement a high triangularity pumped divertor in stages .....	1-20
1-7.	The DIII-D upgrade plan includes contingency options to adapt to evolving scientific outcomes .....	1-20

2.1-1.	DIII-D Program linkages provide intellectual inputs, research inputs and staff opportunities .....	2.1-3
2.1-2.	The DIII-D research plan culminates in integrated, Advanced Tokamak operating scenarios .....	2.1-5
2.1-3.	DIII-D program schedule .....	2.1-7
2.2-1.	The 1999–2003 research plan advances facility capability in step with advancing confinement, stability, boundary and current drive science .....	2.2-4
2.2-2.	ECH barrier control is illustrated by a three-case comparison .....	2.2-20
2.3-1.	$E \times B$ shear suppression enables transport barrier control.....	2.3-4
2.3-2.	An opposing NB will enable transport barrier control through manipulation of $E \times B$ shear .....	2.3-7
2.3-3.	DIII-D $E \times B$ shear regulation occasionally results in modest electron transport reductions.....	2.3-9
2.3-4.	Energy confinement enhancement factor increases with pedestal pressure in ITER .....	2.3-15
2.3-5.	Stability limits for the $n=1$ ideal kink mode .....	2.3-24
2.3-6.	Wall stabilization is predicted to allow ideal $n=1$ kink stability.....	2.3-25
2.3-7.	Simulations with good experimental foundation indicate additional particle pumping will maintain higher $q(0)$ .....	2.3-29
2.3-8.	Better bootstrap alignment could increase $\ell_i$ while preserving NCS .....	2.3-31
2.3-9.	Strong emissivity peaks at low temperatures is the key to a radiative divertor .....	2.3-36
2.3-10.	The standard model predicts radiated heat flux limits for the divertor .....	2.3-36
2.3-11.	Radiation evenly distributed from the X–point region is in stark contrast to standard divertor model predictions .....	2.3-38
2.3-12.	$T_e$ measurements do not support model predictions of significant electron conduction .....	2.3-39
2.3-13.	Divertor measurements and modeling show $< 2$ eV $T_d$ , permitting volume recombination to compete with ionization .....	2.3-40
2.3-14.	Volume recombination remains small until the momentum is reduced via ion-neutral interactions .....	2.3-41
2.3-15.	Carbon radiation dominates partially detached divertor operation induced by deuterium puffing .....	2.3-42
2.3-16.	Either impurities or better neutral baffling are needed to achieve the AT scenario .....	2.3-44
2.3-17.	Slanted RDP structures should aid in obtaining impurity enrichment in the divertor.....	2.3-45
2.3-18.	Pellet fueling with divertor pumping shows the Greenwald limit is not an obstacle .....	2.3-52
2.3-19.	Scientific progress: DIII-D fusion performance has doubled every 2 years .....	2.3-53
2.3-20.	A large pressure decrease in ELMing H–mode discharges is rewarded with an increase in confinement quality .....	2.3-54
2.3-21.	Models predict the RDP baffles will reduce core ionization by an order of magnitude .....	2.3-55
2.3-22.	A 26 MW energy loss per Type I ELM is predicted for ITER.....	2.3-57
2.3-23.	Localized noninductive current drive can yield improved confinement and stability .....	2.3-64
2.3-24.	The allowable power range of DIII-D AT scenarios can be estimated from simple relationships .....	2.3-66
2.3-25.	Optimum ramp-up begins at $\beta_p$ close to the equilibrium limit .....	2.3-70
2.3-26.	One–dimensional simulations show bootstrap overdrive can generate 1 MA in 2 s .....	2.3-72
2.4-1.	DIII-D research connects to four possible tokamak program directions .....	2.4-2
2.4-2.	The major radius of superconducting tokamaks is constrained by wall loading at low aspect ratio and by stress at high aspect ratio .....	2.4-8

2.4-3.	High aspect ratio superconducting tokamaks have relatively low fusion power .....	2.4-8
2.4-4.	DIII-D research projects to a spherical tokamak power system .....	2.4-16
2.5-1.	The DIII-D tokamak facility spans a half city block .....	2.5-2
2.5-2.	The heart of the facility is the DIII-D tokamak with its many support systems, utilities and diagnostics .....	2.5-3
2.5-3.	DIII-D capabilities allow a wide range of research and technology issues to be addressed .....	2.5-5
2.5-4.	The entire DIII-D first wall is graphite .....	2.5-5
2.5-5.	The upper divertor cryopump is optimized to pump highly triangular double-null divertor discharges .....	2.5-6
2.5-6.	An extensive array of computer systems operates the tokamak and collects and analyzes the data .....	2.5-7
2.5-7.	Quarterly boundary radiation levels show the site is maintained well below the 40 mrem operating limit .....	2.5-9
2.5-8.	Proposed facility development incorporates ideas from GA, collaborators and the February, 1998 workshop .....	2.5-10
2.5-9.	The carbon first wall and divertor targets protect the vacuum vessel and limit high-6 impurities .....	2.5-16
2.5-10.	The planned completion of the Radiative Divertor installation includes the lower baffle and the private flux baffles .....	2.5-17
2.5-11.	Divertor and first wall surface options will be tested on DIII-D .....	2.5-19
2.5-12.	The toroidal field coil is capable of 10 s and longer pulse operation with the completion of the proposed upgrade .....	2.5-21
2.5-13.	Additional coils would give an improved match to the outer vacuum vessel wall mode structure .....	2.5-24
2.5-14.	The new MSE system features a tangential and radial view of a single beam line .....	2.5-32
2.5-15.	New interferometer concept overcomes the difficulty with measurement of the first order term .....	2.5-36
2.5-16.	Several possible beamline rotation options would allow counter-injection .....	2.5-48
2.5-17.	The LANL RACE compact toroidal injector is of the size needed for DIII-D .....	2.5-51
2.5-18.	Operation of DIII-D at 3.4 T requires upgrades .....	2.5-52
2.6-1.	The DIII-D program advances fusion energy science and improves the tokamak concept .....	2.6-2
2.6-2.	DIII-D collaborates with the world's premier tokamak facilities .....	2.6-4
2.6-3.	The DIII-D tokamak is capable of producing plasma shapes of other tokamaks .....	2.6-14
2.6-4.	The DIII-D program is implemented through a line management organization which includes collaborators and four GA research divisions .....	2.6-35
3-1.	Scientific progress: DIII-D fusion performance has doubled every two years .....	3-12

## LIST OF TABLES

1-1.	DIII-D program collaborators insure coordination of national and international tokamak optimization .....	1-4
2.1-1.	Advanced tokamak program — objectives, challenges, and targets .....	2.1-6

2.1-2.	DIII-D program collaborators .....	2.1-11
2.2-1.	Program logic defines tools and approaches .....	2.2-5
2.2-2.	Parameters of DIII-D scenarios .....	2.2-18
2.3-1.	Results of dimensionless parameter scaling experiments in DIII-D for various regimes .....	2.3-11
2.3-2.	Tools for L–H transition physics studies .....	2.3-14
2.3-3.	Elements of divertor physics .....	2.3-36
2.3-4.	Enrichment of neon and argon is presented for four cases of induced deuterium flow .....	2.3-43
2.4-1.	$\rho_*$ scaling from ITER to various tokamaks .....	2.4-3
2.4-2.	From ITER to DIII-D and Alcator C–Mod varying $v_*$ and $\rho_*$ .....	2.4-5
2.4-3.	DIII-D contributions to ITER .....	2.4-6
2.4-4.	$\rho_*$ scaling from an optimized superconducting power plant to DIII-D .....	2.4-10
2.4-5.	DIII-D contributions to the superconducting tokamak path .....	2.4-12
2.4-6.	$\rho_*$ scaling from DIII-D to a compact ignition experiment .....	2.4-14
2.4-7.	DIII-D contributions to the compact ignition path .....	2.4-15
2.4-8.	$\beta$ scaling from an ST pilot plant to DIII-D .....	2.4-19
2.4-9.	DIII-D contributions to the ST path .....	2.4-20
2.4-10.	DIII-D contributions to future tokamak paths .....	2.4-21
2.5-1.	Power to plasma of auxiliary heating systems .....	2.5-6
2.5-2.	Power capability of heating systems after proposed upgrades are complete .....	2.5-11
2.5-3.	Summary of the five areas of research into nonaxisymmetric magnetic phenomena and how they would be addressed by the proposed external and internal coil systems .....	2.5-23
2.5-4.	Diagnostic systems installed on DIII-D .....	2.5-29
2.5-5.	Upper divertor diagnostic additions .....	2.5-30
2.5-6.	Lower divertor diagnostic modifications .....	2.5-31
2.6-1.	DIII-D program collaborators .....	2.6-1
2.6-2.	Recent SBIR collaborations with the GA Fusion Group .....	2.6-9
2.6-3.	DIII-D 1997 experiments emphasized urgent ITER physics R&D .....	2.6-16
2.6-4.	General Atomics provides ITER support in addition to DIII-D program support .....	2.6-17
2.6-5.	Past and present graduate and post-doctoral students at DIII-D .....	2.6-19
2.6-6.	DIII-D collaborations related to stability and disruption physics .....	2.6-21
2.6-7.	DIII-D collaborations related to transport and fluctuations .....	2.6-22
2.6-8.	Recent collaborations related to DIII-D work in the wave/particle topical area .....	2.6-23
2.6-9.	DIII-D collaborations related to divertor and boundary physics .....	2.6-24
2.6-10.	Programmatic responsibilities of major DIII-D U.S. collaborators .....	2.6-25
2.6-11.	Programmatic roles of DIII-D university collaborators (1997) .....	2.6-25
2.6-12.	Programmatic roles of other collaborations .....	2.6-26
3-1.	Changes in five-year plan since July 1997 .....	3-1
3-2.	Comparison of 1993 upgrade plan with actual upgrades implemented .....	3-7
3-3.	An assessment of progress on the 1993 advanced tokamak research goals .....	3-8

3-4.	An assessment of resolution of 1993 divertor research program functions/needs issues .....	3-10
3-5.	An assessment of accomplishments of 1993 divertor program goals and guidelines .....	3-10
3-6.	Integrated advanced tokamak parameter goals and achievements .....	3-11
3-7.	Comparison of 1993 plan and actual GA funding levels and operations weeks .....	3-17
3-8.	Facility improvements planned and implemented in FY94–98 .....	3-18
3-9.	An assessment of the 1993 five-year DIII-D new diagnostic plan and accomplishments .....	3-19
3-10.	New diagnostics implemented on DIII-D that were not anticipated in the 1993 five-year plan .....	3-20

# 1. THE DIII-D FIVE-YEAR PROGRAM SUMMARY

## 1.0.1. THE DIII-D NATIONAL PROGRAM OVERVIEW AND MISSION

The strategy for the recently restructured U.S. Fusion Energy Sciences Program focuses on innovation and scientific discovery to strengthen the program's ties to other fields of science, to position the United States to continue playing a meaningful role in the world fusion energy effort within available resources, and to preserve the basis for a future expanded U.S. Fusion Energy Program. The DIII-D Research Program is a cornerstone element in this national fusion program strategy (see 2.1). The problem addressed by this proposal is the optimization of the tokamak. Within this context, the DIII-D Program mission is:

**To establish the scientific basis for the optimization of the tokamak approach to fusion energy production.**

The DIII-D Program is an Advanced Tokamak (AT) Program using and advancing fusion energy science to provide the basis for future fusion initiatives. Tokamak optimization has been a basic organizing thrust of the DIII-D Research Program for several years. In implementing the new DIII-D research plan, we will pursue AT science and integrated performance optimization as the most promising direction for determining the tokamak's highest potential. The DIII-D Program mission seeks to develop and exploit fusion science (confinement, stability, power and particle control, and current drive) to advance fusion energy. DIII-D will produce demonstrated, scalable plasma performance; backed up by a firm, comprehensive theoretical model; and achieved in a configuration that has the potential to be attractive as a power plant concept. Thus, the proposed research will contribute significantly to the three legs of the U.S. Fusion Program: fusion energy science, concept innovation, and burning plasmas.

In support of the DIII-D overall mission, the specific goals of DIII-D AT research in the period 1999–2003 are:

- To attain the theoretically predicted minimum in the cross-field transport of heat and energy;
- To extend the operation of DIII-D to the theoretically predicted limits of plasma stability;
- To seek a plasma that exhibits full recombination in the divertor before it reaches a material surface, thus achieving the simple description of magnetic confinement as using magnetic fields to prevent hot plasma from touching a material surface;
- To develop methods of plasma current generation (initiation, ramp-up, sustainment, and profile control) to provide future devices the basis for full steady-state transformerless operation; and

- To integrate the above objectives in single steady-state operational scenarios to demonstrate the possibility of simultaneous optimization of the tokamak in the four major areas of fusion science.

The DIII-D National Program consists of a tokamak facility with its operating staff and a national collaborative research team that utilizes the facility to carry out research to support the goals of the U.S. Fusion Energy Sciences Program. DIII-D is the world's most flexible tokamak and the largest magnetic fusion device in the U.S. program. Its ability to control a variety of complex plasma shapes and its diagnostic instrument set are the best in the world. It has reliable heating and current drive systems, pumped divertor systems, and a digital plasma control system capable of achieving the plasma control essential to the tokamak optimization mission. The DIII-D open data system architecture enhances the effectiveness of the large collaborative national team.

The DIII-D Program has strong linkages (Section 2.6) to foreign and domestic experiments (the U.S. Theory Program) enabling technology development programs, the general science community, and the designers of future fusion initiatives such as International Thermonuclear Experimental Reactor (ITER). Links to universities and laboratories provide broad intellectual input to the DIII-D Program and provide paths for flow of research results between other groups and the DIII-D Program.

## 1.0.2. THE PROPOSED DIII-D FIVE-YEAR PROGRAM PLAN

An outline of the proposed research plan is presented in Fig. 1–1. Two major in-vessel installations divide the upcoming five-year time frame into three major experimental periods. The research emphasis progresses from short pulse AT physics to extended pulse and more optimized AT physics, and then to sustained 10 second AT physics. During the fall of 1999, we expect to complete the private flux baffle and pump in the upper divertor of the DIII-D vessel. In year 2000, we expect to complete installation of a set of external asymmetric magnetohydrodynamic (MHD) feedback coils. During the fall of 2001, we expect to complete installation of the lower divertor upgrade. By adding 110 GHz microwave gyrotrons, the ECH power will reach 6 MW in the fall of 2000 and 10 MW by 2003. These installations naturally separate the experimental program into three parts:

- The first period will continue the present research program into 1999. We expect to obtain deeper understanding of transport, obtain results on the improvement of stability limits using wall stabilization, elucidate the mechanisms which lead to edge instabilities that limit high confinement regimes and reduce the maximum beta, exploit the microwave heating and current drive, increase understanding of the physics of parallel heat transport in the scrapeoff layer and divertor, and further explore plasma shape optimization.
- The period 1999–2001 will be an intensive AT experimental period devoted to exploring the open-versus-closed divertor question and to developing pressure and current profile control and fueling techniques for sustained, quasi-stationary operation. Further experiments to implement theoretically predicted optimized profiles will also be undertaken.

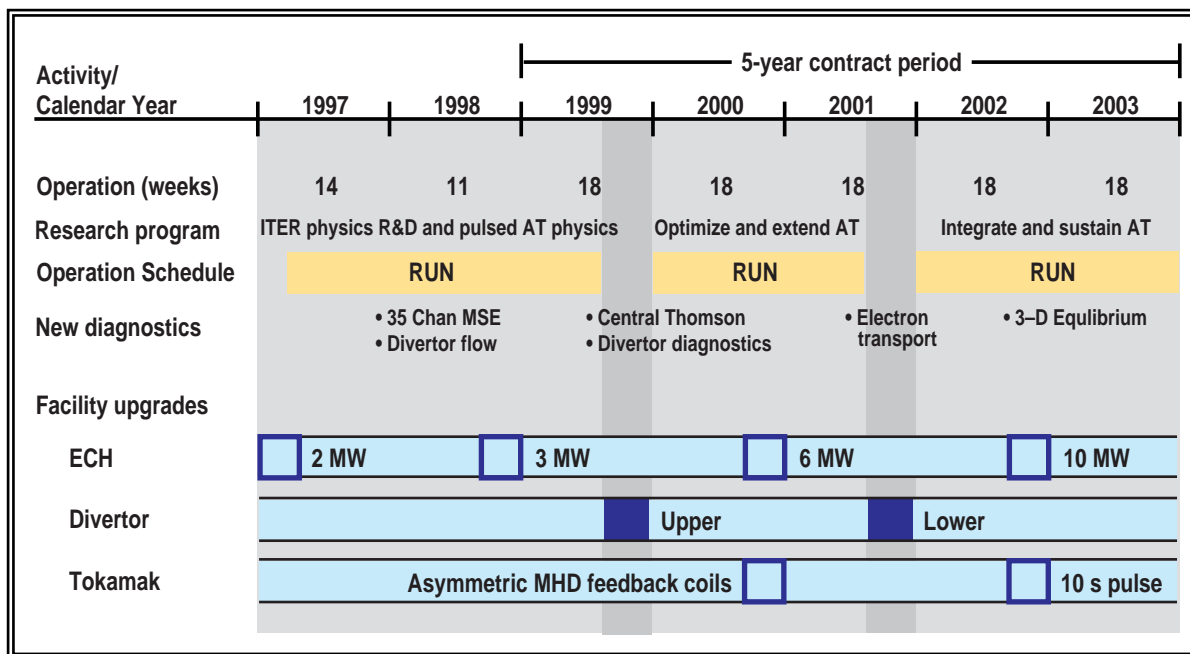


Fig. 1–1. The DIII-D program plan progresses from short pulse Advanced Tokamak physics, through optimization, to 10 s operation. The baseline plan is to operate 18 weeks per year for each of the next five years. The electron cyclotron heating capacity will increase to 6 MW by 2001 and 10 MW by 2003 and installation of the upper and lower radiative divertors are scheduled for 1999 and 2001.

- The third intensive experimental period, from the end of 2002 through 2003, will be devoted to using the systems installed in 2001 to develop integrated, near steady-state (10 s), optimized AT scenarios. There will be a particularly intensive effort to control the current profile and the pressure profile using rf systems using the full double-null divertor.

### 1.0.3. LEADERSHIP

A key responsibility of the DIII-D Program, for the period 1999–2003, is to provide national program leadership in optimization of the tokamak approach to fusion energy. We propose to accomplish this mission with the diverse capabilities of the DIII-D National Team consisting of about 120 operating staff and 100 research scientists drawn from 8 U.S. National Laboratories, 19 foreign laboratories, 17 universities, and 5 industrial partnerships (see Table 1–1 and Section 2.6).

As the contractor for the DIII-D National Fusion Facility, GA will provide leadership for the DIII-D Program of toroidal fusion research. GA is responsible for optimizing the pace for the research program for the most scientific and cost-effective output, and for safe and environmentally sound operation in accordance with applicable DOE, federal, state, and local government rules and regulations.

**TABLE 1-1**  
**DIII-D PROGRAM COLLABORATORS INSURE COORDINATION OF**  
**NATIONAL AND INTERNATIONAL TOKAMAK OPTIMIZATION**

National Laboratories	Universities	International Laboratories
ANL	Cal Tech	ASIPP (China)
INEL	Columbia U.	Cadarache (France)
LANL	Hampton U.	CCFM (Canada)
LLNL*	Johns Hopkins U.	Culham (England)
ORNL*	Lehigh	FOM (Netherlands)
PNL	MIT	Frascati (Italy)
PPPL*	Moscow State U.	Ioffe (Russia)
SNL*	Palomar College	IPP (Germany)
	RPI	JAERI (Japan)
	U. Maryland	JET (EC)
<u>Industry Collabs</u>	U. Texas	KAIST (Korea)
CompX	U. Washington	Keldysh Inst. (Russia)
CPI (Varian)	U. Wisconsin	KFA (Germany)
GA*	UCB	Kurchatov (Russia)
Gycom	UCI	Lausanne (Switzerland)
Orincon	UCLA*	NIFS (Japan)
	UCSD*	Troitsk (Russia)
		SWIP (China)
		Tsukuba U. (Japan)

\*DIII-D Executive Committee Membership.

General Atomics' leadership responsibilities include maintaining:

- A **DIII-D Executive Committee**, including GA and collaborator members to advise the director on program planning, direction, priorities, and budgets.
- A **DIII-D Program Advisory Committee** composed of technical experts from other laboratories to provide outside peer review.
- A **DIII-D Long-Range Plan** to chart DIII-D Program goals and milestones coordinated with major DIII-D collaborators.
- A **DIII-D Research Plan** to detail planned activities for at least a one-year period.

### 1.1. TOKAMAK RESEARCH USING THE DIII-D NATIONAL FACILITY (SOW AND WBS TASK 1)

The technical approach which we will use to pursue the DIII-D Program mission and goals can usefully be described in different cross-cutting ways. At the highest level, we see the Program as two main lines, core plasma and boundary plasma physics, both of which work toward an eventual integration demonstrated by sustaining a 5% beta plasma for 10 seconds. Figure 1-2 of this volume gives some of our numerical targets for tokamak optimization and indicates some of the areas of integrated research between core and boundary physics.

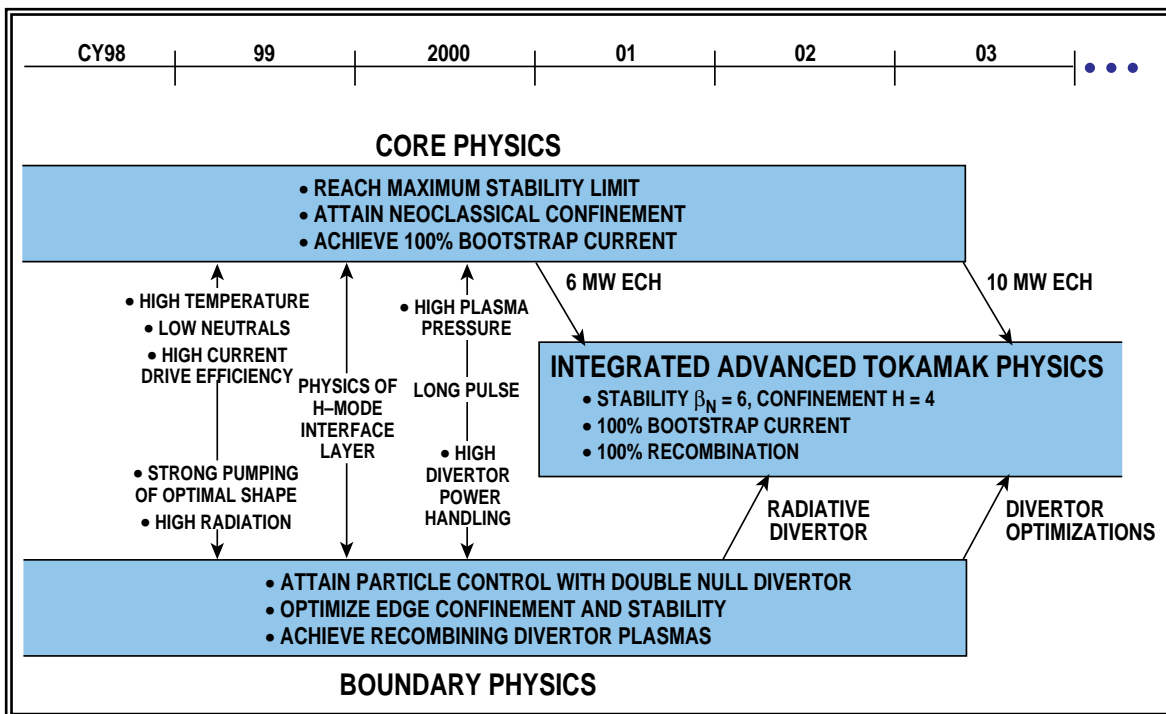


Fig. 1-2. DIII-D Advanced Tokamak research plan will integrate the upgraded heating and divertor to optimize performance. Core plasma physics and boundary physics studies will culminate in 10 second, 5% beta operations.

The second way we view the program is as an integrated AT Program (see Section 2.2). The AT Program approach to optimizing the tokamak is expressed in lines of action or research thrusts. Our ability to pursue these research thrusts motivates the plasma control tools and diagnostics the program needs. Finally, the broadest view of the DIII-D Program is by the science topical areas (confinement, stability, power and particle control, and steady state). We present the program in those WBS categories.

## RESEARCH THRUSTS

The four principal DIII-D research thrusts are:

1. Controlling interior plasma profiles and wall stabilization for higher stability and confinement.
2. Controlling the plasma edge for sustained AT performance and better confinement.
3. Developing the basis of steady-state operation.
4. Developing advanced divertor operating modes.

Figures 1–3 and 1–4 of this section show diagrammatically the required plasma control tools and diagnostic upgraded needed to pursue the DIII-D Research Program. Detailed descriptions of these upgrades and enhancements to DIII-D are given in Section 2.5. The research thrusts are described in Sections 2.2.1.4 and 2.2.3.1 and briefly below. These four principal AT research thrusts are cross cutting activities which integrate elements from the four topical science areas to achieve AT progress.

1. **Controlling the Interior Current and Pressure Profiles.** Controlling the current density profile is the key to attaining the high plasma stability levels sought. The current profile also enters into determining the growth rates of turbulence. The principal objectives are to sustain negative central shear (NCS), to sustain high internal inductance (high  $\ell_i$ ) profiles (peaked current profiles), and to suppress sawteeth. The transport barrier location will greatly affect the current profile since the bootstrap current peaks where the pressure gradient is large. Principle tools to directly control  $J(r)$  are the electron cyclotron current drive (ECCD) for off-axis current drive and the fast wave current drive (FWCD) for on-axis current drive.

The tokamak core has a complex feedback loop which if it is optimized can create transport barriers. Introducing shear in  $E \times B$  flow at a particular point in the plasma can reduce fluctuations locally, reducing the local transport which increases gradients of pressure and flows, which in turn amplifies the radial electric field, thus closing the loop. Principal tools to intervene in this loop are off-axis ECH to control the pressure profile and divertor pumping to control the density to control the neutral beam injection (NBI) deposition profile.

The presence of a nearby conducting wall can stabilize long wavelength MHD modes, and thereby increase the limiting beta. Present nonideal MHD theory indicates that with a resistive wall and plasma dissipation, sufficient rotation leads to stability. In the five-year program, we plan to use feedback controlled nonaxisymmetric coils to improve the wall stabilization concept. Initially, we will use the existing six magnetic field error correction coils (C-coil) for “smart shell” stabilization techniques. Then we will add segmented coils outside the vessel, above and below the midplane, to greatly improve the spatial mode structure of the coil system.

2. **Controlling the Plasma Edge for Sustained AT Performance and Better Confinement.** The high energy confinement (H-mode) shear layer is a battleground of conflicting requirements, providing both the boundary condition for the core plasma and setting the scrapoff layer (SOL) density, temperature, and power flow boundary conditions.

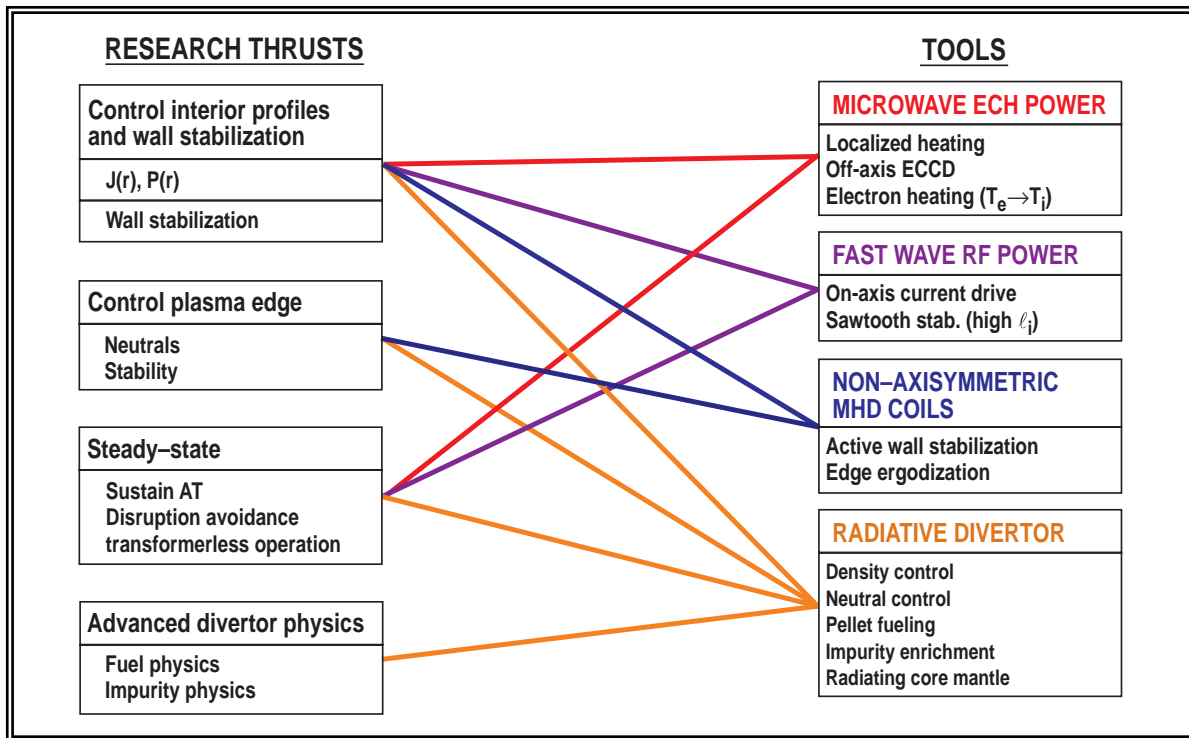


Fig. 1-3. Implementation of the proposed DIII-D research requires the plasma control tools defined in the facility upgrades.

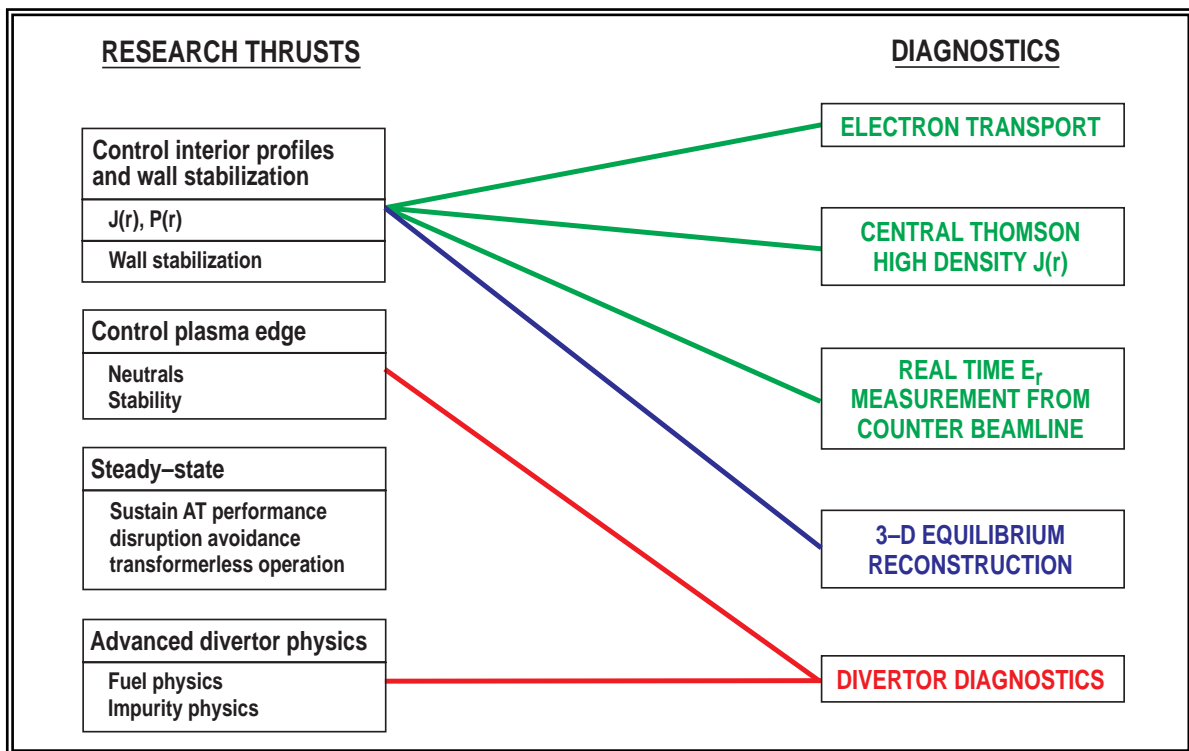


Fig. 1-4. Pursuit of the key research thrusts requires the diagnostic upgrades included in the DIII-D Plan.

The desire for a high quality H-mode edge is motivated by the correlation between decreasing neutral fueling and increasing H-factor and the correlation of the height of the H-mode pedestal with decreasing neutral fueling. The highly baffled Radiative Divertor Project (RDP) installation is expected to make the edge more neutral free. Pellet fueling with inside and outside launch is also being substituted for gas fueling to further lower the neutral gas source at the separatrix.

The large pressure gradient that forms in the H-mode edge leads to a large bootstrap current which is unfavorable for kink modes. A variety of active control techniques are being proposed {the use of a radiating mantle [e.g., the TEXTOR radiative impurity improved confinement mode (RI-mode)], the use of marginally diverted plasmas, control of the plasma shape, the use of non-axisymmetric coils to ergodize the plasma edge, and the regulation of ELMs} to reduce the edge pressure gradient through degraded H-mode edges or even low energy confinement (L-mode) edge.

3. **Developing the Basis of Steady-State Operation.** The extremes of tokamak performance have thus far been achieved under transient conditions. The DIII-D Program will work to extend quasi-stationary operation to 10 s pulses.

AT operation relies on having a significant fraction of the total plasma current produced by the bootstrap effect which closely couples current profile evolution to stability and transport. Control of the current and current profile will require both direct external noninductive sources [neutral beam current drive (NBCD), ECCD, FWCD] and indirect control through bootstrap current manipulation via the density and temperature profiles by heating or transport barrier control.

The potential for plasma disruptions requires a means to avoid or mitigate disruptions. We plan to pursue two approaches. The first is to gain a sufficiently predictive scientific basis of plasma stability to be able to operate using real-time control near, but not exceeding, stability boundaries. Even if this goal is achieved, however, disruptions will still occur (but rarely) owing to random events injecting material from plasma-facing component surfaces into the plasma or faults in the control system. So the second major development for those remaining disruptions is a reliable disruption mitigation system.

Density control techniques are needed for three reasons. First, back-projection from promising power plant designs (see Section 2.4) leads to DIII-D scenarios with  $n/n_{Greenwald} \approx 0.2$  to 0.4, roughly a factor of two lower than usually obtained in H-modes. Second, the efficiency of noninductive current drive varies inversely with density, placing a premium on low density/high-temperature operation. A third, practical consideration for DIII-D is that the cutoff density for the 110 GHz ECH system is  $7 \times 10^{19} \text{ m}^{-3}$ , so the density should be kept below this level. In the near term, divertor pumping will be used to lengthen the high performance phase of DIII-D plasmas using the baffle and cryopump of the proposed divertor upgrades. Neutral beam and central pellet fueling will be used in DIII-D to feed density inside a forming transport barrier to drive up the density gradient. To improve penetration, high-field-side pellet injection is planned.

We will explore several techniques for transformerless operation, including ECH, helicity injection, or use of the outer poloidal field coils for initiation and initial ramp-up. Overdriving the bootstrap current is a promising idea for ramp-up over a wide range of plasma current. Helicity injection startup will also be explored.

4. **Developing Advanced Divertor Operating Modes.** The pattern of recirculation of neutrals in the divertor is governed by the shape of the divertor structures. Encouraging more convective parallel heat transport (instead of conduction) may be a route to increasing divertor radiation. The shaping of the divertor structures that determines the 2-D patterns of fuel flow also dominates the impurity transport problem. We will explore the use of entraining fuel flow to enrich impurities in the divertor while limiting their buildup in the core plasma in AT modes. Impurity radiation in the divertor and fuel flow physics are also emerging as the keys to obtaining a plasma that fully recombines before reaching a material surface. Our goal is to find a regime of radiative and/or detached divertor operation that allows low heat flux to divertor surfaces and low erosion of those surfaces, and is compatible with a low impurity content, high performance core plasma. Finally, the boundary interface between the plasma and the wall must be controlled in order to regulate recycling of fuel and sources of impurities.

### 1.1.1. SCIENCE RESEARCH (WBS SUBTASK 1.1)

The research science is managed and organized by the four key fusion energy science topical areas: confinement, stability, power and particle control, and steady state. The motivations, scientific issues, instruments required, and proposed studies in each area are discussed in depth in Sections 2.3 and 2.5 of this volume. The following paragraphs briefly clarify the scientific content of each of these categories, summarize the research tasks we expect to undertake during the period covered by this plan, and present the manpower loading proposed in each area. The scientific staff activities include design and conduct of experiments, developing and operating diagnostics, analysis of data, support of theory and modeling efforts, comparison to theoretical models, and publication of results. In addition to the four topical science areas, we present the plans and required labor in the three principal areas of science support: applications programming, new diagnostics, and general physics support. In each of these seven subtasks, we indicate the required labor effort. For reference, we give the FY98 labor [in full-time equivalent (FTE)] for GA as well as for collaborators. In our plan, in accordance with DOE guidance, we have assumed that the collaborator level remains constant during the period FY99–FY03.

**1.1.1.1. CONFINEMENT (WBS SUBTASK 1.1.1).** The scope of confinement research on DIII-D covers the transport of particles, angular momentum, and heat within the tokamak core plasma from neoclassical and turbulent processes. Our objective is the suppression and stabilization of turbulence, leading to optimized confinement. Neoclassical thermal transport levels have been reached for the ions. We seek high confinement per unit current (H factor up to 4). Our primary approach is stabilization of turbulence by means of E×B velocity shear, leading to the appearance of transport barriers. Regimes of principal interest are the NCS and high  $\ell_1$  regimes. More broadly, our goal is to improve the fundamental understanding

of turbulent transport and of the dynamics of transport barrier formation and control to obtain a predictive modeling capability for projection to future machines. The particular areas of confinement study that we propose to undertake in the coming five year period are all in this volume (2.2–7):

- Understanding E×B shear stabilization of turbulence (2.3–3ff).
- Producing and controlling transport barriers through suppression of turbulence (2.3–7ff, 2.3–64, 2.2–11).
- Reducing electron thermal transport (2.3–8ff).
- Testing and further developing models of turbulent transport (2.3–10).
- Investigating nondimensional scaling to extrapolate to future devices (2.3–10).
- Understanding fuel and impurity ion transport (2.3–12).
- Exploring regimes with high electron temperature (2.3–10, 2.3–74, 2.2–22).
- Testing and further developing models for the transition from low energy to high energy confinement mode (L–H transition) and the H–mode edge pedestal (2.3–14,15, 2.2–15).
- Investigating confinement physics of novel configurations, like RI–mode (2.3–16).
- Developing diagnostics needed for turbulent transport investigations (see p. 2.5–33).

**1.1.1.2. STABILITY (WBS SUBTASK 1.1.2).** The scope of this subtask is ideal and non-ideal MHD stability research. Our objective is to advance understanding of MHD stability and develop active and passive means of improving it. Advanced tokamaks leading toward a more compact, economical, and reliable fusion power plant need approximately twice the value of normalized beta ( $\beta_N$ ) on which ITER is based. Our approach to obtaining operation at such high  $\beta_N$  is to employ wall stabilization along with optimization of the plasma shape and current and pressure profiles, particularly profiles near the plasma edge. The goals of this work are higher  $\beta_N$  operation and a sufficient basis of understanding to project such operation to future machines, and to operate in such regimes in a manner to avoid creating physics-driven disruptions. For those remaining disruptions triggered by system hardware faults, we have proposed a disruption mitigation approach. In the next five years, we propose to investigate the following issues affecting stability (2.2–9, 2.3–21):

- Optimizing plasma shape (2.3–23).
- Optimizing and controlling the pressure profile (2.3–23).
- Optimizing and controlling the current profile (2.3–23).
- Understanding and applying wall stabilization (2.3–25).
- Seeking profiles with good bootstrap current alignment (2.3–64).

- Understanding and stabilizing nonideal instabilities (2.3–28).
- Avoiding and mitigating disruptions (2.3–31).

**1.1.1.3. POWER AND PARTICLE CONTROL (WBS SUBTASK 1.1.3).** The scope of this subtask encompasses divertor physics, boundary conditions for the core plasma, and plasma-material interactions. Our primary objective is to achieve a detached, radiating divertor plasma compatible with an advanced tokamak core plasma, particularly in regard to providing the needed density control for steady-state regimes. The simplest way to increase radiated power is to raise the density at the separatrix, but that can be inconsistent with the need to maintain a low collisionality core plasma or with density limits. Our approach is to seek increased radiation at fixed density using impurity enrichment in the divertor, 2-D patterns of heat and fuel flow, and plasma recombination. A strongly pumped, double null divertor (implemented in stages) is our approach to providing the density and impurity control and management of neutral fueling for a high triangularity, high performance core plasma. A secondary line of investigation that may be compatible with a thrust toward L-mode edge core plasmas is the use of radiating mantles. The issues in this area revolve around impurity sources from the divertor, core plasma impurity transport, and synergistic effects of impurities on confinement (e.g., RI-mode). Besides achieving plasmas with core/divertor compatibility, our goal is a verified 2D divertor and surface modeling codes that can be used predictively. In the next five years, we propose to investigate the following plasma boundary issues that are all in this volume (2.2–10, 2.3–36):

- Understanding the roles of conduction and convection in parallel heat transport and optimizing the divertor using this physics (2.3–39, 2.3–47).
- Obtaining high degrees of plasma recombination (2.3–41).
- Increasing impurity concentration enrichment in the divertor (2.3–42).
- Finding compatible detached divertor and advanced tokamak core configurations (2.3–44).
- Assessing double versus single null divertor operation (2.3–47).
- Providing density control for the advanced tokamak core plasma (2.3–49).
- Developing pellet fueling (2.3–51).
- Understanding the physics of density limits (2.3–52).
- Understanding the role of neutrals in core confinement (2.3–53).
- Understanding the role of neutrals in H-mode access and the H-mode shear layer structure (2.3–56).
- Understanding and controlling edge localized modes (ELMs) (2.3–58).
- Understanding impurity source mechanisms and surface erosion (2.3–59).

**1.1.1.4. STEADY STATE (WBS SUBTASK 1.1.4).** The scope of this subtask is the scientific issues associated with the physics of heating plasmas to high temperatures and of driving electrical currents in plasmas, including self-generated currents like the bootstrap current and the Pfirsch-Schluter current. For processes using waves, this includes the physics of wave generation, propagation, absorption, and effects on the distribution function like those giving rise to plasma current. Our objective is to provide the scientific basis for noninductive plasma current initiation, ramp-up, maintenance, and current profile control. Our approach will be to utilize various plasma initiation schemes, bootstrap and rf for ramp-up, and ECCD and FWCD for current maintenance and current profile control. Our goal is to provide the basis for full transformerless operation of the tokamak. Some of the issues of current drive and heating (2.2–10, 2.3–63) that we expect to explore during the plan period include:

- Controlling the current profile using ECCD and FWCD (2.3–64).
- Controlling transport barrier thresholds and locations (2.2–18ff).
- Developing off-axis current drive by mode conversion of fast waves to ion Bernstein waves (2.3–68).
- Initiating the plasma current without using the ohmic heating (OH) transformer (2.3–71, 73).
- Ramping up the plasma current using the bootstrap effect (2.3–72).
- Maintaining the plasma current with ECCD, FWCD, and bootstrap (2.3–64ff).
- Studying electron versus ion heating ( $T_e = T_i$  operation) (2.3–74).
- Studying wave absorption by fast ions (2.3–75).
- Using wave power versus NBI to sort out the role plasma rotation and rotational shear on transport barrier formation (2.3–76).
- Stabilizing sawteeth (2.3–77).
- Stabilizing neoclassical tearing modes (2.3–77).
- Controlling ELMs (2.3–78).
- Studying transport by localized heat pulses (2.3–10).

**1.1.1.5. APPLICATIONS PROGRAMMING (WBS SUBTASK 1.1.5).** The scope of this task is to provide the necessary database and data analysis support to the scientific staff on the DIII-D Program (see Section 2.5.6). Our objective is to provide researchers with easy, timely access to all necessary experimental results, and thereby enhance the productivity of DIII-D as a national user facility serving researchers from many institutions both on site and off site. Our approach is to modernize the computing environment to provide the ability for remote participation and a distributed data analysis and modeling capability. Our goal is an open data system that facilitates fast and efficient analysis of data by the DIII-D National Team. Our approach to this goal requires the following actions to be taken:

- Implementing a common I/O file standard to facilitate data transfer.
- Installing a modern, commercially available data warehousing software to archive and retrieve a variety of data.
- Developing user-friendly tools for code invocation, data visualization, and data transfer.
- Constructing a programmable environment for code coupling and continuous improvement of comprehensive simulation capability.

**1.1.1.6. NEW DIAGNOSTICS (WBS SUBTASK 1.1.6).** The scope of this subtask is the diagnostic upgrades and modifications necessary to support the scientific program (see Section 2.5.5). Our objective is to permit the new areas of research necessary to achieve the scientific subtasks defined previously by providing new measurement capability or changes in the DIII-D machine hardware or, (in some limited number of cases such as the core Thomson scattering diagnostic), to fill in gaps in our existing measurement capability. Our approach is to use the DIII-D National Team to implement new measurement systems targeted at key physics issues. Our goal is to enable sufficient measured data to decisively confront theoretical models and enable the development of predictive models based on DIII-D research. Some of the areas of diagnostic upgrade are listed below.

- Radiative Divertor Diagnostics. (See Section 2.5.5.2 Table 2.5–5 and Table 2.5–6).
- Plasma Control Diagnostics (2.5–31).
- Electron Transport Diagnostics (2.5–33).
- Study of Small-Scale Turbulence Via Scattering (2.5–33).
- Magnetic Field Fluctuation Measurements (2.5–34).
- Measurement of Turbulent Temperature Fluctuations (2.5–34).
- Central Thomson Scattering (2.5–34).
- 3-D Equilibrium Reconstructions (2.5–35).
- Current Profile Measurements at High Densities (2.5–35).
- Laser Pumping to Improve Beam Emission Spectroscopy Diagnostics (2.5–36).

**1.1.1.7. PHYSICS SUPPORT AND LEADERSHIP (WBS SUBTASK 1.1.7).** The scope of this task covers GA support for both incoming and outgoing collaborations. Our objective is to support the interface of the DIII-D Program to the collaborators, other laboratories both domestic and foreign, and the external fusion community. This objective is supported by four principal activities:

- Research Program Leadership (program direction and development, research plan development, and advisory committees).
- On-site Collaborator Support (phones/offices, diagnostic operations and maintenance support for

collaborators, data acquisition support for collaborators)

- External Collaboration Support (international cooperation and ITER Expert Group participation)
- Technical Publications Support for the DIII-D Scientific Staff (including collaborators).

### 1.1.2. DIII-D FACILITY OPERATIONS (WBS SUBTASK 1.2)

The scope of this subtask is the operation of the DIII-D facility (see Section 2.5). This subtask is subdivided into seven subordinate subtasks: Tokamak Systems, Neutral Beams, ECH Heating, Ion Cyclotron Resonance Frequency (ICRF) Heating, Diagnostics, Data Systems, and Operations Support. The objective is to provide and organize the resources necessary to enable the DIII-D National Fusion Facility to provide sufficient run time and capability to carry out a wide range of state-of-the-art tokamak experiments. Operation of the DIII-D facility is the responsibility of GA, who provides the core operational engineering and technical staff, along with the appropriate infrastructure to organize the effort. At the heart of the facility is the DIII-D tokamak which is capable of operating at plasma currents up to 3.0 MA with a magnetic field of 2.2 T. The DIII-D tokamak has a unique capability for varied highly noncircular limiter and divertor plasma configurations. Substantial plasma heating and current drive capability is available from 20 MW (delivered) of neutral beam heating, 6 MW (source) of ICRF power and 2 MW (source) of ECH power. The DIII-D diagnostics set provides over 50 diagnostic systems capable of providing definitive measurements of plasma parameters in the core, edge, and boundary regions of the plasma. Control of the tokamak, heating systems, and auxiliaries is managed through a set of interconnected computers and sophisticated internally developed algorithms.

The approach we have taken to this task, and plan to continue, to take is to maximize the productivity of individual run days and run periods. Owing to its operational flexibility and the excellence of its diagnostic set, DIII-D can complete an experiment in a single run day. Research operations have been carried out on a five-day-a-week basis for three weeks of operation followed by two weeks of maintenance, calibration, and testing. Typically one longer period is set aside each year for new installations and major refurbishments. In recent years, the number of operating weeks has been limited by funding (8 weeks in FY97 and 13.6 weeks in FY98, compared to up to 27 weeks earlier). This DIII-D proposal calls for 18 weeks of single shift operation in the annual research operation of the DIII-D facility for the period 1999–2003. A proposed option would extend the operation to 18 shift-and-a-half weeks. Such a schedule allows the maintenance time necessary to keep the machine in a high state of operational efficiency. Our goal is that the planned increased operation will enable up to 50 experiments per year, longer campaigns that require several days, exploratory studies and efforts into new regimes, and additional opportunities for collaborators.

**1.1.2.1. TOKAMAK SYSTEMS (WBS SUBTASK 1.2.1).** The scope of this subtask is to support the operation of the Ohmically heated DIII-D tokamak and its support systems. Besides normal operations and maintenance, this task also requires continuous refurbishment and improvement of aging subsystems, installa-

tion of asymmetric MHD feedback coils, and increasing the electrical substation capacity to enable high power and longer pulse plasma heating and magnet system operation. Our approach is to maintain our historically effective operations and maintenance programs. This subtask provides for the operation and maintenance of the following systems:

- Toroidal coil.
- Ohmic heating coil.
- Eighteen independently controlled poloidal field shaping coils each powered by an independent current regulator.
- A set of six coils which correct the residual error fields.
- Graphite vacuum vessel first wall protection system.
- The 400°C baking and outgassing system.
- The boronization wall conditioning system.
- The glow discharge cleaning system.
- The upper and lower divertor cryopump systems (liquid helium, 40,000 l/s each pump).
- Hardwired systems that implement critical safety limitations.
- State-of-the-art high speed digital plasma control system.
- Programmable fuel and impurity gas injection systems.
- Cryogenic D<sub>2</sub> pellet injector and room temperature lithium pellet injector.
- Prime power substations from the local utility's power mains.
- Two flywheel energy storage motor generators (525 and 260 MVA).
- A set of phase controlled power supplies for the coils.
- A system of switching current regulators (choppers) for the field shaping coils.
- Twelve high-voltage power supplies (6 MW each) for the auxiliary heating systems).
- A 150 l/h helium liquifier to support beamline and divertor cryopump operation.
- A substantial high pressure, high purity water cooling system.
- The radiation shield (the wall and moveable roof of the machine hall).
- The radiation monitoring system to comply with DOE and Nuclear Regulatory Commission (NRC) as low as reasonably achievable (ALARA) principles.

**1.1.2.2. NEUTRAL BEAMS (WBS SUBTASK 1.2.2).** The scope of this subtask is to operate and maintain the DIII-D neutral beam systems, which consist of four beamlines. Each beamline has two positive ion

sources in parallel, focused through a common drift duct. These neutral beam systems were designed for 5 s deuterium beam operation at beam energy of 80 keV with 16 MW of total injected neutral beam power from eight sources. They routinely operate at this level. Improvements in operational technique and in system hardware have led to the routine operation in deuterium at beam power level of 20 MW for 3.5 s. Successful testing and operation of three ion sources at 93 keV deuterium beam energy also leads to the possibility of enhancing system capability to 28 MW. Control and data acquisition computers have recently been upgraded, along with several instrumentation and control systems to improve system functionality, availability, and reliability.

The 20 MW, 80 kV neutral beam system is the workhorse of day to day operation. Four beamlines are routinely available on demand to provide heating at their design levels. They have also become an important source for a number of diagnostics including ion temperature, plasma rotation, radial electric field, current profile, and turbulence. Our approach will be to maintain this excellent capability to meet the high availability objective.

**1.1.2.3. ECH (WBS SUBTASK 1.2.3).** The scope of this subtask is to operate and maintain the installed ECH systems. At present, we have two 110 GHz gyrotrons operating at a nominal 1 MW (source) power level. The first gyrotron is made by Gycom in Russia. It has an edge-cooled window of boron nitride which limits the pulse length to 2.0 s at a power level of 1 MW. It has achieved power levels of 960 kW for 2.0 s pulses in tests in Russia. The other gyrotron is made by CPI (formerly Varian). It has a face-cooled window of sapphire which limits the power to 1 MW for 0.8 s or 0.5 MW for 2 s. Both vendors indicate their designs are steady state compatible except the window. These gyrotrons have injected power into DIII-D through the transmission system, and the beam patterns and locations generated in the vacuum vessel correspond approximately to those expected from the theory of Gaussian beam propagation and from vacuum ray tracing using a 3D computer model. A third gyrotron is expected from CPI in late 1997

The transmission system for these gyrotrons is evacuated corrugated waveguides of diameter 31.75 mm propagating the HE<sub>11</sub> hybrid mode. The waves are launched into the vessel via a rotatable mirror which can steer the beams in the vertical direction in order to control the poloidal location of the power deposition. The steering in the toroidal direction can be changed, but only during a vent of the vacuum vessel. The present mirrors are tilted 19 deg in the toroidal direction in order to generate co-current drive.

Power supplies for the gyrotrons are modified neutral beam supplies. A single neutral beam power supply has sufficient power to support the operation of two 1 MW gyrotrons. However, Gycom gyrotrons operate near 72 kV and CPI gyrotrons operate near 80 kV, so gyrotrons of mixed brands cannot be operated by a single supply. At present, we use a modified Mirror Fusion Test Facility (MFTF) neutral beam supply for the Gycom gyrotron and a modified DIII-D Universal Voltronic Corporation neutral beam supply for the CPI gyrotron.

Our approach will be to continue to operate existing and newly commissioned gyrotron systems for physics experiments while implementing the ECH power upgrade. The objective of the physics experiments will evolve from basic physics tests to major demonstrations as the total available power rises. Our goal is a gradual increase in reliable operational power from the present 2 MW to 6 MW and eventually to 10 MW.

**1.1.2.4. ICRF HEATING (WBS SUBTASK 1.2.4).** The scope of this subtask is to operate the three existing ICRF power sources, eventually a fourth source to be installed, and the associated power transmission and antenna systems. A modified Fusion Materials Irradiation Testing (FMIT) system has power of 2 MW for at least 10 s over the frequency range 30 to 60 MHz. Two Asea Brown Boveri (ABB) transmitters have rf power of 2 MW for at least 10 s over the range 30 to 55 MHz with power falling off to 0.4 MW at 120 MHz. The FMIT power is coupled to an uncooled four strap antenna which is limited to a 2 s pulse length. The ABB transmitters are connected to the water cooled four strap antennas at 0 and 180 deg which can operate for 10 s.

A transmission line configuration more tolerant to variations in plasma-antenna loading is being installed, which is based upon a traveling wave concept. This configuration uses a less efficient coupling factor between the antenna strap and the plasma, which results in a lower perturbation back at the transmitter for any change in plasma edge condition. However, the loss in coupling efficiency is recovered by recirculating the uncoupled power back to the antenna using a resonant ring loop.

Our approach will be to support ICRF operations to allow steady progress in gradually building up the necessary physics tools and approaches toward the advanced tokamak goal.

**1.1.2.5. DIAGNOSTICS (WBS SUBTASK 1.2.5).** The scope of this subtask is to operate and maintain the DIII-D plasma diagnostic set, which is made up of more than 50 instruments built and operated by the DIII-D National Team. This ensemble of instruments is the most complete of any tokamak in the world and routinely produces the high quality data required to fuel the DIII-D scientific research program. The DIII-D diagnostics set includes extensive divertor and edge measurement capability, plasma core profile measurements of density, temperature and plasma current, and a large suite of fluctuation diagnostics. Our approach is to utilize the present mixed team of GA personnel and collaborators to continue the effective operation of the DIII-D diagnostics. A complete list of the diagnostic systems installed on DIII-D and the measurements that they make is shown in Section 2.5, Table 2.5-4.

**1.1.2.6. DATA SYSTEMS (WBS SUBTASK 1.2.6).** This subtask supports data acquisition and control computing and the general DIII-D computing infrastructure. The extraction of data from the experiment, the production of results through data analysis, and the dissemination of information to national and international researchers involves computer systems and programming at all levels. As a national facility, the number of collaborators on-site, and more importantly collaborators at remote sites are expected to increase. Our goal is to support the projected 40%/year increase in the data rate due to participation of

more collaborators, more diagnostics, more operation and longer pulses, and to support the increasing sophistication of the DIII-D control system. The computer systems supported are:

- Neutral beam control systems.
- Plasma control system.
- General purpose facility CAMAC-based data communication and timing system.
- Interlinked local computer network infrastructure.
- The tokamak control computer that monitors the entire operating cycle.
- The data acquisition and archival computer system.
- The local and off-site mass data storage system.
- Numerous front end diagnostic control and data acquisition computers.

**1.1.2.7. OPERATIONS SUPPORT (WBS SUBTASK 1.2.7).** Operations support is a diverse collection of tasks which support the DIII-D operation and research activities including planning, safety, facilities operation and maintenance, stockroom, quality assurance, engineering analysis, computer-aided design (CAD) system, document center, collaboration laboratories.

Our objective is to provide the services and tools required for the operators and research staff to carry out a safe, documented, quality program.

## 1.2. UPGRADE DIII-D COMPONENTS AND SYSTEMS TO ACHIEVE PROGRAM OBJECTIVES (WBS AND SOW TASK 2)

In order to carry out the proposed five year research program, certain upgrades to the DIII-D facility are required: an increase in the 110 GHz microwave power, modification of the divertor, and extension of the tokamak pulse length to 10 s.

The ultimate opportunity for carrying out the AT Program begins in 2002 when DIII-D is equipped with the three principal tools it needs for this integrated research (see Fig. 1–1):

- Precise off-axis current drive and heating from electron cyclotron microwave power sources to sustain and control the optimal current profile. The 110 GHz ECH power will be increased from 2 to 6 MW in 2000 and to 10 MW in 2003 with 1 MW 10 s pulse gyrotrons. Figure 1–5 of this section depicts some of the key, recent technical advances upon which our proposal is based.
- A double-null divertor system which can strongly pump the optimal high-triangularity plasma shape to maintain the core plasma in the required high temperature regime of low-collisionality while producing detached divertor plasmas through advanced divertor physics effects. Such a divertor will be operational in 2001. Figure 1–6 of this section shows the various stages of implementation of the Radiative Divertor Project.
- Modest improvements to the magnet system to enable operation for 10 s pulse lengths.

This upgrade plan was selected as the highest priority among many options. However, recognizing that specific future scientific outcomes cannot be assured, the DIII-D Plan includes contingency options which could be implemented in lieu of the proposed baseline plan. The strategy for contingency options is outlined in Fig. 1–7 of this section. The initial facility upgrades are the ECH 3 to 6 MW upgrade and the upper divertor upgrade. Based on results from experiments with these new tools, at an intermediate decision point (December 2000), we would assess

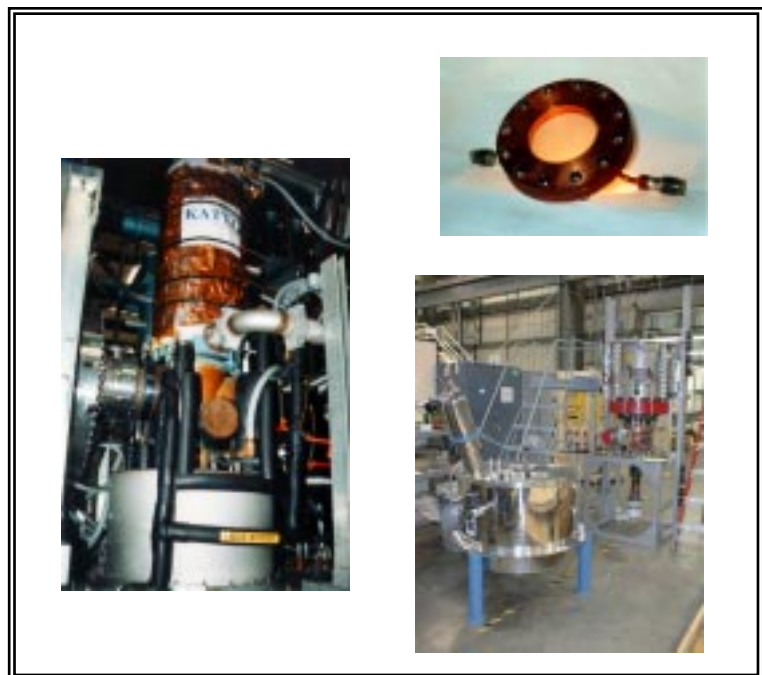
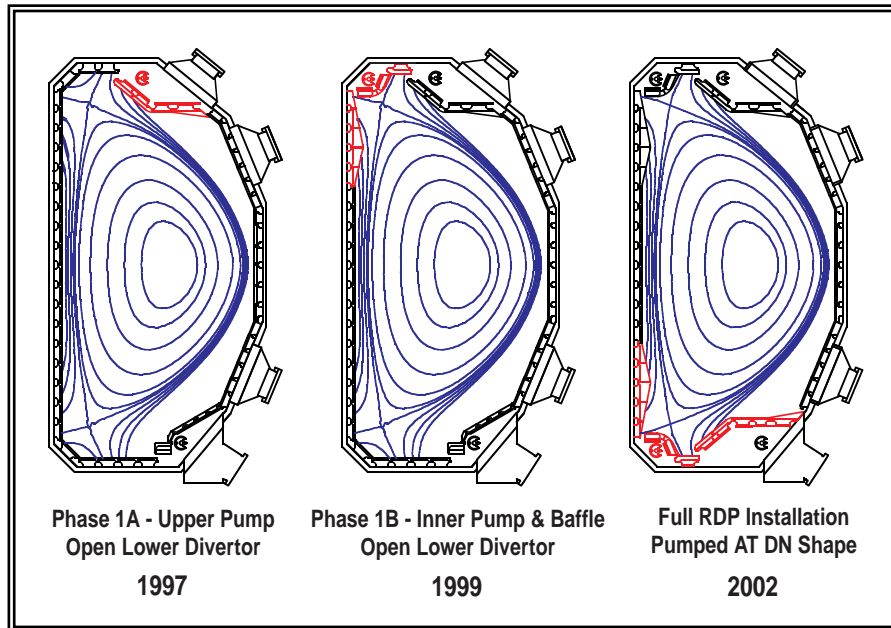


Fig. 1–5. Recent technical developments of 110 GHz gyrotrons and a high-power diamond window (upper right) motivate an accelerated ECH program. The importance of microwave heating and current drive to our advanced tokamak research program lies in off-axis current profile control, transport barrier control,  $T_e = T_i$ , probing transport, momentum versus heating, and two component plasmas.



continuing with the Baseline Upgrade Plan or to decide to implement one or more alternate upgrade contingency options (described in Section 2.5). These contingency options are not costed in this proposal but could be implemented by a DOE change order within the cost envelope of this proposal, in lieu of the proposed baseline upgrade and/or operations activity.

Fig. 1–6. We plan to implement a high triangularity pumped divertor in stages. These divertor modifications provide particle control of advanced tokamak shape plasmas.

### 1.2.1. ECH UPGRADE (WBS SUBTASK 2.1)

The scope of this subtask is the development of a high power microwave system for the DIII–D Research Program for electron heating and current drive (Section 2.5.1). The deposition of microwave

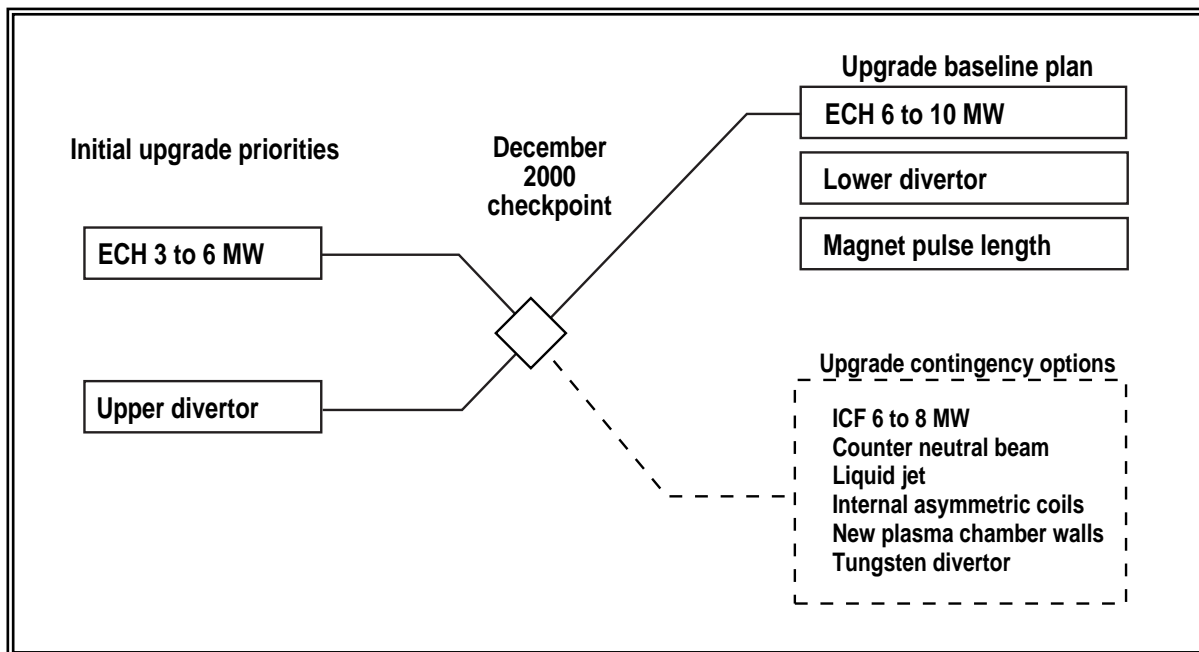


Fig. 1–7. The DIII–D upgrade plan includes contingency options to adapt to evolving scientific outcomes.

power is very localized because of the strong electron cyclotron absorption and can be accurately deposited either by antenna aiming of the narrow microwave beam or by varying the toroidal magnetic field (and thereby the resonant magnetic field location). Our objectives in implementing this exceptionally precise controlled research tool are to enable:

- Localized and transient energy transport studies.
- Control of the electron to ion temperature ratio for transport studies.
- Current drive off-axis for negative central shear advanced tokamak experiments.
- On-axis current drive for high  $\ell_i$  advanced tokamak experiments.
- Highly localized heating for studies of control of internal transport barriers.
- Studies of electron energy transport.

The 110 GHz ECH system consists of two 1 MW gyrotron systems which are operational, and a third system with a diamond window which is expected to be operational in late 1998. The 110 GHz ECH Upgrade is proposed to be implemented in two phases. In the first phase an increase in power from 3 to 6 MW with the addition of three 1 MW gyrotron systems. In the second phase, the power would be increased from 6 to 10 MW.

Our approach to the ECH upgrade will be to build on currently proven GA transmission line technology and to purchase gyrotrons from commercial suppliers. The ECH Upgrade will be implemented using 1 MW 110 GHz gyrotrons with diamond windows, power supplies, and transmission line systems similar to those now operating on DIII-D. Several manufacturers now build 110 GHz gyrotrons (CPI, Gycom, Thomson, and Toshiba) so they can be procured on a fixed cost basis. Power supplies will be modified 80 kV MFTF supplies as are now operating on DIII-D. The transmission system (mode converter, low loss waveguide, and launcher) would be a replica of the present system. The labor and costing for this upgrade are thus based on experience with the prototype systems now operating on DIII-D. Further details are given in Section 2.5.1.

### 1.2.2. DIVERTOR UPGRADE (WBS SUBTASK 2.2)

The scope of this subtask is the divertor upgrades needed to effect the eventual integration of core and boundary physics into integrated, steady-state scenarios (Section 2.5.2). The objectives of the divertor installation are:

- Provide density control (density reduction) to
  - increase current drive efficiency in advanced tokamak core plasmas (Reducing the plasma density increases the plasma electron temperature; which doubly increases the current drive efficiency by the ratio  $T_e/n_e$ )

- maintain the core plasma in the correct regime of collisionality for extrapolation to a reactor ( $n_e < 0.4 n_{GW}$ ) and below the ECH cutoff density ( $7 \times 10^{19} \text{ m}^{-3}$ ).
- Provide baffling to control (reduce) edge neutral effects on confinement and the L–H transition and encourage divertor recombination.
- Provide recycling structures to optimize fuel flow patterns in the divertor for impurity retention and enhanced divertor impurity radiation.
- Provide a divertor structure suitable for answering the design questions posed by future machines:
  - Single or double null?
  - Optimal triangularity?
  - Pumping the inner, outer, or private flux regions?
  - Optimal baffle geometry?

Our approach will be to continue implementing the eventual double-null divertor (Fig. 1–7) in stages. The first stage was the installation in 1996 of the upper, outer baffle and the cryopump behind it. This installation has enabled the pumping of high triangularity plasmas while maintaining the excellent diagnostic capability for divertor studies in the open lower divertor. The second step will be the completion in 1999 of the upper divertor with the private flux dome (and cryopump behind it), and some shaping of the inner wall tiles to obtain the capability to operate a highly baffled divertor for upper single null plasmas and to pump the inner leg of the divertor. Lower, open single null divertor research can continue. Depending on results in the interim from the plasma shape optimization studies and the divertor studies, the lower divertor would be similarly modified in 2001 to enable full double null capability. In the divertor upgrade, we plan to continue to use technology proven already in DIII–D, which is the operational cryopumps and the long proven and trouble-free inertially cooled graphite tiles and associated mounting arrangements.

Our goal is to eventually provide the operational and scientific basis for the choice of optimal divertor geometry and plasma shape in future tokamaks, taking account of the constraints of integrating divertor performance with advanced tokamak core plasma modes.

Costing for the divertor upgrade was based on actual costs of the previous modifications. The estimated FTEs for these WBS labor categories are:

### 1.2.3. MAGNET PULSE LENGTH UPGRADE (WBS SUBTASK 2.3)

Extending the pulse length of the DIII–D tokamak from 5 to 10 s for a 2 MA plasma at 2T magnetic field requires only minor modifications to the tokamak and additional auxiliary heating required for current profile control (Section 2.5.3). The changes needed are the interconnecting busswork between the

bundles of the toroidal field coil, upgrade of the poloidal field shaping coil regulators (choppers), and an upgrade of the cables on the patch panel and the cables connecting the motor generator to the dc power supplies. One dc power supply will be required for the poloidal field coils.

#### 1.2.4. UPGRADE CONTINGENCY OPTIONS

The DIII-D National Facility has the capability and flexibility to pursue a very broad range of fusion research and facility upgrades. Funding ultimately constrains the range of upgrades that can be implemented. Through discussion with the national collaborative team, we have identified the highest priority upgrades included in the baseline costing for the next five years (ECH, divertor, and magnet pulse length upgrades). However, new experimental or theoretical results, or programmatic priorities could dictate plan changes. Alternate contingency options have been discussed in the technical section (Section 2.5) and in Fig. 1-8.

These alternate upgrade options which are described further in Section 2.5 include:

1. Increase of ICRF power to 8 MW and/or the installation of mode conversion current drive combline antenna (Section 2.5.7).
2. Reorientation of one neutral beam line for counter injection (Section 2.5.8).
3. Construction and installation of a liquid jet for disruption mitigation studies (Section 2.5.9.1).
4. Internal MHD coils to control plasma rotation to provide feedback stabilization of resistive wall modes (Section 2.5.4).
5. Replacement of divertor walls with tungsten or replacement of main chamber tiles with B4C or Si doped graphite walls (Section 2.5.2.3).

## 2. TECHNICAL DISCUSSION: THE DIII-D FIVE-YEAR PROGRAM PLAN

### 2.1. THE DIII-D FIVE-YEAR PROGRAM PLAN

This document presents the DIII-D Program Plan for the period 1998–2003. The plan was developed by the national collaborative team that operates, plans, and carries out research using the DIII-D facility. This research program addresses the problem of establishing the scientific basis for the optimization of the tokamak approach to fusion energy production.

#### 2.1.1. THE DIII-D MISSION

Development of the scientific basis of the fusion energy source for future generations represents a grand challenge for science and offers the prospect of great benefits for mankind. The strategy for the recently restructured U.S. Fusion Energy Sciences Program focuses on innovation and scientific discovery, strengthens the program's ties to other fields of science, positions the U.S. to continue playing a meaningful role in the world fusion energy effort within available resources, and preserves the basis for an expanded U.S. Fusion Energy Program when national needs require.

Significant advances have occurred recently in tokamak research. Techniques for producing high temperature plasmas have become routine and reproducible, measurements of plasma internal magnetic and electric fields are now routinely available during experiments, and methods for controlling the plasma current and pressure profiles are being deployed. Transport barriers have reduced ion energy transport to neoclassical levels, plasma pressures have reached MHD theoretical limits, current drive by neoclassical bootstrap currents and rf current drive are at theoretical levels, and divertor operation with active particle pumping and radiative power dissipation has been demonstrated and modeled with numerical codes. The experimental advances have been observed in discharges for short periods and generally in isolation. However, using such advances to help build understanding of the underlying processes, tokamak research is developing a capability for truly theory-based discharge manipulation, which is fairly mature in some areas and less so in others.

Within this context, the DIII-D Program mission goal is:

***To establish the scientific basis for the optimization of the tokamak approach to fusion energy production.***

“Optimization” means experimentally demonstrating performance parameters at the theoretically predicted limits for the tokamak confinement system and achieving to the greatest degree possible an integrated, steady-state demonstration of optimized performance that projects to an attractive fusion power system. “Scientific” means developing a solid understanding of the underlying physical principles and incorporating it into useful predictive modeling tools. The integrated optimization sought, and the scientific basis established, will allow the definition of optimal paths to fusion energy using the tokamak approach.

The DIII-D Program mission seeks to develop and exploit fusion science to the betterment of the fusion energy goal: demonstrated, scalable plasma performance that is backed up by a firm, comprehensive theoretical model and achieved in a total configuration that is attractive as an eventual power plant concept. In DIII-D we quantify this goal as sustaining for 10 s a plasma with 5% beta (the ratio of plasma to magnetic field pressure).

The AT has been the basic organizing thrust of the DIII-D Research Program for several years. The AT is now recognized, partially because of early DIII-D successes in this area, as potentially making possible a variety of attractive near-term development steps for magnetic fusion energy. In implementing the new DIII-D Research Plan, we will continue along this path and pursue AT science and integrated performance optimization as the most promising direction for determining the tokamak’s highest potential. Advancing and benchmarking modeling tools will go hand-in-hand with these investigations.

The DIII-D National Program will support the six near-term (five-year) objectives established by the U.S. fusion community. Primary contributions will be made to two of these objectives:

- Marked progress in scientific understanding and optimization of toroidal plasmas.
- Improved integrated modeling based on theory and experiments.

as well as secondary, but significant, contributions to the other four objectives:

- Participation in international collaboration to study burning plasma physics and related fusion technologies.
- Strengthened general science and education and connection to other scientific communities.
- Evaluation of several nontokamak fusion approaches.
- Marked progress in understanding technologies and materials for fusion power.

In the newly restructured U.S. Fusion Energy Science Program, DIII-D is called “to move toward full, maximally productive utilization, including some upgrades, as a user facility to pursue the rich science to be gained.” The role of DIII-D is to advance fusion science, to lead the development of tokamak improvements, to link to our international partners, and to provide critical physics R&D for ITER. The plasma physics issues being addressed in DIII-D are aimed at maturing the tokamak knowledge base for future applications, whether tokamaks or alternate concepts. The plasma science also has applications to a

wider and broader scientific understanding of natural plasma phenomena, application to other branches of science, and industrial application.

### 2.1.2. THE DIII-D PROGRAM

The DIII-D Program is an AT Program using and advancing fusion energy science to provide the basis for future fusion initiatives. DIII-D (Fig. 2.1-1) consists of a national facility with its operating staff and a national collaborative research team that utilizes the facility to carry out research to support the goals of the U.S. Fusion Energy Sciences Program. DIII-D is the world’s most flexible tokamak and the largest magnetic fusion device in the U.S. Program. Its ability to control a variety of complex plasma shapes and its diagnostic instrument set are the best in the world. It has a reliable 20 MW neutral beam heating system; radio-frequency heating and current drive systems and pumped divertor systems are being developed and are the principal system upgrades in this plan. Its digital plasma control system will control the heating and other systems to achieve the interior plasma profiles essential to the tokamak optimization mission. The DIII-D open data system architecture has facilitated the development of the large collaborative national team.

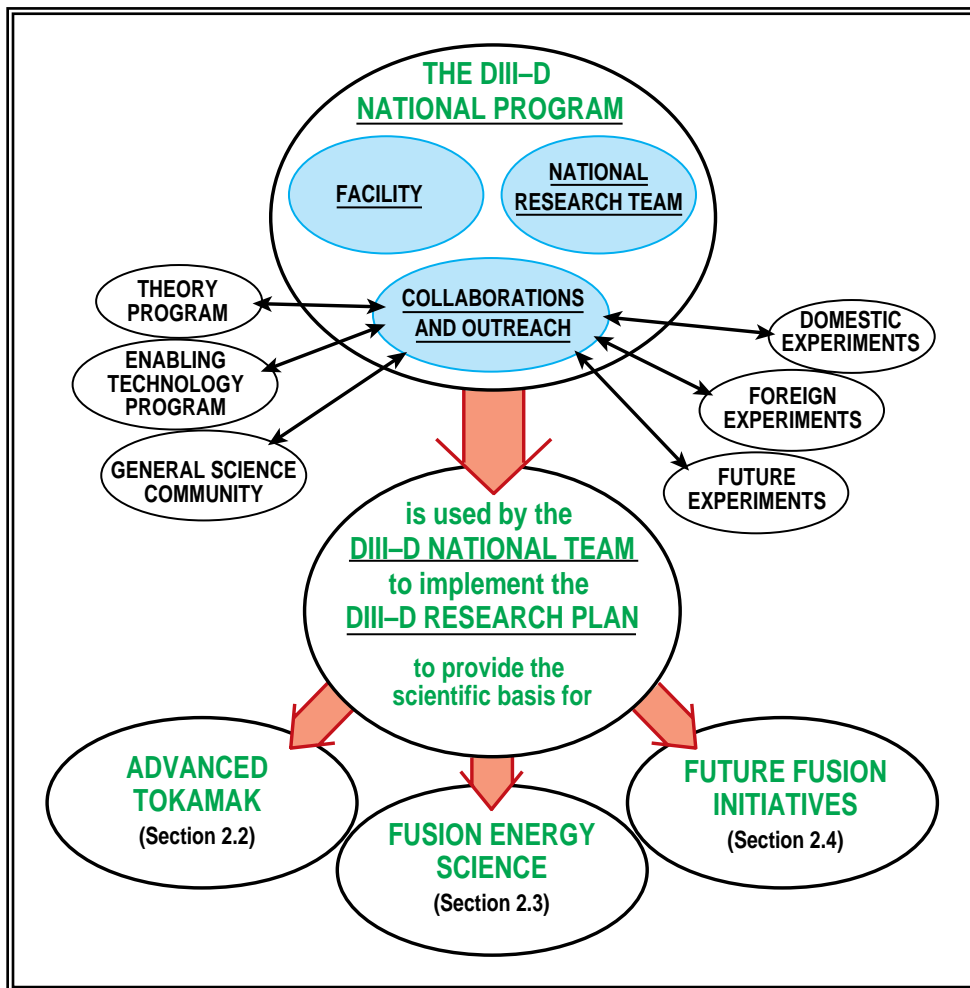


Fig. 2.1-1. DIII-D Program linkages provide intellectual inputs, research inputs, and staff opportuni-

GA operates the DIII-D Program for the U.S. DOE. About 50 institutions participate in the DIII-D Research Program which is managed by an effective system of governance. The primary governance body is the DIII-D Executive Committee, which advises the DIII-D Program Director on matters of program planning, direction, task priorities, and budgets. The committee is comprised of program leaders from GA and the major collaborating institutions. A DIII-D Program Advisory Committee, consisting of technical experts from other national and international fusion programs, provides advice semi-annually to the DIII-D Executive Committee on plans and other major programmatic issues. A multi-institutional Research Planning Committee develops and peer reviews the annual Experiment Plan and reviews, approves, and schedules experiments. Such plans, as was the case with this Long Range Plan, arise from meetings open to the entire National Team and then study and working groups commissioned by the Executive Committee develop the ideas into programmatic research thrusts.

The DIII-D team consists of about 120 technical operations staff and 100 research scientists drawn from 9 U.S. national laboratories, 19 foreign laboratories, 16 universities, and 5 industrial partnerships. The team ranges from undergraduates to those with three decades of experience in fusion research. This staff has been recognized for its outstanding research: 5 winners of the Excellence in Plasma Physics Award and 30 Fellows of the APS.

The DIII-D Program has strong linkages to foreign and domestic experiments, the U.S. Theory Program, enabling technology development programs, the general science community, and the designers of future fusion initiatives (Fig. 2.1–1). These links to universities and laboratories provide broad intellectual input to the DIII-D Program, provide opportunities for DIII-D staff to enrich their professional experience, and provide paths for input of research results from other groups into the DIII-D Program.

**2.1.2.1. RESEARCH GOALS.** In support of its overall mission, the specific goals of the DIII-D AT Research Plan in the period 1999–2003 are:

- To attain the theoretically predicted minimum in the **cross-field transport** of heat and energy.
- To extend the operation of DIII-D to the theoretically predicted limits to **plasma stability** for a tokamak at the DIII-D aspect ratio.
- To seek a plasma that exhibits **full recombination** in the divertor before it reaches a material surface, thus achieving the simple description of magnetic confinement as using magnetic fields to prevent hot plasma from touching a material surface.
- To develop methods of **plasma current generation** (initiation, ramp-up, sustainment, and profile control) to provide future devices the basis for full steady-state transformerless operation.
- To integrate the above objectives in single steady-state operational scenarios to demonstrate the possibility of **simultaneous optimization** of the tokamak in the above four major areas of fusion science.

This set of research goals defines the ultimate expression of what is called the AT. We see the Research Plan (Fig. 2.1–2) as two main lines, core plasma and boundary plasma physics, which both work toward an eventual integration demonstrated by sustaining a 5% beta plasma for 10 s.

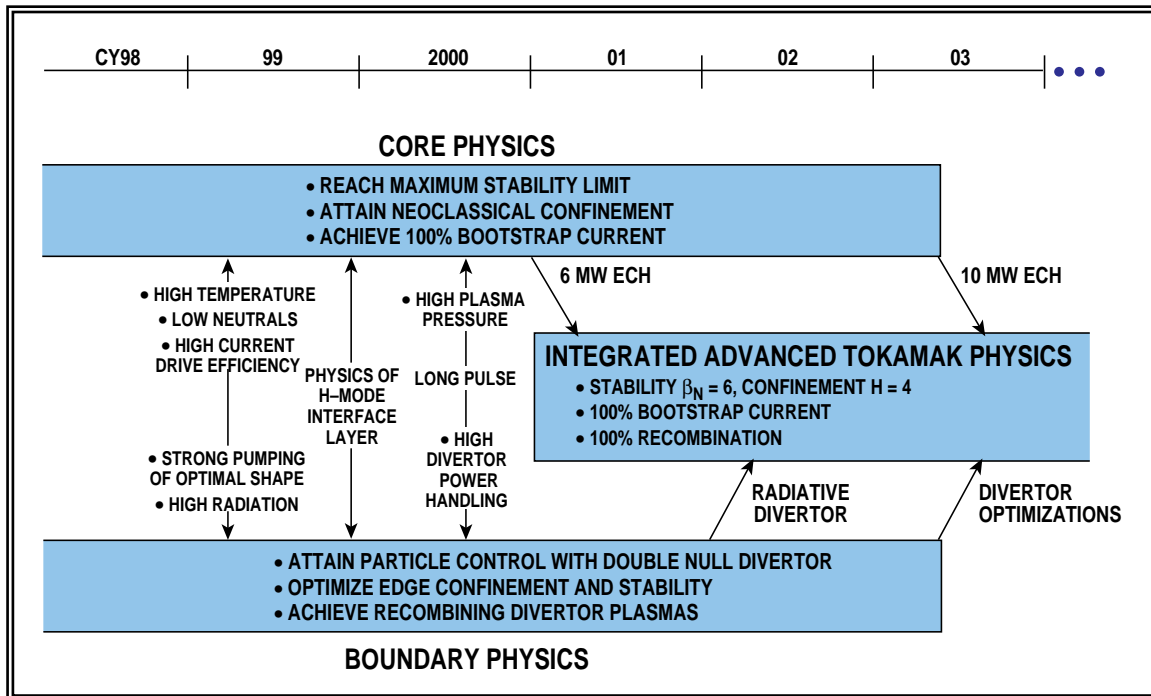


Fig. 2.1–2. The DIII-D research plan culminates in integrated, Advanced Tokamak operating scenarios.

In Table 2.1-1, we show in each of the typical science areas the programmatic objectives, the toughest challenges we anticipate, and some quantitative targets. The H-factor is the confinement quality normed to ITER–89P scaling.  $\beta_N \equiv \beta_T(\%)/I_p/aB_T$ . Enrichment is the ratio of impurity concentration in the divertor to the core plasma. The quantity  $f_{bs}$  is the bootstrap fraction.

**2.1.2.2. FACILITY UPGRADES AND IMPROVEMENTS.** The principal opportunity for carrying out the AT Program begins in 2002 when DIII-D is equipped with the two principal tools it needs for this integrated research (see Fig. 2.1–2):

- Precise off-axis current drive and heating from electron cyclotron microwave power sources to sustain and control the optimal current profile. The electron cyclotron heating (ECH) power will be increased from 2 to 6 MW in late 2000 and to 10 MW in early 2003 with 10 s pulse gyrotrons.
- A double-null divertor which can strongly pump the optimal high-triangularity plasma shape to maintain the core plasma in the required high temperature regime of low-collisionality while producing detached divertor plasmas through advanced divertor physics effects. Such a divertor will be operational in 2001.

**TABLE 2.1–1**  
**ADVANCED TOKAMAK PROGRAM — OBJECTIVES, CHALLENGES, AND TARGETS**

Area	Programmatic Objectives	Toughest Challenges	Quantitative Targets
Confinement	Neoclassical confinement through transport barrier control	Sufficient understanding of underlying turbulence; extension to long pulse	$H \rightarrow 4$ (>5 s)
Stability	Long-pulse, high $\beta_N$ , AT operation	Profile control; neoclassical islands; wall stabilization	$\beta_N \rightarrow 6$ (>5 s)
Divertor	Fully recombining divertor plasma	Compatibility with low-collisionality AT plasmas	Recombination $\rightarrow 100\%$ Enrichment $\rightarrow 8$ Peak heat flux reduction $\rightarrow 5$
Steady state	Fully transformerless operation	Profile control; extension to long pulse; startup	$f_{bs} \rightarrow 100\%$

Our near term plans are to: implement improvements to the data analysis and database systems to support greater access to the data and efficiency of data analysis by the national research team; improve diagnostics such as installing a Central Thomson Scattering System, a package of diagnostics aimed at studying electron transport, a real time radial electric field measurement, and a package of upgrades and modifications connected with the new divertor; improvements to the rf transmitter power, reliability, and antenna systems; and improvements to the plasma control system to drive the divertor and current drive control tools for real time control of plasma profiles.

Longer term upgrades and enhancements, being considered for the period 1999–2003 based on research results are as follows:

- Additional diagnostics improvements could include packages for 3D reconstruction of equilibria, magnetic turbulence, temperature fluctuations, advanced current profile measurements, and laser pumped beam emission spectroscopy.
- Nonaxisymmetric coils are being designed to enhance wall stabilization by rotating the plasma or by feedback controlling low order modes and/or ergodizing the plasma edge.
- Tokamak systems to enable the study of long pulse physics at full parameters. In our baseline plan, the pulse length will be extended to 10 s by 2003.
- RF antenna modifications are expected to enable transport barrier control and mode conversion current drive.

- Possible divertor optimizations and first wall modification options include a longer divertor slot, a geometry modification toward increased convective parallel heat transport, or a geometry that optimizes helicity injection.
- One of the four DIII-D neutral beamlines may be re-oriented to inject in the counter-direction to control the radial electric field through toroidal rotation and to facilitate precise real-time measurement of the radial electric field.

The upgrades and improvements proposed for the DIII-D facility are described in Section 2.5.

**2.1.2.3. FACILITY OPERATION.** The DIII-D Plan calls for 18 single-shift operation weeks in the annual research operation of the DIII-D facility for the period 1999–2003 (Fig. 2.1–3). An unsolicited option is proposed to extend the operation to 18 shift-and-a-half weeks. Such a schedule allows sufficient off time for the operating staff to perform the necessary maintenance and the scientific staff to carefully prepare experiments, benefiting from analysis of previous weeks. The maturity of the diagnostic systems enables complete data sets to be obtained in one discharge resulting in completing one experiment on an average of a day and a half. The planned increased operation will enable DIII-D to include longer campaigns that require several days, to support exploratory studies and efforts into new regimes, and to provide additional opportunities for collaborators.

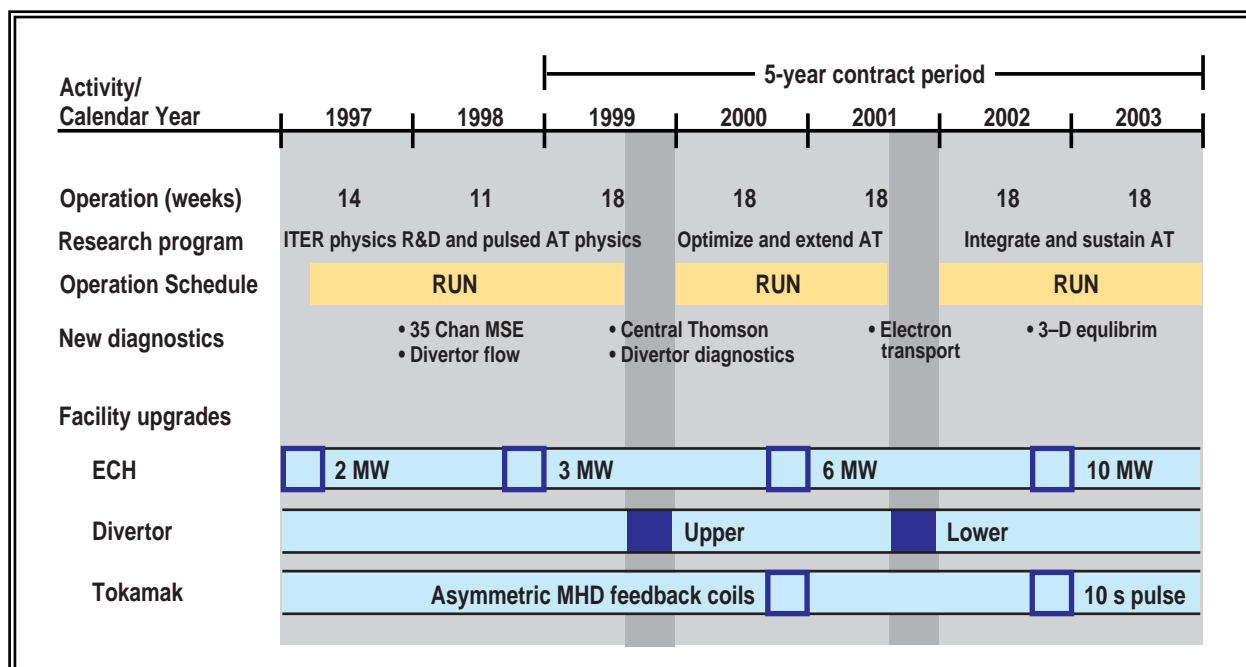


Fig. 2.1–3. DIII-D Program schedule. The reference plan is to operate 18 weeks per year with an option for an additional 9 weeks (27 week total).

The DIII-D Plan outlined here is expected to take five years to complete, depending on resources available and rates of research progress. Almost certainly, some of the longer term activities described above will extend beyond 2003. Around 2001, we will evaluate the possibilities for the period after 2003.

### 2.1.3. NATIONAL LEADERSHIP

A key element of this DIII-D Program Plan is to provide national program leadership in the area of the DIII-D mission; optimization of the tokamak approach to fusion energy. This extends the responsibility of the DIII-D National Team in six directions (indicated in Fig. 2.1-1) beyond the conduct of the DIII-D Research Program using the DIII-D facility:

- The DIII-D Program will identify the critical theoretical effort needed for the mission, and will seek to obtain that effort from the broader Theory Program.
- The DIII-D Program will identify enabling technologies that need to be developed to advance its mission.
- The DIII-D Program will continue its active program of collaboration and coordination with national and foreign experiments to assist their progress with DIII-D results and to benefit from their input into the DIII-D research directions.
- The DIII-D Program will be pro-active in identifying experimental research from other programs, especially smaller university experiments which can support the DIII-D mission, and will form linkages to assist those experiments to succeed and to obtain timely input of their results into the DIII-D Program.
- The DIII-D Program will continue and strengthen its coupling to the design teams for future devices to assure timely and accurate input of the important research results from DIII-D into the planning for future facilities.
- The DIII-D Team will promote interaction with the broader U.S. scientific community, making available when appropriate the well-diagnosed DIII-D high temperature plasma facility for nonfusion plasma physics research and communicate the excitement and progress of fusion energy science to a broad community.

### 2.1.4. BENEFITS OF DIII-D RESEARCH

In line with the three “legs” of the restructured Fusion Energy Sciences Program, three constituencies will benefit greatly from the results of the DIII-D Research Program.

**Fusion Energy Science.** The DIII-D Program will advance fusion energy science in the topical areas of plasma confinement, plasma stability, power and particle exhaust, current generation, and plasma control. The intent of the Program is to incorporate what is learned into theory based, predictive modeling packages. Such packages are well advanced in the areas of plasma stability and current generation, less advanced for confinement and power and particle exhaust. Ultimately, these topical packages will be integrated into a

comprehensive predictive model for the tokamak as part of a national effort. The physical principles to be studied are of general value to the science of magnetic confinement of plasmas, especially but not exclusively in toroidal systems. These activities are described extensively in Section 2.3 of this document.

**The Advanced Tokamak (Innovation).** DIII-D will integrate the topical science elements into discharge scenarios which support the feasibility of steady-state AT operation and which simulate fusion power systems by appropriate scale-size extrapolation. The notion of AT incorporates many of the improvements in tokamak performance which have been demonstrated in short pulse experiments over the last few years into a composite picture of an attractive fusion power system. The principal challenge for the DIII-D Program is to demonstrate these characteristics under integrated and near steady-state conditions. As the most successful means to date of confining fusion plasma, the tokamak warrants a thorough exploration of its highest potential as a fusion power candidate. The development and implementation of AT operation is discussed in Section 2.2.

The DIII-D Program has played and will continue to play the lead role internationally in the AT thrust. The flexibility of the DIII-D device allows early testing of new approaches that can, if successful, later be implemented on the larger tokamaks in Europe (JET) and Japan (JT-60U). DIII-D scientists have participated in such experiments on foreign machines, transferring techniques developed on DIII-D. Working with foreign tokamaks of various sizes, DIII-D has played a key role in developing the dimensionless parameter approach to the scale size dependence of confinement. The path of developing AT approaches on DIII-D, and confirming those approaches on the larger foreign tokamaks, will provide the scientific basis for use of AT operating modes on future international Fusion Development Steps.

**Next Steps in Fusion Development.** The science base built by DIII-D and the integrated demonstration of AT operating modes will provide a broad basis on which to define optimal national or international next steps toward magnetic confinement fusion energy using the tokamak approach. Able to simulate ITER discharges at one-fifth scale, DIII-D today plays a prominent role in ITER physics R&D. The AT thrust points directly at optimized superconducting tokamak fusion devices and compact ignition experiments. The AT physics elements also lead in new directions; for example when expressed in a low aspect ratio device, these become the basis of the spherical torus approach to the volume neutron source or a pilot plant. The projection of DIII-D results to future devices is developed in Section 2.4.

**DIII-D Research Provides Pathways to the Future.** DIII-D's high temperature plasmas have dimensionless parameters close to those of a fusion power facility, except for size as measured by normalized gyroradius  $\rho_*$ . DIII-D's integrated AT operation and radiative divertor provide a high-performance configuration capable of steady-state enhanced plasma performance with good particle and heat exhaust. This combination opens up a variety of future steps for fusion energy development:

- For the ITER design, DIII-D results extend to ITER along a dimensionless parameter scaling path varying only  $\rho_*$ . Key elements are confinement at least as favorable as Bohm scaling and radiative divertor physics compatible with a collisionless core.

- For a moderate-aspect-ratio tokamak reactor, DIII-D results provide a basis for a minimum-sized superconducting design like Advanced Reactor Innovations and Evaluation Study — Reverse Shear (ARIES–RS). Key elements to this demonstration are confinement at least as favorable as Bohm scaling, wall stabilization for high normalized beta, transformerless operation, and a radiative divertor compatible with the ARIES–RS collisionless core.
- For a moderate-aspect-ratio ignition experiment, DIII-D points to a small-sized, high-field device if confinement scaling is at least as favorable as gyroBohm.
- For either an ignition experiment or reactor with low aspect ratio, DIII-D forms the basis for projection along  $\beta$ -scaling paths and can address a number of key issues, e.g., wall stabilization for high beta, transformerless operation, and radiating-mantle power exhaust.

### 2.1.5. THE DIII-D NATIONAL TEAM

DIII-D is a national fusion science facility. The DIII-D Program is conducted as a national program with approximately 50 participating institutions. Among these collaborators, seven institutions have broad based multitopic research programs or have broad programmatic responsibilities and management roles. These seven institutions (indicated by asterisks in Table 2.1–2) work together to formulate strategic program directions and form the membership of the DIII-D Executive Committee. Planning, execution, and peer review of the scientific research experiments is carried out by a multi-institutional Research Planning Committee. An international DIII-D Advisory Committee provides overall peer review. Further information on program participants, governance, and linkages to national and international Fusion Energy Science Programs is given in Section 2.6.

**TABLE 2.1-2**  
**DIII-D PROGRAM COLLABORATORS**

<b>National Laboratories</b>	<b>Universities</b>	<b>International Laboratories</b>
ANL	Cal Tech	ASIPP (China)
INEL	Columbia U.	Cadarache (France)
LANL	Hampton U.	CCFM (Canada)
LLNL*	Johns Hopkins U.	Culham (England)
ORNL*	Lehigh	FOM (Netherlands)
PNL	MIT	Frascati (Italy)
PPPL*	Moscow State U.	Ioffe (Russia)
SNL*	RPI	IPP (Germany)
	U. Maryland	JAERI (Japan)
	U. Texas	JET (EC)
<u>Industry Collabs</u>	U. Washington	KAIST (Korea)
CompX	U. Wisconsin	Keldysh Inst. (Russia)
CPI (Varian)	UCB	KFA (Germany)
GA*	UCI	Kurchatov (Russia)
Gycom	UCLA*	Lausanne (Switzerland)
Orincon	UCSD*	NIFS (Japan)
		Troitsk (Russia)
		SWIP (China)
		Tsukuba U. (Japan)

\*DIII-D Executive Committee Membership.

## 2.2. THE DIII-D ADVANCED TOKAMAK (AT) PROGRAM

The DIII-D Program for the years FY98–FY03 will be directed toward a synthesis of the critical elements needed to address its mission in order to further the objectives of the U.S. Fusion Energy Sciences Program. The science components of our research: confinement and transport, stability, boundary physics, and the science of plasma heating and current drive are all directed toward the overall mission of optimizing the tokamak for eventual fusion power production.

In this section, we present the details of the DIII-D Five-Year Research Plan as it has been developed from the DIII-D Mission Statement. We describe schedules for the research activities, for principal improvements in facility capabilities, and for upgrades and enhancements to DIII-D. Following the plan and schedule, we define AT and indicate why this idea is at the core of the program (Section 2.2.2). We then expand on the elements of the program from two points of view: the scientific topical areas and the integrated development issues formulated in terms of aspects of plasma control (Section 2.2.3). Finally, we illustrate some possible operating scenarios for DIII-D (Section 2.2.3.4).

### 2.2.1. THE PLAN

**2.2.1.1. DEVELOPING THE RESEARCH PLAN — APPROACHES TO PROBLEMS.** The selection and prioritization of research tasks is based on three considerations.

- **The long-standing DIII-D objective of developing and implementing AT operation.** This requires optimization of tokamak AT performance through active intervention and control of plasma characteristics and behavior. Successful AT operation can significantly reduce the size and cost of future fusion initiatives, pilot plants, and fusion power plants. Because plasma control is an integral part of AT development, the theme of control runs throughout this plan. We emphasize particularly the need to develop steady-state operation of the tokamak. Although this is part of the AT goal, it is important to make the steady-state objective explicit because it does enter into making choices between avenues of research.
- **Identification of target scenarios which are extrapolatable to interesting fusion power (or prototype) systems.** In this connection, we emphasize the use of nondimensional scaling, which lends confidence that DIII-D experiments are exploring the same physical processes that will occur in the larger systems.
- **Support of efforts to develop a burning plasma experiment (ITER).** The flexibility of DIII-D enables it to address many issues relevant to ITER and to other, less well developed, toroidal magnetic fusion concepts.

The plan presented here represents a considered assessment of the scientific studies needed to address each of these issues. In addition, we have incorporated a significant measure of realism in folding into the plan the sequencing of new hardware tools required for this research, taking into consideration the need to

plan major acquisitions well in advance, to avoid conflicts between experiments, and to maintain a smoothly varying budget profile.

**2.2.1.2. DIII-D RESEARCH OBJECTIVES.** The DIII-D Five-Year Research Plan develops from five primary fusion energy science objectives associated with the AT goal. These are:

- To attain the theoretically predicted minimum in the cross-field transport of heat and energy.
- To extend the operation of DIII-D to the theoretically predicted limits to plasma stability for a tokamak at the DIII-D aspect ratio.
- To seek a plasma that exhibits full recombination in the divertor before it reaches a material surface, thus achieving the simple description of magnetic confinement as using magnetic fields to prevent hot plasma from touching a material surface.
- To develop methods of plasma current generation (initiation, sustainment, and profile control) to provide future devices the basis for full transformer-less steady-state operation.
- To integrate the above objectives in steady-state operational scenarios.

The specific research efforts needed to approach these goals are summarized in Section 2.2.3.1, and described much more fully in Section 2.3.

**2.2.1.3. RESEARCH SCHEDULE.** An outline of the research schedule was given in Fig. 2.1–3. Although there will be a continuous process of adding to DIII-D capabilities, we envision two major installation vents during the five-year plan period. These vents divide the five-year time frame into three major experimental periods. During the fall of 1999, we expect to complete the private flux baffle and pump of the RDP in the upper portion of the DIII-D vessel and install a set of external nonaxisymmetric coils. During the fall of 2001, we expect to complete the RDP with installation of the lower divertor. By adding gyrotrons, the ECH power will reach 6 MW in the fall of 2000 and 10 MW by 2003. These installations naturally separate the experimental program into three parts:

- The first period will continue the present research program into 1999. We expect to obtain deeper understanding of transport, results on the improvement of  $\beta_N$  limits using wall stabilization, on the mechanisms which lead to edge instabilities that limit high confinement regimes and reduce the maximum beta, exploitation of microwave heating and current drive, on understanding the physics of parallel heat transport in the SOL and divertor, and on plasma shape optimization.
- From 1999–2001 will be an intensive experimental period devoted to exploring the open versus closed divertor and to developing profile control and fueling techniques for sustained, quasi-stationary operation. Further experiments to implement theoretically predicted optimized profiles will be undertaken.
- The third intensive experimental period, from the end of 2001 through 2003, will be devoted to using the systems installed in 2001 to develop integrated, steady-state (10 s), optimized scenarios. There will be a particularly intensive effort to control the current profile and the pressure profile using rf systems, modified beams, and fueling using the full double-null RDP.

**2.2.1.4. RESEARCH THRUSTS.** Another way to look at the DIII-D AT Program is in terms of the principal lines of research activity, the sum total of which will culminate in integrated, long pulse AT operating scenarios. We see these principal research thrusts as:

1. Controlling interior plasma profiles for higher  $\beta_N$  and H.
2. Controlling the plasma edge for sustained AT performance and better confinement.
3. Developing the basis of steady-state operation.
4. Developing advanced divertor operating modes.

In Fig. 2.2–1, we present these four principal AT research activities, their sub-issues (green dots), and the approximate time scale of the main activities (yellow) aimed at these issues.

Looking at the program this way begins to make explicit the integrations of elements from the four science areas (confinement, stability, boundary, current drive) that are needed to achieve an AT progress element. For example, consider the elements “control edge stability” and “sustain AT mode for 5–10 s.” The principal problem in extending AT modes to long pulse appears to be instabilities that originate in the plasma edge. The causes of these instabilities must be better identified in the period 1997–1999 (see Stability Science, Section 2.3.2). It is felt that the likely solution is to lower the edge pressure gradient and therefore bootstrap current through either marginally diverted radiative divertor mode (RI-mode) plasmas or ultimately an ergodic boundary (2000–2001, Section 2.3.3 Boundary Science). Presuming success in stabilizing the edge, to sustain AT modes for 5–10 s requires in addition an understanding of rf current drive efficiency (1998–99) and the application of localized ECCD to stabilize neoclassical MHD (1999–2000) (see Section 2.3.4 Physics of Current Drive and Heating). The primary scenario for long pulse, the NCS will be developed starting in earnest in 2000 (see Sections 2.3.2 and 2.3.4). Ultimately the NBI power will be brought in (2001–2003) and the full RDP will be needed to handle the power and particle throughput for 10 s.

The AT activities in Fig. 2.2–1 are explained in more detail in Section 2.2.3 and in much more detail in Section 2.3 on Fusion Energy Science. To provide here a maximally compact overall summary of the AT activities, we have constructed Table 2.2–1. The table is laid out as follows:

- Major Activity Heading
  - Sub-topical area



Most of the tools and new hardware proposed in this plan are shown in Table 2.2–1 as derived from the key research efforts that need to be made. Detailed descriptions of these upgrades and enhancements to DIII-D are given in Section 2.5.

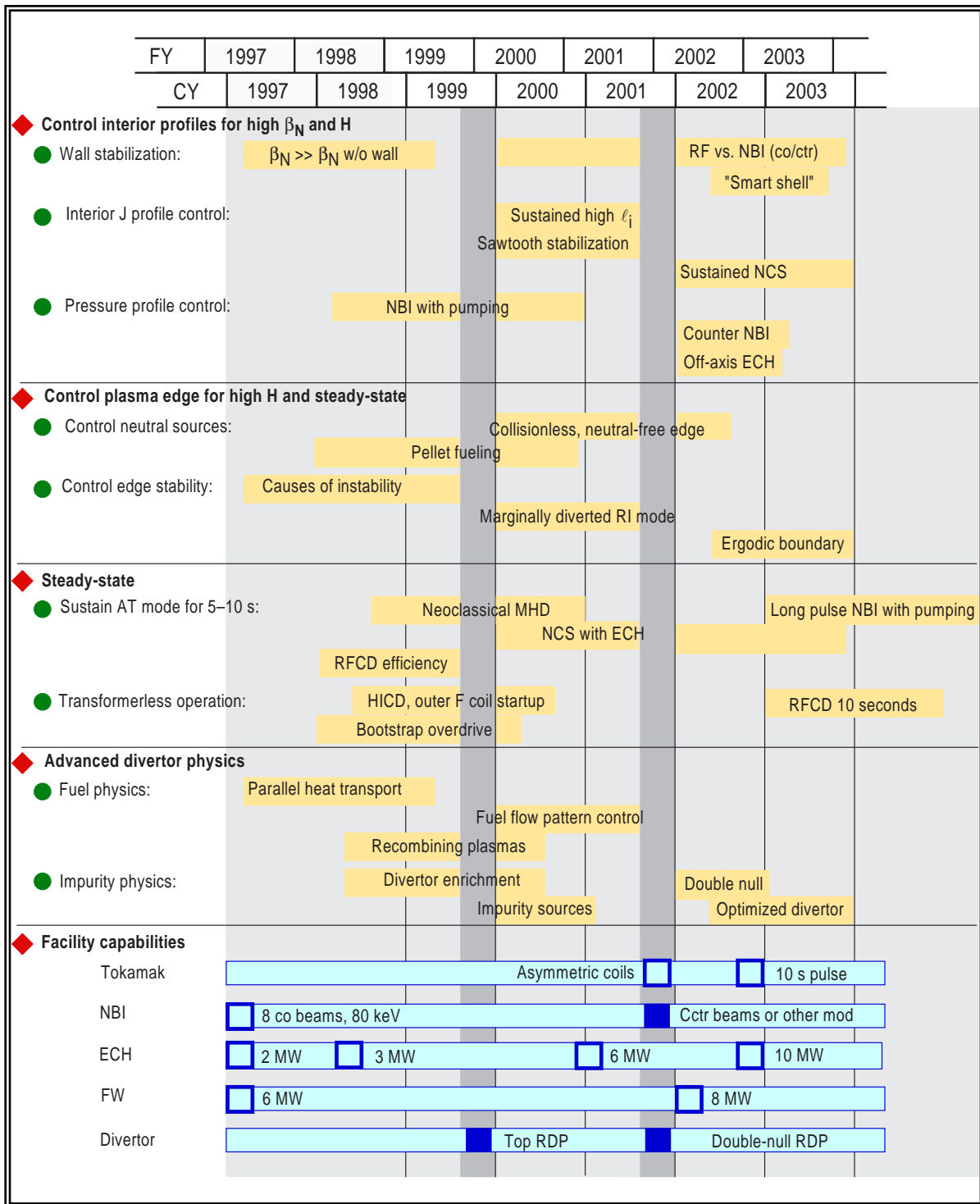


Fig. 2.2–1. The 1999–2003 research plan advances facility capability in step with advancing confinement, stability, boundary and current drive science.

**TABLE 2.2-1**  
**PROGRAM LOGIC DEFINES TOOLS AND APPROACHES**

<p><b>• Control Interior Profiles for Higher <math>\beta_N</math> and H</b></p>	
<p>— Wall Stabilization</p> <ul style="list-style-type: none"> <li>+ Show wall stabilization works if the plasma rotates.</li> <li>+ Study by trading off co/counter NBI and rf</li> <li>+ Make the plasma stay rotating (esp. edge)</li> <li>+ Make the wall appear "superconducting"</li> </ul>	<p>⇒ Smart Shell Counter beamline</p>
<p>— Interior J Profile Control</p> <ul style="list-style-type: none"> <li>+ Make hollow q profiles with <math>q_0 &gt; 2</math> and <math>q_{\min}</math> at large radius.</li> <li>+ Make high <math>I_i</math> profiles with <math>q_0 &lt; 1</math>.</li> <li>+ Sawtooth stabilization with ICRH.</li> </ul>	<p>⇒ Control density to control NBCD profile and increase RFCD efficiency ECCD (&gt;6MW) for off axis current drive Comblines for MCCD off-axis FWCD for on axis current drive Control location of bootstrap peak (see below)</p>
<p>— Control Pressure Profiles</p> <ul style="list-style-type: none"> <li>+ Control radial location of the pressure gradient and bootstrap peak by controlling the transport barrier location, by controlling the ExB profile.</li> <li>+ Control the plasma shape, magnetic well, and Shafranov shift.</li> </ul>	<p>⇒ Pump to control the density to control NBI deposition profile Counter beamline and/or low voltage beams. Off-axis NBI and ECH Plasma shape control</p>
<p><b>• Control the Plasma Edge for Sustained AT Performance and Better Confinement</b></p>	
<p>— Control Neutral Sources</p> <ul style="list-style-type: none"> <li>+ Understand impact of neutrals in confinement</li> <li>+ Create a more collisionless, neutral free edge.</li> </ul>	<p>⇒ Pump for lower density Baffled divertor for lower core gas fueling Pellet fueling instead of gas Lithium wall conditioning Radiative mantle</p>
<p>— Solve the Edge Stability Problem</p> <ul style="list-style-type: none"> <li>+ Understand stability properties of the edge.</li> <li>+ Lower the edge pressure gradient (bootstrap current).</li> </ul>	<p>⇒ Understand L-H and H-L to find a way to retain L-mode edge Radiative mantle Marginally diverted plasmas Ergodize the edge</p>
<p><b>• Develop Steady-State Operation</b></p>	
<p>— Sustain AT modes</p> <ul style="list-style-type: none"> <li>+ Sustain an AT mode for a current profile relaxation time.</li> <li>+ Suppress Neo-Classical MHD</li> </ul>	<p>⇒ Upgrade the tokamak for 10 s at 2 T Long pulse rf for J(r) control Pump to regulate density for enhanced RFCD and to regulate NBI deposition Radiate in divertor to lower heat flux a factor of 2-3 to enable 10 second operation</p>
<p>— Develop the basis of transformerless operation.</p> <ul style="list-style-type: none"> <li>+ Develop methods of transformerless current initiation.</li> <li>+ Develop a method of noninductive current ramp-up.</li> <li>+ Develop sustaining current drive.</li> </ul>	<p>⇒ HICD                      Outer PF coils only Bootstrap overdrive    Early NBI 10 s upgrade            ECCD, FWCD assist Develop science        ECCD, FWCD, MCCD of current drive</p>
<p><b>• Develop Advanced Divertor Operating Modes</b></p>	
<p>— Fuel Physics</p> <ul style="list-style-type: none"> <li>+ Understand the mechanism of parallel heat transport</li> <li>+ Understand how to achieve recombining plasmas</li> </ul>	<p>⇒ Use RDP structures to alter flow patterns Encourage/increase convective heat flow</p>
<p>— Impurity Physics</p> <ul style="list-style-type: none"> <li>+ Understand impurity transport and sources</li> <li>+ Develop ways to increase divertor radiation</li> <li>+ Maintain a clean core plasma.</li> </ul>	<p>⇒ RDP to produce divertor enrichment Dome to lower chemical sputtering C source Impurity entrainment Baffled divertor</p>

## 2.2.2. WHAT IS AN ADVANCED TOKAMAK?

The fundamental distinction between the concept of the “Advanced Tokamak,” and the “ordinary” tokamak is the use of active external intervention and control in all of these areas to improve tokamak performance.

It is possible to describe a tokamak power plant without AT features. Such a machine would have a low beta plasma and produce neutron and thermal surface power fluxes low enough to satisfy conservative neutron damage and surface heat loading criteria. Its plasma core would be large. We know of no development path toward this conservative power system that does not soon require large ignition devices, DEMOs, pilot plants, etc. This is the present conundrum of the U.S. and world fusion programs.

Application of the features associated with ATs can address these difficulties. A simultaneous improvement in stability (to give higher beta and lower magnetic field and plasma current), in transport (to ignite the plasma with less external power), in boundary control and heat removal (to ease the demands on the material walls and divertor), and in the efficiency and control of current drive and heating (to increase the energy gain of the reactor) can provide both a more affordable development path for fusion power and an ultimate reactor which produces power at lower unit cost.

Although a portion of the proposed DIII-D Program is to conduct individual investigations in each of these areas, in order to gain a better understanding of the underlying science, we also continue to maintain our focus on using this understanding to demonstrate that integrated active control for optimization in all aspects leads to a better product for the fusion program.

## 2.2.3. THE SCIENCE, THE TOOLS, AND THE INTEGRATION

There are three different motivating objectives of the proposed DIII-D Program. These are:

- The advancement of the plasma and fusion science underlying the behavior of tokamak plasmas.
- The development of techniques, methods, and tools for maintaining the plasma in a condition giving higher performance than otherwise possible.
- The integration and demonstration of the successful application of these tools and this understanding.

Success in all three is needed to make real progress toward the goal of advancing the prospects for fusion energy. In this plan, we describe these elements sequentially. However, one should bear in mind that in the DIII-D Program as it will be carried out, these threads will be pursued simultaneously and interactively.

**2.2.3.1. ADVANCING SCIENTIFIC UNDERSTANDING.** The plasma physics important to the development of tokamaks is somewhat arbitrary divided into four categories. In shorthand terms, these are “confinement,”

“stability,” “boundary,” and “current drive and heating.” The motivations, scientific issues, principles, techniques and instruments required, and proposed studies and solutions in each area are discussed in depth in Sections 2.3 and 2.5. The following sections briefly clarify the scientific content of each of these categories (i.e., what physics is included) and summarize the research tasks we expect to undertake during the period covered by this plan.

**Confinement.** Confinement studies are concerned with the physics which affects the transport of particles, angular momentum and heat within the tokamak plasma. These fluxes are determined by a combination of neoclassical (collisional) and turbulent processes. Suppression and stabilization of the turbulence can lead to optimized confinement. For the AT Program, the present concentration in this area is on stabilization by means of  $E \times B$  velocity shear, in narrow radial regions (leading to the appearance of “transport barriers”) or over the entire plasma cross section. We need to improve the fundamental understanding of turbulent transport [low energy confinement (L-mode)], and of the dynamics of transport barrier formation and control. This should lead to a predictive modeling capability. High beta, intermediate wavelength electromagnetic turbulence can also affect transport and lead to pressure limits, but experimental studies have thus far been limited. Work on high magnetic shear, high  $\ell_1$  configurations will be expanded. The particular areas of confinement study that we propose to undertake in the coming five year period are:

- $E \times B$  shear stabilization of turbulence.
  - Make more detailed and quantitative comparisons between experiment and theories of turbulence stabilization.
  - Develop and test transport models including  $E \times B$  shear stabilization.
  - Investigate synergistic effects between electric and magnetic shear.
- Produce and control transport barriers through suppression of turbulence.
  - Utilize profile control of current, density, toroidal rotation, temperature and poloidal rotation to manipulate  $E \times B$  shear.
  - Investigate transport of particles, angular momentum and heat in the presence of  $E \times B$  shear.
  - Determine whether poloidal rotation agrees with neoclassical prediction.
- Test and further develop models of turbulent transport.
- Utilize results of nondimensional scaling investigations to extrapolate DIII-D results to future devices.
- Explore regimes with high electron temperature.
  - $T_e \sim T_i$  with direct electron heating.
- Test and further develop models for the high energy confinement (H-mode) edge.
  - L to H and H to L transition models.
  - Models for the H-mode edge pedestal, including physics of edge localized modes (ELMs).

- Investigate confinement physics of novel configurations.
  - RI-mode (high density, good confinement, with radiating edge).
- Encourage diagnostic development needed for turbulent transport investigations.
  - Direct  $E_r$  measurements.
  - Measurement and visualization techniques for  $S(\omega, k, \rho)$ .
  - Measurement of higher frequency, shorter scale length electron-scale turbulence.

**Stability.** ITER is designed for MHD-stable operation at a normalized beta value  $\beta_N \sim 2.5$ . ATs leading toward a more compact, economical, and reliable fusion power plant need approximately twice this value. Wall stabilization is the key requirement. Our stability research aims at advancing the physics understanding of MHD behavior in high performance tokamak plasmas and at developing active and passive means of improving tokamak stability. Research in the past has shown that the plasma's stability to both ideal and resistive MHD instabilities depends strongly on the profiles of current density, pressure, and angular momentum, as well as the discharge shape. To improve stability, we need to optimize both plasma shape, internal pressure and current profiles, and particularly profiles near the plasma edge. The results of this work should allow higher beta operation. A second important result will be a sufficient basis of stability understanding to operate a tokamak in a manner to avoid creating disruptions for physics reasons. Of course, disruptions will still occur, triggered by material from surfaces falling into the plasma or system hardware faults. For these cases, it is important to develop a disruption mitigation approach. In the next five years, we propose to investigate the following physics issues affecting stability:

- Plasma Shape
  - Investigate effects of triangularity on ideal and resistive stability.
  - Confirm predicted synergism of shaping and profiles in raising stability limits.
  - Use plasma shape to control pressure driven edge modes.
  - Use extreme shaping to access predicted higher beta and second stability regime.
- Profile Effects
  - Improve stability limits of NCS plasma by increasing  $\ell_i$ .
  - Develop high performance high  $\ell_i$  regime with H-mode edge.
  - Demonstrate feedback control of current density profile with rf.
  - Demonstrate edge pressure profile control with pellet injection and edge ergodization.
  - Control core pressure profile with ECH and ECCD (and possibly mode conversion).
- Wall Stabilization
  - Determine rotation requirements for wall stabilization.
  - Enhance and sustain wall stabilization using external coils.
  - Use internal coils for angular momentum input.
- Bootstrap Current Alignment
  - Explore theoretical and experimental solutions with better alignment.

- Develop high performance discharges with ELMing H-mode edges.
- Demonstrate long pulse sustainment with large bootstrap fraction and modest rf current drive.
- Nonideal instabilities
  - Verify neoclassical tearing mode theories.
  - Avoid neoclassical tearing instability by reducing sources of seed islands.
  - Assess neoclassical tearing mode stabilization by ECCD.
  - Investigate Alfvén instabilities in NCS.
- Disruptions
  - Investigate and characterize halo currents and runaway electrons during disruption.
  - Evaluate disruption mitigation techniques using impurity pellets, gas puffing and liquid jets.
  - Explore disruption avoidance using neural network systems.

**Boundary.** In divertor physics, there exist certain conventional assumptions that might be termed the “standard model” (classical conduction limited heat flow along the field lines, constant pressure along the field lines (attached plasmas), coronal equilibrium radiation rates, constant impurity concentration everywhere in the system, sheath limited heat flow at the divertor plate). Within this model, the amount of power that can be radiated in the SOL/divertor is in-principle limited. The only way to increase radiated power is to raise the density at the separatrix which can be inconsistent with the need to maintain a low collisionality core plasma or in conflict with density limits. To realize an AT, advanced divertor physics is needed that goes beyond the standard model to enable increased SOL/divertor radiation compatible with AT core conditions.

The elements of such advanced divertor physics that we will investigate in the five-year period are listed below. Another line of investigation that may be compatible with a thrust toward L-mode edge core plasmas is the use of radiating mantles. The issues in this area revolve around impurity sources from the divertor, core plasma impurity transport, and synergistic effects of impurities on confinement (e.g., RI-mode). Finally, the divertor provides the means of fuel and impurity exhaust and primary management of neutral fueling for the core plasma. Our main lines of investigation in these areas are listed below. We will seek to express success along these lines in verified 2D divertor and surface modeling codes that can be used predictively.

- Advanced Divertor Physics Elements
  - The roles of conduction and convection in parallel heat transport.
  - Impurity concentration enrichment in the divertor.
  - Noncoronal equilibrium radiation rate enhancements.
  - 2-D flow patterns of heat and fuel.
  - Non-LTE enhancements of radiation.
  - Plasma recombination.

- Radiative Mantle Issues
  - Core plasma impurity transport, especially in AT regimes.
  - Synergistic effects on confinement.
  - Understanding impurity source mechanisms and surface erosion.
- Core Plasma Boundary Condition Issues
  - The role of neutrals in core confinement.
  - The role of neutrals in H-mode access and the shear layer structure.
  - Density control and density limits.
  - Fueling without gas injection — pellets, compact tori.

**Current Drive and Heating.** Current drive and heating studies aim at resolving scientific issues associated with the physics of heating plasmas to high temperatures and of driving electrical currents in plasmas, including self-generated currents like the bootstrap current and the Pfirsch-Schluter current. For processes using waves, this includes the physics of wave generation, propagation, absorption, and effects on the distribution function like those giving rise to plasma current. Some of the issues of current drive and heating that we expect to explore during the plan period include:

- Wave generation, propagation, absorption, and current drive.
  - Definitively determine effect of magnetic well on current drive efficiency, for ECH and FWCD, and compare to Fokker-Planck codes.
  - Study physics of mode conversion of fast waves to ion Bernstein waves at the ion-ion hybrid frequency and subsequent propagation and damping of the Bernstein waves, including generation of radial shear in  $E_r$ .
  - Determine limits and behavior of nonthermal and nonlinear wave physics including effects on resistivity which affect the relaxation times.
- Effects of wave fields on the transport of particles and heat in a plasma.
  - Study anomalous transport caused by wave fields.
  - Study nonlocal effects on transport.
  - Use localized heating as a perturbation or diagnostic.
  - Study effect on transport barriers.
- Effect of wave power on plasma rotation and rotational shear.
- Physics of the bootstrap current.
  - Elucidate the physics of bootstrap generation and compare with the many theories; include the effects of fast ions.

**2.2.3.2. DEVELOPING TOOLS AND TECHNIQUES.** Pursuit of the objective of using active intervention and control to improve tokamak performance requires more than an understanding of the underlying scientific principles governing tokamak plasma behavior. We also require proven techniques for applying this control — actuators in the language of control systems.

In past and present studies, the DIII-D Program has demonstrated the benefits derived from control of the details of the shape and location of the plasma. The steadily improving DIII-D plasma shape control system, now an expanded digital plasma control system, has contributed greatly to both developing understanding of the dependence of MHD stability and transport on plasma shape, and to the achievement of outstanding performance.

The principles and past experience with plasma control in the DIII-D Program form the basis for the proposed program for the next five years. With improved understanding of the dynamics of tokamak plasmas, and with increasing recognition of the need to control many aspects of the plasma, we are proposing expanded programs in the areas of “interior pressure and current profile control, wall stabilization, density control, control of the core plasma boundary, steady-state operation, and control of the plasma-wall interface. This list follows the list of issues in Fig. 2.2-1 and Table 2.2-1 in moving from the plasma center out into the SOL and finally to the wall of the vacuum chamber. Again, these are shorthand phrases for groups of complex interactive systems we propose to develop. These areas have also been referred to as “composite issues” because a successful outcome of these research lines requires contributions from several of the scientific topic areas.

In addition to describing the activities in each of these areas, we also discuss tools and techniques specifically associated with the steady state aspects of the DIII-D AT Program.

**Interior Pressure and Current Profile Control.** Present control systems focus on control of plasma shape and global plasma parameters. To reach theoretical optimum performance, control of local profiles becomes important. Both gross stability and the turbulence levels that determine confinement are determined by the pressure, current, fluid flow, and radial electric field. These are coupled through the requirement of radial pressure balance to form the sheared  $E \times B$  flow that suppresses turbulence. Transport of the related quantities (heat, particles, angular momentum) is determined by the turbulence levels that develop as a result of the gradients and profile shapes. Thus the tokamak core has a complex feedback loop which if it is optimized can create transport barriers. Introducing shear in  $E \times B$  flow at a particular point in the plasma can reduce fluctuations locally, changing the local transport, modifying the profiles over a wider region, in turn affecting turbulence, transport, and stability limits for the entire plasma cross section. Principal tools to control the pressure profile are off-axis ECH, pumping to control the density to control the NBI deposition profile, and the counter beamline.

Controlling the current density profile is the key to attaining the high plasma stability levels sought. The current profile also enters into forming the  $E \times B$  shear flow and in determining the growth rates of turbulence. The principal objectives are to make sustained hollow  $q$  profiles with  $q_0 > 2$  and  $q_{\min}$  at large radius (NCS), to make sustained high  $\ell_1$  profiles (peaked current profiles), and to suppress sawteeth. The transport barrier location will greatly affect the current profile since the bootstrap current peaks where the pressure gradient is large. Tools to directly control  $J(r)$  are the ECCD for off-axis current drive, mode conversion current drive (MCCD) for off-axis current drive, FWCD for on-axis current drive, and density control to control the NBCD profile.

Feedback control involves using diagnostic measurements to calculate discharge parameter profiles, comparison to the required profiles and modification of actuators to change the profiles to correct any error. To improve our ability to control profiles, both new actuators and improvements in the plasma control system are needed. New actuators such as a counter-injection neutral beam, nonaxisymmetric coils to force plasma rotation, and increased ECH and fast wave power are being planned. To improve the system, hardware will be installed to allow real time profile data acquisition and reduction. The counter beam-line will enable real time measurement of  $E_r$ . Further enhancement in computing power will be required for equilibrium reconstruction including the additional information.

The challenge is to produce quasi-stationary plasmas that simultaneously minimize transport and maximize beta.

**Wall Stabilization.** The presence of a nearby conducting wall can stabilize long wavelength MHD modes, and thereby increase the limiting beta. Present nonideal MHD theory indicates that with a resistive wall and with plasma dissipation, sufficient rotation leads to stability. The beta-limiting instabilities are then purely internal to the plasma. So far, it has been difficult to sustain wall-stabilized plasmas, perhaps because of the difficulty of maintaining the necessary plasma rotation. In the five-year program, we plan to develop several approaches which make use of nonaxisymmetric coils to improve the wall stabilization concept.

External coils can be used to stabilize modes even with little or no plasma rotation. An asynchronous rotating field may be applied, so that a mode stationary with respect to the vessel wall is stabilized by this “fake rotating shell.” Synchronous fields may be applied using feedback control, either with a coil set optimized for a particular instability, or with a “smart shell” consisting of autonomous coils controlled to simulate a perfectly conducting wall. Also, a rotating field applied can add angular momentum to the plasma and keep it rotating rapidly enough to maintain stabilization by the resistive wall. The coil set may be either inside or outside the vacuum vessel. The inside coil is more difficult and expensive, but its high frequency capability allows for additional applications.

We envision several phases to the development of these techniques in DIII-D. Initially, we will use the existing C-coil for “fake rotating shell” and “smart shell” stabilization techniques. Second, we will add segmented coils outside the vessel (similar to the C-coil) above and below the midplane to greatly improve the spatial mode structure of the coil system. Finally, we will install segmented inside coils with a much faster time response for feedback control and angular momentum input. With an appropriate design, it should also be possible to use the same internal coil set for edge pressure profile control by ergodization of the edge magnetic field, and for other applications.

**Disruption Avoidance and Mitigation.** There are two key approaches that need to be developed in the tokamak to remove disruptions as a major operational issue for future tokamak devices. The first is to gain a sufficiently predictive scientific basis of plasma stability to be able to operate a tokamak using real-time control near but not across stability boundaries. Even if this goal is achieved, however, disruptions will still occur (but rarely) owing to random events injecting material from plasma-facing component sur-

faces into the plasma or faults in the control system, particularly the poloidal field (PF) coil system. So the second major development for those remaining disruptions is a reliable disruption mitigation system.

Essentially, the entire purpose of the DIII-D research in the stability area is to build the scientific base of plasma stability so that disruptions may be avoided. We have developed the diagnostic techniques to measure the current and pressure profiles. Work is ongoing to enable these measurements to be made in real time so that they can be used as the sensors in plasma feedback control loops. The various actuators (NBI, rf, the “smart shell,” etc.) will be the active elements of such control loops. The stability code work ties these efforts together in building predictive understanding. An integrated approach to the disruption avoidance control is being pursued with the use of real-time neural networks to identify the disruption boundaries. By incorporating the set of advanced profile diagnostics now available on DIII-D, more advanced numerical techniques, and training on a more complete ensemble of DIII-D disruptions including advanced tokamak operating modes, an early warning system will be developed to avoid disruptions and maintain stable operation or allow implementation of a soft shutdown or disruptions mitigation system.

Disruptions mitigation involves two main activities. The first is the identification of the physical phenomena that occur before and during a disruption in order to know what has to be done to mitigate the consequences and the second is to develop an active method of disruption mitigation. In the area of disruption characterization, the physics of the thermal quench will be examined in order to understand the mechanism of the energy loss and the resulting time scales and spatial distributions of the lost energy. Current quench processes that will be investigated include halo currents, the role of impurities and turbulence in the plasma resistivity during the disruption, and the generation and confinement of runaway electrons.

Finally, it is necessary to develop a reliable, active disruption mitigation system. Our primary candidate for such a system is a combination of a supersonic liquid helium jet injection followed by injection of a high-Z impurity pellet. The combined effect should significantly reduce halo currents, radiate most of the plasma thermal and magnetic energy, and avoid the production of runaway electrons. This approach requires a significant hardware development that has been separately proposed to the OFE Technology Division. In addition to the hardware development, the physics issues of the liquid jet approach will be investigated.

**Density Control.** Control techniques are needed for both the average plasma density and for the density profile in DIII-D. First, back-projection from promising power plant designs (see Section 2.3) leads to DIII-D scenarios with  $n/n_{\text{Greenwald}} \approx 0.2-0.4$ , roughly a factor of two lower than usually obtained in H-modes. Second, the efficiency of noninductive current drive varies inversely with density, placing a premium on low  $n$  operation. A third, practical consideration for DIII-D is that the cutoff density for the 110 GHz ECH system is  $7 \times 10^{20} \text{ m}^{-3}$ , so the density should be kept below this level. Local fueling and density profile control is closely coupled to the formation and maintenance of transport barriers. Density control becomes a means for current and current profile control in plasmas with a large fraction of bootstrap current.

In the near term, divertor pumping will be used to try to lengthen the high performance phase of NBI-driven NCS plasmas. Transport simulations have predicted that multisecond sustainment of this AT mode could be made if density control through pumping these high triangularity plasmas were available. For that reason, the installation of the upper, outer baffle and cryopump of the RDP was made in this last year. This density control capability will be available in the next two years and will be extended from the present 40,000 l/s capability to 160,000 l/s when the full RDP is installed in 2001.

NBI and central pellet fueling can be used in DIII-D to feed density inside a forming transport barrier to drive up the density gradient. In future machines, NBI and pellets will not be able to fuel the center of the plasma. To improve penetration, high-field-side pellet injection is planned for 1998.

**Control of the Core Plasma Boundary.** The H-mode shear layer is a battleground of conflicting requirements. It both provides the boundary condition for the core plasma and sets the SOL density, temperature, and power flow boundary conditions. Since this is also where neutral influx is primarily attenuated, giving rise to a strongly spatially varying neutral source density, this region is in-principle not described solely by the dimensionless parameters of plasma physics. The complications of this region account for the conflicting strategies for controlling its properties.

The desire for a high quality H-mode edge is well understood. There is a correlation between decreasing neutral fueling (coupled to wall conditioning) and increasing H factor. Recently emphasis has been placed on the height of the H-mode pedestal, which is also correlated with decreasing neutral fueling. To make the edge more neutral-free and collisionless, the highly baffled RDP installation is expected to lower the core fueling a factor of 8 for fixed neutral reflexes from the divertor targets. Pellet fueling is also being substituted for gas fueling to further lower the neutral gas source at the separatrix. Further efforts in lithium wall conditioning are also planned, in addition to boronization. Finally we must note that the RI-mode radiating-mantle approach, though it seems contradictory to this line, nevertheless has been shown to improve the core plasma confinement.

However, the large pressure gradient that forms in the H-mode edge is linked to the termination of AT modes. This pressure gradient leads to a large bootstrap current which is unfavorable for kink modes. Thus, there is interest in controlled reduction of the edge pressure gradient through degraded H-mode edges or even an L-mode edge. L-mode edges are preferable from a divertor physics point of view. A variety of active control techniques are being proposed: the use of a radiating mantle (*a la* RI-mode), the use of marginally diverted plasmas, the use of nonaxisymmetric coils to ergodize the plasma edge, and the regulation of ELMs.

**Steady-State Operation.** The extremes of tokamak performance have thus far been achieved under transient conditions. When studies are done of long-term behavior, other effects enter in a way which complicates plasma behavior and tends to reduce performance. These include current profile changes, wall modifications in response to the changing plasma, and resistive and neoclassical effects on stability. In this plan, the DIII-D Program will work to extend quasi-stationary operation to 10 s pulses. These

experiments will not be truly steady-state because 10 s is not enough time for the plasma to reach full equilibrium with the walls and divertor, and there will certainly be residual current profile relaxation effects on this time scale.

The principal area of study and source of control requirements is the plasma current (or equivalently poloidal flux) profile. AT operation relies on having a significant fraction of the total plasma current produced by the bootstrap effect, which closely couples current profile evolution to stability and transport. Control of the current and current profile will require both direct external noninductive sources (NBCD, ECCD, FWCD) and indirect control through manipulation of the density and temperature profiles by heating or transport barrier control. The long term dynamical stability of these profiles, on the flux transport time scale, is a major research topic for the next five years. Another consideration is that the transport and relaxation of the current profile is certainly affected by the level of turbulence or large scale instability (sawteeth, ELMs) in the plasma. Control of the steady-state plasma in the presence of these processes is not presently understood.

When steady-state versions of the AT operating modes are achieved, we will have the opportunity for much more extensive study and optimization of these configurations. The accurate determination of transport properties can be done without concern about corrections (e.g., the contentious  $dW/dt$  term in the energy balance). Experiments requiring high precision, such as the dimensionless scaling determinations, will then be possible for the advanced regimes. Measurements requiring signal averaging will benefit from the huge increase in observation time at optimum conditions.

The DIII-D Program will make major contributions to establishing the basis for fully noninductive formation of a high performance plasma. Noninductive current initiation and ramp-up require determination of an optimal time-dependent path through parameter space, to avoid instability and produce the desired profile. We will explore several techniques for transformerless operation, including ECH, helicity injection, or use of the outer poloidal field coils for initiation and initial ramp-up. Overdriving the bootstrap current is a promising idea for ramp-up over a wide range of plasma current. With a better understanding of current diffusion processes, helicity injection may also find useful application.

**Control of the Plasma Wall Interface.** The interface between plasma and divertor structures is a critical control element in achieving advanced divertor physics. The pattern of recirculation of neutrals in the divertor is governed by the shape of the divertor structures. Our recent research has shown that encouraging more convective parallel heat transport (instead of conduction) may be a route to beating the radiation constraint of the standard divertor model. We will investigate this in the RDP and are developing an advanced version of this solution to the divertor problem which seeks to create strong convective flows in the divertor. The shaping of the divertor structures that determines the 2-D patterns of fuel flow also dominates the impurity transport problem. It is the entraining fuel flow (if it exceeds the thermal force) that can give rise to impurity enrichment in the divertor. We also must find a way to retain impurities in the divertor to limit their buildup in the core plasma in AT modes. Impurity radiation in the divertor and fuel flow physics are also emerging as the keys to obtaining a recombining plasma. A plasma that fully recombines before reaching a material surface offers the best possible interface.

Finally, the boundary interface between the plasma and the wall must be controlled in order to regulate recycling of fuel and sources of impurities. Presently, we feel the principal source of carbon is chemical sputtering in the private flux region. The dome of the RDP should lower this chemical sputtering source. Wall sources of carbon cannot be overlooked. Much more work needs to be done on characterizing these sources before we can plan an intervention.

**2.2.3.3. THEORY OBJECTIVES.** Even at the presently reduced budget level, the U.S. theory effort has been able to maintain a leadership role in the world fusion program. The ITER–EDA has increasingly relied on U.S. theory help in resolving outstanding issues. Similarly, U.S. experiments have recognized that increased coupling with theory and modeling provides a means to make more effective use of our remaining facilities. The success of the DIII–D Program will depend critically on the contributions of theory. In particular, forming teams of experimentalists and theorists cutting across traditional disciplinary areas has been found to be a most effective way of stimulating progress in physics understanding. The key objectives of theory and modeling in support of DIII–D are to:

- Develop quantitative models which can be validated by experiments leading to deeper understandings and contributing to the long-term goal of comprehensive simulation of fusion systems.
- Provide innovative ideas for concept improvement which can be tested on DIII–D leading to advances in the design of a commercially attractive fusion power plant.

For the next five-year program on DIII–D, focusing theoretical efforts in the following issues would be of particular relevance.

- Elucidate the effects of sheared flow, shape and magnetic shear on core transport barrier formation.
- Clarify  $\rho_*$ ,  $\beta$ ,  $v_*$  scaling in relation to microstability physics.
- Identify physics processes responsible for electron heat transport.
- Develop quantitative models for L–H transition and edge pedestal.
- Elucidate the physics of ELMs and their impact on stability and confinement.
- Ascertain the effects of shape, profiles and resistive wall on ideal MHD stability.
- Investigate resistive instabilities and their role in long-pulse stability limits.
- Understand the MHD triggers for disruptions and develop mitigation techniques.
- Evaluate the impact of bootstrap alignment on stability.
- Study the efficacy of EC and fast wave (FW) for current and pressure profile control.
- Elucidate the physics of MCCD and the optimum regime for off-axis current profile control.
- Explore transport barrier formation using EC and FW.

- Validate the physics of divertor detachment, impurity transport and impurity enrichment.
- Confirm the theoretical model for heat and particle transport in the SOL.
- Explore the compatibility of an effective radiative divertor and good core performance.

In addition, continuous development of a comprehensive, time-dependent simulation capability is required. This would include the ability to evolve strongly shaped magnetic geometry including separatrices, nonstandard  $q$ -profiles, shear flows, and physics-based heat and particle transport models. The simulation should distinguish between heat input to different species, hence quantitative heat, particle and momentum sources should be incorporated. The coupling between core simulation and SOL/divertor should be strengthened. Finally, a first step in coupling transport simulations to a fully nonlinear resistive MHD stability code should be undertaken.

While the DIII-D Program will make contributions in many of these areas, making needed progress toward establishing the scientific basis for fusion will require national cooperation in addressing these issues.

#### 2.2.3.4. DEVELOPING INTEGRATED SCENARIOS

**Common Characteristics.** Development of these scenarios serves several purposes. In addition to illustrating the plasma configuration and parameters that are the target of the AT Program, the scenarios highlight the requirements which have to be met to achieve these configurations. The scenarios point out the present uncertainties in performance, help identify the most important research tasks, and illustrate the needs for new techniques and new hardware to carry out this development path. Development of scenarios is an on-going process.

Table 2.2–2 presents several scenarios which try to use and extend the most recent advances in our understanding of plasma transport. These scenarios are 1D simulations developed with the ONETWO code. They represent several realizations of the beneficial results of NCS current profiles — both the formation of a transport barrier for improved confinement and improved stability at high  $\beta_N$ .

These cases represent a range of  $\beta$  from 5% to 11.5%. The toroidal magnetic field is 1.95 T and the plasma currents are 1.6–2.2 MA. All have strong shaping ( $\kappa=2.1$ ,  $\delta=0.8$ ). The heating and current drive power is 15–20 MW, made up of roughly equal contributions of NBI, ECH, and FW. Fast wave heating is used to achieve a high core electron temperature. We should note that the power levels quoted here are delivered to the plasma (what's important to plasma simulations). The system power capability at the sources is necessarily higher. Thus, the 6–7 MW of ECH indicated in Table 2.2–2 corresponds to a 10 MW source specification, and 4 MW of fast wave power requires a nominal 6 MW rf system.

They also seek high bootstrap fractions and make up any difference in the plasma current and the bootstrap current by use of rf current drive. The resulting plasmas have rather low  $\rho_*$  and very low  $v_{*r}$ , but they match up well along dimensionless parameter scaling paths to future tokamak

**TABLE 2.2–2**  
**PARAMETERS OF DIII-D SCENARIOS**

Case	1	2	3	4	5
$\beta$ (%)	7.5	5.0	8.1	8.7	11.5
$\beta_N$	5.7	3.8	6.2	5.8	6.0
$I_p$ (MA)	1.6	1.6	1.6	1.8	2.2
$I_{bootstrap}$	1.07	1.45	1.85	1.92	2.1
$I_{ECCD}$	0.35	0.50	0.03	0	0
$I_{FWCD}$	0	0	0	0	0
$I_{NBCD}$	0.25	0.11	0	0	0
$I_{OH}$	–0.07	–0.46	–0.28	–0.12	–0.10
$q_{95}$	6.5	5.0	5.0	5.3	3.6
$q_0$	3.8	2.3	2.5	3.9	3.4
$q_{min}$	2.6	3.3	2.1	2.3	
$T_i(0)$ keV	15	12.3	18.5	14.5	19
$T_e(0)$ keV	8.5	9.7	7.0	12.7	13
$n_e(0)$ $10^{20} \text{ m}^{-3}$		0.59	0.89	0.72	0.88
$\bar{n}$ $10^{20} \text{ m}^{-3}$	0.57	0.35	0.54	0.48	0.53
$n_{edge}$ $10^{20} \text{ m}^{-3}$		0.23	0.23	0.23	0.21
$\bar{n}/n_G$	0.4	0.26	0.4	0.32	0.3
P (MW)	20	14	12	14	14
$P_{NBI}$ (MW)	6.5	4.0	4.0	4.0	4.0
$P_{EC}$ (MW)	7.0	6.0	4.0	6.0	6.0
$P_{FW}$ (MW)	6.5	4.0	4.0	4.0	4.0
W (MJ)		1.25	1.3	4.6	6.0
$\tau_E$ (s)		0.21	0.29	0.28	0.4
$H_{99p}$	3.5	3.4	4.4	4.0	4.95
$\rho_{*e}$ at $\bar{T}_e$	$2.3 \times 10^{-4}$	$2.5 \times 10^{-4}$	$2.1 \times 10^{-4}$	$2.8 \times 10^{-4}$	$2.9 \times 10^{-4}$
$\rho_{*i}$ at $\bar{T}_i$	$1.3 \times 10^{-2}$	$1.2 \times 10^{-2}$	$1.5 \times 10^{-2}$	$1.3 \times 10^{-2}$	$1.5 \times 10^{-2}$
$v_{*e}$ at $\bar{T}_e$	$1.2 \times 10^{-2}$	$4.2 \times 10^{-3}$	$8.0 \times 10^{-3}$	$2.9 \times 10^{-3}$	$2.1 \times 10^{-3}$
$v_{*i}$ at $\bar{T}_i$	$2.7 \times 10^{-3}$	$1.8 \times 10^{-3}$	$0.8 \times 10^{-3}$	$1.6 \times 10^{-3}$	$0.7 \times 10^{-3}$

Case 1: SSC-VH [Turnbull PRL 74, 718 (1995)]

Case 2:  $\beta = 5\%$ ,  $P = 16$  MW,  $n$  &  $v_\phi$  transported

Case 3:  $\beta = 8\%$ ,  $P = 15.2$  MW,  $n$  &  $v_\phi$  transported

Case 4:  $\beta = 8\%$ ,  $P = 17$  MW

Case 5:  $\beta = 11\%$ ,  $P = 17$  MW

devices (see Section 2.3). The scenarios all have rather low densities and high temperatures. The combination of low density (well below the Greenwald limit) and high power will make it particularly challenging to obtain radiating, detached divertors in these scenarios.

**Second-Stable Core Very High Confinement Operating Mode (SSC–VH).** For reference, the first scenario is that published by Turnbull [Turnbull (1995)]. At that time, DIII–D had seen plasmas with hollow current profiles and very high central beta. The plasma core was calculated to be in the second stable regime for ballooning modes [Lazarus (1992)]. We had also seen in other highly shaped discharges the very high confinement mode (VH–mode), with a transport barrier forming near  $\rho=0.8$ . The VH–phase was correlated with  $q_0 > 1$  [Lazarus (1994)]. This scenario considered combining these two features. With the inverted  $q$  profile, stability calculations gave  $\beta_N = 5.7$ , assuming wall stabilization. Electron heat diffusivities were modeled by the INTOR scaling and the ion diffusivity was taken to be neoclassical near the core and rising to  $5\times$ neoclassical near the edge. A combination of bootstrap current which peaked off axis and ECCD and NBCD were used to sustain the hollow current profile. Fast wave heating sustained the core electron temperature. A limitation of this scenario was the use of a fixed density profile; no density transport was considered. The rather broad density profile did not contribute much bootstrap current.

**New Scenarios with Transport Barrier Simulation.** Since the SSC–VH scenario was constructed, considerable progress has been made in understanding the characteristics of that regime. Very strong internal transport barriers have been seen, first with strongly NCS in the  $q$  profile and later with weak central shear (WCS). The formation of these transport barriers has come to be understood in terms of stabilization of turbulence by sheared  $E\times B$  flow. We have constructed a full transport model that can exhibit transport barrier formation in all channels (see Section 2.4.1 for details) and have used that transport model to construct scenarios 2–5 in Table 2.2–2. This model of transport barrier formation contains many feedback loops, since the radial electric field depends on all the profiles, and a very rich set of phenomena, some of which have been seen in DIII–D. Perhaps more important than the specific numbers in the table are the qualitative features we have seen from the barrier formation model.

**The Plasma Edge.** The cases considered all model an L–mode edge. The transport barrier forms where the shearing rate from the gradient of the radial electric field exceeds the local growth rate of the turbulence. Gyrokinetic calculations of the radial profile of the growth rate for ion temperature gradient (ITG) trapped-electron modes generally show a peak around  $\rho\approx 0.6$ , with smaller values in the core and at the edge. Hence it is easiest to form transport barriers in the plasma edge (H–mode) and in the center (NCS). Our basic task is to join these two regions, overcoming the peak in the growth rate. When density transport is turned on in the code, the strong local fueling source at the edge easily forms an edge transport barrier quickly leading to excessive edge pressure gradients. To avoid this problem, we imposed a large edge growth rate to keep the edge in L–mode and fixed the edge density. Development of a high performance discharge with an L–mode-like edge in order to avoid MHD instability is one of the DIII–D main AT thrusts. However, because of the high power flow through that edge, some means to suppress the L–H transition is needed. A configuration with substantial mantle radiation is one possible approach. We leave this study to future simulation work.

**Role of Density Gradients.** One of the most important new features we have seen in the core plasma is the role of density transport in forming a transport barrier. When turbulence is suppressed, strong density gradients appear. Density gradients are more effective than temperature gradients in creating bootstrap current and for that reason, we obtain more bootstrap current than in the original SSC–VH scenario. Also, we have moved the transport barrier further out in radius, which also increases the total bootstrap current. We find it rather easy (in fact too easy in these simulations) to obtain full bootstrap current. It appears that with central fueling from beams or pellets and a longer time for the density to accumulate, in the future we should see strong transport barrier formation with large density gradients and with accompanying large bootstrap fractions.

**ECH is a Precision Tool.** Another important observation is that the ECH is very effective at transport barrier control. The ECH deposition profile is about as narrow as the gradient regions of the transport barrier, and so the ECH is a precision tool for barrier control. The use of ECH for barrier control is illustrated in Fig. 2.2–2. A beam heated (6 MW) target plasma (solid curves) is near the critical point for an internal transport barrier. If 6 MW of ECH power is deposited centered at  $r/a = 0.7$  (dashed curves), a transport barrier in the electron density [Fig. 2.2–2(c)] and temperature [Fig. 2.2–2(d)] develops at the deposition radius. If the ECH deposition is centered at  $r/a = 0.3$  (dot-dashed curves), then no barrier forms due to the large background transport (156 times electron neoclassical for the electron thermal diffusivity) near the magnetic axis. Developing suitable feedback algorithms for producing and maintaining the desired transport barriers will be a challenge.

**Transport Assumptions and Consequences.** The various cases 2–5 have varying assumptions about how low the transport rates become inside the transport barrier. In DIII–D we have already seen ion neoclassical

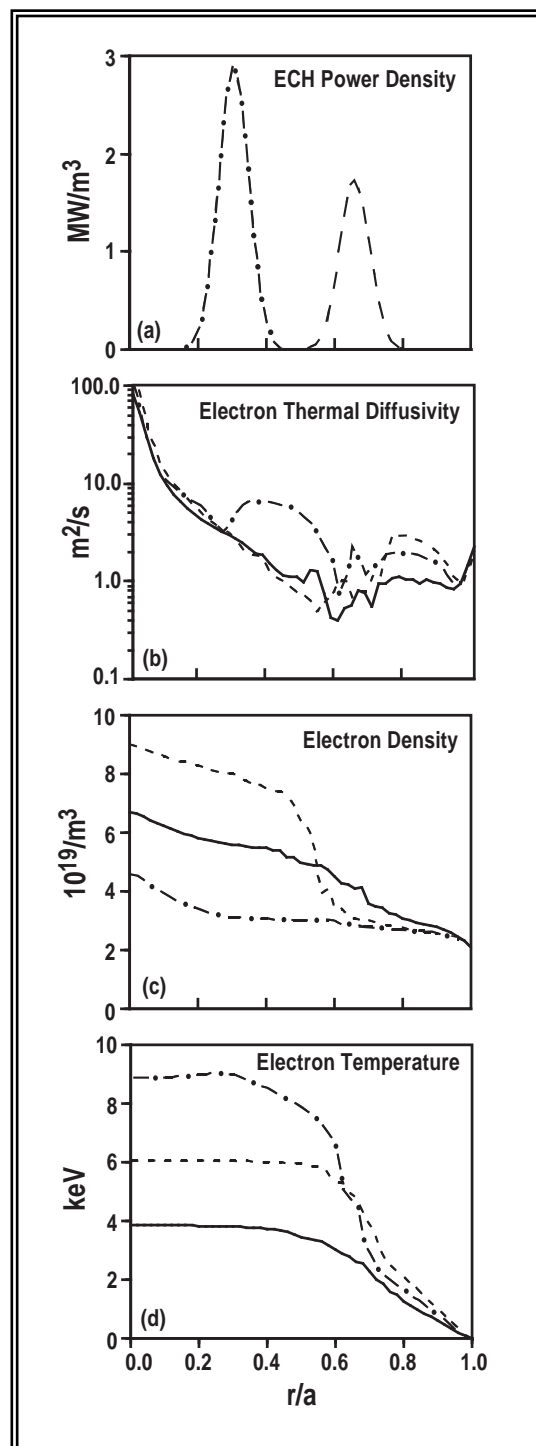


Fig. 2.2–2. ECH barrier control is illustrated by a three-case comparison: 6 MW NBI only (solid), 6 MW NBI + 6 MW ECH at  $r/a \sim 0.7$  (dashed), 6 MW NBI + 6 MW ECH at  $r/a \sim 0.3$  (dot dashed). Shown are profiles of (a) ECH power density, (b) model electron thermal diffusivity, (c) electron density, and (d) electron temperature.

transport rates all across the cross section so this assumption for the residual transport was made in all cases. But it is clear that similarly low levels for transport rates for electrons and particles in DIII-D are too good. Beta limits would be quickly exceeded. DIII-D does not presently see as much transport reduction in the electron and particle channels as in the ions and apparently will not require such reduction to reach the scenarios shown.

**Long Pulse Equilibration of Ions and Electrons.** One regime not yet adequately explored in experiments is that of equal electron and ion temperatures. In larger steady-state systems ions and electrons will reach substantially the same temperature, affecting turbulence growth rates and the overall power balance. In alpha-heating dominated reactors, the principal power flow will be from alphas to electrons to ions. In these scenarios, all of the fast wave and ECH power heats the electrons, along with a fraction of the neutral beam power. Even then, it is difficult to produce plasmas with  $T_e=T_i$ . To more closely approach these conditions will lead us in the direction of increasing the fraction of the power input going directly to electrons with either ECH or fast waves.

These are some of the striking phenomena we have seen in our initial exploration of the possibilities for AT physics in the plasma core. The simulations presented give a feeling for the parameter regimes achievable, the power levels in various systems to achieve them, the density and edge control that may be required. But the main value of such simulations is to indicate a wide vista of new phenomena that should open up as the auxiliary capabilities of DIII-D are developed toward the goal of long pulse sustainment of AT operating modes.

## References for Section 2.2

Turnbull, A.D., et al., Phys. Rev. Lett. **74**, 718 (1995).

Lazarus, E.A., et al., Phys. Fluids B **4**, 3644 (1992).

Lazarus, E.A., et al., Proc. 15th Int. Conf. on Plasma Physics and Controlled Fusion Research, Seville, Spain (International Atomic Energy Agency, Vienna 1995) p. 609.

## 2.3. FUSION ENERGY SCIENCE IN DIII-D

The advancement of plasma science is an intrinsic part of the Fusion Energy Research Program. The tokamak, being the most mature magnetic configuration, has contributed significantly to the cumulative knowledge base of high temperature plasma physics. The DIII-D tokamak, with its flexibility and a comprehensive suite of diagnostics, has been and will continue to be a major contributor in this mission; in turn, it will apply the knowledge gained toward the optimization of the tokamak concept as an economically attractive fusion power plant. In the next five years, the DIII-D tokamak will deliver valuable scientific information in many areas. Some key deliverables include:

- **Determine Mechanisms for the Suppression of Turbulent Transport.** A general mechanism for reducing turbulence attributed to  $E \times B$  shear flow damping is emerging and theoretical models to understand this effect are maturing. Experimental optimization of transport barriers in all channels and further study of the dynamics of shear flow suppression will provide a stringent test of the models. A goal of reducing the transport rates to the theoretical minimum (neoclassical) appears possible (Section 2.3.1).
- **Understand Pressure Limits at Very High Temperatures.** The science of MHDs predicts fundamental pressure limits to plasma confinement. Theory and experiment in recent years have shown that these limits are sensitive to plasma shapes as well as internal profiles. There is evidence suggesting that nonideal effects come into play. Understanding and circumventing ideal and nonideal effects in long pulse discharges in order to reach the theoretical stability limits will be a major focus (Section 2.3.2).
- **Understand the Physics of Interfacing Hot Plasma to a Material Wall.** Recent advances in divertor diagnostics have opened up investigations of the basic physics of the divertor. Realizing a fully recombining divertor plasma seems a real possibility. The plasma boundary interacts strongly with core plasma confinement, stability, and edge currents (Section 2.3.3).
- **Elucidate the Transfer of Energy and Momentum Among Waves, Charged Particles, and Plasma.** The study of rf heating and current drive has evolved from experiments performed in low density plasmas aimed at extracting the intrinsic physics to high power experiments under reactor relevant conditions. The science issues involving current drive have become strongly related to transport of particles and energy, transport of current, and generation of off-axis current. In addition, the difference in momentum content between waves and neutral beams (NB) provides a powerful tool for probing the role of rotation in transport. A goal of full transformerless operation appears within reach (Section 2.3.4).

### 2.3.1. CONFINEMENT SCIENCE AND TRANSPORT BARRIER CONTROL

*The discovery of transport barriers in the DIII-D tokamak has established the basis for an exciting program of confinement research in the next five-year period. DIII-D work in this area began with the H-mode transport barrier, progressed to the VH-mode transport barrier, and recently has extended further into the plasma in the interior transport barriers formed with NCS. We believe that one physical mechanism,  $E \times B$  shear stabilization of turbulence, underlies all three of these transport barrier formations. The physics of  $E \times B$  shear stabilization is very rich in providing feedback mechanisms which motivate the control of the profiles of density, ion temperature, electron temperature, current, and toroidal and poloidal rotation in order to control transport barrier formation. The conceptual basis given by  $E \times B$  shear stabilization gives a framework for theory work on the underlying anomalous transport, the properties of the turbulence (such as the radial correlation lengths and the decorrelation rate), and the residual transport rates after suppression. The promise for fusion application of this major advance in our understanding is achieving neoclassical levels of residual transport everywhere across the plasma. This has already been demonstrated in the ion heat channel. Understanding the transport in the electron channel and lowering it remains a principal challenge. Understanding the particle transport, especially that of impurities, inside the transport barriers is also a major area of future work.*

*We begin this section by reviewing the scientific basis for  $E \times B$  shear stabilization of turbulence. In Section 2.3.1.2, we present the scheme of transport barrier control implied by the  $E \times B$  shear stabilization theory. In subsequent sections, we discuss some particular important elements of the transport barrier research. Our plan to attack the electron transport problem is presented in Section 2.3.1.4. Theoretical and experimental work on the basic anomalous transport mechanisms and the turbulence suppression mechanism is presented in Section 2.3.1.5. The general plan for dimensionless parameter scaling studies for both the anomalous and the residual transport is discussed in Section 2.3.1.6. The problem of fuel and impurity transport is discussed in Section 2.3.1.7. The important remaining problems of the trigger mechanism for the L-H transition and the structure and stability properties of the H-mode shear layer are discussed in Sections 2.3.1.8 and 2.3.1.9. Finally, we discuss the new area of the RI-mode, whose radiating mantle with improved confinement may be a path to combining a high performance core plasma with effective power exhaust.*

**2.3.1.1. E×B SHEAR STABILIZATION OF TURBULENCE.** One of the scientific success stories of fusion research over the past decade is the development of the E×B velocity shear model to explain the formation of transport barriers in magnetic confinement devices. This model was originally developed to explain the transport barrier formed at the plasma edge in tokamaks after the L-to-H transition. As has been recently discussed [Burrell (1997)], this concept has the universality needed to explain the edge transport barriers seen in limiter and divertor tokamaks, stellarators, and mirror machines. More recently, this model has been applied to explain the further confinement improvement from H-mode to VH-mode seen in some tokamaks [Greenfield (1993), La Haye (1995), Burrell (1995)] where the edge transport barrier becomes wider. Most recently, this paradigm has been applied to the core transport barriers formed in plasmas with negative or low magnetic shear in the plasma core [Burrell (1997), Strait (1995), Lao (1996), Mazzacuatto (1996), Kimura (1996)].

It is not often that a system self-organizes to reduce transport when an additional source of free energy is applied to it. In addition to its intrinsic physics interest, the transport decrease that is associated with E×B velocity shear effects has significant practical consequences for fusion research. The best fusion performance to date in the DIII-D and JT-60U tokamaks has been obtained under conditions where transport reduction through E×B velocity shear decorrelation of turbulence is almost certainly taking place [Lazarus (1996), Ushigusa (1996)]. In the DIII-D case, for example, the ion thermal transport is at the minimum level set by interparticle collisions over the whole discharge [Lazarus (1996)]. At least in the ion channel, it appears that anomalous transport is totally absent.

The fundamental physics involved in transport reduction is the effect of E×B velocity shear on the growth of and radial extent of turbulent eddies in the plasma. Both nonlinear decorrelation [Chiueh (1996), Biglari (1990), Shaing (1990)] and linear stabilization [Shaing (1990), Waltz (1995), Hassam (1991), Staebler (1991), Wang (1992), Carreras (1992), Dominguez (1993)] effects have been considered. The basic nonlinear effect is the reduction in radial transport owing to decrease in the radial correlation length and the change in the phase between density, temperature and potential fluctuations. There are a multitude of linear effects specific to various modes; however, one general feature of linear stabilization is coupling to more stable modes caused by the E×B velocity shear.

The same fundamental transport reduction process can be operational in various portions of the plasma because there are a number ways to change the radial electric field  $E_r$ . A schematic of the entire process of E×B shear suppression of turbulence is shown in Fig. 2.3–1. The radial force balance equation

$$E_r = (Z_i n_i e)^{-1} \nabla P_i - v_{\theta i} B_\phi + v_{\phi i} B_\theta \quad , \quad (1)$$

indicates that there is a connection between  $E_r$  and the cross field heat and particle transport ( $\nabla P_i$ ), cross field angular momentum transport ( $v_{\phi i}$ ) and poloidal flow ( $v_{\theta i}$ ). Since sheared E×B flow also affects turbulence and transport, there are several feedback loops whereby  $E_r$  and its shear can change allowing the



plasma access to different confinement regimes. For example, both  $v_{\theta i}$  and  $\nabla P_i$  are important in the H-mode edge [Burrell (1997)] while  $v_{\phi i}$  appears to play the major role in VH-mode [Greenfield (1993), La Haye (1995), Burrell (1995)]. Both  $v_{\phi i}$  [Lao (1996)] and  $\nabla P_i$  [Mazzucato (1996)] appear to play a role in the core transport barriers. This multiplicity of feedback loops ultimately provides a number of possibilities for active control of transport. NBI, for example, has been used to alter  $v_{\phi i}$  [Greenfield (1993), La Haye (1995), Burrell (1995), Strait (1995), Lao (1996), Mazzucato (1996)] while ion Bernstein wave (IBW) input has apparently changed  $v_{\theta i}$  [Bernabei (1993)]. The diamagnetic component of  $E \times B$  (decreasing with smaller  $\rho_*$ ) is expected to have a poor scaling with increasing B-field and the momentum component with increasing density where it is more difficult to get large rotation. The L-H transition [and the balanced beam tokamak fusion test reactor (TFTR) ERS barrier] is likely a diamagnetic type and the VH-mode and NCS barrier (in DIII-D) likely momentum dominated.

One of the important themes in this area is the synergistic effects of  $E \times B$  velocity shear and magnetic shear. Although the  $E \times B$  velocity shear appears to have an effect on broader classes of microturbulence, magnetic shear can mitigate some potentially harmful effects of  $E \times B$  velocity shear and facilitate turbulence stabilization. For example, there are many similarities in velocity shear effects in magnetized plasmas and neutral fluids [Hunt (1991)]; however, in neutral fluids, the increased turbulent drive owing to the free energy provided by the velocity shear usually overcomes the stabilizing effects of reduced radial correlation length to drive Kelvin-Helmholtz instabilities. In a plasma with magnetic shear, both in the ideal case [Scott (1988)] and the resistive case [Biglari (1990)], Kelvin-Helmholtz modes are rendered ineffectual. As a second example, in the case of core transport barriers, the magnetic shear effects play a role by linearly stabilizing several modes (e.g., sawteeth and ideal ballooning modes) while reducing the growth rates of others [Lazarus (1996), Scott (1988), Lebedev (1996)], thus allowing the core gradients to steepen. A transport bifurcation, similar to those previously discussed [Hinton (1993), Staebler (1994)], results and the core transport barrier forms [Diamond (1997), Lebedev (1996), Hinton (1993), Staebler (1994)].

Considerable experimental work has been done to test this picture of  $E \times B$  velocity shear effects on turbulence. The experimental results are consistent with the basic theoretical models. The  $E \times B$  velocity shear model has the universality needed to explain: (1) H-mode edge confinement improvement seen in limiter and divertor tokamaks, stellarators, torsatrons and mirror machines produced with a variety of heating and plasma biasing schemes; (2) the confinement improvement in the outer half of the plasma seen in VH-mode and high  $\ell_i$  discharges [Lao (1993)]; and (3) the formation of core transport barriers in a number of tokamaks. In addition, there is both qualitative and quantitative agreement between theory and the experimental results. Finally, in the last several years, there have been several rigorous tests of causality; the experimental results are consistent with  $E \times B$  velocity shear causing the reduction in turbulence and transport in both the plasma edge and the core.

Although the  $E \times B$  velocity shear theory has considerable experimental support, there are still areas where it needs to be tested further. For example, more quantitative comparisons need to be made between

the turbulence decorrelation rate and the  $E \times B$  shearing rate under various plasma conditions to verify the expected inequality. A more readily quantified criterion is that the  $E \times B$  shearing rate  $\omega_{E \times B}$  should exceed the maximum gyrokinetic linear mode growth rate  $\gamma_{\max}$ . This rule describes  $E \times B$  shear in nonlinear gyrofluid simulations [Waltz (1995)]. It has been incorporated in transport models with some success in describing the DIII-D NCS transport barrier [Waltz (1996, 1997), Lao (1996)]. However the stability criterion is based on nonlinear flux 2-D simulations for circular geometry in the limit of vanishing  $\rho_*$  and generalization to regimes with significant diamagnetic components (generally the actual case) or with profile curvature are unclear. In addition, although ion thermal transport at the neoclassical level has been seen in DIII-D [Lazarus (1996)], electron transport and angular momentum transport are still anomalous, indicating that not all turbulence effects have been totally suppressed [Lao (1996)]. One possibility is that high wave number  $\eta_e$  modes could support electron heat transport [Waltz (1996, 1997)]. New DIII-D diagnostics may be able to detect a shift to very high wave number turbulence inside core transport barriers. We need to investigate these questions further. A further reduction in angular momentum transport would be especially significant since it would reduce the amount of NB torque needed to influence the electric field by changing the toroidal plasma rotation.

Since synergistic effects occur between  $E \times B$  shear and magnetic shear, it is important to sort out the relative role of  $E \times B$  shear and magnetic configuration in improved confinement. It is known that either large magnetic shear or reverse shear, particularly large alpha or Shafranov shift, suppress growth rates making it easier for  $\omega_{E \times B}$  to exceed  $\gamma_{\max}$ . Some simulations suggest the critical  $\omega_{E \times B}$  decreases with shear  $|s|$  but others find that it is independent. There is a general result on DIII-D that magnetic configurations which have enhanced MHD stability usually exhibit improved energy confinement as well. Accordingly, we will investigate what role magnetic shear and magnetic configuration have in reducing turbulent transport, either directly or by facilitating the effects of  $E \times B$  shear. DIII-D is in a unique position to carry out such investigations because of its flexible shaping control and because of the variety of current drive techniques which will be available during the next five years.

Magnetic topology effects may even lead to a bifurcation mechanism from Shafranov (alpha-) stabilization of the gyrokinetic ballooning modes not unlike the root to second stability for ideal ballooning modes. The alpha-stabilization can actually lead to a natural heat flow bifurcation [La Haye (1995), Beer (1996)] strongest at high- $q$ , weak or negative shear, and high beta. It seems likely that low wave number gyrokinetic modes are not completely stabilized in an MHD second stable core. Verifying this requires a detailed gyrokinetic stability study with real geometry. While it seems to be a subdominant mechanisms in most DIII-D transport barriers, it may be possible to design DIII-D experiments at high field and high density with sufficient power to get high beta so that alpha-stabilization may dominate. Having no  $\rho_*$  or momentum dependence, this mechanism has a much better scaling to ITER and is generally compatible with ideas about AT profile configuration.

**2.3.1.2. CONTROL OF TRANSPORT BARRIERS.** The results from DIII-D and other tokamaks cited in the previous section indicate that control of transport barriers is equivalent to control of the  $E \times B$  shear. The

simplest way for DIII-D to change  $E_r$  is to alter the toroidal rotation using NBs. Unbalanced NBI has led to toroidal rotation speeds as large as 700 km/s. Indeed, in all improved performance NCS discharges in DIII-D, the  $E_r$  is dominated by the effects of toroidal rotation. In order to enhance our control of the rotation, this proposal includes the installation of a NB which will inject in the opposite direction to the standard beam direction. This will enable us to alter the rotation separately from changes in the heating power. Figure 2.3–2 shows the great change that can be made in the turbulence shearing rate profile between co- and counter-injection. Fundamental investigations of angular momentum transport need to be performed as part of this work, to understand the effects of  $E \times B$  shear on angular momentum transport. Because this transport is still anomalous in the DIII-D NCS discharges, further reductions are (in principle) possible which could lead to much reduced requirements for the input torque needed to maintain a given rotation speed. Density control (to be provided by the divertor cryopumping system) also couples in to this part of the work since  $E_r$  depends on the rotation speed, which increases as density is lowered.

If neoclassical theory is correct (this aspect is in question), the poloidal plasma rotation and the ITG are intimately linked. Indeed, the poloidal rotation is directly proportional to the temperature gradient, leading to almost complete cancellation of these two terms in Eq. (1) in the banana regime if the theory is correct [Staebler (1997)]. The portion of neoclassical theory which makes this prediction is the same portion which leads to the prediction of the bootstrap current, which has been experimentally verified. A key question that we will confront experimentally is whether the predicted cancellation of these two terms is true. If it is, attempting to manipulate  $E_r$  through temperature gradient modifications would be fruitless. However, there are theoretical indications that turbulent Reynolds stress can break this connection between poloidal rotation and temperature gradient, which would open up other avenues for control of  $E_r$ . Localized heating, for example with ECH, could then be used to manipulate  $E_r$ .

If, as was discussed above, temperature gradients are ineffective at producing a transport barrier, then the role of control of the density profile takes on great importance. A transport barrier formed from a density gradient has the added advantage of producing more bootstrap current for a given pressure gradient. Our on-going transport simulation

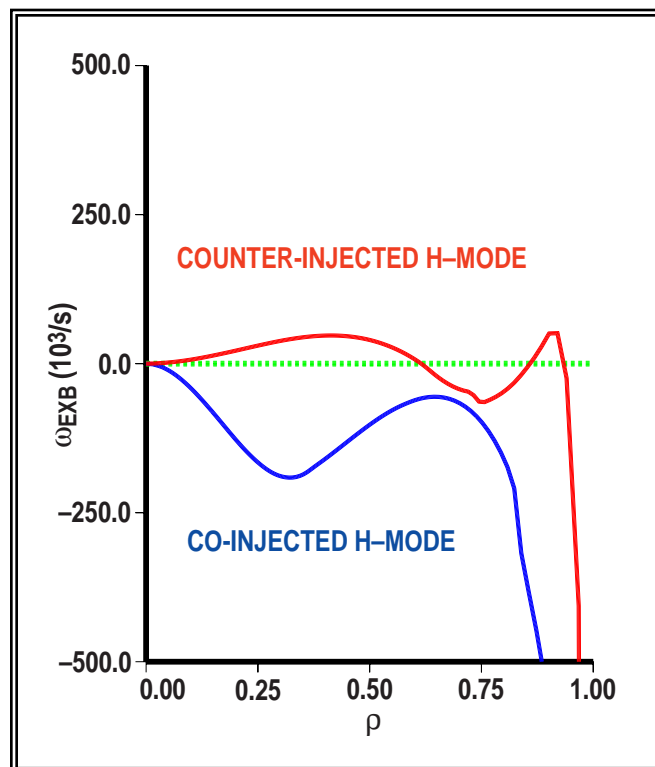


Fig. 2.3–2. An opposing NB will enable transport barrier control through manipulation of  $E \times B$  shear.

work with ONETWO using the transport model shown in Fig. 2.3–1 has shown the density gradient can dominate the transport barrier formation and the current profile through its strong bootstrap contribution. Density gradient transport barriers may have been formed close to the plasma center in DIII–D, but the lack of Thomson scattering data in the core has prevented a definitive study. A core Thomson system is proposed in the next plan period. The science involved in density control is the physics of particle transport. The tools available to manipulate the density are core fueling with NBs and pellets and edge pumping with the divertor cryopumps. One theory of the L–H transition considers the strongly spatially varying edge neutral fueling as the trigger mechanism through the density feedback loop in Fig. 2.3–1. We will seek to intervene in this mechanism by restricting the neutral source available to the core plasma using the well baffled RDP divertor. A possible use of Compact Toroid injection to develop a fueling technique for future tokamaks is described in Section 2.5. Fundamental investigations of particle transport in the presence of  $E \times B$  shear, coupled with these tools, will allow us to manipulate the density profiles to optimize the transport barriers.

Since the general geometry form for the  $E \times B$  shearing rate involves both electric and magnetic shear [Hahm (1995)], shaping of the current profile is an important tool for the control of transport barriers in addition to its importance for improving MHD stability. Figure 2.3–1 shows the loop in which the current profile affects both the turbulence shearing rate and decorrelation rate. Small or reverse magnetic shear may just be the mechanism to lower the growth rates in NCS discharges. We plan to intervene in this loop using the sources of noninductive current drive (ECCD and FWCD) planned for DIII–D.

Most of the discussion in this section has been devoted to improving transport barriers. However, there are cases where the barriers are already too good and some reduction would be appropriate. For example, the VH–mode phase of discharges in DIII–D is terminated by an MHD event (kink mode) which is triggered when gradients in the plasma edge become too steep. Control of the edge gradient to extend the VH–mode to steady state is an important topic for our research. This could be achieved either through plasma shaping, bringing on the onset of ELMs before the kink mode strikes, or possibly by edge radiation, similar to the work that is discussed later for the RI–mode.

**2.3.1.3. ANOMALOUS ELECTRON TRANSPORT.** Control of plasma transport via theoretically predicted  $E \times B$  shear regulation of turbulence levels has culminated in neoclassical levels of ion thermal transport across the entire plasma radius on DIII–D. However, while ion transport can now be controlled, transport in the electron channel is still a puzzle. Part of the puzzle is the variability in results from machine to machine; on TFTR no improvement in electron transport is observed, on DIII–D modest improvements are observed on occasion but not always, while on JT–60U reduced electron transport is routinely observed in NCS discharges. An example of DIII–D data showing neoclassical levels of ion transport, while electron transport remains anomalous is shown in Fig. 2.3–3. Thus, the central remaining challenge in understanding turbulence and transport in fusion plasmas is the determination of what mechanisms are responsible for anomalous electron transport and how can electron transport be controlled?

DIII–D has unique capabilities to address and clarify this issue of anomalous electron transport. First, DIII–D has a uniquely comprehensive set of turbulence and transport diagnostics, with excellent spatial and temporal coverage. We believe that the current combination of advanced diagnostic development capabilities, detailed transport measurement and analysis capabilities, and close coupling to theory make



are competitive with statistical global scaling law descriptions (given H-mode boundary conditions.) In particular, the theoretical models with E×B shear stabilization are able to describe core transport barriers [Waltz (1997)]. On the other hand, it appears that best fitting model may not be significantly better than several good models using standard L- and H-mode data sets (e.g., 15% versus 25% deviations). Further, the database does not clearly distinguish models with radically different underlying physics [e.g., ITG models versus current diffusive ballooning mode (CDBM) or inertial MHD]. The U.S. modeling community is largely in agreement on the basic correctness of the standard picture with ITG and trapped electron core modes and resistive edge modes consistent with gyrokinetic stability and gyrofluid nonlinear simulations. Nevertheless, there is no direct evidence for the existence of the ITG critical gradient length and its demonstration is of highest priority. A DIII-D working group has planned experiments to demonstrate the critical gradient by ECH modulation studies. These exploit the unique feature that the critical gradient decreases with increasing  $T_e/T_i$  which leads to a phase reversal of the pulses (hot pulse propagating to cold pulse and vice versa, perhaps, as seen in TEXT and TFTR). Careful modeling of the pulses should distinguish ITG from CDBM models. The current ITG models also differ greatly in stiffness ( $\chi_{\text{heat-pulse}}/\chi_{\text{power-balance}}$ ) and from preliminary modeling, we expect that the amplification of the ECH-induced electron and ion temperature pulses to measurably differ. Additional studies along this line are possible looking at L–H transition edge front propagation and pellet perturbations.

**2.3.1.5. TRANSPORT SCALING USING DIMENSIONLESS PARAMETERS.** The related methods of dimensional analysis, similarity, and scale invariance in physics provide a powerful technique for analyzing physical systems. The application of these techniques to various approximations of the Vlasov-Maxwell system of equations yield sets of dimensionless parameters that characterize the plasma dynamics [Kadomtsev (1975), Connor (1977)]. For example, the scale invariance principle leads to the thermal diffusivity being written in the form

$$\chi = \chi_B F(\rho_*, \beta, \nu_*, q \dots) \quad , \quad (2)$$

where  $\chi_B$  is the Bohm diffusion coefficient,  $\rho_*$  is the normalized Larmor radius,  $\beta$  is the plasma beta,  $\nu_*$  is the collisionality,  $q$  is the safety factor and the function  $F$  depends upon the specific transport mechanism. Since the scale invariance principle can serve as a framework for an empirical as well as a theoretical approach to plasma physics, recently there has been interest in measuring the dependence of the plasma transport on the dimensionless parameters in Eq. (2). This allows one to differentiate between various proposed instability mechanisms for turbulent transport and has important implications for the scaling of fusion devices to the ignition regime.

The invariance approach to confinement physics makes it possible to determine the required size for an ignition device based upon data from a single machine. This eliminates the possibility of systematic machine-to-machine differences in confinement skewing the ignition projections. Existing fusion experiments such as DIII-D can operate with all of the dimensionless parameters at values expected for ignition devices with the exception of  $\rho_*$ . In particular, DIII-D discharges with ITER dimensionless parameters

(including  $T_i/T_e$ ) the same except  $\rho_*$  have been demonstrated [Petty (1997)]. The heat and particle transport from DIII-D can, therefore, be scaled to larger devices by decreasing  $\rho_*$  while keeping the other dimensionless parameters fixed. GyroBohm-like transport, for which  $F$  is proportional to  $\rho_*$ , projects to ignition in much more compact devices than Bohm-like transport, for which  $F$  is independent of  $\rho_*$  [Petty (1997)]. Therefore, if high confinement is desired for a compact ignition device in the future, it is important to identify a robust gyroBohm-like confinement mode in present day machines. On the other hand, if a mode of apparently high confinement in present day machines is found to have worse-than-Bohm  $\rho_*$  scaling, then it will not scale attractively to future devices.

The scaling of transport with dimensionless parameters also illuminates the underlying physics of anomalous transport. For example, the  $\rho_*$  scaling distinguishes between short wavelength (gyroBohm) and long wavelength (Bohm) turbulent transport models, the  $\beta$  scaling differentiates between electrostatic and electromagnetic mechanisms, and the  $v_*$  scaling discriminates between dissipative trapped particle modes and  $\eta_i$  (or collisionless trapped electron) modes. Initial experiments have begun on DIII-D to measure the dimensionless parameter scaling of transport for a few basic regimes, as shown in Table 2.3–1. This table shows that progress has been made for L-mode and ELMing H-mode plasmas; however, advanced modes of operation such as NCS, high- $\ell_i$  and VH-mode have not been studied yet. The differences between the L-mode and H-mode results have demonstrated that different ion physics are important in these two regimes, and certain classes of turbulent transport mechanisms have already been ruled out. The DIII-D Program intends to complete these dimensionless parameter scaling studies for the various advanced modes shown in the table. The result will be a scaling principle for both the anomalous and residual transport parts of the transport coefficients in Fig. 2.3–1. Dimensionless parameter scaling studies require carefully prepared discharge parameters, which is difficult to do in transient situations. That is the main reason why the advanced modes in Table 2.3–1 have not been studied. Solution of the stability problems discussed in Section 2.3.2 and the extension of the advanced modes to long pulse will be the key to enabling these dimensionless parameter studies.

**TABLE 2.3–1**  
**RESULTS OF DIMENSIONLESS PARAMETER SCALING EXPERIMENTS**  
**IN DIII-D FOR VARIOUS REGIMES**

Regime	$\rho_*$	$\beta$	$v_*$	$q$
L-mode ELM-free H-mode	$\chi_e \propto \rho_*, \chi_i \propto \rho_*^{-1/2}$	$\chi_e, \chi_i \propto \beta^0$	$\chi_e, \chi_i \propto v_*^0$	
ELMing H-mode VH-mode NCS High- $\ell_i$	$\chi_e, \chi_i \propto \rho_*$	$\chi_e \propto \beta^0, \chi_i \propto \beta^{-1}$	$\chi_{\text{eff}} \propto v_*^{1/3}$	

**2.3.1.6. FUEL AND IMPURITY ION TRANSPORT.** As was discussed in Section 2.3.1.2 above, the possibility that temperature gradients may not be effective in creating transport barriers places increased emphasis on studying transport barrier formation using density gradients. Moreover, density gradients are more effective at producing bootstrap current than temperature gradients. The study of fuel particle transport is closely coupled to the divertor physics discussed in Section 2.3.3 below since the recycling from the divertor plates is ultimately the neutral source for the core plasma. In practical terms, the fitting of the divertor parameters with the SOL modeling code UEDGE and Monte Carlo neutral codes [DEGAS, EIRENE, and a code under development at Massachusetts Institute of Technology (MIT)] is how the neutral source for the core plasma gets determined. A program of study to use divertor baffling to alter the core fueling from the divertor and perhaps affect the core plasma confinement is described in Section 2.3.3.2. Pellet and NB sources are available for deep fueling of the core. The pellet system makes possible transient transport experiments.

Electron particle transport coefficients for L-mode, ELM-free H-mode and ELMing H-mode have been measured using deuterium gas puffing into DIII-D and modeling of the density rise after the L-H transition. For L-mode and ELMing H-mode plasmas, the diffusion coefficient ( $D$ ) increases with  $\rho$ , rising at the edge to several times that of the center. The central values of  $D$  are about the same in both modes, but for L-mode the edge value is almost twice that for ELMing H-mode. In ELM-free H-mode, the central value of  $D$  is also about the same as in the other modes, but the edge value decreases to approximately one-fifth of the central value.

A physics based model which predicts the steady-state density profile in tokamak plasmas with high transport has been developed and compared with measured profiles. The resulting steady-state profiles are independent of the absolute magnitude and the radial dependence of the particle diffusion coefficient but does depend on the relative transport of trapped versus passing particles. This model is valid for ohmic, L-mode and ELMing H-mode plasmas.

The plans for the future include a sequence of experiments which will measure the electron particle transport coefficients and energy transport coefficients for identical plasmas. Comparing the particle and energy transport will further elucidate the physical mechanisms responsible for the transport in different confinement regimes.

**Helium Transport.** The efficient transport and removal of helium ash is an integral part of any fusion-based power plant solution. Over the past few years, DIII-D has carried out an intensive experimental campaign to assess helium transport and exhaust in a variety of confinement modes with particular emphasis placed on ELMing H-mode. The main results of these studies can be summarized as follows: (1) helium exhaust rates sufficient for a reactor (i.e., exhaust efficiency of the pump and not by the core transport rate of helium); (2) no preferential peaking of the helium density profile (relative to the electron density profile) has been observed in any confinement regime including VH-mode and NCS discharges; and (3) scaling path to ITER (i.e., they have the same collisionality,  $\beta$ ,  $q$ , etc.). These results have convinced the ITER JCT that helium transport rates in ITER should not be a limiting factor in the ITER design.

As part of this five-year plan, it is envisioned that the same type of experimental studies will be carried out with particular emphasis placed on characterizing helium transport in enhanced confinement regimes, especially those based on core transport barriers. These regimes offer the potential advantage of improved energy transport and stability, but these improvements may be mitigated by reduced helium transport rates, leading to unacceptable levels of fuel dilution. Many of the tools that were used for the studies outlined above are expected to be upgraded substantially. The charge exchange recombination (CER) spectroscopy system has 40 channels with 8 channels specifically devoted to impurity density profile measurements, allowing helium transport data to be obtained in piggyback mode. The addition of two inner-strikepoint divertor cryopumps will increase the flexibility in exhausting helium as it appears from spectroscopic measurements that the helium density on the inboard side of the divertor is substantially larger than that at the outboard side at the outer strike point.

**Impurity Transport.** Contamination of the plasma fuel from impurities either generated from interactions between the edge plasma and plasma facing surfaces or intentionally injected to aid in dissipating the plasma energy flow to these surfaces via radiation is inevitable. In this regard, it is important to understand the core transport properties of these impurities both in terms of controlling the impurities and also in taking advantage of the natural transport properties of the impurities. In this regard, several studies have been carried out on DIII-D using the CER system and small, nonperturbative gas puffs from the plasma edge. The results of these studies to date can be summarized as follows: (1) in L-mode and H-mode, the transport properties of all low- $Z$  impurities (including helium, carbon, nitrogen, and neon) is approximately the same with the steady-state density profile for these impurities being the same as the electron density profile; and (2) in VH-mode plasmas, the transport properties of helium is considerably different than those for carbon and neon (e.g., the helium density profile is the same as the electron density profile but the profiles for carbon and neon are extremely hollow). As the electron density profile in VH-mode is generally quite flat, this hollowness is suggestive of a “temperature” screening effect predicted by neoclassical theory. Although the connection with theory has not been completed yet, the existence of such a screening effect has the natural outcome that plasmas with flat electron density profiles will inevitably have hollow impurity density profiles, provided the collisionality of the impurity is in the proper range. If this effect could be coupled with the impurity enrichment results outlined in Section 2.3.3.1, an attractive solution for impurity and radiation control would be possible.

As confinement regimes with ion energy transport near neoclassical levels have been obtained on DIII-D, a natural extension of these studies for the five-year plan would be an assessment of neoclassical impurity transport and the ramifications of the obtained transport properties (neoclassical or anomalous) on the performance of these regimes. The  $Z$ -dependence of the transport properties is an important clue as to the nature of the transport since anomalous transport is expected to  $Z$ -independent (i.e., transport driven by electrostatic fluctuations) and neoclassical transport is strongly dependent on the impurity charge. DIII-D is equipped with a 40-channel CER system capable of measuring the density profile of two impurities simultaneously and has the capability of introducing many different impurities through gas puffing or via small pellets of various impurities using the lithium pellet injector.

**2.3.1.7. L–H TRANSITION PHYSICS.** Studies of L–H transition physics have elucidated the crucial role of  $E \times B$  shear effects in modifying transport in magnetized plasmas and have provided a paradigm for transport barrier formation which has been quickly transferred to the study of core transport barriers in tokamaks. Achieving the long term goal of understanding the physics of the H–mode transition now requires a much deeper qualitative and quantitative confrontation of theory and experiment in order to understand the local conditions required to produce the H–mode state. From the theoretical side, this confrontation is being made possible by present and anticipated advances which include increasingly realistic models of the relevant edge physics, including finite beta and diamagnetic effects, the effects of neutrals, and the connection between the edge (confined) plasma and the SOL plasma. From the experimental side, the confrontation is being furthered by the maturing of edge diagnostics and the development of increasingly sophisticated techniques for the analysis of the resulting data. L–H studies in DIII–D will provide data required to quantitatively evaluate L–H transition models based on physics mechanisms such as those listed in Table 2.3–2. These measurements will utilize existing DIII–D capabilities to measure edge density and temperature profiles (of both electrons and ions), edge rotation and radial electric field profiles, the edge magnetic shear, edge density and potential fluctuations, and the turbulent-driven particle flux. Existing divertor diagnostics will be used to measure or compute divertor quantities including the electron temperature and density, radiated power, the spatial distribution of deuterium neutrals and cross field fluxes of particles and heat due to neoclassical  $\text{grad-B}$  drift effects. On-going diagnostic developments are expected to provide measurements of edge electron temperature fluctuations and estimates of the turbulent-driven Reynolds stress. An important aspect of future experimental studies will be to provide databases of relevant data for comparison with theoretical models of the transition.

**TABLE 2.3–2**  
**TOOLS FOR L–H TRANSITION PHYSICS STUDIES**

Physics Mechanism	Measurement	Tools
Turbulence-generated flows	Reynolds stress, main ion rotation	C–coil
Pressure gradients	Edge temperature and density profiles	Pellets, ECH
Ion diamagnetism	Edge ion temperature and density	Pellets
Flows driven by ion orbit loss	Main ion rotation, orbit calculations	RDP, counter beam

The program outlined above must be augmented by additional studies in order to more clearly differentiate between the different possible physics mechanisms for the transition. In DIII–D, this will be done by developing perturbative techniques, as suggested in Table 2.3–2, which can perform the required discrimination. These techniques, which can be attempted with existing DIII–D hardware capability (including some anticipated modifications to the pellet injection system), include modulating plasma flows with the C–coil, modulating the edge pressure and density profiles with shallow pellet injection, modulating the edge electron temperature with edge ECH heating, and altering the neutral distributions around the

plasma using the baffled RDP system. These techniques and this work will also be directly relevant to active control of the H-mode transition — another long-term goal of L–H studies.

**2.3.1.8. THE H-MODE SHEAR LAYER AND PEDESTAL.** Stiff turbulent transport models [Kotschenreuter (1996), Waltz (1996)] predict an improvement of the global energy confinement with increasing H-mode pedestal temperature. This is consistent with the DIII–D data in that the energy confinement enhancement factor,  $H$ , is positively correlated with the pedestal electron pressure (Fig. 2.3–4). The factors which may play a role in setting the pedestal parameters are: (1) the parameters that set the width of the H-mode transport barrier, which could relate to such things as ion poloidal gyroradius, [Kikuchi (1993)] or the edge particle source; (2) the critical parameters for the ELM instability which may be related to ballooning modes although ballooning modes may set the edge pressure gradient but not be the ELM trigger; and (3) the divertor conditions which may set a boundary condition on the open field lines.

In the DIII–D ITER shape database, the width of the ELMing H-mode transport barrier,  $\Delta$ , is fit equally well by  $(\beta_p^{\text{PED}})^{1/2}$  or  $(\rho_{\text{pol}}^{\text{PED}})^{2/3}$ . These two scalings, along with ballooning mode scaling of the edge pressure gradient, give an edge temperature of 6 and 1 keV respectively for ITER, which would significantly affect the fusion power output according to the Institute for Fusion Studies — Princeton Plasma Physics Laboratory (IFS–PPPL) model. [Kotschenreuter (1997)]. The uncertainty in choosing between these scalings is due largely to the correlation between density and current in H-mode. More work is needed on DIII–D and in intermachine comparison (perhaps through the ITER database) to distinguish these scalings and to understand if other variables such as divertor effects are important.

Many of the H-mode pedestal parameters cycle between ELMs. Although it is not completely clear that the ballooning mode is the trigger of the Type I ELM, several experiments indicate that the edge pressure gradient before the ELM scales consistently with what would be expected for ideal ballooning. Comparison with ballooning mode stability calculations did not give quantitative agreement. It is difficult to predict, at present, what edge pressure gradient would be obtained in ITER.

Further work needs to be done relating the divertor conditions to the H-mode pedestal parameters. In some theories [Hinton (1992)], the edge turbulence suppression zone can be set by the edge particle source. There is also evidence

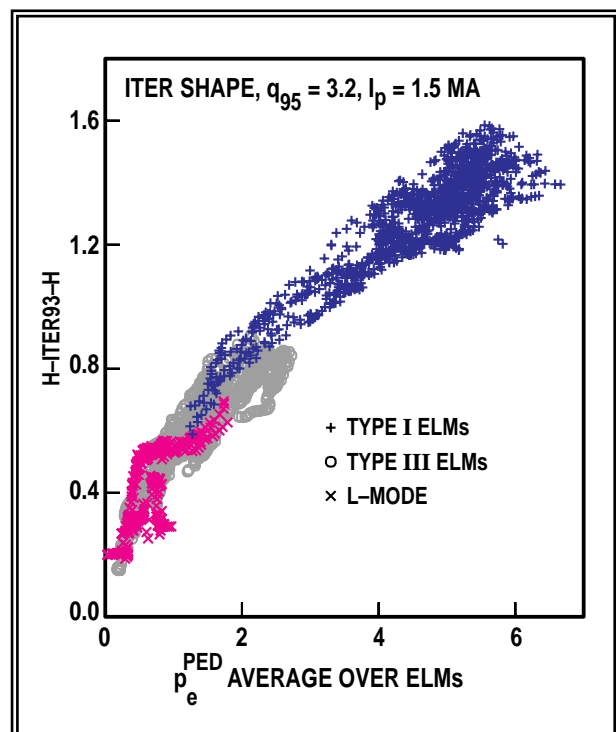


Fig. 2.3–4. Energy confinement enhancement factor increases with pedestal pressure in ITER shape discharges consistent with stiff turbulent transport models.

that resistivity may play a role in the ELM stability, in particular, for Type III ELMs. One might also expect that the separatrix values of temperature and density would be strongly affected by the neutral fueling that escapes the divertor and that these values would be combined with the H-mode transport barrier to set the pedestal values.

**2.3.1.9. CORE RADIATIVE MANTLE AND LIMITER PLASMA REGIMES.** Discharges with a highly radiating mantle and ELM free H-mode energy confinement have many advantages for future fusion devices such as ITER. The radiating mantle keeps edge temperatures and physical sputtering to acceptable values and limits long-term wall erosion. Under some conditions, radiative mantle discharges have no ELMs, eliminating potential problems associated with transient heat pulses. H-mode confinement scaling provides the confinement enhancement for a radiating mantle fusion device to ignite if core impurities can be minimized. Recent work on the TEXTOR tokamak has demonstrated that such discharges [named radiating improved confinement mode (RI-mode)] can be maintained for up to 100 energy confinement times using neon or silicon to produce a radiating mantle with little increase in central impurity accumulation [Messiaen (1996)]. These discharges were obtained using a pumped limiter geometry.

We propose to extend the work done on TEXTOR by performing radiating mantle experiments on DIII-D. The DIII-D shaping and diagnostics capabilities will complement the TEXTOR work and explore several key physics issues such as the role of rotation in radiating mantle discharges, the possible existence of transport barriers, the effect of shape (elongation and divertors), size scaling, power thresholds, core impurity influx, and potential reductions in density fluctuations (both edge and core). In addition, we will explore “parameter space” in these discharges, particularly, the issue of extending radiating mantle quasi-steady-state discharges to higher values of  $\beta_N H$ . The recent addition of the high triangularity upper DIII-D cryopump will allow pumping of marginally limited discharges, allowing more effective control of the edge neon radiation, found to be important for TEXTOR in operating at  $P_{\text{rad}}/P_{\text{in}}$ . This work on radiating mantle discharges lies in the general line of using core plasma radiation to produce an L-mode edge or at least an edge with a lower pressure gradient, one of the approaches to promoting longer pulse operation of advanced core modes as discussed in Section 2.3.2.

A primary goal of this DIII-D work will be to develop a physics understanding of the underlying mechanisms leading to high confinement discharges with low temperature radiating mantles. For example, Becker (1996) has examined radiating mantle CDH-mode discharges and found that the density profile peaking is a function of  $Z_{\text{eff}}$  and that the inward pinch term,  $v_{\text{in}}$ , is proportional to  $Z_{\text{eff}}$ . We propose to extend this work to radiating mantle discharges in DIII-D. If this model is valid for DIII-D discharges, it will be useful in predicting impurity profiles which can minimize central impurity accumulation while maintaining H-mode with low edge temperatures.

### References for Section 2.3.1

- Becker, G., Nucl. Fusion **36**, 1751 (1996).
- Beer, M.A., and G.W. Hammett, Phys. Plasmas **3**, 4046 (1996).
- Bernabei, S., R. Bell, M. Chance, T.K. Chu, M. Coneliussen, W. Davis G. Gettlefingher, T. Fibney, N. Greenough, R. Hatcher, H. Hermann, D. Ignat, S. Jardin, R. Kaita, S. Kaye, C. Kessel, T. Koaub, H. Kugel, L. Lagin, B. LeBlanc, J. Manickam, M. Okabayshi, H. Oliver, M. Ono, S. Paul, S. Preische, P. Roney, N. Sauthoff, S. Schweitzer, S. Sesnic, Y. Sun, H. Takahashi, W. Tighe, E. Valeo, S. von Goeler, K. Voss, M. Mauel, G. Navratil, R. Cesario, S. Batha, F. Levinton, F. Rimini, N. Asakura, S. Jones, J. Kesner, S. Luckhardt, F. Paoletti, P. Woskow, A. Zolfaghari, T. Seki, J. Bell, J. Dunlap, A. England, D. Greenwood, J. Harris, G. Henkel, S. Hirshman, R. Isler, D. Lee, L. Blush, R. Conn, R. Doerner, Y. Hirooka, R. Lehmer, L. Schmitz and G. Tynan, Phys. Fluids B **5**, 2562 (1993).
- Biglari, H., P.H. Diamond, and P.W. Terry, Phys. Fluids B **2**, 1 (1990).
- Biglari, H., M. Ono, P.H. Diamond, G.G. Craddock, in Proc. 9th Top. Conf. on Radio-Frequency Power in Plasmas, Charleston, 1991 [American Institute of Physics, New York (1992)] Vol. 244, p. 376.
- Burrell, K.H., Phys. Plasmas **4**, 1499 (1997).
- Burrell, K.H., M.E. Austin, T.N. Carlstrom, S. Coda, E.J. Doyle, P. Gohil, R.J. Groebner, J. Kim, R.J. La Haye, L.L. Lao, J. Lohr, R.A. Moyer, T.H. Osborne, W.A. Peebles, C.L. Rettig, T.L. Rhodes, D.M. Thomas, Plasma Physics and Controlled Nuclear Fusion Research 1994 [International Atomic Energy Agency, Vienna (1995)] Vol. 1, p. 221.
- Carreras, B.A., K. Sidikman, P.H. Diamond, P.W. Terry and L. Garcia, Phys. Fluids B **4**, 3115 (1992).
- Chiueh, T., Ph.D. Thesis, University of Texas (1985).
- Connor, J.W., and J.B. Taylor, Nucl. Fusion **17**, 1047 (1977).
- Diamond, P.H., V.B. Lebedev, D.E. Newman, B.A. Carreras, T.S. Hahm, W.M. Tang, G. Rewoldt, K. Avinash, Phys. Rev. Lett. **78**, 1472 (1977).
- Dominguez, R.R., and G.M. Staebler, Phys. Fluids B **5**, 3876 (1993).
- Greenfield, C.M., B. Balet, K.H. Burrell, M.S. Chu, J.G. Cordey, J.C. DeBoo, N. Deliyianakis, E.J. Doyle, R.J. Groebner, G.L. Jackson, S. Konoshima, D.P. O'Brien, L. Porte, C.L. Rettig, T.H. Osborne, H. St. John, A.C.C. Sips, G.M. Staebler, E.J. Strait, P.M. Stubberfield, T.S. Taylor, S.J. Thompson, K. Thomsen, A.D. Turnbull, and The JET and DIII-D Teams, Plasma Physics and Controlled Fusion **35**, B263 (1993).
- Hahm, T.S., and K.H. Burrell, Phys. Plasmas **2**, 1648 (1995).
- Hassam, A.B., Comments Plasma Phys. Controlled Fusion **14**, 275 (1991).
- Hinton, F.L., and G.M. Staebler, Phys. Fluids B **5**, 1281 (1993).
- Hinton, F.L., and G.M. Staebler, Proc. 14th Int. Conf. on Plasma Physics and Controlled Nuclear Fusion Research, October 1992, Würzburg [International Atomic Energy Agency, Vienna, (1993)] IAEA-CN-56/A4-17.

- Hunt, J.C.R., et al., in *New Perspectives in Turbulence* [Springer Verlag, New York (1991)] p. 55.
- Kadomtsev, B.B., *Sov. J. Plasma Phys.* **1**, 295 (1975).
- Kikuchi, M., et. al, “Hot Ion H-mode Characteristics in JT-60U,” *Proc. Euro. Conf. on Controlled Fusion and Plasma Physics*, Lisbon, 1993, I-179.
- Kimura, H., the JT60 Team, *Phys. Plasmas* **3**, 1943 (1996).
- Konings, J.A., and R.E. Waltz, “Comparison of Transport Models with a Transport Profile Database,” to be published in *Nucl. Fusion* (1997).
- Kotschenreuter, M., et al., “First Principles Calculations of Tokamak Transport,” in *Proc. 16th Int. Conf. on Plasma Physics and Controlled Nuclear Fusion Research*, October 1996, Montréal, [International Atomic Energy Agency, Vienna (1997)] IAEA-F1-CN-64/D1-5.
- Kotschenreuter, M., and W. Dorland, “Memorandum on Confinement Projections,” FESAC ITER Review, December 14, 1997.
- La Haye, R.J., T.H. Osborne, C.L. Rettig, C.M. Greenfield, A.W. Hyatt, J.T. Scoville, *Nucl. Fusion* **35**, 988 (1995).
- Lao, L.L., K.H. Burrell, T.S. Casper, V.S. Chan, M.S. Chu, J.C. DeBoo, E.J. Doyle, R.D. Durst, C.B. Forest, C.M. Greenfield, R.J. Groebner, F.L. Hinton, Y. Kawano, E.A. Lazarus, Y.R. Lin-Liu, M.E. Mauel, W.H. Meyer, R.L. Miller, G.A. Navratil, T.H. Osborne, Q. Peng, C.L. Rettig, G. Rewoldt, T.L. Rhodes, B.W. Rice, D.P. Schissel, B.W. Stallard, E.J. Strait, W.M. Tang, T.S. Taylor, A.D. Turnbull, R.E. Waltz, and the DIII-D Team, *Phys. Plasmas* **3**, 1951 (1996).
- Lao, L.L., J.R. Ferron, T.S. Taylor, K.H. Burrell, V.S. Chan, M.S. Chu, J.C. DeBoo, E.J. Doyle, C.M. Greenfield, R.J. Groebner, R.A. James, E.A. Lazarus, T.H. Osborne, H. St. John, E.J. Strait, S.J. Thompson, A.D. Turnbull, D. Wróblewski, H. Zohm, and the DIII-D Team, *Phys. Rev. Lett* **70**, 3435 (1993).
- Lazarus, E.A., G.A. Navratil, C.M. Greenfield, E.J. Strait, M.E. Austin, K.H. Burrell, T.A. Casper, D.R. Baker, J.C. DeBoo, E.J. Doyle, R. Durst, J.R. Ferron, C.B. Forest, P. Gohil, R.J. Groebner, W.W. Heidbrink, R.-M. Hong, W.A. Houlberg, A.W. Howald, C.-L. Hsieh, A.W. Hyatt, G.L. Jackson, J. Kim, L.L. Lao, C.J. Lasnier, A.W. Leonard, J. Lohr, R.J. La Haye, R. Maingi, R.L. Miller, M. Murakami, T.H. Osborne, L.J. Perkins, C.C. Petty, C.L. Rettig, T.L. Rhodes, B.W. Rice, S.A. Sabbagh, D.P. Schissel, J.T. Scoville, R.T. Snider, G.M. Staebler, B.W. Stallard, R.D. Stambaugh, H.E. St. John, R.E. Stockdale, P.L. Taylor, D.M. Thomas, A.D. Turnbull, M.R. Wade, R. Wood, and D. Whyte, *Phys. Rev. Lett.* **77**, 2714 (1996).
- Lebedev, V.B., P.H. Diamond, M.B. Isichenko, P.N. Yushmanov, D.E. Newman, B.A. Carreras, V.E. Lynch, T.S. Hahm, W.M. Tang, G. Rewoldt, K. Avinash, and A. Smolyakov, “Developments in the Theory of Core and Edge Plasma Transport Barrier Dynamics and Control,” to be published in *Plasma Physics and Controlled Nuclear Fusion Research 1996* (International Atomic Energy Agency, Vienna).

- Mazzucato, E., S.H. Batha, M. Beer, R.E. Bell, R.V. Budny, C. Bush, T.S. Hahm, G.W. Hammett, F.M. Levinton, R. Nazikian, H. Park, G. Rewoldt, G.L. Schmidt, E.J. Synakowski, W.M. Tang, G. Taylor and M.C. Zarnstorff, *Phys. Rev. Lett.* **77**, 3145 (1996).
- Messiaen, A., et al., APS–DPP invited talk (1996), to be published in *Phys. Plasmas* (1997).
- Petty, C.C., and T.C. Luce, *Nucl. Fusion* **37**, 1 (1997).
- Scott, B.D., P.W. Terry, and P.H. Diamond, *Phys. Fluids* **31**, 1481 (1988).
- Shaing, K.C., E.C. Crume, Jr., and W.A. Houlberg, *Phys. Fluids B* **2**, 1492(1990).
- Staebler, G.M., R.R. Dominguez, *Nucl. Fusion* **31**, 1891 (1991).
- Staebler, G.M., and F.L. Hinton, *Phys. Plasmas* **1**, 909 (1994).
- Staebler, G.M., R.E. Waltz, J.C. Wiley, *Nucl. Fusion* **37**, 287(1997).
- Strait, E.J., L.L. Lao, M.E. Mauel, B.W. Rice, T.S. Taylor, K.H. Burrell M.S. Chu, E.A. Lazarus, T.H. Osborne, S.J. Thompson, and A.D. Turnbull, *Phys. Rev. Lett.* **75**, 4421 (1995).
- Ushigusa , K., and the JT–60 Team, “Steady State Operation Research in JT–60U,” to be published in *Plasma Physics and Controlled Nuclear Fusion Research 1996* (International Atomic Energy Agency, Vienna)..
- Waltz, R.E., et al, “A Comprehensive Gyro-Landau Fluid Transport Model,” in *Proc. 16th Int. Conf. on Plasma Physics and Controlled Nuclear Fusion Research, October 1996, Montréal* [International Atomic Energy Agency, Vienna (1997)] IAEA-F1-CN-64/D1-6.
- Waltz, R.E., G.D. Kerbel, J. Milovich, and G.W. Hammett, *Phys. Plasmas* **2**, 2408 (1995).
- Waltz, R.E., G.M. Staebler, W. Dorland, G.W. Hammett, M.Kotschenreuther, and J.A. Konings, “A gyro-Landau-fluid transport model,” to appear in *Phys. Plasmas*.
- Wang, X.-H., P.H. Diamond, and M.N. Rosenbluth, *Phys. Fluids B* **4**, 2402 (1992).
- Zohm, H., et al, “Study of H–mode Physics on ASDEX Upgrade,” *Proc. 16th Int. Conf. on Plasma Physics and Controlled Nuclear Fusion Research, October 1996, Montreal* [International Atomic Energy Agency, Vienna (1997)] IAEA-F1-CN-64/A5-1.

## 2.3.2. STABILITY SCIENCE

*The goals of the DIII–D stability program are to advance the understanding of MHD stability in high performance tokamak plasmas, and to develop active and passive means of improving tokamak stability up to the theoretically predicted limits, ultimately leading to the DIII–D long-term goal of an integrated demonstration of optimized performance through active control. This program will help provide the scientific foundation for improvement of the tokamak concept toward a more compact, economical, and reliable device.*

*Stable operation at high beta is essential for ITER or other next-generation tokamaks as well as for “advanced” tokamaks. The past decade of tokamak research has seen much theoretical and experimental progress in understanding the dependence of ideal and resistive MHD stability limits on the pressure, current density and rotation profiles and the presence of a conducting wall. New operating regimes have been explored which have both good stability properties and enhanced energy confinement, in particular the VH–mode, high  $\ell_p$ , and NCS regimes. The desire to develop plasmas capable of steady-state operation now adds another constraint, that the pressure and current density profiles be consistent with a large fraction of bootstrap current. The DIII–D stability program, while continuing to advance the understanding in these areas, will also develop the scientific basis for active control of plasma stability, in order to extend the stability limits and provide more reliable operation near those limits. The goal is reliable operation without disruptions near stability limits and a disruption mitigation strategy for the remaining class of disruptions that occur from random events like material ingress or system faults.*

**2.3.2.1. INTRODUCTION.** Stability at high beta is needed in order to take advantage of regimes of improved energy confinement in creating a compact fusion plasma with high power density. In a steady-state fusion plasma, assuming a fixed plasma size and a simplified form for the energy confinement  $\tau_E \propto H I P_{\text{loss}}^{-1/2}$ , we find that the loss power scales approximately as  $P_{\text{loss}} = W/\tau_E \propto (\beta_N B/H)^2$ , while the ratio of fusion power to loss power scales approximately  $P_{\text{fus}}/P_{\text{loss}} \propto (HB/q)^2$ . The fusion gain  $Q$  increases with  $P_{\text{fus}}/P_{\text{loss}}$ , so the fusion gain can be improved by increasing the confinement factor  $H$ , at a fixed toroidal field  $B$  and safety factor  $q$ . However, if the larger  $Q$  is to translate into greater fusion power rather than

reduced loss power,  $\beta_N$  must increase in proportion to  $H$ . For reasonable neutron wall loading,  $H \sim 4$  and  $\beta_N \sim 6$  are projected by some system studies as optimal for an attractive power plant.

Steady-state operation with low recirculating power for current drive also implies operation at high normalized beta. Maximizing the fusion power  $P_{\text{fus}} \propto p^2 V \propto \beta_t^2 B^4 V$  at fixed toroidal field and plasma volume  $V$  calls for maximizing the toroidal beta  $\beta_t$ . On the other hand, steady-state operation requires a large bootstrap current fraction  $f_{\text{bs}} = I_{\text{bs}}/I \propto \epsilon^{1/2} \beta_p$  which calls for maximizing the poloidal beta  $\beta_p$ . For a fixed plasma shape, the normalized beta can be written as  $\beta_N^2 \propto \beta_t \beta_p$ , so increasing the bootstrap fraction without reducing the fusion power requires increasing the normalized beta.

Reliable operation at high beta without potentially damaging disruptions requires control of the plasma's stability. Operation near stability limits implies that small changes in the plasma profiles can lead to an instability which may damage the vacuum vessel or its internal components. This danger can be avoided by extending the stability limits so that the operating point no longer lies near a limit, by closely controlling the plasma parameters to prevent excursions across a stability boundary, or by mitigating the effects of a disruption when it does occur. All of these avenues will be pursued by the DIII-D stability program.

**Approach.** Tokamak stability research is guided by advances in both physics understanding and research tools. Early work in testing the “Troyon scaling,” [Troyon (1984)] focused largely on limits on global parameters of the plasma with some optimization of profiles, and demonstrated that ideal MHD theory could predict these stability limits with some accuracy. Strong shaping was shown to be important in raising the beta limit. As the subject matured, advances in theory and diagnostic measurements {most notably measurements of the  $q$ -profile [Levinton (1992), Wròblewski (1992)]} led to a more detailed understanding of the role played by the pressure, current density, and rotation profiles in ideal MHD stability. Initial experiments in profile modification have opened several regimes of enhanced confinement and stability, but so far these are achieved only transiently. In many cases the limitations result from nonideal instabilities such as neoclassically destabilized tearing modes and fast particle-driven modes, and the emphasis on understanding these nonideal instabilities will continue to grow. In the future, new tools will allow active control of plasma stability through profile modification, active enhancement of wall stabilization, and direct MHD mode control, leading to improved physics understanding, extension of stability limits, and sustainment of high performance plasmas.

**Research Program.** The DIII-D Stability Science Research Program for the next five years can be separated into five phases: shape and profile optimization, wall stabilization, nonideal instabilities, disruption avoidance and mitigation, and steady-state issues. Although there is some overlap between these topics, the emphasis of the program will shift from one to the next during the five-year period as we work toward the goals of advancing the scientific understanding of tokamak plasma stability and improving the tokamak concept.

In the first phase, we will continue the ongoing work on optimizing the discharge shape and profiles for stability and confinement. As tools for profile control become available, including rf current drive, they will be used to create and modify these optimized profiles. The second phase, emphasizing wall stabilization, grows naturally from the first, since one aspect of profile optimization will be development of profiles which benefit from stabilization by the resistive vacuum vessel wall. Later in the five-year period, external and internal active coils will be installed to enhance and sustain the effects of wall stabilization. The third phase focuses on several types of nonideal MHD instabilities. Both profile control and local current drive at the rational surface will be developed as methods to stabilize resistive modes, in particular neoclassical tearing modes. Internal coils will also be utilized for stabilization of tearing modes through rotation control or direct coupling to the modes. Alfvén eigenmodes, normally driven by fast particles, will be studied by exciting them with the internal coil set. The nonideal physics of disruptions will be studied, and active means of mitigating the effects of disruptions will be explored. Disruption avoidance through profile control and real-time prediction of instability thresholds will be developed in order to enable operation close to stability limits. Techniques to mitigate the consequences of disruption will be developed. In the last phase, all of these techniques will be brought together to maintain the stability of near steady-state discharges at high beta. Such discharges have the additional requirement that the bootstrap current be well aligned with the total current density profile in order to minimize the requirements for noninductive current drive.

**2.3.2.2. SHAPE AND PROFILE OPTIMIZATION.** The distinguishing feature of the AT concept relative to the conventional inductive tokamak scenario embodied in the ITER design, is the focus on enhancing the tokamak performance by taking advantage of the details of the 1-D and 2-D profiles and plasma shape, in contrast to the essentially zero D scalings, such as the Troyon scaling, used to predict or design the conventional scenario. A combination of experiments and theoretical and numerical calculations for AT operating regimes has identified several characteristics of the profiles and cross section shape which are critical in determining the stability limit.

The current density profile (or  $q$  profile) is clearly a crucial determinant of the beta limit since it essentially distinguishes the different AT regimes: low central shear with  $q_0 \sim 1$  and high edge shear for the high  $\ell_i$  regime [Ferron (1990), Navratil (1991), Lao (1993)], nonmonotonic  $q$  with  $q_{\min} > 1$  for the NCS regime [Kessel (1994), Levinton (1995), Strait (1995), Turnbull (1995)], high  $q$  for the high  $\beta_p$  regime [Politzer (1994)], and conventional monotonic  $q$  with  $q_0 \geq 1$  for the VH-mode [Jackson (1992)]. In the high  $\ell_i$  regime, the optimum beta limit is predicted to increase with increasing  $\ell_i$ . Conversely, in the wall-stabilized NCS scenario, the coupling to the wall, and thereby the beta limit is a strong function of lower  $\ell_i$ . This dependence on  $\ell_i$  has been shown by current and elongation ramp experiments; the only clear exceptions to the resulting  $\beta_N \sim 4 \ell_i$  scaling are discharges which appear to be wall stabilized at low  $\ell_i$ . The importance of keeping  $q_0 > 1$  in obtaining high performance has been demonstrated in both VH-mode and NCS discharges in DIII-D. In both these regimes, the edge current density is also a crucial determinant of the beta limit; positive edge current density or an edge current density gradient can seriously degrade the beta limit by destabilizing low to intermediate n edge peeling modes, which often degrade or destroy edge confinement.

The pressure profile peakedness has been found from systematic stability calculations to be a critical parameter in optimizing both the high  $\ell_1$  [Turnbull (1986), Howl (1992)] and NCS scenario [Turnbull (1997a)] beta limits; the ideal  $n = 1$  kink limit increases with broader pressure in both cases. This improvement in the beta limit has been clearly confirmed in both high  $\ell_1$  and NCS configurations — the latter by transitions from L-mode to H-mode which doubled the observed beta limit [Lao (1996)]. The physical reasons for this dependence should apply to the high  $\beta_p$  and VH-mode scenarios as well. In addition, the pressure gradient profile essentially determines the steady-state bootstrap current and therefore affects stability limits through their dependence on the current density profile. This is important when large pressure gradients associated with transport barriers are present since large pressure and current density gradients are generally destabilizing. This is an especially serious concern for the VH-mode and the NCS H-mode scenarios which are presently limited by unstable low  $n$  peeling-like modes; the build up of positive edge current density from finite edge pressure gradients associated with edge transport barriers has been identified as the driving mechanism for the observed modes, and this is presently the major limitation to higher beta in both scenarios.

It has been well-known for some time that the plasma elongation and triangularity are important shape parameters, largely through the increased current carrying capacity of highly elongated Dee-shaped cross sections at fixed  $q$ , but also partly from increases in the normalized beta limit,  $\beta_N = \beta/(I/aB)$  from higher triangularity [Strait (1994)]. The importance of cross section shaping on the operationally achievable beta limit has been clearly demonstrated in both conventional and AT discharges by controlled systematic DIII-D experiments. More recently, other shaping parameters, such as indentation, squareness, up-down asymmetry, and the presence of an external separatrix have been found to also affect the stability. These effects are now being investigated in on-going experiments. Moreover, recent calculations for the NCS configuration have shown that coupled with wall stabilization, the dependence of the beta limit on cross section shape is even stronger than for conventional profiles [Turnbull (1997a)]. The cross section shape and profile dependence are synergistic in the sense that the degree of this enhancement is also strongly dependent on the profiles, especially the pressure profile. Conversely, the sensitivity of the NCS beta limit to the pressure profile peakedness is also strongly dependent on the cross section shaping, ranging from a weak dependence in circular cross section to roughly a factor 2 to 3 increase in beta between L-mode peaked pressure and broad pressure H-mode-like profiles in a strongly Dee shaped cross section (Fig. 2.3–5). This predicted synergistic relationship between shape and pressure optimization for NCS scenarios has not yet been fully demonstrated due to the limited control over the edge pressure and current density profiles achievable up till now. With improved control, the anticipated synergism can be more fully explored and exploited.

Over the past few years, there has been an increased awareness of the importance of the rotation profile in obtaining high performance AT operation. This new awareness was pioneered at DIII-D and is continuing to be pursued. The role of the rotation profile in stabilization of the ideal kink by a resistive wall has been positively identified in controlled experiments. Rotation relative to the resistive wall is now understood to be both necessary and effective for maintaining wall stabilization for

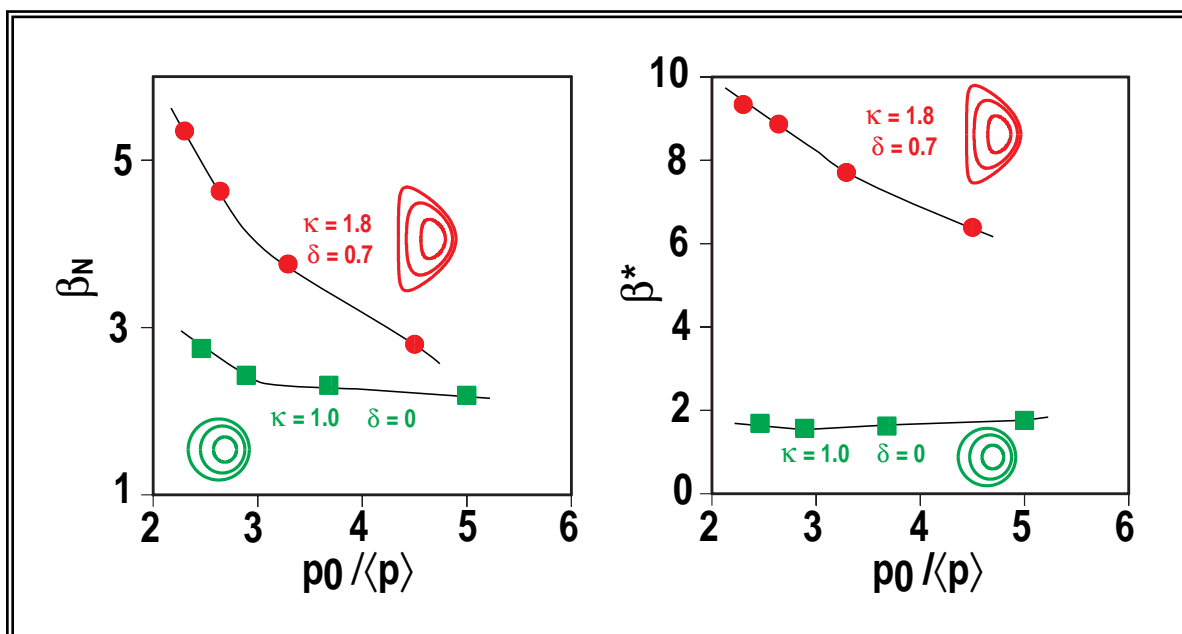


Fig. 2.3-5. Stability limits for the  $n=1$  ideal kink mode in (a) normalized beta,  $\beta_N = \beta (I/aB)^{-1}$  and (b) fusion-weighted beta,  $\beta^* = \langle p^2 \rangle 2\mu_0/B^2$ , both increase as the pressure profile peaking factor  $\rho_0/\langle p \rangle$  decreases. The effect is much greater for a strongly shaped discharge than for a circular discharge.

more than an  $L/R$  time. Agreements with theories remain qualitative. Competing theories predict widely varying critical rotation speeds and the experimental evidence to date suggests a lower critical rotation can provide stabilization than any of the predictions.

The near-term DIII-D Program will continue to investigate the roles of shape and profiles, including confirmation of the predicted “synergy” between discharge shaping and profiles in raising low- $n$  ideal stability limits. Mild to strong current profile peaking (raised  $\ell_i$ ) will be used to improve the stability limits of high-performance discharges with internal transport barriers (NCS) or edge transport barriers (H-mode). Preliminary experiments will investigate the use of noninductive current drive to create and sustain the current density profiles needed for high-performance regimes with high stability limits, including central FWCD for high  $\ell_i$  and off-axis ECCD for NCS.

As more profile control tools become available in the first years of the five-year plan, the emphasis will move toward active control of the pressure and current density profiles. Improved diagnostics and real-time profile analysis will provide input for feedback control of the current density profile with rf current drive. In particular, the counter neutral beamline will significantly improve the real time motional Stark effect (MSE) current profile measurement resolution. Steerable ECH antennas will provide more precise control. Controlled pellet injection will allow modification of the central pressure, while edge ergodization will be applied to control the edge pressure.

**2.3.2.3. WALL STABILIZATION.** In order to make a significant improvement in tokamak performance while also sustaining the plasma current primarily by well-aligned bootstrap current, the level of  $\beta_N$  for tokamaks in the usual aspect ratio range ( $R/a \sim 2$  to 5) must be increased to about 6, and for lower aspect ratio tokamaks like the spherical torus (ST) ( $R/a < 2$ )  $\beta_N$  must be increased to levels above 8 [Turnbull (1997b)]. The most promising approach which has been found from MHD equilibrium studies with good bootstrap alignment and high bootstrap current fraction, rely on equilibria with elevated central  $q_0$  and negative magnetic shear in the central region of the plasma [Kessel (1994), Turnbull (1995)]. However, this necessarily leads to equilibria with relatively broad current profiles (low  $\ell_i$ ) and in all of these cases a conducting boundary placed relatively close to the plasma edge ( $\leq 30\%$  minor radius) is necessary to provide stability against the  $n = 1$  ideal kink mode. The effect of plasma edge/conducting wall separation calculated for  $n = 1$  stability in second stable core VH-mode plasmas is shown in Fig. 2.3–6. The ratio of the wall stabilized  $\beta_N$  limit to the no-wall  $\beta_N$  limit is typically 2 to 3 for both ST and conventional aspect ratio tokamaks; hence, the achievement of plasma operation near the predicted wall stabilized beta limit well above the no-wall limit is essential for the development of improved tokamak reactor designs. Since the best documented performance in any experiment has been only 30% above the no-wall beta limit in DIII-D [Taylor (1995)], the demonstration of stable, long pulse operation of a tokamak plasma well above the no-wall ideal beta limit remains an outstanding research goal.

Recent progress in both theory and experiment has brought into clearer focus potential limitations on the effectiveness of conducting wall stabilization of low- $n$  ideal modes. It was first shown by Pfirsch and Tasso (1971) that a plasma unstable to an ideal MHD mode which is stabilized by a perfectly conducting wall near the plasma boundary cannot be stabilized by a resistive wall at any distance. Freidberg (1987) showed that as a close fitting wall with finite conductivity is moved near to the plasma, the low- $n$  mode which grows on the ideal MHD time scale is stabilized, but a slower growing mode which grows up on the time scale for flux penetration into the resistive wall is now destabilized. This “resistive wall” mode (RWM) is now believed to present a serious obstacle to achieving high levels of wall-stabilized  $\beta_N$  predicted by ideal MHD modeling.

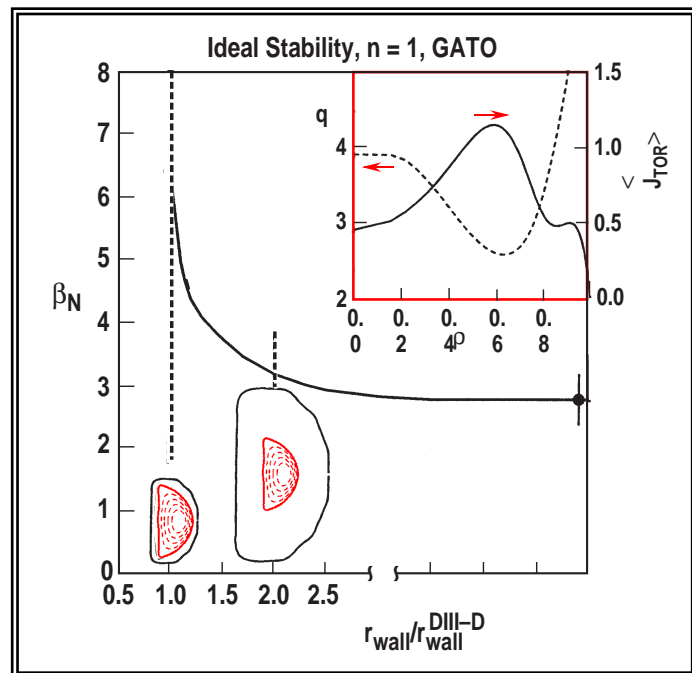


Fig. 2.3–6. Wall stabilization is predicted to allow ideal  $n=1$  kink stability with  $\beta_N > 6$  in a NCS equilibrium. An equilibrium with monotonic  $q$ -profile is only stable up to  $\beta_N = 4$  (dotted line in the inset  $q$ -profile, shaded region in the main plot). The abscissa is the minor radius of the conducting wall divided by the minor radius of the DIII-D vacuum vessel; a value  $R_{\text{wall}}/R_{\text{DIII-D}} = 1$  corresponds to a conducting wall at the actual position of the vacuum vessel wall.

A promising approach to stabilizing the RWM was identified by Bondeson (1994) and Ward (1995) who used the MARS code to show that if the plasma is rotating sufficiently fast (usually a few percent of the Alfvén frequency) with respect to the resistive wall, that the wall begins to appear like a perfect conductor and the RWM can be stabilized. The onset of the RWM and the stabilizing effect of rotation has been observed in experiments on DIII-D where a critical rotation speed of about 2 kHz was observed for a plasma above the no-wall beta limit. Several schemes have been proposed to exploit this rotation stabilization effect and these can be divided into two classes: passive stabilization and active stabilization.

In the case of passive stabilization of the RWM, a source of angular momentum input is used to drive toroidal plasma rotation relative to the fixed resistive wall which is typically assumed to be the vacuum vessel in present experiments. The two approaches which are easiest to implement and have been demonstrated in present experiments are to use the momentum input from NBs or to apply an electromagnetic torque to the plasma with a rotating nonaxisymmetric magnetic field generated by a set of external coils. In recent DIII-D experiments controlled “braking” of the NBI rotation profile at the plasma edge by application of a static  $n=1$  perturbation field has been used to study the onset of the RWM [Mauel (1995)]. However, there is a complex interaction between the onset of resistive modes and their island structure on low order rational surfaces in the outer region of the plasma and rotation of the plasma. Typically, as  $\beta_N$  is increased above the no-wall ideal beta limit,  $2/1$  and  $3/1$  rotating islands can develop which cause a rotational “drag” against eddy currents induced in the resistive wall. Since the rotation profile is maintained by cross-field momentum transport from the centrally deposited NBI momentum, the eddy current induced drag on rotating magnetic islands can exceed the local NBI rotational drive as the resistive modes grow in amplitude leading to slowing rotation, mode “locking” and finally disruption. One approach to this problem is to apply a rotating resonant magnetic perturbation field with a set of external saddle coils to apply torque to the rotation islands directly and maintain their rotation. Despite the rotating perturbation field, the rotation of the islands relative to the wall provides stabilization. Driven mode rotation has been demonstrated on  $2/1$  islands in DITE [Morris (1990)] and in HBT-EP [Ivers (1996)] and it is proposed that a saddle coil set be installed inside the DIII-D vacuum vessel to maintain toroidal rotation of  $2/1$ ,  $3/1$ , and  $4/1$  resonant surfaces up to 10 kHz for study of RWM onset and control.

In the case of active stabilization of the RWM, it has been proposed that an active feedback network could be used which would simulate a perfectly conducting wall, thus stabilizing the RWM. Suggested approaches to implementing this form of active mode control are the “smart shell” [Bishop (1989)] and the “fake rotating shell” [Fitzpatrick (1996), Jensen (1996)]. In both cases, the resistive wall is covered by a network of sensor loops mounted on the surface of the wall, with an array of current-carrying coils nearby. In the “smart shell” approach, flux loops sense the radial magnetic field,  $B_r$ , soaking through the resistive wall and feedback control is used to apply a correction field which maintains very closely a net zero  $B_r$  through the resistive wall, eliminating the RWM. In the “fake rotating shell” approach, a phase shift is applied to the response coils to reproduce the leading phase shift response that the plasma would experience if the resistive wall were in fact rotating toroidally which

leads directly to stabilization of the RWM. Both of these approaches will first be tested on DIII-D through an extension of the existing C-coil structure combined with an array of radial flux sensors.

Near-term experiments will be aimed at further experimental testing of “passive” wall stabilization and comparison to theories. We will extend the database of wall-stabilized discharges and attempt to verify the wall-stabilized ideal limit at high beta. The rotation required for wall stabilization will be compared with theory.

Under the DIII-D Five-Year Plan, we will investigate active means of enhancing and sustaining wall stabilization using external and internal coils. This will be done in several stages. Two approaches have been suggested to use external coils to stabilize the RWM: the so-called “fake rotating wall” and “smart shell” methods. A power supply upgrade will allow a preliminary test of both schemes with the existing C-coil. Additional external coils to be added later will allow selection of the poloidal mode number for better coupling to specific instabilities. Finally, internal coils will provide angular momentum input to sustain plasma rotation. Building on the results of the previous research phase, we will determine the optimum pressure and current density profiles for maximizing the benefits of wall stabilization.

**2.3.2.4. NONIDEAL INSTABILITIES.** As theoretical and experimental understanding moves beyond ideal MHD to a more realistic description of the plasma, a wide range of nonideal instabilities will be investigated under the DIII-D Five-Year Plan, including resistive instabilities with and without a significant contribution from neoclassical effects, sawteeth, Alfvén eigenmodes driven by fast particles, and disruptions.

**Resistive “Locked Modes.”** Resistive “locked modes” induced by helical field errors have become well understood but are still of concern for ITER. Locked modes arise either from naturally unstable tearing modes which induce eddy currents in the resistive vessel wall that exert drag on the mode singular surface or in naturally stable plasmas without rotating tearing modes in which helically resonant static error fields induce eddy currents at the rotating singular surface with concomitant drag. The first kind of locked mode which arises from rotating tearing modes can be avoided by  $j(r)$  control to reduce the local current gradient, seed island control by avoiding sawteeth or ELMs, or by injecting additional momentum into the plasma from the co-beams and/or rotating fields from internal saddle coils so as to keep the vessel eddy current drag from stopping the rotation. (Locked modes are particularly bad as H-mode is usually lost, impurities can come in from local wall interaction, etc.) The second kind of locked mode due to static error fields is predicted to be very problematic for ITER because of its large size and thus low rotation frequency [La Haye (1997a)] and could induce disruption in the early ohmic target phase. It is avoided by (1) careful multimode correction of low  $m$ ,  $n = 1$  static error fields by a multielement correction coil; (2) applying radially localized ECCD at  $q = 2$ , particularly in the island O-point, which would oppose the 2/1 helical current which supports the island and by island reduction reduce the drag allowing the momentum input to unlock it [Hegna (1996)]; or (3) by applying momentum input to keep the island from developing with low voltage, high momentum input co-beams or rotating helical fields from internal saddle coils.

**Neoclassical Effects.** Recent theoretical developments [Carrera (1986), Hegna (1992)] have led to an understanding of the importance of **neoclassical effects** (i.e., the bootstrap current) for resistive instabilities in collisionless plasmas. Preliminary experiments in DIII-D and other devices are consistent with these predictions. In ITER-like ELMing H-mode, single-null divertor (SND) discharges with sawteeth,  $q_{95} \gtrsim 3$  and low collisionality as in ITER  $[(v_i/\epsilon)/\omega_{bi} \approx 0.05]$ , the practical long pulse beta is limited by neoclassically destabilized tearing modes. This occurs in DIII-D [La Haye (1997b)] as well as COMPASS-D and ASDEX-U. The  $m/n = 3/2$  islands reduce confinement by up to 30% at  $\beta_N = \beta (\%) / I/aB \approx 2$  and the  $m/n = 2/1$  islands typically lead to beta collapse, locking, and disruption. As the destabilization is driven by low collisionality, high beta perturbed bootstrap currents due to sawteeth and/or ELM “seeds,” these resistive modes are projected to be the beta limitation for ITER.

The modes are driven by a helically perturbed bootstrap current in response to a “seed” island. In practice, the flattening of the pressure gradient in the seed O-point (but not in the X-point) reduces the bootstrap current there. This is confirmed by comparing DIII-D ONETWO transport code bootstrap current profiles before and after a 2/1 rotating mode, which shows the time averaged bootstrap current decreases locally at  $q = 2$  over the island width. It has been suggested [Hegna (1996), Zohm (1997)] that replacing the “missing” bootstrap current with radially localized co-current drive such as by ECCD can suppress the mode island width (open loop) and/or stabilize the mode (closed loop). The necessary current to stabilize is about 6 kA. One gyrotron can conservatively drive 34 kA at 500 kW so that only 0.5 MW is needed.

**Central  $q$  Control.** A key feature of the VH-mode is that  $q(0)$  rises above unity when the beams are injected into a (sawtoothed) discharge [Lazarus (1995)]; sawtoothed ceases, and both central temperatures and  $q(0)$  rise. The resulting  $q$  profile provides second-stable access. The time evolution of Shot 78136, an excellent VH-mode, has been modeled using the WHIST transport code [Houlberg (1982)], with the thermal and particle diffusivities adjusted to match the measured temperature and density profiles. These simulations show that for the case where the perturbing current source is introduced on a time-scale that is short compared to the resistive time-scale, the radial profile of the noninductive current source (bootstrap current plus co-injected NB current) has a positive gradient near the axis. It is a consequence of Faraday’s law that this initially drives  $j(0)$  down, raising central  $q$ . Additionally, the equilibrium condition with lower  $j(0)$  requires increased  $\kappa(0)$ , which contributes equally to the rise in  $q(0)$ . The simulation shows  $q(0) > 1$  lasting about 0.6 s, in good agreement with the experimental measurement of about 400 ms, as seen in Fig. 2.3–7. [The simulation has only resistive diffusion, whereas an infernal  $n=1$  mode is observed in the experiment when  $q(0)$  drops below 1.2.]

Particle control should allow this favorable  $q$  profile to be sustained. The simulation shows that the broadening beam deposition profile is responsible for the return of  $q(0)$  to unity as both the NBCD and bootstrap contributions fade away. This is also consistent with the experiment, which shows longer  $q(0) > 1$  intervals and lower  $q(0)$  maxima with slower increases in the density which occur when the beam power is reduced. If we were to pump the same discharge well enough to maintain  $\bar{n}_e = 7 \times 10^{19} \text{ m}^{-3}$ ,

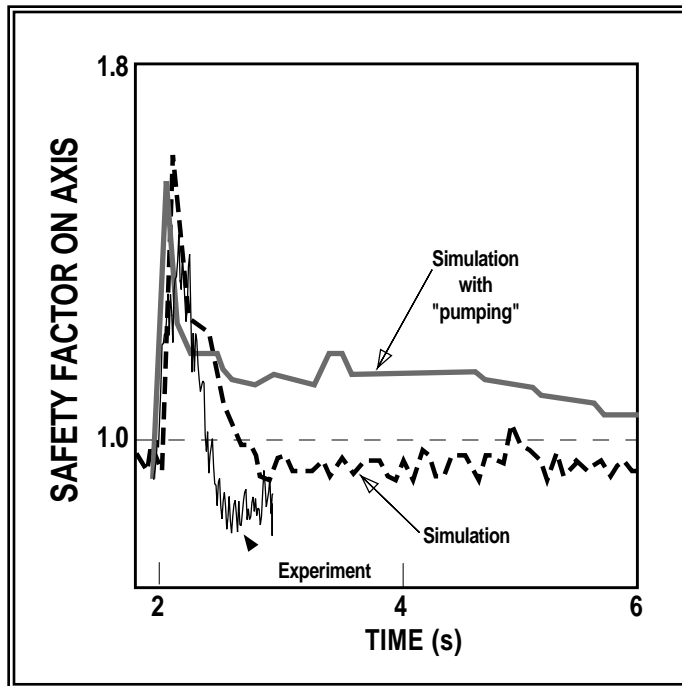


Fig. 2.3–7. Simulations with good experimental foundation indicate additional particle pumping will maintain higher  $q(0)$ .

pressure profile and reducing the energy confinement. In addition, coupling of the internal kink to other rational surfaces can create seed islands which destabilize neoclassical tearing modes. The sawtooth can be avoided by maintaining  $q(0)$  greater than unity, which also tends to open access to the second stable regime in the core of the discharge. Central rf counter-current drive is one means to maintain  $q(0) > 1$  in a long-pulse discharge. Another promising approach is to use off-axis beam-driven current and bootstrap current, taking advantage of the density control capabilities of DIII-D's pumped divertors.

**Alfvén eigenmodes** driven by alpha particles also remain a concern for ITER and any future burning-plasma devices. Alfvén eigenmodes can be destabilized by beam ions, by ion cyclotron heating (ICH) tail ions, and by alpha particles. Modes with frequencies both below and above the TAE were identified, including the BAE/KBM, the KTAE, the EAE, and the NAE. Modes with frequencies that vary rapidly in time, or “chirp”, were also observed. Recently, stable eigenmodes were studied with external antennas. Despite this substantial progress, many important issues remain poorly understood. To date there has been only preliminary investigation of the dependence of Alfvén eigenmode stability on current density profiles and discharge shape.

Our principal new tool will be an antenna to measure the frequency and damping of stable Alfvén eigenmodes. This technique was successfully demonstrated at JET [Fasoli (1995)]. Application of this technique at DIII-D will allow improved comparison of the damping rates and eigenfunctions with theory; study of the shape dependence of the damping rates; measurement of the fast-ion drive; and obtaining nondimensional scaling to a reactor. A crucial parameter in the theory of the TAE mode is the ratio of the

but other than that make no change in the modeling of 78136, WHIST predict the discharge would be maintained near peak conditions with  $T_i(0) \approx 25$  keV,  $T_e(0) \approx 9$  keV, and  $n_e(0) \approx 9 \times 10^{19} \text{ m}^{-3}$ . With the density peaking eventually brought about by the beam fueling of the core, such a discharge might exhibit a more substantial occupation of the second-regime of ballooning stability. Under this scenario, 88% of the current is noninductive, asymptotically, 0.9 MA from bootstrap and 0.5 MA from NBCD. The evolution shows that, after thermal and particle equilibrium have been reached,  $q(0)$  slowly decreases but remains above unity for several seconds (Fig. 2.3–6).

Avoidance of **sawteeth** is desirable for several reasons. Sawteeth create a large-scale redistribution of pressure, flattening the

thermal ion gyroradius to mode scale length,  $k_0\rho_i$ , which determines the relative importance of nonideal effects such as “radiative damping.” Experimentally, we can vary this quantity by scanning the toroidal field at constant values of  $q$  and  $v_F/v_A$  (the ratio of fast-ion speed to Alfvén speed). Another focus of study will be “BAE” modes. Although modes in the 50–150 kHz frequency band have been observed in most large tokamaks, the correct theoretical identification of these dangerous instabilities is still uncertain.

In **nonideal instability research**, the near-term DIII-D Program will continue to investigate the requirements for plasma rotation and minimization of error fields to avoid locked modes. More detailed verification of neoclassical tearing mode theories will be made, including measurement of the mode structure with improved profile diagnostics, and means of avoiding neoclassical tearing modes by current density and pressure profile modification to reduce the sources of seed islands will be investigated. Disruption processes will be studied with new diagnostics including imaging of runaway electron profiles, and means of mitigating the effects of disruptions with injection of pellets or gas jet will be explored.

As the five-year plan progresses, active profile control tools will be used to avoid resistive instabilities, including stabilization by ECCD at rational surfaces. Later, real-time profile analysis with precise current density profile control through plasma positioning or steerable ECH antennas will allow feedback control for avoidance of resistive instabilities. Internal coils will be used for momentum input to maintain plasma rotation, as well as for direct mode control. The internal coils will also be used as antennas to study the damping rates of stable Alfvén eigenmodes. Disruption effects will be mitigated using real-time detection of their onset, or avoided by real-time prediction of instability thresholds.

**2.3.2.5. DISRUPTION AVOIDANCE AND MITIGATION.** We propose to extend the present work of the DIII-D disruption program with the goal of demonstrating operation of an AT in which the frequency and severity of disruptions are reduced to a level at which they are no longer a major design consideration for future machines. We propose to build and routinely operate a system on DIII-D that accomplishes this goal.

To achieve this, experiments and modeling on DIII-D will focus on three main areas of study: (1) develop a better understanding of critical physics that determines the evolution of the thermal and current quench and the resulting heat loss, forces, and runaway electron generation; (2) develop and implement disruption detection and avoidance systems; and (3) develop and implement a disruption mitigation system to reduce the effect of those disruptions that do occur.

In the area of disruption characterization and modeling, the physics of the thermal quench will be examined in order to understand the mechanism of the energy loss and the resulting time scales and spatial distribution of the loss. A new fast infrared (IR) radiometer diagnostic provided by University of California, San Diego (UCSD) will augment our present disruption diagnostic set and permit investigation of the energy loss. Current quench processes that will be addressed include the structure and magnitude of the halo currents, understanding the role of impurities and turbulence in determining the plasma resistivity, and the generation and confinement of runaway electrons. Existing analysis has clearly shown

that there are large toroidal asymmetries in the heat flux, halo currents, and the plasma flux surfaces during disruptions. It is also predicted that structure of the flux surfaces will affect the generation and confinement of runaway electrons. Identification of the three dimensional structure of the plasma and its effect on these disruption phenomena will be investigated using three new arrays of magnetic probes and the existing toroidal halo current array.

Disruption detection and avoidance will be achieved by extending the existing successful work on the use of real-time neural networks developed by ORINCON Corporation [Wròblewski (1997)] to identify the disruption boundaries. By incorporating the set of advanced profile diagnostics now available on DIII-D, more advanced numerical techniques including wavelet analysis, and training on a more complete ensemble of DIII-D disruptions including AT operating modes, an early warning system will be developed to avoid disruptions and maintain stable operation or allow implementation of a soft shutdown system.

The final leg of the disruption program will be the development and implementation of a disruption mitigation system. The primary candidate for this system is a combination of supersonic liquid helium jet injection followed by injection of a high- $Z$  impurity pellet. Based on existing data and modeling, the combined effect should significantly reduce halo currents, radiate most of the plasma thermal and magnetic energy, and avoid the production of runaway electrons. In addition to an extensive hardware development program [involving GA, Idaho Nuclear Engineering Laboratory (INEL), and ORNL], issues of jet deformation and ablation, jet propagation and disruptive boiling in a vacuum, and high- $Z$  pellet ablation and radiation will be studied.

**2.3.2.6. STEADY-STATE ISSUES.** One important constraint in achieving high  $\beta$  steady-state discharges is that the bootstrap current must be properly aligned. The flux surface averaged parallel current profile is given by  $\langle J \cdot B \rangle = \langle J \cdot B \rangle_{bs} + \langle J \cdot B \rangle_{\text{current drive}}$  where  $\langle J \cdot B \rangle_{\text{current drive}}$  includes any ohmic current. At times long compared to the resistive timescale, the ohmic current will become the monotonic profile  $\langle J \cdot B \rangle_{\text{ohmic}} \rightarrow E_0 B_0 / \eta$ , where  $\eta$  is the plasma resistivity. Thus, in the absence of NB or rf current drive, a rough guide to bootstrap alignment is that peaks in the current profile must occur at the same radial locations as peaks in the gradient of the pressure profile. Figure 2.3–8 shows the pressure profile and the parallel current profile for the NCS discharge 87072 at 1.7 s [Rice (1996)]. It is evident that the bootstrap current is well-aligned at the edge of the plasma but not so well aligned in the center. The peak in the bootstrap occurs at  $\rho = 0.3$  while the

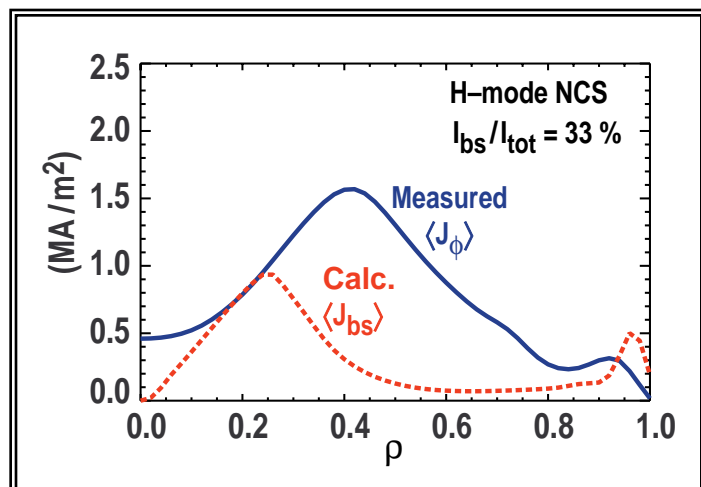


Fig. 2.3–8. Better bootstrap alignment could increase  $\ell_i$  while preserving NCS.

peak in the current occurs at  $\rho = 0.5$ . This lack of bootstrap alignment means that the current profile will continue to evolve in time. The two profile modifications which can improve alignment in the NCS discharges are to move the current peak to a smaller radius or to move the pressure peak to a larger radius.

High  $\ell_1$  discharges tend to have better bootstrap alignment than NCS discharges at small  $\rho$  because the current is typically peaked on axis. Also, confinement and  $\beta_N$  are observed to increase with increasing  $\ell_1$ . However, the bootstrap current near the edge of the plasma limits the peakedness of the current profile and limits the value of  $\ell_1$ , and these discharges lack the internal transport barrier of NCS. One way to improve bootstrap alignment and preserve the advantages of NCS (internal transport barrier, second stable ballooning, etc.) may be a combination of high  $\ell_1$  with NCS. For discharge 87072 this means the peak in the current profile in Fig. 2.3–8 should be moved to a smaller radius, towards the peak in the bootstrap current. This could increase  $\ell_1$  while improving the bootstrap alignment and preserving NCS.

The techniques that can be used to move the peak in the current density,  $\rho(q_{\min})$ , include varying the amount of early beam power during  $I_p$  ramp and varying the speed of the  $I_p$  ramp. Beam current and ECH or FWCD can also be used in combination with the ramp techniques to influence the current profile. Alternatively, the peak of the pressure gradient can be altered. The peak arises from a combination of the local heating and fueling sources, which can be varied, and the location of the transport barrier in NCS, which is related to the low or negative shear but not fully understood at the present time. We anticipate that the combination of the application of these techniques and the continuing increased understanding of the transport barrier will lead to self-consistent “steady-state” high  $\beta$  discharges in DIII-D.

Later in the five-year period, the development of self-consistent solutions with a large fraction of well-aligned bootstrap current will be combined with the other active stabilization techniques described above to achieve the goal of a long pulse discharge with modest rf current drive and no inductive current drive. The next step will then be to explore stable, self-consistent approaches to noninductive startup and current ramp-up, as needed for a high beta, low aspect ratio torus with transformerless operation.

### References for Section 2.3.2

- Bishop, C.M., Plasma Phys. and Contr. Fusion **31**, 1179 (1989).
- Bondeson, A., and D.J. Ward, Phys. Rev. Lett. **72**, 2709 (1994).
- Carrera, R., et al., Phys. Fluids **29**, 899 (1986).
- Chang, Z., et al., Phys. Rev. Lett. **74**, 4463 (1995).
- Fasoli, A., et al., Nucl. Fusion **35**, 1485 (1995).
- Ferron, J.R., et al., Phys. Fluids B **2**, 1280 (1990).
- Fitzpatrick, R., Phys. Plasmas **2**, 825 (1995).
- Fitzpatrick, R., and T.H. Jensen, Phys. Plasmas **3**, 2641 (1996).
- Freidberg, J., **Ideal MHD**, Plenum Press, New York (1987)
- Hegna, C.C., and J.D. Callen, Phys. Fluids B **4**, 1855 (1992).
- Hegna, C.C., and J.D. Callen, “On the Stabilization of Neoclassical MHD Tearing Modes Using Localized Current Drive or Heating,” Report UW-CPTC96-7 (1996).
- Howl, W., et al., Phys. Fluids B **4**, 1724 (1992).
- Houlberg, W.A., et al., Nucl. Fusion **32**, 935 (1982).
- Ivers, T.H., et al., Phys Plasmas **3**, 1926 (1996).
- Jackson, G.L., Phys. Fluids B **4**, 2181 (1992).
- Jensen, T.H., and R. Fitzpatrick, “Resistive Wall Feedback Stabilization,” General Atomics Report GA-A22526, to be published in Phys. Plasmas (1997).
- Kessel, C., et al., Phys. Rev. Lett **72**, 1212 (1994).
- La Haye, R.J., “Physics of Locked Modes in ITER,” General Atomics Report GA-A22468 (1997a).
- La Haye, R.J., et al., Nucl. Fusion **37**, 397 (1997b).
- Lao, L.L., et al., Phys. Rev. Lett. **70**, 3435 (1993).
- Lao, L.L., et al., Phys. Plasmas **3**, 1951 (1996).
- Lazarus, E.A., et al., in Plasma Physics and Controlled Nuclear Fusion Research [International Atomic Energy Agency, Vienna (1995)] Vol. 1, p. 609.
- Levinton, F., Rev. Sci. Instrum. **63**, 5157 (1992).
- Levinton, F.M., et al., Phys. Rev. Lett. **75**, 4417 (1995).
- Mauel, M.E., et al., in Proc. 22nd EPS Conf. on Controlled Fusion and Plasma Physics [International Atomic Energy Agency, Vienna (1995)] Vol. 19C, p. 137.
- Morris, A.W., et al., Phys. Rev. Lett. **64**, 1254 (1990).
- Navratil, G.A., et al., in Plasma Physics and Controlled Fusion Research 1990 [International Atomic Energy Agency, Vienna, (1991)] Vol. I, p. 209.
- Pfirsch, D., and H. Tasso, Nucl. Fusion **11**, 259 (1971).
- Politzer, P.A., et al., Phys. Plasmas **1**, 1545 (1994).
- Rice, B.W., et al., Phys. Plasmas **3**, 1983 (1996).
- Strait, E.J., Phys. Plasmas **1**, 1415 (1994).
- Strait, E.J., et al., Phys. Rev. Lett. **75**, 4421 (1995).

- Taylor, T.S., et al., *Phys. Plasmas* **2**, 2390 (1995).
- Troyon, F., et al., *Plasma Physics and Controlled Fusion* **26**, 209 (1984).
- Turnbull, A.D., et al., *J. Comput. Phys.* **66**, 391 (1986).
- Turnbull, A.D., et al., *Phys. Rev. Lett.* **74**, 718 (1995).
- Turnbull, A.D., et al., “Optimization of negative central shear discharges in shaped cross-sections,” in *Plasma Physics and Controlled Nuclear Fusion Research 1996*, [International Atomic Energy Agency, Vienna, in press (1997a)].
- Turnbull, A.D., and R.L. Miller, *Int. Sherwood Fusion Theory Meeting* (1997b).
- Ward, D.J. and A. Bondeson, *Phys. Plasmas* **2**, 1570 (1995).
- Wilson, H.R. et al., *Phys. Plasmas* **2**, 248 (1996).
- Wròblewski, D., and Lao, L., *Rev. Sci. Instrum.* **63**, 5140 (1992).
- Wròblewski, D., et al., “Tokamak disruption Alarm Based on a Neural Network Model of the High Beta Limit,” submitted to *Nucl. Fusion* (1997).
- Zohm, H., “Stabilization of Neoclassical Tearing Modes by Electron Cyclotron Current Drive,” *Nucl. Fusion* **37**, to be published (1997).

### 2.3.3. BOUNDARY SCIENCE

*Boundary science covers three main areas: divertor physics, boundary conditions for the core plasma, and plasma material interactions. The primary purpose of these studies is to lay the scientific groundwork for the divertors in future machines. We seek to develop the physics basis for power and particle exhaust. Future machines require a divertor that can provide copious radiation in the divertor for power exhaust while simultaneously providing core plasma boundary conditions that maximize core confinement, control core plasma impurity levels, and exhaust fuel and impurities, especially helium, at the required rates. The goal of this research is to incorporate the physics elements that are established in the experiments in codes that can be used productively for future machines. In the near term, the divertor in DIII-D must also supply the functions of impurity control, density control, confinement optimization, and power exhaust for the DIII-D AT Program. Much of the physics in this area, the physics of open field lines, atomic physics, and plasma material interaction physics, is generic to any magnetic confinement concept that bounds closed flux surfaces with open field lines or which uses open field lines.*

**2.3.3.1. DIVERTOR PHYSICS.** Just as L-mode confinement establishes a baseline of confinement behavior in the tokamak that enables definition of what we mean by enhanced or advanced confinement modes, there is a “standard model” of divertor physics that enables definition of what we mean by advanced divertor physics. The elements of the standard model are listed in the top of Table 2.3–3. The goal of the divertor component of the DIII-D AT Program is to develop the advanced divertor physics elements.

The standard model can be worked out almost analytically and implies some well known in-principle limitations to divertor performance that are exhibited in Figs. 2.3–9 and 2.3–10. The two governing equations are for impurity radiation extracting heat from the parallel heat conduction, which has a very strong temperature dependence.

$$\frac{\partial q_{\parallel}}{\partial \ell_{\parallel}} = n_e^2 f_I L(T_e) = (n_e^2 T_e^2) f_I L(T_e) / T_e^2 \quad , \quad (3)$$

$$q_{\parallel} = \kappa_0 T_e^{5/2} \frac{\partial T_e}{\partial \ell_{\parallel}} \quad . \quad (4)$$

**TABLE 2.3–3  
ELEMENTS OF DIVERTOR PHYSICS**

---

- Elements of Standard Divertor Physics
  - Classical conduction limited heat flow along the field lines
  - Constant pressure along the field lines (attached plasmas)
  - Coronal equilibrium radiation rates
  - Constant impurity concentration everywhere in the system
  - Sheath limited heat flow at the divertor plate.
  
- Elements of Advanced Divertor Physics
  - Impurity concentration enrichment in the divertor
  - Noncoronal equilibrium radiation rates
  - 2-D flow patterns of heat and fuel
  - Non-Maxwellian enhancements of radiation
  - Plasma volume recombination

---

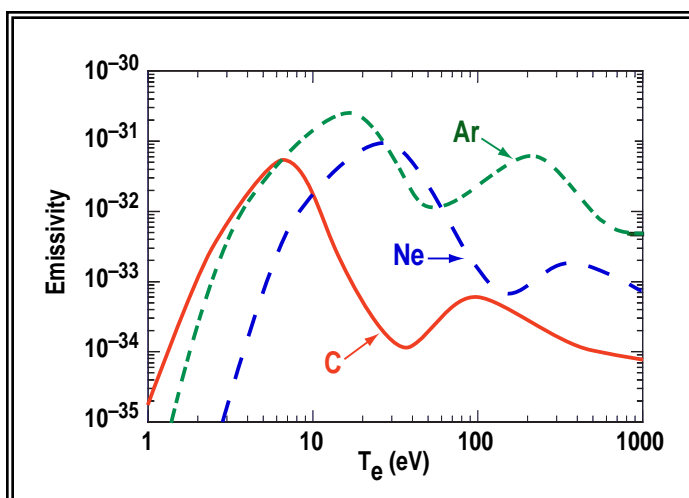


Fig. 2.3–9. Strong emissivity peaks at low temperatures is the key to a radiative divertor.

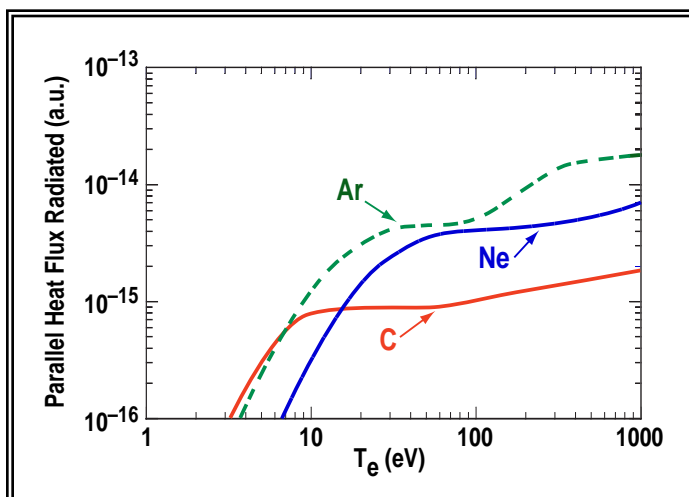


Fig. 2.3–10. The standard model predicts radiated heat flux limits for the divertor.

Here  $f_I$  is the impurity concentration and  $L(T_e)$  is the emissivity given in Fig. 2.3–9. The coronal radiation rates are shown in Fig. 2.3–9 for the impurities of most interest to DIII-D and ITER. Clearly, one wishes to make use of the very strong emissivity peaks at low temperatures to make a radiative divertor. This would seem consistent with the desire to produce low temperatures in the divertor by the same radiation. However, the strong temperature dependence of the parallel heat conduction means that as the plasma temperature drops, the plasma becomes increasingly unable to conduct the heat to the cold zone where it might be radiated. This conflict results in an in-principle limitation to the amount of radiation that can be achieved in the SOL/divertor. By making use of the constant pressure assumption, Eqs. (3) and (4) can be combined into a single integral for the square of the total parallel heat flux that can be radiated along the field lines from  $T_e = 0$  up to  $T_e$ .

$$q_{\parallel}^2(T) = 2\kappa_0 P_e^2 f_I \int_0^T L(T) T^{1/2} dT \quad (5)$$

These in-principle maximum values of  $q_{\parallel}$  that can be radiated are shown in Fig. 2.3–10. Carbon accumulates all the radiation it can make below 10 eV and is a good choice for making a radiating divertor, but the total radiation that can be made is limited. Neon and Argon can produce more total radiation, but most of that radiation will be accumulated at temperatures above 20 eV. These standard model limits for the total radiation give about 100 MW maximum SOL/divertor radiation for ITER. Although that suffices for the nominal power balance case in ITER, advanced divertor physics is required to open up the operational flexibility to shift more radiation from the core plasma into the divertor (to a maximum of 300 MW in ITER). Thus ITER defines the need from advanced divertor physics as a factor of 3 increase in achievable SOL/divertor radiation. A higher power density future system like ARIES-RS needs up to a factor of 8 enhancement.

The radiation limit in the standard model also produces conflicts with core plasma physics. As can be seen from Eq. (5) if the integral over temperature is constrained, the only way to increase the total SOL/divertor radiation is to increase the core plasma separatrix density or the core plasma impurity concentration. Increasing the core density can run into density limit problems or just increase core collisionality into regimes that are not of interest from a dimensionless parameter point of view (Section 2.2). Increasing the impurity concentration can be detrimental to core confinement and causes unacceptable fuel dilution. Hence, advanced divertor physics is needed to enable increased divertor radiation at restricted core plasma densities and impurity concentrations.

The standard model has other undesirable features. The characteristic solution for the standard model has all the temperature gradient near the divertor plate, all the carbon radiation in a spatially very narrow region right against the divertor plate, and essentially no reduction of parallel heat flow until just at the divertor plate. Advanced divertor physics is required to stretch the divertor radiation more uniformly up the leg of the divertor in order to radiate the power to the large area of sidewall in the ITER divertor. Another constraint of the standard model that was realized early in the ITER considerations is that with

the anticipated particle fluxes to the divertor plate, just the recombination energy would exceed the desired  $5 \text{ MW/m}^2$  heat load. Hence, detached plasma operation must be sought in which the plasma pressure along the field lines is lowered by charge exchange dissipation of momentum or plasma recombination.

The elements of advanced divertor physics attack limitations of the standard model. Increasing the concentration of impurities in the divertor with respect to the core plasma (divertor enrichment) can increase divertor radiation over the standard model. Short residence times of the impurities in the plasma and/or substantial neutral densities in the plasma can enhance radiation rates over the coronal equilibrium values. The DIII-D Program in these areas of impurity transport and radiation physics is described below. DIII-D data disagree greatly with the standard model picture of parallel heat flow — the program of research in this area is also discussed below. Experimental evidence for plasma recombination has only now emerged from many tokamaks in the last year — this exciting area is in its infancy; this section reviews DIII-D work on plasma recombination. The actual divertor problem is 2-D and cross field heat flow may ameliorate the constraint of parallel heat conduction in a way that allows more radiation. The program to manage fuel and heat flow patterns in the divertor is described below. Possible longer range divertor optimizations are discussed here as well.

**Heat and Fuel Particle Transport in the SOL and Divertor.** On DIII-D, we have produced radiating divertor plasmas that are in stark contrast to the implications of conduction dominated transport of the standard divertor model. In Fig. 2.3–11, the radiation produced by deuterium puffing is shown to be distributed evenly from the X-point region to the divertor target. The uniformity in radiation is approximately 2:1 and exceeds the requirements of ITER divertor design. Spectroscopy indicates that carbon radiation dominates in the X-point region with deuterium radiation peaking near the target.

To understand how so much power could flow to the lower portion of our divertor channel, we have compared the electron temperature profile measured in our radiative

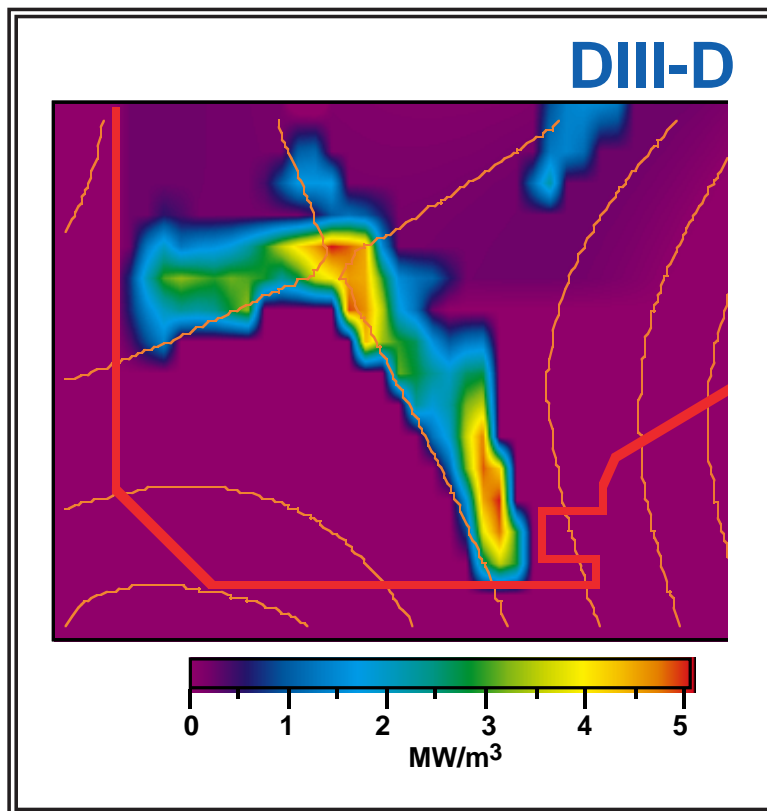


Fig. 2.3–11. Radiation evenly distributed from the X-point region is in stark contrast to standard divertor model predictions.

divertor plasmas with that predicted by electron conduction from the standard model. If conduction is dominating the heat transport, then the required electron temperature profile (shown in Fig. 2.3–12) must rise above 20 eV a short distance from the divertor target. In contrast to the predicted  $T_e$  profile, we also plot in Fig. 2.3–13  $T_e$  measurements from the Divertor Thomson System which show  $T_e \sim 1$  to 2 eV throughout the divertor. Because of the strong temperature dependence, conduction can support essentially no heat flux at this temperature range.

Plasma convection can explain our dissipation of heat flux by radiation throughout the divertor. If the plasma is flowing as a fluid, then the thermal energy of the plasma and its ionization potential can be carried down the divertor without the temperature gradient required for conduction. By measuring the divertor density and temperature, we find that our measured heat flux profile can be supported by plasma flowing near the ion sound speed throughout the divertor. Plasma flowing at the ion sound speed

is also seen in UEDGE simulations of DIII-D radiative divertor plasmas and will be discussed below. When the divertor temperature drops significantly below 10 eV, ionization of neutral deuterium moves further upstream away from the divertor plate. The upstream ionization then becomes the source of plasma flow through the divertor. Plasma flow then brings heat flux into a low temperature region where ultimately recombination can dissipate the plasma ionization potential.

Our **future work** will investigate the transition region where conduction dominated transport gives way to convection. Our studies will seek to determine the 2-D relationship between power flux, intrinsic impurity radiation, ionization, and plasma flow. Understanding the interaction of these processes is important for designing a high power divertor, such as ITER, that dissipates the heat flux yet meets the requirements of a high confinement core plasma. Our plans for optimization of convection in the divertor for dissipation of heat flux will be presented in the section on the Convective/Radiative Divertor.

**Recombination.** The divertor plate heating can be minimized by obtaining the plasma conditions which permit volume recombination of the ion current above the plate, thus eliminating the heating which accompanies recombination within the plate.

The electron temperature must be reduced below 2 eV to permit volume recombination to compete with ionization. We have been able to produce such conditions in DIII-D. The divertor Thomson scattering

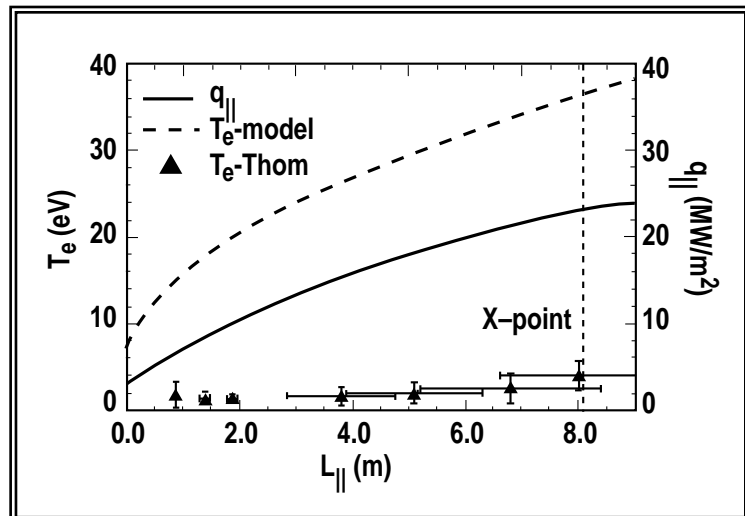


Fig. 2.3–12.  $T_e$  measurements do not support model predictions of significant electron conduction.

system in DIII-D is able to make 2-D images of the temperature in the divertor. Figure 2.3–13 shows a wide region of 1 to 2 eV plasma measured by the Thomson system. UEDGE is able to simulate these recombining plasmas and that simulation is also shown in Fig. 2.3–13. The recombination process is rather slow. The plasma momentum must also be reduced to permit the recombination process to compete with particle losses via flow to the plate. Figure 2.3–14 shows that volume recombination on the inner leg. As expected, volume recombination becomes significant only in the region with  $T_e < 2$  eV, but it remains relatively small until the momentum is reduced via ion-neutral interactions (as indicated by the reduction in the parallel Mach number). Volume recombination is maximized when the recombination time is comparable to the flow time to the plate. Poloidal profiles of the parallel Mach number similar to that shown in the bottom of Fig. 2.3–14 have been inferred from the bolometer data on DIII-D. Evidence of recombination has also been seen spectroscopically on both C-Mod and, more recently, on DIII-D [Isler (1997)]. Thus, both modeling and experiment indicate that volume recombination is playing a significant role in reducing the ion currents to the divertor plates and thus in reducing the plate heating.

Our **future research** in this area will continue to exploit the unique 2-D Thomson scattering measurements. We are adding spectroscopic and probe diagnostics to measure plasma flows. We will improve our direct spectroscopic evidence for recombination. The spatial resolution of the bolometer system will be improved.

**Impurity Transport and Radiation in the SOL and Divertor.** The impurity transport studies on DIII-D will continue to emphasize the detailed 2-D structure of impurity transport and radiation. The transport of impurities in the divertor results predominantly from forces from the primary plasma (including the ITG force) and the frictional force from the ion flow patterns induced by recycling and puffing with pumping. Anomalous radial transport and wall sources and sinks are also important.

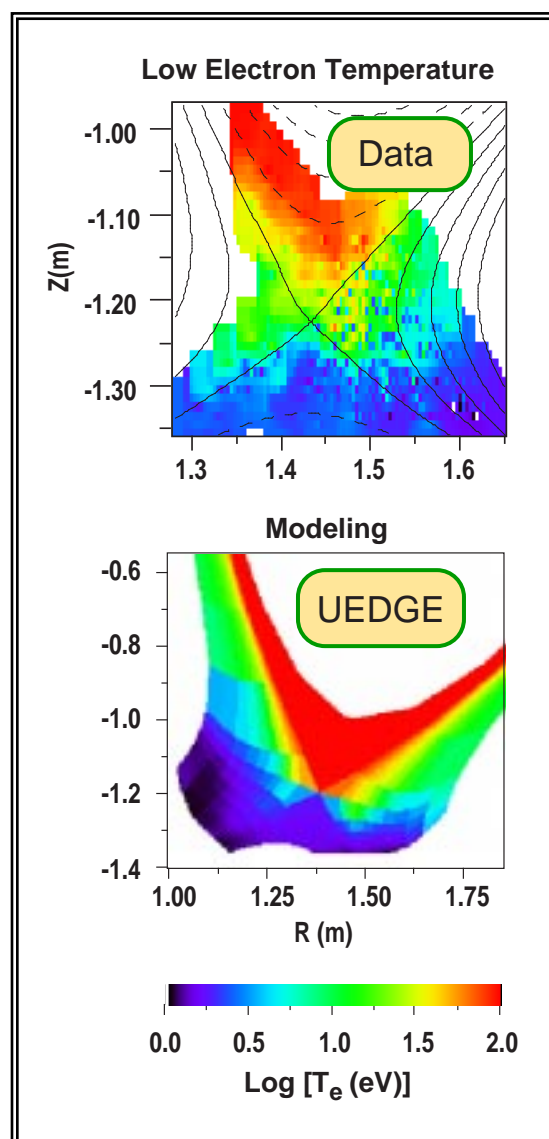


Fig. 2.3–13. Divertor measurements and modeling show  $< 2$  eV  $T_d$ , permitting volume recombination to compete with ionization.

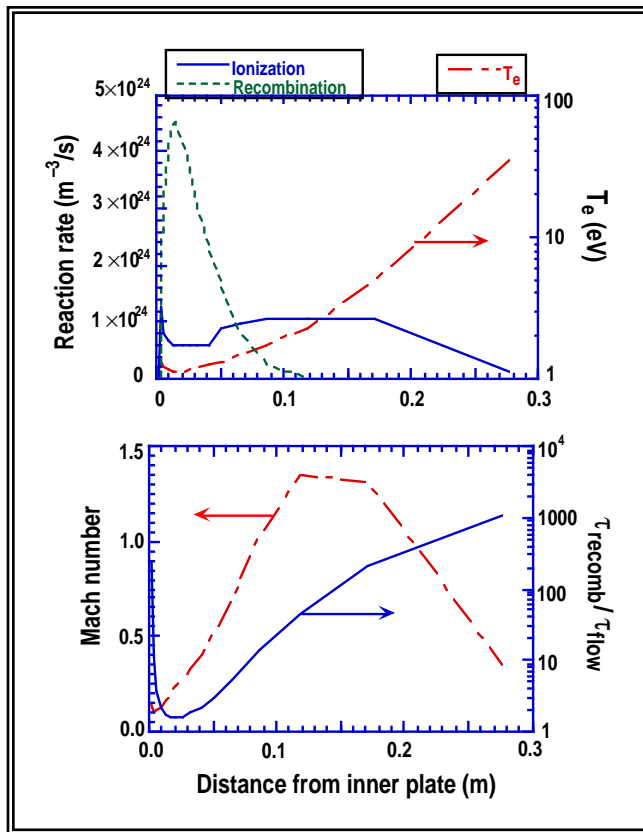


Fig. 2.3-14. Volume recombination remains small until the momentum is reduced via ion-neutral interactions.

The open lower divertor readily yields two-dimensional divertor plasma data. Recent results have clearly shown that during partially detached divertor operation induced by deuterium puffing, (Fig. 2.3-15) [Wood (1996)] when the EUV spectrometer line of sight passes through the X-point region, carbon radiation is heavily dominant. When, the sight line passes through the strike point, deuterium radiation is important. These quantitative measurements are confirmed qualitatively by tomographic inversions of tangential visible TV images [Fenstermacher (1996)]. Recently, the EUV survey instrument, poor resolution, extended domain (SPRED) spectrometer, which views the lower divertor region of DIII-D, has been upgraded to allow measurement of the emission intensity from Lyman alpha and from the strongest lines of CIII (1175 Å) and CIV (1550 Å). The direct measurement of these lines will improve dramatically our confidence in the collisional radiative modeling of total radiation from both carbon and deuterium.

The addition of new viewing channels to an existing high resolution visible spectrometer [multichord divertor spectrometer (MDS)], through Doppler shift measurements, will allow determination of toroidal flow velocities. Doppler shifts of CIII, CIV, and  $H_{\alpha}$  will be measured in the divertor from the X-point to the floor. Using the divertor sweeping capability in the open configuration, a 2-D picture of divertor impurity flow will emerge.

Other recent studies on DIII-D [Schaffer (1996)] were designed to investigate the possibility of using induced plasma flow to enhance the divertor impurity enrichment (in these studies, enrichment is defined as the ratio of the divertor pumping plenum concentration to the core plasma concentration). The results are summarized in Table 2.3-4, where it is shown clearly that puffing  $D_2$  gas at the top of a single-null plasma, combined with strong pumping in the divertor, can provide a mild increase in the enrichment of neon and a fairly sizable increase in argon enrichment. The results for argon are fairly promising.

The well baffled RDP structure will provide tight baffling of recycling deuterium and impurity neutrals. Such baffling should strongly reduce the source of neutrals to the X-point and midplane regions. In addition, the divertor recycling patterns should change dramatically. Thus, we expect significant changes

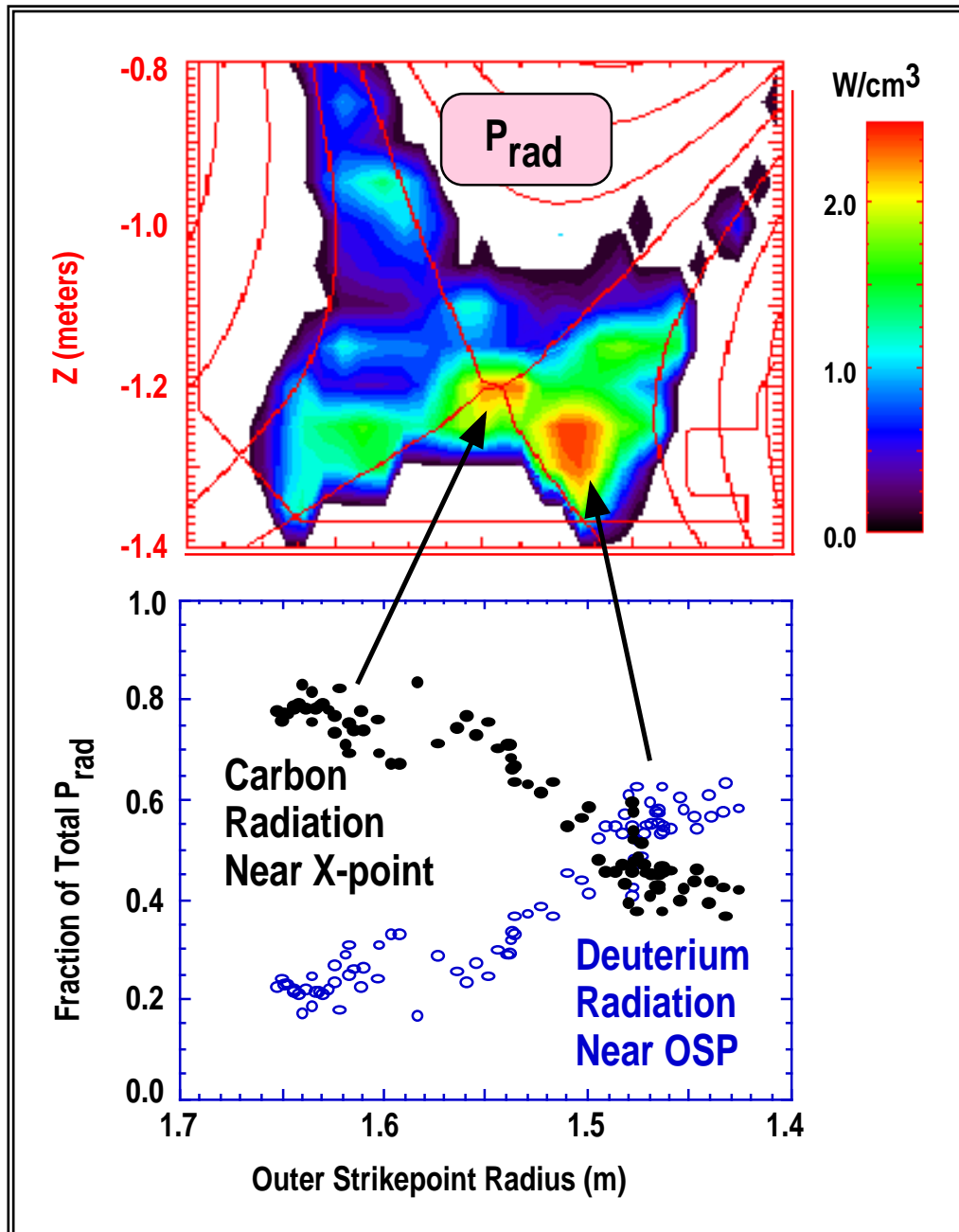


Fig. 2.3-15. Carbon radiation dominates partially detached divertor operation induced by deuterium puffing.

to the impurity transport. To provide the same level of diagnostic capability for impurity flow, line emission, and radiation that we now have in the open divertor, will require significant modifications and upgrades to our diagnostic set. These changes are proposed for this plan period and are discussed in some detail in Section 2.5.5.

**TABLE 2.3–4**  
**ENRICHMENT OF NEON AND ARGON IS PRESENTED**  
**FOR FOUR CASES OF INDUCED DEUTERIUM FLOW**

<b>D<sub>2</sub> Flow Location</b>	<b>Top</b>	<b>Divertor</b>	<b>Top</b>	<b>Divertor</b>
Flow (Torr-l/s)	150	150	80	80
Line-averaged density	$6.2 \times 10^{19}$	$6.1 \times 10^{19}$	$6.0 \times 10^{19}$	$6.1 \times 10^{19}$
Baffle pressure (mTorr)	4.0	3.5	1.6	1.5
ELM frequency (Hz)	60	55	60	55
Neon enrichment	1.4	1.0	1.2	1.0
Argon enrichment (relative) <sup>(a)</sup>	6.9	2.2	1.7	1.0

<sup>(a)</sup>Normalized to enrichment in 80 Torr-l/s, divertor fueling case.

**Detached Divertor Scenarios, AT Compatibility.** DIII–D faces a significant challenge in integrating detached divertor operation with AT core plasma modes. As is discussed in Sections 2.2 and 2.4, the main AT scenarios devised for DIII–D involve operation with densities less than 40% of the Greenwald limit. In fact, in DIII–D the detached divertor operating space and the confinement data operating space are disjoint. Virtually, the entire confinement database used to support ITER is taken at densities less than 50% of the Greenwald limit; whereas virtually the entire detached plasma database has densities over 50% of the Greenwald limit. While pursuit of AT and detached divertor physics in disjoint regimes suffices to provide the science basis for ITER, the use of advanced divertor physics to join these two regimes at low density is necessary for higher power density machines like ARIES–RS. Here we present the status of our investigations of the operating regimes for detached plasmas. We believe it will be necessary to install the full RDP to gain access to detached plasmas at the low densities desired by the AT Program.

**Deuterium Only Operation.** In pure deuterium, UEDGE was used to determine the range of detachment in terms of the heating power which flows into the SOL together with the density just inside the separatrix. The results are summarized in Fig. 2.3–16. Unfortunately, the AT scenario described in Section 2.2 lies at about 10 MW and  $0.5 \times 10^{20} \text{ m}^{-3}$  where both the inner and outer legs of the divertor should be attached. We either need impurities or better neutral baffling to lower the detachment threshold in density or raise it in power. The effect of well baffling the divertor in JET has largely been a reduction in the density needed for detachment.

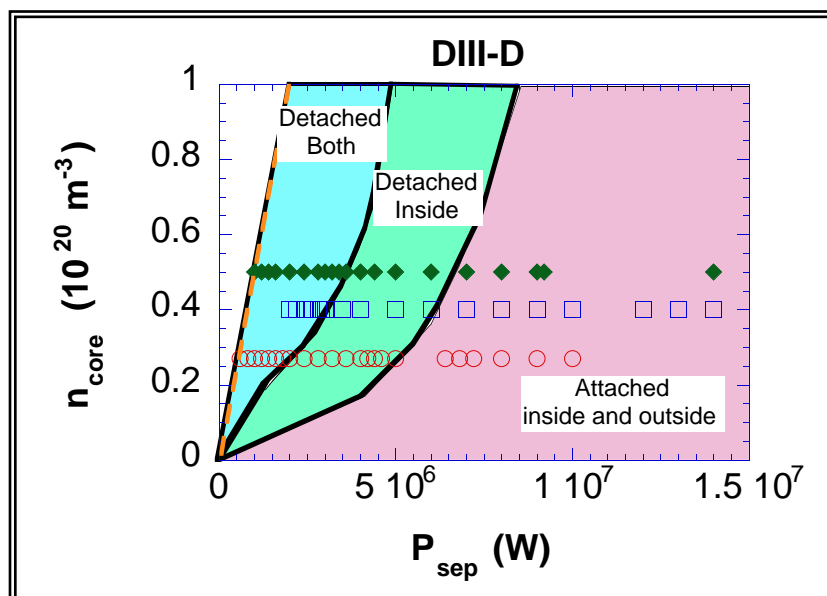


Fig. 2.3-16. Either impurities or better neutral baffling are needed to achieve the AT scenario.

the device. This process is modeled in UEDGE by assuming the existence of a flux of neutral carbon which is proportional to the incident flux of deuterium at the plates and the wall. The constant of proportionality is referred to as the sputtering coefficient. We started with a “best fit” to a particular discharge (Shot 87506) and varied this sputtering coefficient until we achieved detachment at both the inner and outer divertor plates. The plasma modeled has a density of  $6.5 \times 10^{19} \text{ m}^{-3}$  on the 96% poloidal flux surface and 3.4 MW of heating power into the SOL. We find the inner plasma detaches easily, with a sputtering coefficient of only  $2 \times 10^{-5}$ . When the sputtering coefficient exceeds  $10^{-4}$ , the impurity source has become strong enough (due to the rise in private flux pressure) to alter the impurity flows, and we see impurity radiation cool the outer leg. When the sputtering coefficient is increased 25% from  $4 \times 10^{-4}$  to  $5 \times 10^{-4}$ , the plasma detaches from the outer leg. The plasma behavior at this point is very different from that seen in simulation of pure deuterium plasmas. Rather than being able to easily control the position of the ionization front on the outer leg, we find the ionization front moves rapidly up to the X-point. The neutral pressure in the divertor region increases as the plasma pumping is decreased due to the low temperatures. This increased pressure leads to enhanced carbon production, and we find a runaway process with a few millisecond time scale.

We find the window between detachment of the outer leg and the development of a core MARFE is very small when we include the effect of impurity production and transport. The low power level for detachment is favorable for integrated AT operation, but the density we have considered is twice what should be looked at in the AT cases. The planned RDP installation addresses some of the limitations we have seen in our study. The divertor dome (based originally on JAERI work) is expected to reduce the chemical sputtering carbon source to provide more control against runaway thermal collapse. The dome in

### Multispecies Impurity Model.

We have recently been able to use the multispecies ion model in UEDGE to analyze some of the phenomena we are seeing in DIII-D and to assess effects we may see with the RDP installation. We assume the only impurity is the intrinsic carbon which comprises the entire plasma facing wall in the device. After an initial study found that physical sputtering off the divertor plates could not produce detached plasmas, we have moved to an examination of the effect of chemical sputtering from all the walls of

the RDP also decouples the inner and outer divertor channels and both can be pumped which should make it easier to balance the detachment process more equally between the inner and outer legs.

We also expect the slanted RDP structures to exert a major influence over the fuel flow patterns in the divertor which should aid in obtaining impurity enrichment in the divertor. The effect of the impurity source on the plasma flow in the present divertor geometry is shown in Fig. 2.3–17. Negative parallel velocities represent flow toward the inner plate and positive represent flow toward the outer plate. We see flow reversal near the separatrix on both the inner and outer plates at low sputtering coefficients (or in pure deuterium plasmas). This arises because there is efficient ionization of the recycling neutrals, leading to a high density very near the plates. The plasma tends to flow away from this source region. Both the thermal gradients and the flow terms tend to force the impurity ions into regions of high temperature at low sputtering coefficients. The carbon is then removed by flowing radially via anomalous transport, then flowing to the plates where the parallel plasma velocity is not reversed.

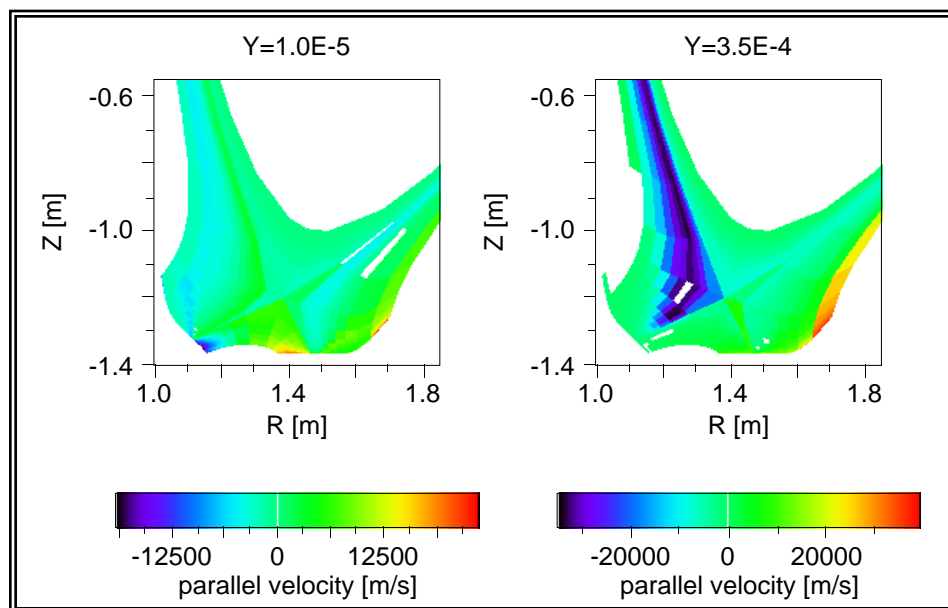


Fig. 2.3–17. Slanted RDP structures should aid in obtaining impurity enrichment in the divertor.

The picture is very different under detached conditions as seen on the right of Fig. 2.3–17. In this case, the ionization front has moved off the plate on the inside, and plasma flowing away from the source moves toward the inner plate. Both the thermal gradient and the flow moves the impurity which is introduced on the outside to the inner plate. Overall, the upstream carbon concentration is reduced a factor of 2–3. We will extend these studies soon to the actual RDP structures.

**Double-Null Divertor Issues.** The present DIII–D device is uniquely qualified to study double-null divertors, and this capability will be maintained in future upgrades and modifications of the device. A double-null divertor is desirable from the standpoint of reducing the peak heat flux on the divertor plate

as there are four strike points rather than two compared with a single-null configuration. However, DIII-D experiments have shown that there is a definite in-out asymmetry of the heat flux. The profiles are more symmetric at lower densities ( $\sim 5 \times 10^{13} \text{ cm}^{-3}$ ) where AT operation with current drive will be carried out. We need to understand the physical processes connected with this asymmetry and thereby control it. In addition, we observe an in-out asymmetry in the particle flux so that plasma pumping (exhaust) will be asymmetric. Experimental results suggest that it may be possible to symmetrize both the particle and heat flux by pumping at the inner strike point. Experiments on TdeV and preliminary experiments on DIII-D indicate that the power and particle up-down symmetry can be controlled in double-null plasmas by carefully controlling the distance between the two separatrices. In fact, a balanced heat flux requires an unbalanced magnetic configuration.

Double-null operation has several advantages from the AT standpoint. Theoretically, the stability limit for edge ballooning modes is predicted to be higher in high triangularity plasmas. The influence on the edge ballooning modes can, in turn, increase the edge density pedestal which has been correlated with increased energy confinement. Edge density control with both inside and outside cryopumping can also be important for determining the bootstrap current fraction, which depends more strongly on the density gradient than the temperature gradient. Careful particle control at both the inner and outer strike points will be important.

Another advantage of double-null plasmas is their inherent up-down symmetry which results in a more robust plasma configuration in the case of disruptions. During the thermal quench, the plasma usually exhibits rapid motion either up or down. The divertor plate ultimately becomes the connection path for the poloidal current with a resulting “halo current” through the structure. In the case of double null, the plasma, vessel, and coils are much more symmetric so this motion and thereby forces are expected to be reduced.

The DIII-D RDP will provide a unique opportunity in the world to study double-null plasmas at high power and triangularity.

**The Convective/Radiative Divertor.** In the conduction limited heat flow regime, the impurity radiation zone in the divertor is expected to be a narrow slab near the target plate. However, we have been able to produce nearly uniform radiation along the entire divertor leg. This was not done so much by circumventing the parallel heat conduction constraint but by introducing volume recombination in the lower portion of the divertor channel. Then, even though the plasma temperature was 1–2 eV, enough energy could be “convected” along the field lines to produce the radiation seen from the recombining region. This “convection” requires some explanation. There is not enough kinetic energy in the flowing particles to produce impurity radiation; the only way radiation gets produced is from release of the potential energy that can be considered to be flowing down the divertor channel. This potential energy is turned into photons during recombination.

The idea that this physics has stimulated is to try to force Mach 1 flows down the field lines in regions where the plasma is hot, 20–60 eV. In that case, the convection of kinetic energy can be competitive with conduction and the convection can serve to carry the energy of excitation downstream to impurities where they can be made to radiate. The result should be a much longer (in the parallel direction) region of impurity radiation than can be produced only by heat conduction. The goal would remain sufficient cooling of the plasma so that recombination ultimately occurs in the lower portion of the divertor channel. Our preliminary analytic calculations and UEDGE simulations indicate that such a regime may be feasible. The hardware embodiment of such an approach would be a divertor structure that collects gas created from recombination at the bottom of the divertor channel and ducts a portion of that gas back upstream and admits it to the divertor plasma stream where that plasma stream is hot. The key problem is getting the gas to penetrate that plasma stream; creation of local turbulence may be necessary. We intend to develop this idea toward a possible divertor optimization in DIII-D that would compete in the 2002 time frame with other major divertor modifications like the 43 cm slot modification.

**Use of Nonaxisymmetric Coils.** A substantial body of research shows that the width of the SOL can be increased by producing a stochastic magnetic layer at the edge of the plasma. This stochastic layer shields impurities from the core plasma and reduces the divertor heat load. The heat load reduction is further amplified by quadratic increase of the radiated power with the SOL width. Such coils may afford a controlled way to reduce the edge pressure gradient and bootstrap current, the driver of edge instabilities that are terminating AT phases. A new set of nonaxisymmetric  $\beta_r$  perturbation coils, designed in such a way that they do not perturb the core plasma but provide a relatively uniform homogeneous stochastic boundary layer, will be considered for DIII-D in the CY02 time frame.

Based on extensive numerical modeling results and a wide range of experimental measurements using both external and internal resonant  $\beta_r$  coils on TEXT, JIPP T-IIU, and Tore Supra, we have found that the best design for such coils is one which employs moderately high  $n,m$  mode numbers with multiple sets of rationally identical or near neighbor modes (i.e.,  $n=3,m=9$  and  $n=5,m=15\pm 1$ ) in order to insure good mode mixing on the resonant  $q$  surface of interest. Previous experiments were not equipped to produce the mode spectrum required for a truly effective stochastic boundary layer.

There is a delicate balance between minimizing the power in the low  $q_{n,m}$  rational perturbations and driving the required mode spectrum for  $q_{n,m} = 3$  resonant perturbations. Since the amplitude of the  $\beta_r$  perturbations falls off roughly as  $e^{(m-1)(r-r_c)}$  for  $r < r_c$ , large amplitude high  $m$  perturbations imply the need for relatively large coil currents ( $\sim 15$  to  $20$  kA-turns) assuming the coils are located at a reasonable distance from the  $q = 3$  resonant surface. These coil currents can create substantial near field (i.e., nonresonant) effects on the local magnetic equilibrium which induce toroidal and poloidal asymmetries in the edge plasma parameters. This should be avoided since they unnecessarily complicate our understanding of the boundary layer physics and reduce our ability to control critical plasma surface interactions. These considerations, plus an array of technical design issues, strongly favor placing the  $\beta_r$  coils outside the vacuum vessel where they are both accessible and far enough away from the plasma edge that the near

field effects do not play a significant role in the boundary layer physics. In DIII-D, external  $\beta_T$  coils are much easier and less expensive to secure against  $J_c \times B_\phi$  forces.

**2.3.3.2. BOUNDARY CONDITIONS FOR THE CORE PLASMA.** The divertor and core plasmas share boundary conditions through the H-mode shear layer. The strong temperature dependence of the parallel heat conduction in the SOL essentially restricts the midplane separatrix temperature to less than about 200 eV. But how the density at the midplane separatrix is determined is not precisely known. In steady state, the core plasma density is set by a balance of charged particle outflow across the separatrix and a flux of neutrals in across the separatrix whose magnitude makes the volume integral of their subsequent ionization equal to the charged particle losses. The divertor pumps in DIII-D provide a means of regulating the neutral reflux to the core plasma, providing the necessary means of density control for obtaining core plasmas in relevant collisionality regimes. The program of density control for the core plasma is described in this section. As discussed in the divertor section above, the desire for more divertor radiation generally puts upward pressure on the core plasma density. The physics of limits to the core plasma density is discussed here as well. The two most restrictive limits, complete thermal collapse of the divertor plasma and the origination of thermal collapse just inside the separatrix, are phenomena that originate in divertor and/or radiation physics. Many of the advances in confinement in DIII-D have been produced by wall conditioning efforts whose main effects are to reduce sources of neutral reflux to the core plasma. The highly baffled divertors planned for DIII-D are another step along this line to improve core plasma performance. This use of the divertor is illustrated below. Finally, there is the issue of the interaction of the divertor and the H-mode shear layer: that complicated region of the plasma that sets the pedestal height for the core plasma and the separatrix boundary conditions for the SOL/divertor plasma. Also shown are the various scientific issues in this area.

**Density Control for the AT Core Plasma.** Density control is required to extend the duration of the peak performance phase of high performance plasmas, both VH-modes [Lazarus (1995)] and weak shear discharges. The onset of  $n = 1$  modes (sawteeth) after initiation of the high confinement phase degrades the performance. Magnetic reconstruction shows that  $q(0)$  drops below 1, prompting both sawteeth and internal kink modes. WHIST modeling of one VH-mode discharge shows [Lazarus (1995)] that the main cause of  $q(0)$  reduction is the beam deposition profile becoming broader as the plasma density is rising. Density control should prevent the broadening of the beam deposition profile and lengthen the duration of the high performance phase.

Most of the operational scenarios proposed in Section 2.2 require operation at  $\sim 0.4 n_{GR}$  ( $n_{GR} \equiv$  Greenwald density limit). Density control, to this level, has been demonstrated in ELMy plasmas [Mahdavi (1993)]. The “natural” H-mode density, i.e., the density toward which H-modes normally evolve, was  $\sim 0.6$  to  $0.7 n_{GR}$ , prior to installation of the lower divertor cryopump in FY93. After installation of that pump, we have achieved [Maingi (1996)] density as low as  $0.2 n_{GR}$  in ELMy plasmas. The natural H-mode density after the pump is turned off is now  $\sim 0.4$  to  $0.5 n_{GR}$ .

Density control in ELM-free plasmas has proven more challenging. Early studies [Rensink (1993)] indicated that the density rise after the L–H transition in ELM-free plasmas was caused partly by the decrease in the particle transport rate out of the core and partly by the decrease of the SOL opacity to neutrals which increased the core fueling rate. From a divertor science standpoint, determination of which effect actually dominates under which conditions is important because the answer could affect the lowest density which could be achieved in ELM-free plasmas. If the reduction in transport dominates, then effective density control would require as much of a reduction in core fueling sources as possible, including a large amount of in-vessel pumping/baffling and the use of heating scenarios other than NBI. If the decrease in SOL opacity dominates, then mechanisms to create a denser SOL need to be investigated. Experimentally, we have shown that the use of lower divertor pumping during ELM-free operation does reduce the peak rate of rise of electron density after the L–H transition from  $\sim 50\text{--}60$  torr- $\ell/\text{s}$  to  $\sim 20\text{--}30$  torr- $\ell/\text{s}$ . However, the rate of density rise could not be brought down to zero until ELMing began. Part of the difficulty in demonstrating as good density control in ELM-free discharges is the fact [Hill (1992)] that ELMs account for  $\geq 50\%$  of the total particle outflux in H-mode discharges. Moreover, recent studies [Wade (1996)] of our high performance ELM-free discharges have shown that carbon is largely responsible for the density rise during the high performance phase. Because the origin of the carbon has not been conclusively determined (i.e., from the divertor strike points, private flux region, or outer wall), it may be more difficult to control with divertor pumping than the fuel gas. Nonetheless, analysis [Lasnier (1996)] of our highest performance weak shear discharges has shown that the peak rate of electron density rise was reduced down to the NB fueling rate with aggressive wall conditioning and nonoptimized divertor pumping. To reduce the rate of density rise below the beam fueling rate requires additional pumping/baffling and possibly the initiation of ELMs in high performance discharges.

This additional pumping/baffling will be implemented as part of the radiative divertor program. The estimated combined pumping speed of all four cryopumps is 160,000  $\ell/\text{s}$ . Calculations [Fenstermacher (1995)] with the UEDGE and DEGAS codes have predicted  $\sim 8\times$  reduction in the core fueling rate with the addition of the pumps and baffles, which should lead both to better energy confinement and enhanced duration of the high performance phase.

**Pellet Fueling Research Program.** The mission of the pellet fueling program on DIII–D is to investigate the influence of pellet injection on plasma behavior, quantify the results and use that knowledge to identify pellet injection scenarios that lead to improved plasma performance and control. There are three main areas of emphasis of the pellet injection program on DIII–D to support this mission: plasma particle control, plasma confinement properties, and system particle inventory. Experimental investigations are planned that will help quantify the influence of pellet injection on plasma behavior in each of these areas. The topics of these investigations have been identified as important issues by the ITER program, but they are also very relevant to improved operation of DIII–D and fusion reactor plasmas in general.

There are several potential means of fueling large diverted plasmas and each is expected to have different effects on plasma operating behavior. These include gas injection, low field side (LFS) injection of

conventional speed ( $v \sim 1$  km/s) or high speed ( $v > 4$  km/s) pellets, high field side (HFS) injection of conventional speed pellets and compact toroid injection. Among these, HFS injection experiments on ASDEX-U [Lang (1996)] have shown great promise with improved penetration and fueling efficiency and reduced edge perturbations. The DIII-D pellet fueling program will explore LFS and HFS injection of conventional speed pellets and compare the results with gas injection under a variety of experimental conditions. The experiments will use pellets to help separate the influences of core, edge and divertor physics on plasma behavior, improve our understanding of the interrelationships between the physics processes and thereby establish a more solid foundation for access to improved confinement regimes with greater control over operating characteristics.

Pellet induced perturbations can be a useful means of probing plasma transport characteristics. Particle transport studies are a natural scenario for using pellet perturbations and have been used for such studies in the past [Baylor (1995)]. But perturbations to the local density, temperature and plasma rotation profiles may also induce fundamental changes in the transport characteristics, e.g., they may help trigger the formation of internal transport barriers. The proposed HFS pellet injection is anticipated to produce perturbations deeper in the plasma than LFS injection and also generate less ELM activity, which will allow us to better separate internal and edge physics effects.

**Fueling Efficiency.** Projections of the penetration depth for pellets injected into ITER plasmas on the LFS predict that the pellets will penetrate just inside the ELMing region. A quantitative study on DIII-D that compares the fueling efficiency of shallow pellet injection in ELMing H-mode plasmas from different fueling locations is planned. Injection locations on the outside midplane, inside midplane, and top launch are to be used. We plan the development of a self-consistent model of plasma shielding for pellets injected on the HFS that includes the interaction with ELMs. There is speculation that the same mechanism responsible for the HFS improvement in pellet fueling efficiency also applies to gas puff fueling. An experiment to compare HFS side pellet and gas puff fueling with LFS fueling is planned using helium. It is possible with helium to determine the inward flow rates using the CER diagnostic for helium density measurement.

**Density Profile.** For DIII-D AT plasmas an investigation of controlling the density profile peaking with pellet injection is proposed. The method used to provide the core fueling for density peaking may be either HFS injected pellets (limited to 200 m/s), high speed pellets ( $>2$  km/s), or CT injection. All three methods require proposed hardware upgrades for DIII-D.

**ELM Behavior.** Another aspect of impurity behavior related to pellet fueling is in using pellets to control ELM frequency in otherwise ELM free AT plasmas such as VH-mode. Impurity accumulation invariably occurs in these discharges so the possibility of using pellets to trigger benign ELMs that flush impurities from the plasma core will be investigated. Another important aspect of this study is the interaction of pellets with ELMs. Experiments to date in H-mode plasmas show that LFS pellets cause an ELM under virtually all conditions. A study of the ELM instigation by both LFS and HFS injected pellets and

an investigation of the asymmetry of the ballooning threshold as it applies to HFS pellet injection is part of this scenario plan.

**Internal Transport Barriers.** Earlier pellet-enhanced performance (PEP) mode studies on JET and TFTR have shown that the strong central density peaking from deep pellet fueling can lead to improved core confinement in both the ion and electron channels. The PEP mode has yet to be explored on DIII-D and is proposed for studies of core transport barrier formation. The program will utilize PEP-like conditions to further understand the role of peaked density, low plasma rotation, and  $E \times B$  shear effects on transport barrier physics. It is also proposed to use pellet perturbations to probe existing internal transport barriers (namely the NCS regime) to better understand the role of the density profile on barrier control. Pellets will also be used to investigate whether perturbations in pressure profile can be used to trigger the mechanism responsible for internal barrier formation.

**Plasma Startup.** It has been proposed in the past to use pellet fueling early in the DIII-D discharge formation to limit the amount of gas that gets loaded onto the first wall. Preliminary experiments have shown that up to 40% of the gas used to build the initial discharge density can be eliminated by the use of early pellet fueling. Experiments to utilize this fueling scheme will be executed to investigate the change in AT discharge behavior with reduced wall loading.

**Isotopic Fueling.** The proposed scheme of isotopic tailoring for ITER fueling [Gouge (1995)] uses tritium rich pellets and deuterium gas puffing to preferentially fuel the core plasma with tritium and minimize the tritium inventory in the first wall components. A study of this scheme in DIII-D is proposed by using hydrogen rich pellets in deuterium plasmas to investigate the dynamics of the isotopic fraction in the core plasma.

**The Physics of Density Limits.** An overwhelming body of tokamak data support the Greenwald [Greenwald (1988)] density limit scaling law:  $n_{GW} \approx I_p / \pi a^2$  ( $10^{14} \text{ m}^{-3}$ ). Several machines — notably TFTR, ASDEX-Upgrade, JET and DIII-D (under restrictive conditions) have operated at densities above this scaling, albeit at varying degrees of confinement degradation relative to the H-mode. Although the Greenwald limit is not fundamental, it is apparently very difficult to surpass. We have embarked upon a series of experiments to understand the physics of the density limit in tokamak plasmas. The phenomena studied include: divertor power balance limit, MARFE instability, ballooning mode, tearing mode, and H-L transition. The essential tools to accomplish this effort are a pellet injector, the divertor cryopumps, and arrays of high resolution diagnostics that measure profiles of electron density and temperature, ion temperature, impurity concentration, and current profile.

Normally in DIII-D, with either gas or pellet fueling (depending on divertor geometry and heating power) a density limit in the range 0.7 to 1.1  $n_{GW}$  is observed. This limit is seen following divertor detachment when the most prominent radiation zone reaches the X-point and is attributed to the divertor power balance limit. We have bypassed this limit [Maingi (1996), Mahdavi (1996)] by lowering the divertor density relative to the line average density by simultaneous divertor pumping and pellet injection. As a result, we

have succeeded in obtaining a line-average density of 50% above  $n_{\max}^{\text{GW}}$  with global energy confinement times of 1.8, normalized to the ITER–89P scaling, within a very narrow range of plasma parameters (Fig. 2.3–18). This result shows that there is no fundamental obstacle to achieving line average densities above the Greenwald limit in high confinement plasmas. However, our experiments show that there are numerous obstacles that make the path to high densities very difficult.

Radiation driven instabilities, such as the MARFE, within the core plasma can (in principle) prevent access to the desired densities. Using the data from the high-resolution edge plasma diagnostics, we

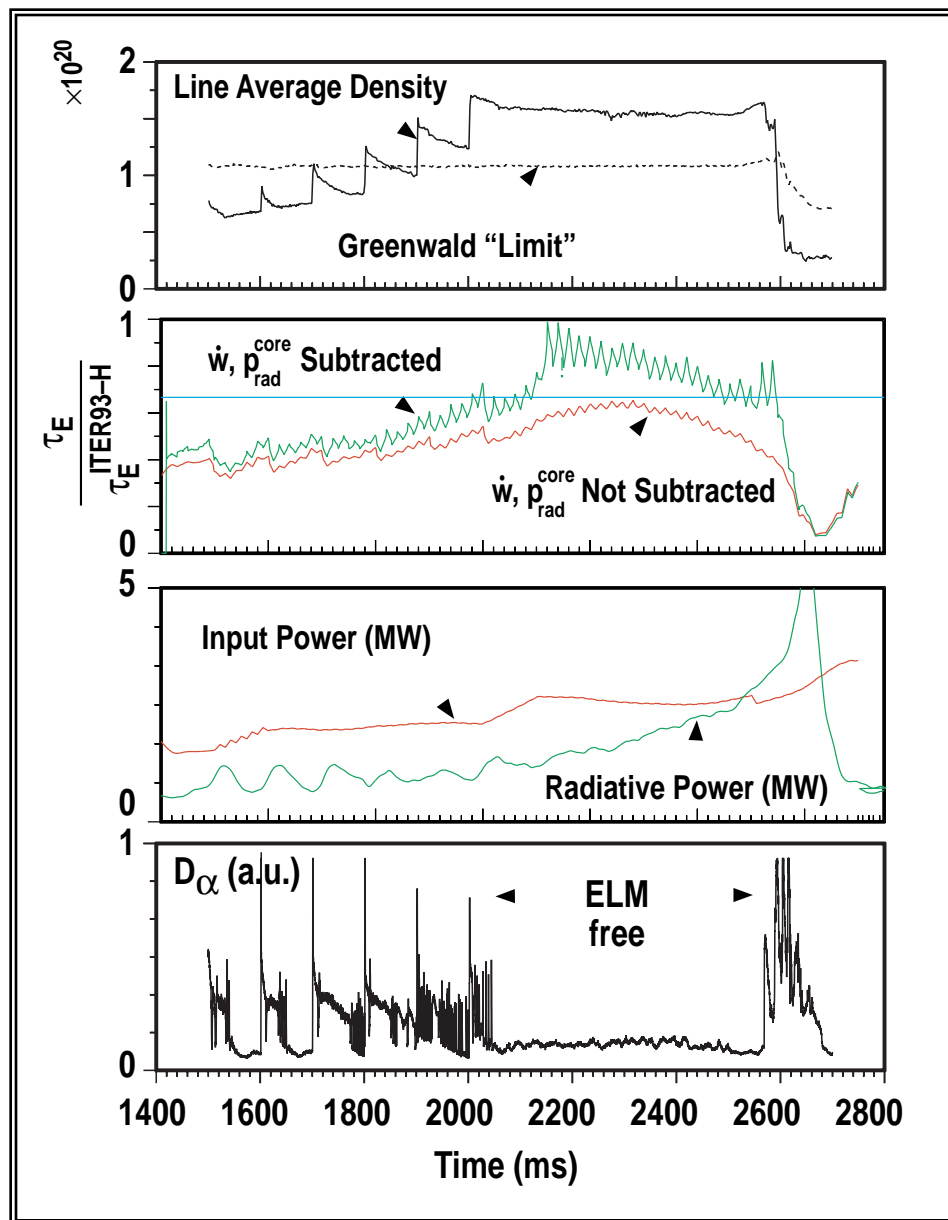


Fig. 2.3–18. Pellet fueling with divertor pumping shows the Greenwald limit is not an obstacle.

have found that the onset of the MARFE is in good quantitative agreement with the theoretical marginal stability condition [Drake (1987)] for this instability.

Several deleterious effects of fueling were observed (H–L transition, pellet-induced ELMs, and MHD modes) and are subjects of our continuing experimental effort on the physics of the density limit. Near the H–mode power threshold, pellets cause transient H–L transitions which result in an unacceptable particle loss. Spontaneous or pellet triggered Type I ELMs, attributed to the ideal ballooning mode, expelled a large fraction of the plasma density which frequently increased the fueling demand beyond the available injection rate. Finally, pellets invariably triggered low number MHD modes which at times continued to grow and lock long after the pellet density perturbation had decayed away. Analysis shows these plasmas to be stable to classical and neoclassical tearing modes. Therefore, additional physics is needed to explain these observations. A phenomena similar to “snakes,” observed on JET, is suspected and is the subject of our current experimental investigations.

**Control of Neutral Fueling for Improved Core Performance.** Most of the major advances in plasma confinement quality in DIII–D (and most other tokamaks) have been made through wall conditioning and management of neutral sources. This linkage in DIII–D is rather clearly shown in Fig. 2.3–19. The parameter

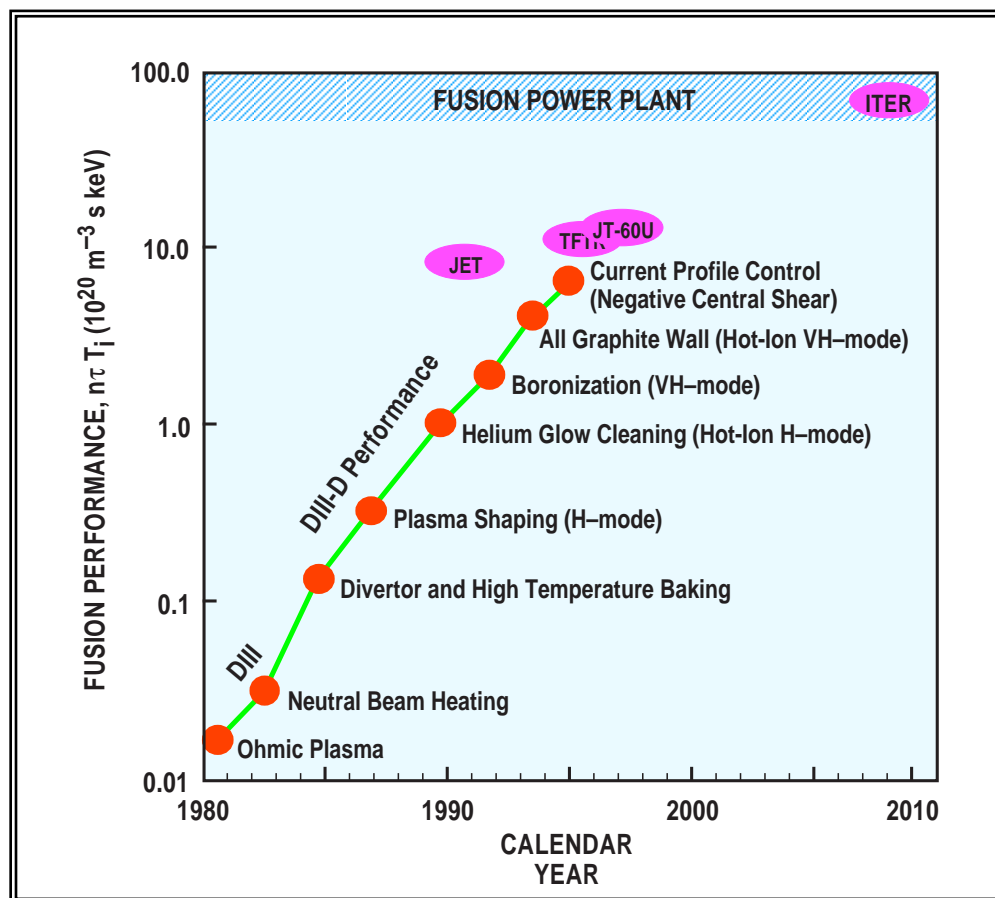


Fig. 2.3–19. Scientific progress: DIII–D fusion performance has doubled every 2 years.

$n\tau T$  was advanced from  $5 \times 10^{18}$  to  $\times 10^{20} \text{ m}^{-3} \text{ s keV}$  by the sequential implementation of divertor operation, baking, carbonization, helium glow wall conditioning, boronization, and the all-graphite wall. Today, experimenters will not attempt high quality confinement mode experiments unless DIII-D has been recently boronized and the helium glow between discharges is available. The quality of confinement in VH-mode reference discharges is used to monitor the condition of the wall.

Most of this effort on wall conditioning is aimed at reducing the immense source of deuterium neutrals that the graphite wall can store. The working hypothesis is that plasma confinement is improved by reducing the available core fueling by gas. In Fig. 2.3–20, we document the increase of confinement quality in DIII-D with decreasing neutral pressure. Clearly there is a reward in lowering neutral pressure although the effort must be made over three decades in neutral pressure!

The highly baffled double-null divertor to be installed in DIII-D is aimed at further improving confinement by further lowering neutral sources available to the plasma. In Fig. 2.3–21, we show calculations in the reduction factor of core fueling from the unbaffled case to cases with varying positions of the outer baffle. These calculations were done by using UEDGE to calculate an attached plasma solution and then using DEGAS to calculate the resulting core fueling rate from the neutrals recycled off the

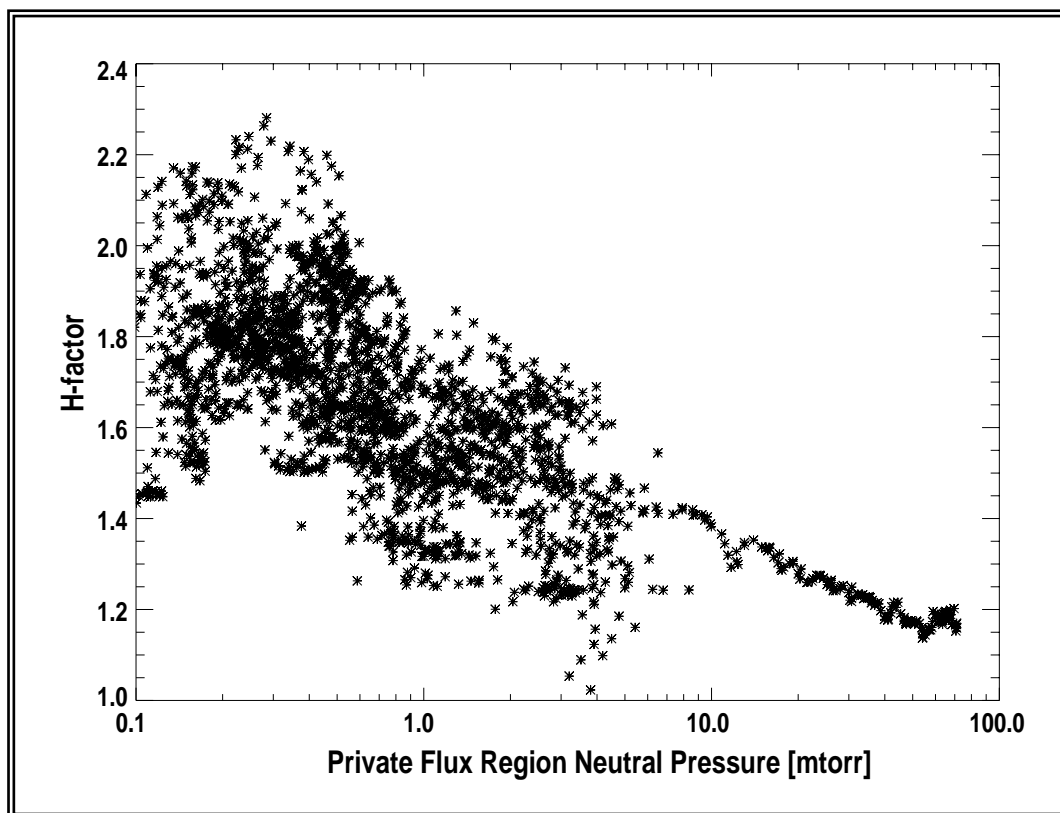


Fig. 2.3–20. A large pressure decrease in ELMing H-mode discharges is rewarded with an increase in confinement quality.

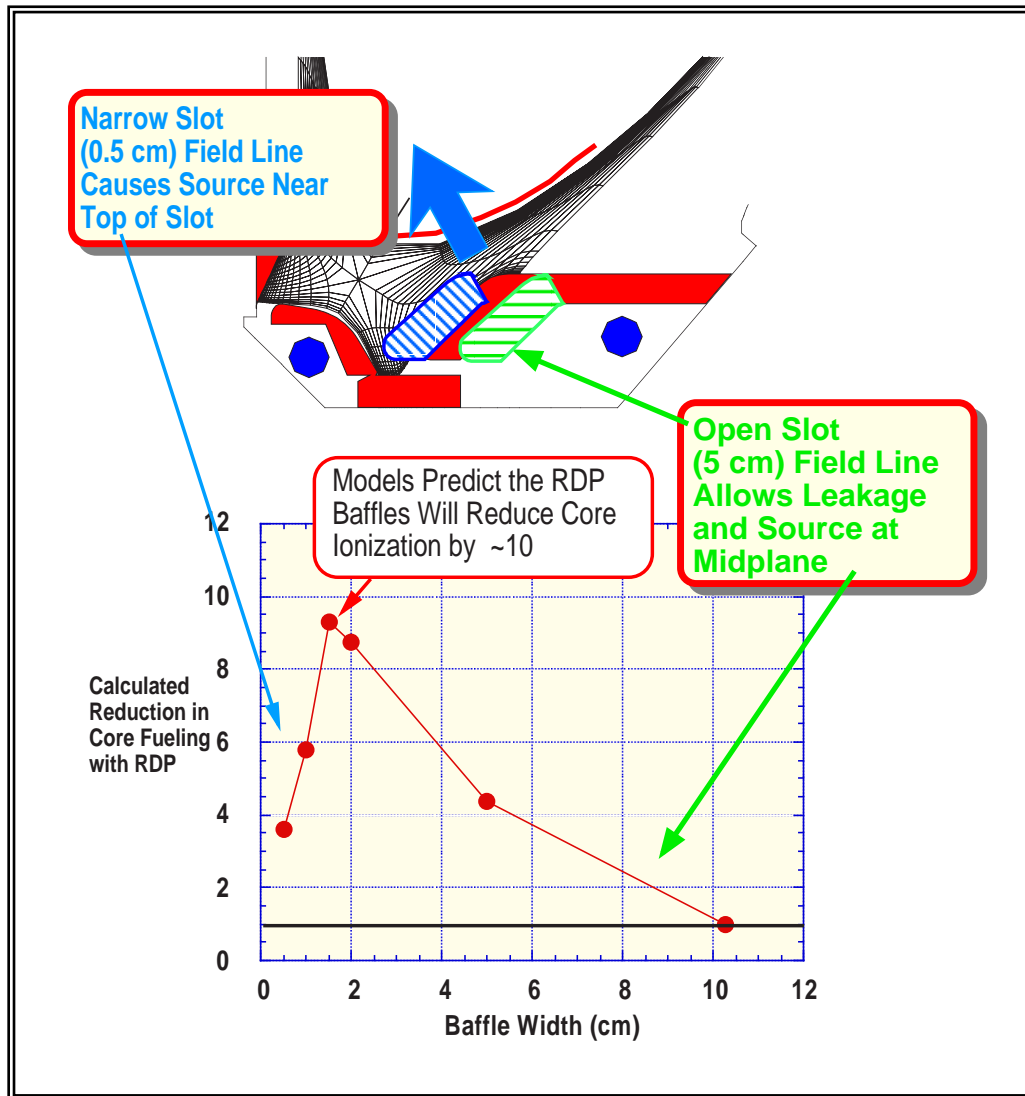


Fig. 2.3-21. Models predict the RDP baffles will reduce core ionization by an order of magnitude.

divertor surfaces. At the optimal baffle position, a factor of ten reduction in core fueling, for the same neutral reflux sources is expected. How the plasma will respond to this altered boundary condition is not clear. On a continuum of possibilities, we can discuss the two endpoint possibilities for a new steady-state particle balance. First, the plasma particle confinement time could increase a factor of 10 along with a factor of 10 reduction in core fueling while the neutral reflux sources at the divertor surfaces remained the same. This would be the path of improved confinement. Second, the particle confinement time could be unaffected (dominated by interior plasma physics, not neutrals); the core fueling would then also have to be the same as the unbaffled case; and the neutral pressures and neutral reflux at the divertor surfaces would rise a factor of 10. Preliminary results from the closed divertor experiment in JET indicate that the JET plasma has chosen the second solution. No change in core plasma confinement was seen. However, the increased neutral pressures in the divertor enable divertor detachment at lower density, a direction that could help

DIII-D couple the detached/radiative divertor operation to the lower core density plasmas of interest to the AT Program.

**Interaction with the H-mode Shear Layer.** A view of tokamak physics has emerged that divides the plasma into three radial regions. The first region, the core plasma, is from the top of the H-mode pedestal inward. The second region is the H-mode shear layer, which comprises only a few centimeters just inside the separatrix in present machines. The third region is the SOL/divertor region from the separatrix to the divertor plate. A subject of current debate is the extent to which a “stiff” transport model determines the entire core performance given the height of the pedestal on the inner side of the H-mode shear layer. The H-mode shear layer connects Regions 1 and 3 and provides boundary conditions for both. The physics of the H-mode shear layer must consider neutrals and so is unlikely to be described solely by the dimensionless parameters of plasma physics. Experimental and theoretical interest is currently focused on this shear layer. On its outer side, it sets the boundary conditions of power flow, density, and temperature for the SOL/divertor.

Various lines of physics investigation are being pursued in regard to the interaction of the SOL/divertor and the H-mode shear layer, especially in regard to neutrals. One theory of the L–H transition has as its key driver the strongly spatially varying ionization source in the H-mode shear layer [Staebler (1994)]. A possible clue to the connection of confinement quality and neutrals is given by the correlation of the pedestal height clearly increasing with decreasing neutral pressure. The role of charge exchange damping of momentum at the edge in the L–H transition is being investigated. Charge exchange damping is dominated by neutral fueling through the separatrix, which may be connected to the very slow L–H transitions (Section 2.3.1.7) that are connected with MARFE formation and are being pursued for studies of H-mode causality. Divertor pumping has been shown to affect the L–H transition threshold power. Another idea being pursued is the suggestion of Miura that collisionless ion orbits will suffer charge exchange primarily in the SOL where the neutral density is high or near the X-point where both the neutral density is high and the orbits spend a lot of time near their banana tips. The charge-exchange of these ions would constitute a radial current flow that would have to be replaced by a cold return current and thus exert the torque on the plasma that may cause the L–H transition. This idea is related to the original suggestion of Shaing that edge ion orbit loss could be the trigger mechanism for the L–H transition.

### Edge Localized Modes (ELMs)

**Type I ELM Divertor Effects.** To determine the effects of Type I ELMs in the ITER divertor we need to understand the scaling of four parameters to an ITER discharge (1) the ELM energy loss from the main plasma, (2) the fraction of that energy deposited on the divertor target, (3) the profile or area of the ELM heat flux, and (4) the  $\Delta t$  of the ELM heat flux.

We obtained a scaling for the Type I ELM energy loss (Fig. 2.3–22) where the absolute energy loss per ELM,  $\Delta E$ , is independent of input power and scales approximately linearly with plasma current. This scaling predicts an energy loss of 26 MJ per Type I ELM in ITER. In ITER shaped discharges we found that

roughly 80% of the ELM energy loss is deposited as heat flux onto the divertor target. The width of the ELM heat flux was about twice that in-between ELMs with up to twice as much energy going to the inner strikepoint as the outer. The time scale for the ELM heat flux was about 1 ms with no discernible systematic variation. If the same fraction of ELM energy loss reached the ITER divertor with similar spatial distribution and time scale, this would be near the limit of what is tolerable.

**Type III ELMs.** Type III ELMs have the desirable feature that the energy loss per ELM is a factor of 5 to 10 times less than for Type I ELMs. Type III ELMs would thus be desirable for ITER if they were compatible with other aspects of ITER operation.

Two distinct classes of Type III ELMs have been identified on DIII-D. The low temperature class, which has been studied extensively on ASDEX-U and DIII-D, occurs below a critical edge temperature. It appears to be possible to achieve energy confinement comparable to the Type I ELM regime with low-temperature Type III ELMs if the density is sufficiently high. An improved understanding of the scaling of the critical temperature for this ELM type will be necessary to determine if they will occur in ITER.

A second class of Type III ELMs has been identified at low density on DIII-D. These ELMs do not exist above a critical edge pressure gradient which is less than the critical pressure gradient for Type I ELMs but which also scales as  $I_p^2$ . This separation in pressure gradients results in reduced energy confinement in the low density Type III regime relative to the Type I regime. In terms of global parameters, low-density Type III ELMs disappear above a critical input power which scales as  $I_p^{2.4}/n_e^2$ . The density dependence may be tied to the rate at which neutrals fuel the edge pressure gradient. The reduction in energy confinement with low-density Type III ELMs may represent a concern for ITER as they can occur at powers well above the H-mode threshold power if the density is low enough. More work needs to be done on the scaling of the threshold conditions for low density Type III ELMs.

**2.3.3.3. MATERIALS AND PLASMA WALL-INTERACTION SCIENCE.** A wide variety of physical and chemical processes are taking place at the interface between the plasma and the wall in a magnetic confinement

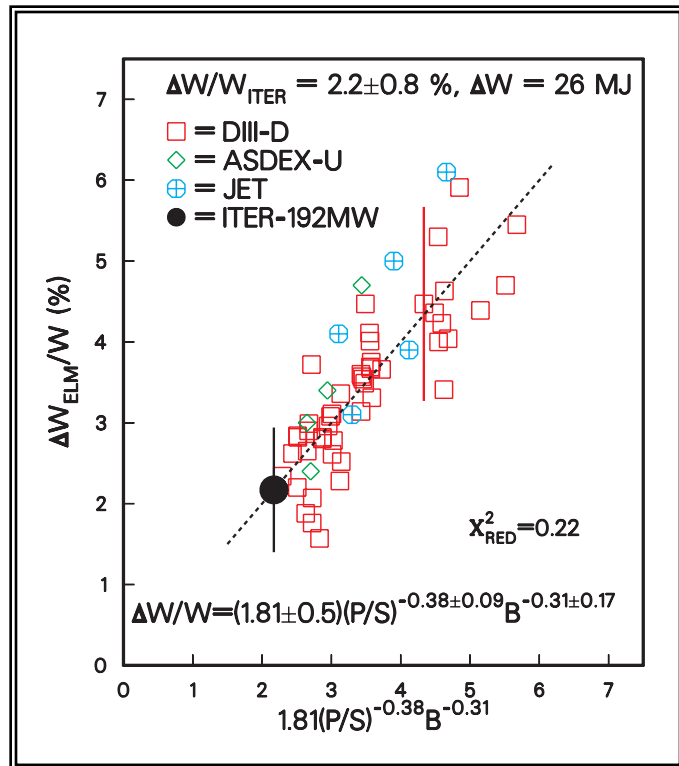


Fig. 2.3-22. A 26 MW energy loss per Type I ELM is predicted for ITER.

device. These processes result in the recycling of plasma particles, in impurity influx into the plasma, in the erosion and redistribution of wall material, and in the uptake of plasma constituents by the wall. The detailed understanding of the combined effect of the multiple plasma/wall interaction processes, the complex magnetic geometry, and the varied conditions in the plasma periphery has not yet been achieved, but progress in both the experimental documentation and detailed modeling has been significant. The demonstration of truly stationary current and pressure profiles for long-pulse AT operation requires that plasma-wall interactions are fully equilibrated. This requires long-pulse operation.

**Atomic Physics and Plasma-Wall Interactions.** The edge plasma is dominated by atomic physics with a strong effect on confinement and plasma performance. To make progress in defining the relation between wall effects and confinement, a much better job of characterization must be done. An accurate description will require advanced spectroscopic studies. This necessitates supporting studies and links to atomic physics and surface science expertise. Given the presently great, and surely increasing, pressure on DIII-D experimental access, the most effective strategy will involve prescreening and evaluation of diagnostic techniques using off-line resources.

## Research Goals

**Equilibration Time.** The first goal is to measure recycling equilibration times as a function of wall conditions, plasma parameters, and external exhaust. This is to establish criteria for stationary conditions with respect to wall conditioning, wall temperature, plasma density, heating power, and pulse duration. Plasma-wall equilibration in discharges without external pumping is assumed to take several hundred seconds; e.g., in Tore Supra the density was still evolving at the end of a 120-s discharge. However, in a discharge with external pumping, the resulting wall equilibration time depends on the effective global recycling coefficient, which, after a few seconds, is determined by the applied external exhaust rate. With an exhaust rate of 10% of the recycling flux, i.e., with a recycling coefficient  $R = 0.9$ , the density response time is  $\tau_p = \tau_p / (1-R) = 10 \times \tau_p$ , i.e., in the order of 5 to 10 s, assuming  $\tau_p^* \sim 0.5$  to 1 s. Thus, from the fuel recycling point of view, pulse durations of 10 to 50 s can provide a reasonable test of wall equilibration if external pumping is applied.

The recycling species will be identified as a function of the wall conditions. Possible species and their fractions to be identified experimentally are: atomic and molecular hydrogen, hydrocarbons, and other impurities. These species need to be identified as a function of the location inside the tokamak, i.e., the divertor area or the inboard/outboard wall, etc. The properties of the wall-emerging species will be determined. This includes densities, temperatures, and drift velocities, as well as ionized fractions, excited electronic states, vibrational states, etc. The atomic processes in the SOL, divertor, and in the edge plasma layer (EPL) inside the separatrix need to be characterized. They depend on the recycling species and their states as well as on the plasma parameters. Some of the prominent processes are: ionization, excitation, dissociation, recombination, elastic collisions, Franck-Condon processes, and charge-exchange reactions. Models need to be developed that incorporate the effects of plasma-wall interactions and atomic physics

in the divertor, SOL and EPL on the basic core transport processes. And finally, the successful models will serve to devise techniques which allow the control of transport mechanisms through atomic and wall processes.

**Supporting Studies and Links to Atomic Physics and Surface Science.** The tokamak, and especially the tokamak edge, presents spectroscopists with a complex and ill-defined plethora of inter-related processes. Since some of the studies on wall interactions, as well as on atomic and molecular processes, will require detailed identification of basic characteristic features, such as band structure, very detailed preliminary experiments must be carried out in a well characterized environment in laboratory-scale facilities to conduct supporting experiments in order to better understand the atomic and molecular physics processes in the plasma edge of tokamaks. Furthermore, for the understanding of specific processes involving the interactions of plasma particles with solid surfaces and resulting in recycling species with particular properties, the surface science expertise available in the laboratories of various collaborators will be important.

**Erosion Studies.** The Divertor Materials Erosion Studies (DiMES) program will continue to be the basis for the erosion/redeposition studies on DIII-D. The DiMES program on DIII-D is an umbrella for close collaboration between the DIII-D scientific staff, materials experts, and plasma/wall interaction modeling experts allowing direct interaction between the multiple experimental efforts required to carry out and analyze the materials exposure and the physical and numerical modeling efforts. The complexity of the problem requires such close interaction if progress is to be timely. The DiMES program, combined with the strong divertor plasma diagnostics effort, has allowed experimental measurement of net erosion of candidate divertor materials under well-characterized attached divertor plasma conditions. However, this effort has only begun to explore the widely varying plasma conditions possible on DIII-D. Laboratory studies of particle/surface interactions indicate that physical and chemical sputtering rates will depend strongly on the incident particles' energy, mass, and flux, as well as the surface material and morphology. The return of eroded particles back to the surface will depend strongly of the plasma density, temperature, and flow as well as the mass, energy and ionization rates of the eroded atoms. DIII-D can achieve a wide variety of divertor plasma conditions, from well attached sheath limited cases, to high recycling, high density attached plasma cases, to fully detached, cold dense cases. Thus the DiMES program on DIII-D provides a unique capability to provide the coupling between the basic particle wall interaction physics, plasma transport physics, and first wall design issues.

**Alternate Wall Materials.** DIII-D is presently an "all graphite" machine, meaning that the first wall is over 90% graphite. The plasma  $Z_{\text{eff}}$  and the radiated power are dominated by carbon. Our wall conditioning techniques are focused on the properties of graphite; and in many cases, our operational scenarios are devised with the properties of the carbon wall in mind. However, the future of magnetic confinement fusion will probably not include graphitic first wall materials. The dominant reasons that graphite is not a suitable wall material are: (1) net divertor erosion rates that lead to an unsuitably short component lifetime, (2) tritium uptake rates that produce a large wall tritium inventory, and (3) neutron damage rates that degrade material structural integrity and thermal conductivity.

The wall physics studies will be used to choose divertor and main chamber first wall materials that provide a suitable test of materials attractive to future devices. Operation of DIII-D with this new wall is proposed for the last year of the plan period.

Tungsten seems to satisfy the divertor's needs for low sputtering, high redeposition, and low tritium uptake. However, because it has a high nuclear charge, the core plasma radiation can be excessive with very low concentrations ( $10^{-4}$ ) of tungsten. Recent experiments on the ASDEX-Upgrade device have indicated successful tokamak operation with a tungsten divertor. For high recycling and detached divertor operation, core contamination was acceptable and, in some cases, too low to observe. Tungsten is likely to remain the material of choice for the divertor first wall.

The main chamber wall materials' requirements are not as stringent (from an engineering point of view) since the peak heat and particle flux will be small compared to the divertor. One primary concern is to provide a low-Z first wall to minimize the deleterious effects from core plasma contamination. Low-Z coatings over graphite tiles will be investigated as a suitable alternative.

### References for Section 2.3.3

- Baylor, L.R., et al., Proc. 22nd Euro. Conf. on Controlled Fusion and Plasma Physics, Bernemouth [European Physical Society, Petit-Lancy (1996)].
- Drake, J., Phys. Fluids **30**, 8 (1987).
- Fenstermacher, M., et al., 12th Int. Conf. on Plasma Surface Interactions in Controlled Fusion Devices, May 20–24, 1996, Saint Raphael, France, to be published in J. Nucl. Mater.
- Fenstermacher, M.E., et al., J. Nucl. Mater. **220–222**, 330 (1995).
- Gouge, M.J., et al., Fusion Technolog.
- Greenwald, M., Nucl. Fusion.
- Hill, D.N., et al., J. Nucl. Mater. **196–198**, 204 (1992).
- Isler, R., et al., "Signatures of Deuterium Recombination in the DIII-D Divertor," to be submitted for publication.
- Lang, P.T., et al., IPP Report 1/304 (1996).
- Lasnier, C.J., et al., in 12th Int. Conf. on Plasma Surface Interactions in Controlled Fusion Devices, May 20–24, 1996, Saint Raphael, France, to be published J. Nucl. Mater.
- Lazarus, E.A., et al., Proc. 15th Int. Conf. on Plasma Physics and Controlled Nuclear Fusion Research, September 26–October 1, 1994, Seville [International Atomic Energy Agency, Vienna, (1995)] Vol. 1, p. 609.
- Mahdavi, M.A., et al., "Divertor Plasma Physics Experiments on the DIII-D Tokamak," in Proc. 16th Int. Conf. on Plasma Physics and Controlled Nuclear Research, October 1996, Montreal, (International Atomic Energy Agency, Vienna) to be published.
- Mahdavi, M.A., Proc. 20th European Conf. on Plasma Physics and Controlled Nuclear Fusion, Lisbon, Portugal, Part II, p. 647 (1994).

- Maingi, R., et al., “Investigation of Physical Processes Limiting Plasma Density in H-mode on DIII-D,” to be published in *Phys. Plasmas* (1996).
- Maingi, R., et al., *Nucl. Fusion* **36**, 245 (1996).
- Porter, G., et al., in Proc. 23rd European Conf. on Controlled Fusion and Plasma Physics, June 24–28, 1996, Kiev [European Physical Society, Petit-Lancy (1996)] Vol. 20C, Part II, p. 699.
- Rensink, M.E., et al., *Phys. Fluids B* **5**, 2165 (1993).
- Schaffer, M., 12th Int. Conf. on Plasma Surface Interactions in Controlled Fusion Devices, May 20–24, 1996, Saint Raphael, to be published in *J. Nucl. Mater.*
- Staebler, G., and F.L. Hinton, *Phys. Plasmas* **1**, 909 (1994).
- Wade, M.R., et al., in Proc. 23rd European Conf. on Controlled Fusion and Plasma Physics, June 24–28, 1996, Kiev [European Physical Society, Petit-Lancy (1996)].
- Wood, R., et al., in Proc. 23rd European Conf. on Controlled Fusion and Plasma Physics, June 24–28, 1996, Kiev [European Physical Society, Petit-Lanc, (1996)] Vol. 20C, Part II, p. 763.

### 2.3.4. PHYSICS OF CURRENT DRIVE AND HEATING

*The science of generating and controlling the plasma current has broadened considerably, both generally and in the DIII-D Program. With the advent of diagnostics that can measure the interior current profile, the role of the current profile in plasma confinement and stability has become prominent; various internal transport barrier modes are identified with their characteristic current profiles. With the ECCD and FWCD systems planned for DIII-D, control of the current profile is a near term possibility. DIII-D will continue to investigate the basic physics of noninductive current drive using electron cyclotron and FWs and NBs. The heating from these systems, with the amplification of transport barrier formation, can control the amount and radial location of the bootstrap current. With the enhanced stability expected with optimized current profiles, achieving 100% bootstrap fractions appears realistic. Indeed, using bootstrap overdrive ( $f_{bs} > 100\%$ ) and other plasma initiation techniques, it appears possible to startup, rampup, sustain the plasma current, and control its profile without use of the OH transformer, providing future machines the basis for the simplification of transformerless design*

**2.3.4.1. INTRODUCTION.** Waves and particles have been used for plasma heating and current drive for many years. In the past, the concentration of research has been on bulk current drive; however, recent research has shown the value of control of the current profile for improved performance. At the same time, the current due to the neoclassical bootstrap effect has been shown to play a major role in AT discharges, thereby reducing the requirements on the efficiency of noninductive current drive. The science issues involving current drive therefore become strongly related to transport of particles and energy (which affect the bootstrap current), transport of current, and generation of off-axis currents. These will be active topics of research.

RF heating and current drive can be used in testing models of heat transport in plasmas. Models of transport due to plasma microturbulence, for example, show strong sensitivity to parameters of the plasma like the radial gradient in the plasma flows and the ratio of the electron temperature to the ion temperature. By modifying these parameters using rf heating or current drive, we can help to determine the role played by the subject instabilities in the transport processes. Raising the temperature ratio  $T_e/T_i$  to near unity through strong electron heating also moves the plasma into a regime more like that of reactor plasma, thereby making studies of transport and stability limits more relevant.

In addition to maintenance of the current profile, an active area of research will be ramping of the plasma current from very low levels. This is motivated by the prospect of a move toward low aspect ratio tokamaks, for which elimination of the OH transformer would be a major benefit. A number of approaches appear feasible.

Current drive and heating can also be used to control or suppress plasma instabilities. Past research has shown effects on sawteeth, ELMs, and other MHD activity. In this plan, the heating and current drive systems are used to suppress sawteeth in order to allow high- $\ell_1$  discharges with central safety factor well below unity. Higher order tearing modes, for example the neoclassical tearing mode with mode numbers (2,1) and (3,2) which are known to limit beta in DIII-D and other tokamaks, will be suppressed using localized current generation.

**2.3.4.2. MAINTENANCE AND CONTROL OF THE CURRENT PROFILES.** Recent experiments on a number of tokamaks have demonstrated the value of optimization of the current profile. Low order core MHD modes can be avoided by keeping the minimum of the safety factor,  $q_{\min}$ , above the low order ratios (1, 3/2, 2), and the ballooning modes can be stabilized by weak or negative shear. With the MHD instabilities suppressed, the plasma pressure can be raised without core MHD instability to a level where the pressure gradient generates sufficient rotational shear to stabilize kinetic instabilities, thereby reducing transport to neoclassical levels. At the same time, the large pressure gradient introduces a large bootstrap current which greatly reduces the need for externally driven currents. Thus, the role of current drive systems is to support the detailed control of the current profile around the bootstrap current, which might supply 70% of the total current [Turnbull (1995)]. The role of magnetic shear, whether weak or strongly negative, is not fully understood at this time, but recent results from JT-60U suggest that a strong barrier in the electron channel, in addition to the more commonly observed barrier in the ion channel, can be obtained with strong NCS [Itam (1997)]. This last reference is particularly notable in that it described improved core confinement in a plasma with an L-mode edge and a radiative divertor in which 70% of the input power was radiated.

The primary role of the current drive systems is therefore to help maintain the plasma current and support the optimization of the magnetic shear. Experiments on DIII-D using FWs [Prater (1997)] and in Tore Supra [Litaudon (1995)] using lower hybrid waves have shown that localized noninductive current drive can affect the  $q$ -profile and that this control can yield improved confinement and stability. An example of this behavior from DIII-D is shown in Fig. 2.3–23. Here, 2 MW of FWCD was applied in the counter-current direction to drive a central current which opposed the inductive current. This dramatically slowed the resistive decay of the central  $q(0)$  and the onset of sawteeth was deferred from 1.6 s with co-FWCD to 2.15 s with counter-FWCD. As the current profile relaxed toward a weak shear condition, a spontaneous transition to a condition of improved confinement occurred at 1.95 s, as highlighted by the shaded area in the figure. Both the electron and ion temperatures increased. This phase ended when the central safety factor decayed to 1 and sawteeth began. Modeling suggests that the weak magnetic shear condition can be maintained more easily by suitable application of off-axis co-current drive than by on-axis counter-current drive.

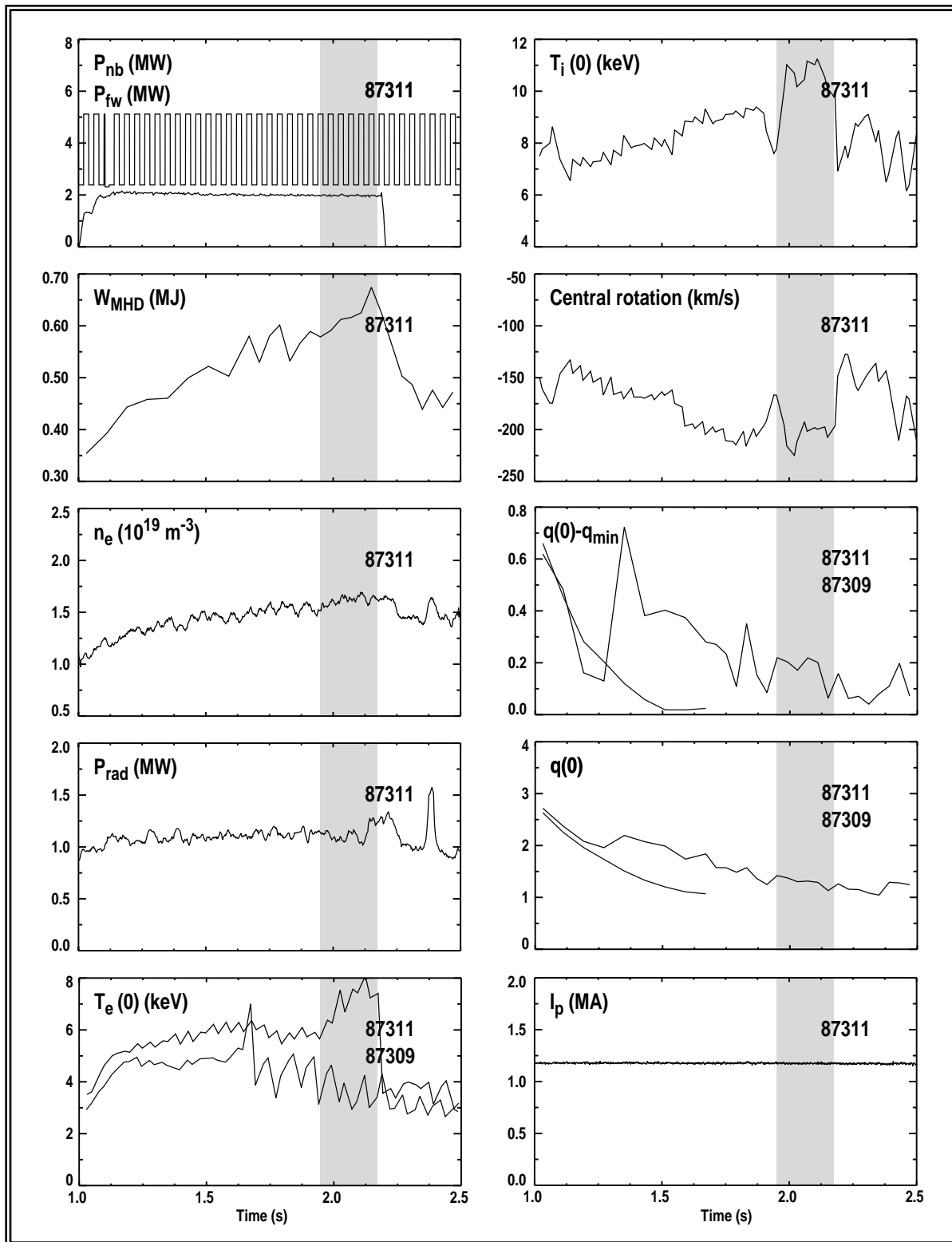


Fig. 2.3-23. Localized noninductive current drive can yield improved confinement and stability.

**Stability of Current Profile.** A key physics issue is the stability of the current profile in a discharge with very high bootstrap fraction. Most proposed steady-state ATs and low aspect ratio tokamaks obtain a large fraction (>70%) of bootstrap current to maintain the plasma equilibrium. These high bootstrap fraction plasmas are characterized by a current profile peaked off-axis with a NCS or WCS configuration. The interplay between the transport barrier and the bootstrap current, which is peaked where the pressure gradients are largest, can introduce a slow current diffusion instability which expands or shrinks the region of improved core confinement. Moreover, the presence of ohmic current, which favors a centrally peaked current profile, tends to destabilize the NCS/WCS configuration. The slow collapse on a resistive time scale of the transport barrier observed in the NCS discharges in JT-60U [Itami (1997)] signifies this type of instability. A localized heating or current drive source such as ECH or ECCD can be used to control the pressure and current profiles and eliminate the instability. More modeling is required to determine the exact conditions and powers required to obtain stability.

**Power Requirements and Limits.** The allowable range of power which can be used in AT scenarios in DIII-D can be estimated from simple relationships between the beta limit and the energy confinement. The beta limit may be expressed in normalized form as a limit on  $\beta_N = \beta/(I_p/aB)$ , where  $I_p$  is the plasma current in MA,  $a$  is the plasma minor radius in m, and  $B$  is the toroidal field, and the confinement may be expressed as a factor  $H$  multiplied by the confinement time calculated from the ITER-89P scaling relation. Putting together the definition of beta,  $\beta = \langle nkT \rangle (B^2/2\mu_0)$ , the energy confinement time,  $\tau_E = 3\langle nkT \rangle V/2P$ , where  $V$  is the plasma volume and  $P$  is the total power, and the ITER-89P scaling gives the relation

$$P_{MW} = 0.0089 \left( \frac{\beta_N}{H} \right)^2 \left( \frac{I_{MA}^{0.3} B_T^{1.6} V^2}{a^{2.6} R^{2.4} \kappa} \right) \dots, \quad (6)$$

so for fixed plasma parameters the required power is proportional to  $(\beta_N/H)^2$ . This behavior is shown in Fig. 2.3–24 for parameters typical of DIII-D.

The power requirements and limits for AT operation in DIII-D can be estimated from Fig. 2.3–24. For example, for the parameters of Fig. 2.3–24 and the target conditions of  $H = 3.5$  a and  $\beta_N = 5.0$ , the required power will lie between 15 and 20 MW. It is necessary that the power requirements for current drive lie below the power which heats the plasma to the beta limit.

**Time Constants and 10 s Operation.** To estimate time constants, the plasma current profile (actually the poloidal flux profile) can be represented as the sum of “normal modes,” each with a shorter radial wavelength [see Mikkelsen, *Phys. Plasmas* B **1**, 333 (1989)]. The longest time constant ( $\tau_0$ ) is for the decay of the total current. This value is important for noninductive current ramp-up experiments. For current profile control in high performance plasmas, the time constants for the next few higher order modes should be used ( $\tau_1, \tau_2$ ). The table gives these times, roughly estimated for various values of  $T_e(0)$  in DIII-D. For time constants appropriate to current profile control in thin regions, the local skin-depth formula is more

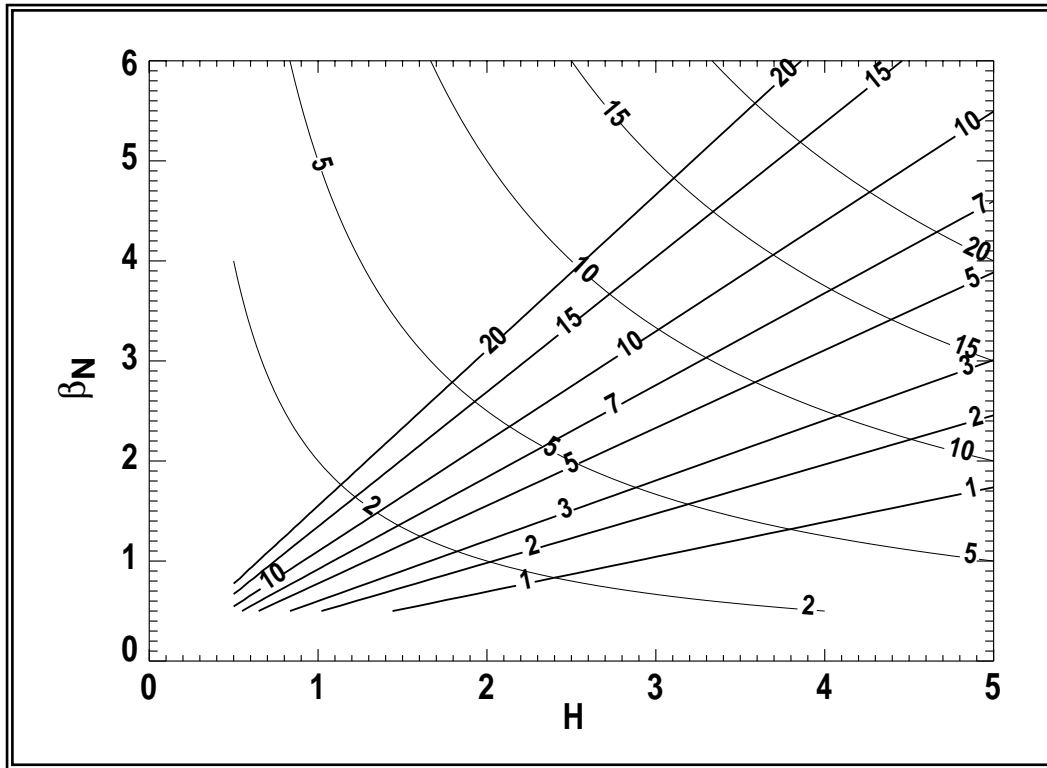


Fig. 2.3-24. The allowable power range of DIII-D AT scenarios can be estimated from simple relationships.

appropriate. The last column gives the approximate time constant for a 10 cm thick layer, at  $r/a = 0.5$ , with  $T_e = T_e(0)/2$ .

$T_e(0)$ keV	$\tau_0$ (s) <sup>(a)</sup>	$\tau_1$ (s) <sup>(a)</sup>	$\tau_2$ (s) <sup>(a)</sup>	$\tau_{skin}$ (s)
1	0.75	0.45	0.13	0.01
3	2.5	1.5	0.4	0.05
6	5.6	3.4	1.0	0.13
12	14	8	2.5	0.4

<sup>(a)</sup> $\tau_0$  at constant surface voltage;  $\tau_1$  and  $\tau_2$  at constant total current.

Current ramp-up experiments require high power input, making it difficult to hold  $T_e$  at very low levels. With  $T_e(0) \approx 3$  keV, we will have time for definitive studies of partial ramp-up. However, it will not be possible in a 10 s pulse to cover the full range from a few 10 s of kA to 1-2 MA.

For high performance operation, we will have to use transient techniques to prepare the plasma and to come close to the “steady-state” current profile. The time constants  $\tau_1$  and  $\tau_2$  represent the time required

for the loop voltage profile to relax in these cases. Clearly, even after 10 s, there will be residual transient effects.

Another consideration to note is that at present, we have nominally 5 s pulse operation. Of this time, 1–2 s are used in the initial transient to raise the current and to bring the profiles to the desired configuration. Thus, at most 3–4 s are available for evolution toward a steady state and for noninductive current profile control studies. Extending the pulse capability of the tokamak and the noninductive rf sources to 10 s operation will extend the duration available for such experiments by significantly more than a factor of two.

**Approaches to Current Drive.** On DIII-D, there are several approaches to current drive, all of which require study. First, FWCD is effective at driving current and electron heating near the center of the plasma. This is very useful for generation of discharges with high  $\ell_1$ , which past research has shown to have the potential for improved performance. Scientific questions regarding FWCD relate to the damping of the wave by ions, particularly those from the NB fast ion population, and the effect of the waves on plasma rotation. The FW system can also be used for minority ion heating, a hydrogen minority in deuterium, for example, which also provides strong electron heating and a nonthermal ion distribution which can be useful for suppression of sawteeth (see Section 2.3.4.5).

For off-axis current drive, ECCD is the best system from the point of view of control of the location of the current drive. ECCD takes place near the cyclotron frequency or, as in the case of DIII-D with 110 GHz ECH power, near the second harmonic. Thus, through control of the magnetic field the absorption location can be easily determined. Scientific issues for ECCD primarily concern the effect of trapping of the electrons in the magnetic well and the diffusion in space of the current carrying electrons, which will manifest itself as a broadening of the driven current profile. For stabilization of MHD tearing modes, which requires large currents highly localized, this is a key issue, but it is unlikely to be very important for obtaining reverse shear profiles, for which the gradients in current density are relatively small.

NBs also drive current, although the profile is highly dependent on the plasma density and not easily controllable. Nevertheless, NBCD contributes to the overall current drive. A counter-current NB would allow NBI heating with the NB currents largely canceling.

Another approach to generation of off-axis current is MCCD [Ram (1995)], in which FWs are launched at around 30 MHz with a toroidally-phased antenna array. The FWs propagate up to the ion-ion hybrid layer in a two ion species plasma, in this case a hydrogen minority of 30% to 50% in a deuterium plasma, where the power is converted to an IBW. The IBW is generally strongly damped on electrons very close to the mode-conversion point, which is the property that allows strong, localized, controllable heating and current drive. The location of the mode conversion surface is controlled either by changing the toroidal magnetic field strength or by varying the minority concentration.

The mode-conversion heating scheme has been previously studied on several tokamaks (TFTR, JIPP-IIU, JFT-2M, PLT) using inside launch antennas. More recently, it was realized that outside launch

antennas could be used as well, if the launched spectrum was peaked at high enough toroidal wave numbers (requiring a phased antenna array) and if competing wave damping mechanisms could be minimized [Majeski (1994)]. This led to successful applications of this heating scheme on TFTR, Tore Supra, JET, Alcator C-Mod, and ASDEX-U. On TFTR, approximately 0.1 MA of current has been driven using MCCD [Majeski (1996)].

In order to implement mode conversion heating and current drive on DIII-D, either an inside or outside launch antenna can be used. The existing outside launch antennas, however, would require some changes in the strap geometry in order to launch the low frequencies effectively. Inside or outside launch has advantages and drawbacks for this application. Outside launch of FWs is technically easier than inside launch but is more sensitive to the minority concentration and toroidal wavelength. The primary advantage of inside launch is that the mode conversion is virtually 100% efficient in a single pass, which should allow for better localization of the heating and current drive. For D(H), a hydrogen minority in deuterium, the required frequency range for DIII-D is 25 to 32 MHz. Since the generators at DIII-D can operate only as low as 30 MHz, mode conversion studies would benefit from reduction of the minimum frequency, but some physics tests can be done at 30 MHz without modification of the transmitters. Some doubt about the quality of confinement in DIII-D with a large hydrogen fraction would lead us also to consider D(He<sup>3</sup>) as an alternative. Here, the frequency would need to be in the range 15 to 20 MHz. This is technically feasible, but major changes in the launchers would be required for effective coupling. For either case, mode conversion heating and current drive can be a valuable supplement to the ECH system on DIII-D.

#### 2.3.4.3. CURRENT INITIATION AND RAMP-UP

**Physics Objectives.** In the “classical” version of the tokamak concept, the toroidal plasma current is produced and sustained by means of induction, using the plasma as the secondary of a transformer. This is the arrangement used in every tokamak experiment built to date.

There are two important consequences of relying on induction to produce and maintain the plasma current. First, a primary transformer coil is required. In order to provide the flux change needed, the field in the centerpost has to be high. This means that an air-core transformer is needed (iron or other ferromagnetic materials would saturate) and that the primary coil must be inboard of the plasma. This requirement uses very valuable real estate for a complex coil system. The other consequence is that the fully inductive tokamak is inherently pulsed — the total change in flux linking the plasma is limited by maximum fields, forces, and currents.

The steady-state requirement can be satisfied by using inductive ramp-up of the tokamak current to its final value, followed by noninductive current drive to sustain the current indefinitely. However, a more elegant solution is to use noninductive means, or at least methods that do not require a transformer solenoid in the tokamak bore. This approach frees up space in the centerpost, and simplifies the construction

of the tokamak. For low aspect ratio tokamaks, including the ST configurations, transformerless startup is a necessity.

Noninductive current maintenance and profile control are discussed in other portions of Section 2.3.4. Here we look at the possible methods we plan to study for initiating the toroidal current in the DIII-D tokamak and raising it to the final operating value without benefit of the transformer solenoid.

**Ramp-Up Physics.** The ramp-up of the plasma current is determined by the relationship.

$$\frac{dI}{dt} = \frac{I_{BS} + I_{CD} - I}{\tau_{L/R}} \quad (7)$$

The total noninductive current is

$$I_{BS} + I_{CD} = C_{BS} \epsilon^{1/2} \beta_p I + \gamma_{CD} \frac{P_{CD}}{nR} \quad (8)$$

where  $\gamma_{CD}$  is primarily a function of temperature (approximately,  $\gamma \propto T$ ).  $\tau_{L/R}$  is determined mainly by geometry and the temperature. In addition, when ramping the current from very low values, we have to avoid both the equilibrium beta limit (expressed as a limit on  $\epsilon\beta_p$ ), and stability limits (expressed as a maximum allowed  $\beta_N$ ). Other considerations entering this problem are that the power available for heating and current drive is limited (also bear in mind that  $P_{CD} \leq P_{heat}$ ), and that the density can be taken to be a fixed fraction of the Greenwald limit. Using the definitions of  $\beta_p$  and  $\beta_N$ , the plasma current is (factors related to size and shape are suppressed):

$$I = C_0 \frac{\beta_N B}{\beta_p} \quad (9)$$

The noninductive current can also be expressed in terms of  $\beta_p$  and  $\beta_N$ :

$$I_{BS} + I_{CD} = C_1 \beta_N B + C_2 \frac{f_{P,CD}}{(n/n_G)^2 H^2} \beta_p \beta_N^2 B^2 \quad (10)$$

where  $f_{P,CD}$  is the fraction of the total power used to drive current, and the energy confinement time has been assumed to be  $\tau_E \propto HI/P^{1/2}$ , to relate the power and pressure. In Fig. 2.3–25, the relationship in Eq. (9) is plotted as a set of curves, each for a fixed  $\beta_N$ . The steady-state condition,  $I = I_{BS} + I_{CD}$ , is also indicated:

$$I_{SS} = C_3 \frac{(n/n_G)^2 H^2 \left( \beta_{p0} - \beta_p \right)}{f_{P,CD} \beta_p^3} \quad (11)$$

where  $\beta_{p0} = 1/(C_{BS}\epsilon^{1/2})$  is the value at which all of the current is bootstrap. Points to the right of this curve give positive  $dI/dt$ . Finally, the relaxation time varies roughly as

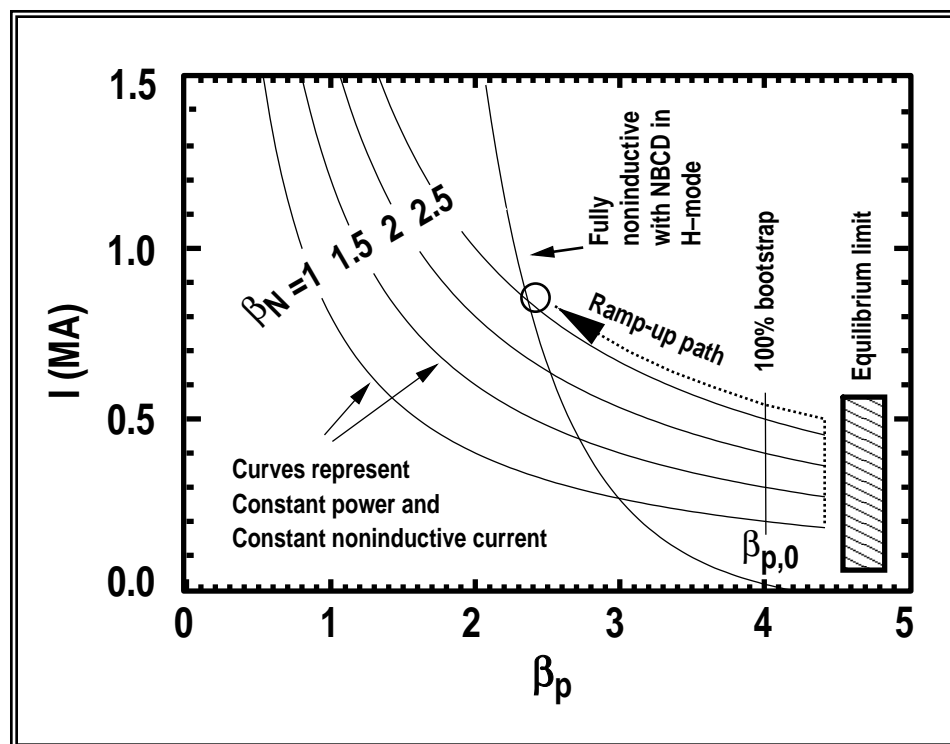


Fig. 2.3-25. Optimum ramp-up begins at  $\beta_p$  close to the equilibrium limit.

$$\tau_{L/R} = C_4 \frac{1}{(n/n_G)^{3/2}} (\beta_N B)^{3/2} \quad (12)$$

The optimum path for ramp-up appears to be to begin at high  $\beta_p$ , close to the equilibrium limit. Raise  $I$  (and  $\beta_N$ ) at constant  $\beta_p$  until the stability limit is approached. Then reduce  $\beta_p$  at constant  $\beta_N$  to increase the current further. One difficulty is that the stability limit may be determined by neoclassical tearing modes, which severely limit  $\beta_N$  as well as the bootstrap fraction, particularly at high  $\beta_p$ . Another is that the time scale for ramp-up increases with  $\beta_N$  as well as the bootstrap fraction. This motivates longer pulse operation of DIII-D.

We note that allowing the plasma size to increase during the current ramp-up extends the range over which ramp-up is possible and reduces the power needed. Determination of the optimum trajectory is a matter for further research.

**Using the Outer PF Coils.** A straightforward, reasonably well understood technique for initiating and ramping up the plasma current to modest values is to use the induction available from the shaping and equilibrium coils located near the centerpost above and below the vacuum vessel. Previous work on DIII-D using ECH pre-ionization and heating [Lloyd (1991)] has shown very reliable low voltage break-

down and ramp-up. This indicates that the modest voltage possible with shaping coils alone should be sufficient.

Experiments are being planned, in collaboration with the TRINITY laboratory, to demonstrate outer PF coil startup on DIII-D using the number 4, 5, and 8 coils to provide volt-seconds and coils 6 and 7 for position control. ECH will be used to initiate the plasma, and to heat it during the current ramp-up. Modeling, using the time-dependent MHD code DINA with full DIII-D coil geometry and vacuum vessel, indicates ramp-up from 20 kA to a final current of 220 kA can be provided with these PF coils alone, using the existing power supplies. Previous experiments on DIII-D have shown that an initial plasma current of 20 kA can be provided by ECH alone. One complication is that at the end of this ramp-up, the PF coils are not in the optimum state for shape and position control of the final, fully developed plasma.

To complete the current ramp-up scenario, the current must be further increased using noninductive techniques. Simultaneously, the PF coil currents must be taken to the values required for the final shape and position control. It appears likely that the PF coil current changes will require the noninductive drive to overcome a back EMF during this phase of ramp-up. Continued modeling and further experimental tests are planned for the five-year plan period.

**Bootstrap Overdrive.** Ramp-up by bootstrap current overdrive is of interest because it does not require external noninductive current drive. Rather, it needs only plasma heating to produce the self-consistent, neoclassical toroidal current associated with density and temperature gradients. Ramping the current using bootstrap alone is accomplished by starting with and maintaining a high value of  $\beta_p$  throughout the ramp-up phase. Initial 0-D studies of this concept were performed for spherical tokamak configurations, and subsequently for DIII-D. These studies came to the conclusion that bootstrap overdrive could generate  $I \geq 1$  MA and  $dI/dt \sim 0.5\text{--}1.0$  MA/s.

Here we show the first results from 1-D simulations using ONETWO. The simulation starts with a full-size DIII-D plasma (with  $\kappa = 1.8$ ,  $\delta = 0.5$ ,  $I = 50$  kA,  $T_e = T_i = 200$  eV, and  $n_e \bar{O} = 0.8 n_{\text{Greenwald}}$ ). The thermal diffusivities are  $\chi_e \approx \chi_i = \chi_{i,\text{neo}}$  which are close to the best values observed in experiments on DIII-D. The results obtained seemed robust, and although other transport assumptions will change details of these results we do not expect them to alter the feasibility assessment. There is no option in ONETWO to set the electric field at the plasma boundary so the total current was prescribed as a linearly increasing function of time. The density is proportional to the current [Fig. 2.3–26(a)].

An rf power source which heats electrons was also specified as a function of time, reaching a maximum of 5.7 MW [Fig. 2.3–26(b)]. The distribution of the power was spatially uniform except during the first 0.25 ms when additional heating was supplied near the edge to support the edge temperature. The residual ohmic current was minimized by adjusting the input power level step-wise in time, and by varying the final current. Figure 2.3–26(a) shows bootstrap-driven ramp-up to 1 MA at  $\sim 0.5$  MA/s.

$\beta_p$  exceeds 1 throughout the discharge [Fig. 2.3–26(c)].  $\beta_N$  is seen to be  $< 2.5$  throughout the ramp-up and therefore MHD instabilities should not be a problem for this ramp-up scenario. Further optimization

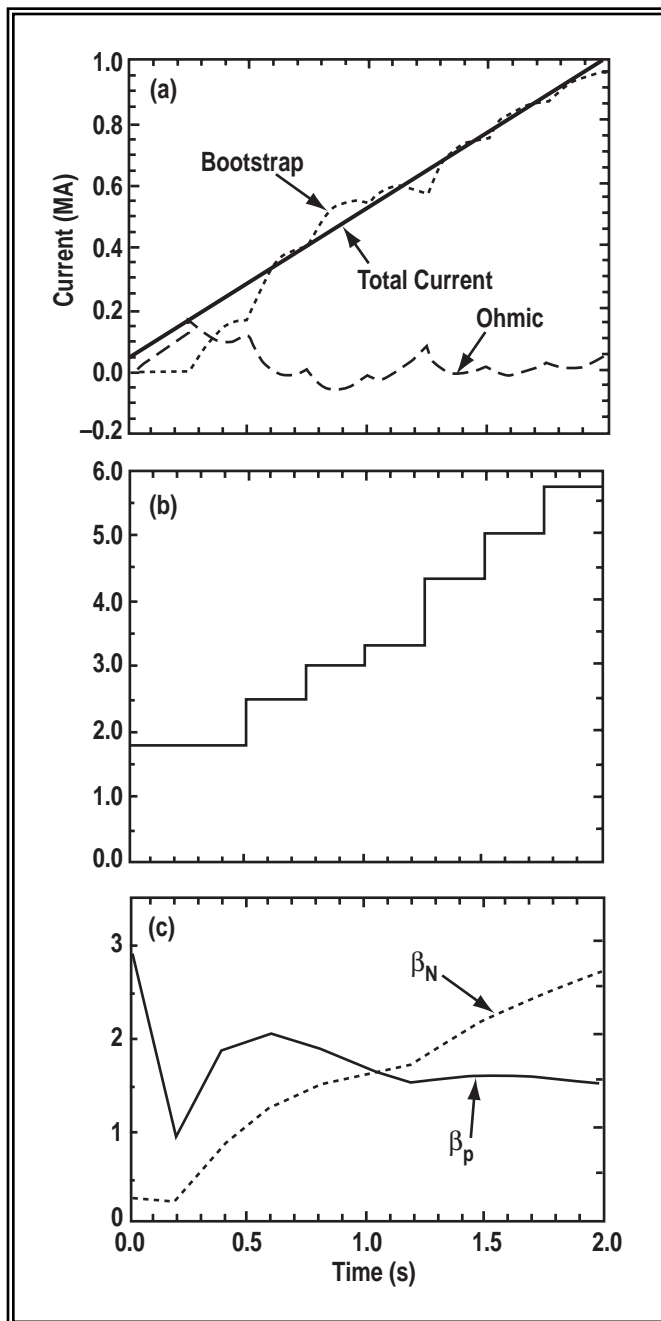


Fig. 2.3-26. One-dimensional simulations show bootstrap overdrive

current,  $\mu = J_{\parallel}/B$ . Turbulent current diffusion is clearly operative in experimental spheromaks and in RFPs and is in qualitative agreement with Boozer theory. The HIT tokamak also seems to be more or less in agreement with Boozer theory, but CDX obeyed neither Boozer nor classical behavior. Thus, if current diffusion in a tokamak is classical, then HICD will be limited to the edge and SOL plasma. If turbulent,

of the first 250–500 ms should be possible by putting in more power and driving  $\beta_p$  higher. An important question to address is the stability of the cold, very low current DIII-D plasma during the early part of this ramp-up.

**Initiation by HICD and ECH.** Helicity injection current drive (HICD) offers the appealing possibility, at least in principle, to drive toroidal current noninductively with a current/power efficiency that scales like ohmic power and is independent of plasma density. HICD itself does not offer current profile control. However, since HICD will probably prove to be most effective near the plasma edge, it could be an efficient tool for edge current control. HICD can also be used to create a target plasma of a few 100 kA, with subsequent ramp-up by more conventional noninductive processes. HICD has successfully formed and sustained current in the CTX [Jarboe (1983)] and SPHEX [Browning (1992)] spheromaks and in the CDX [Ono (1987)], CCT [Darrow (1990)], and HIT [Nelson (1994)] tokamaks.

The principal physics question associated with HICD is the transport of current across magnetic surfaces. In the absence of nonaxisymmetric processes such as turbulence, only slow classical diffusion is possible. Boozer [1986] argued that current diffusion by magnetic turbulence would be driven by the gradient of the normalized parallel current,

then HICD will penetrate more deeply, but it might unacceptably degrade plasma confinement. This is a question for future experiment.

A new DIII-D electrode is proposed that will increase the density near the cathode and consequently increase the current that can be driven in the SOL. Together with good strike point position control and a strong suite of edge and core diagnostics, it will be possible to study HICD under reactor-relevant conditions. In these experiments, the distribution of helicity injection current can be extracted from MSE diagnostic data and classical flux diffusion calculations.

Helicity injection can provide an initial tokamak plasma noninductively. A weak vertical magnetic field magnetized the ring electrode and connected it to the vessel ceiling. Electron cyclotron power was absorbed on the same magnetic surfaces and generated a plasma annulus, through which the electrode drove current. Because  $B_T \gg B_V$ , the current was mainly toroidal. It bulged the vertical field outward (large-R side) and weakened it inward (small-R side) until the poloidal field collapsed and reconnected around a new torus of plasma near the midplane. About 200 A of electrode current generated 10–20 kA tokamaks. The plasmas were subsequently sustained by ECCD.

The main issue with HICD noninductive startup is scalability to toroidal currents of a few hundred kiloampere, where conventional noninductive current drive techniques can take over. Turbulence and poor confinement are not major issues during startup. If the tokamak must be formed directly from the annulus, the required electrode current scales as  $I_p$ . The new DIII-D 110 GHz ECH system will provide more power than in the past, which will work with the new electrode to reduce cathode sheath impedance and accommodate larger currents. If, on the other hand, HICD is as effective as it presently is in HIT, then the required electrode current will be less.

#### 2.3.4.4. PLASMA HEATING

**Electron Versus Ion Heating.** The strong ion heating from the NBI commonly used in present day tokamak experiments is at odds with the strong electron heating expected from alpha particles in future ignition devices. The highest performance discharges in DIII-D have ion temperatures well in excess of the electron temperatures (hot ion modes), whereas the electron temperature will actually be slightly above the ion temperature in an ignition device. Thus, there is some uncertainty as to whether the plasma physics learned in hot ion mode plasmas, especially the confinement physics, will be applicable to plasmas in the ignition regime. Both theory and experiment suggest that adopting hot ion mode physics to ignition projections will lead to too optimistic predictions.

To study the physics of ignition-relevant plasmas with equilibrated electron and ion temperatures, it is necessary to utilize sources of strong electron heating to balance the NB ion heating. Although it is possible to operate at high densities to force the electron and ion temperatures to equilibrate through collisions, this results in high collisionality plasmas (in present day machines) that are no more applicable to the ignition regime than are hot ion modes. On DIII-D, strong electron heating is available through two types of rf

sources, ECH and FW. ECH can be localized on any flux surface in the plasma. The FWs can heat electrons directly through the combination of electron Landau damping and transit time magnetic pumping (TTMP) or through mode conversion, or indirectly through ion cyclotron heating. Using these rf sources in combination with NBI, the ignition-relevant physics of plasmas with equilibrated temperatures and low collisionality can be studied. This is critical due to the sensitivity of the models of turbulent transport to the ratio of electron to ion temperature.

Using strong heating of a hydrogen minority to generate a nonthermal ion distribution, the physics of energetic ions can be studied. This approach has been used in TFTR to examine the physics of TAE modes.

**Wave Absorption by Fast Ions.** The absorption of FWs by energetic ions at high harmonics of the ion cyclotron frequency is a major concern for FWCD in future tokamaks. For ignition devices such as ITER, the undesired absorption of FWs by alpha particles would decrease the amount of wave energy available for current drive, lowering the engineering efficiency of the FWCD. For high-beta low-aspect-ratio tokamaks, the possibility of strong damping of the FWs on NB ions has been identified as a critical rf physics issue. In addition to reducing the FWCD efficiency, such damping may expel energetic beam ions from the plasma, damaging the first wall components, and possibly exciting Alfvén instabilities.

On the DIII-D tokamak, the absorption of FWs by energetic beam ions at high harmonics of the ion cyclotron frequency can be studied [Petty (1997)]. This addresses not only the issue of the interaction between the FWs and beam ions, but also the analogous physics of FW damping on alpha particles. The excitation of Alfvén instabilities by the wave/particle interaction will also be examined, as well as sawtooth stabilization. The FWCD frequencies utilized on DIII-D are between 4 and 16 times the deuterium cyclotron frequency, depending upon the magnetic field strength (1–2 T), and the launched parallel index of refraction can be varied between 3 and 9. The radial profiles of FW driven current and the fast ion pressure can be determined using the MSE diagnostic and magnetic equilibrium reconstruction techniques. The ion distribution function can be measured with neutral particle charge-exchange analyzers. Reflectometers and rf probes can monitor the propagation of the FWs in the plasma. The information gathered from these diagnostics can be compared to calculations of the wave/particle interaction from Fokker-Planck and full wave codes. The close comparison of experiment and theory should allow the relevant physics of high-harmonic absorption of FWs by energetic ions to be determined on DIII-D. Some additional diagnostics, such as charge exchange analysis or energetic ion detectors, would be beneficial.

**Heating at High Density.** Certain operating modes on DIII-D, such as PEP modes and other pellet injection scenarios, have such high central densities that the NBs will not penetrate to heat the plasma center. This limits the performance of these modes since the central pressure cannot be raised by direct heating. Unfortunately ECH cannot solve this problem since the cutoff density for the 110 GHz system is  $7.5 \times 10^{19} \text{ m}^{-3}$  at the second harmonic. However, the FW system can still provide localized central heating for high density plasmas through ICH. Normally the FWs are absorbed by electron Landau damping and TTMP on

DIII-D. This damping mechanism is not effective for electron temperatures below 1 keV, however, given the available antenna phasings. Instead, tuning the FW antennas to 60 MHz and introducing a 10% hydrogen minority allows second harmonic hydrogen heating to be done at 2 T, which is effective even in low temperature plasmas. Modeling of this heating scenario using full wave codes indicates that strong central heating in high density plasmas is possible with FWs, and under some conditions the heating may be well localized. Mode conversion heating is also likely to be effective.

**Rotation Issues.** Recently there has been interest in how rotational shear stabilization of transport may affect heat and particle transport in the plasma. For plasmas that are rotating due to unbalanced NBI heating, as is the case for DIII-D, diamagnetically induced rotational shear is small and the rotational shear rate is directly related to the injected momentum from the NBs. In order to separate the effects of rotational shear from heating, it is important to have additional heating sources which do not inject significant momentum into the plasma. On DIII-D, rf heating with either ECH or FWs satisfies this requirement since these forms of heating have been shown to not result in significant rotation or rotational shear. Therefore, NBI and rf heating can be used to determine the effect of diamagnetic rotation on the plasma confinement properties. The rf heating scenario is especially relevant to future ignition regimes which are expected to not be strongly rotating and are dominated by central electron heating from alpha particles.

**Generation of Transport Barriers.** It is believed that a transition to locally reduced transport can occur when a local profile gradient which enters into the determination of the shear in the radial electric field exceeds a threshold value. In PBX and TFTR, experiments have suggested the potential for IBWs to directly affect the radial electric field, presumably through the Reynolds stress tensor. If this approach is practical, it offers a very attractive means to control the radial location of the transport barrier. Experiments on this topic could be carried out using the FW antennas to generate waves which are mode converted to IBWs at the ion-ion hybrid layer in a two-component (D/H) plasma. Alternatively, the folded waveguide antenna is made to be installed to generate either FWs, for mode conversion, or directly launch IBWs, which is the mode used in PBX and TFTR. A reduction in frequency of the rf generator from 30 to 20 MHz would be useful for this application but not essential for proof of principle. Increase of the gradient in electron temperature through local electron heating by ECH is also predicted to be a means to control the shear in the radial electric field, although in past experiments with 60 GHz the  $T_e$  profile has been difficult to change much.

**2.3.4.5. HEATING AND CURRENT DRIVE FOR STABILIZATION.** The DIII-D rf systems will be used to investigate rf-specific mechanisms for stabilization and control of MHD modes which can arise at various regions within the plasma. These are spatially localized modes within the plasma and so there must be reliable methods to indicate this spatial location and most importantly to determine the phase of the mode in space and time. Modern current density profile diagnostics, such as the DIII-D motional Stark effect (MSE) system, can provide an approximate  $q$ -profile in real time with sufficient accuracy. For reproducible discharges the  $q$  profile is very well determined. External magnetic probes are effective in providing the necessary phase measurement for feedback to the rf systems in those techniques where it is required.

**Sawtooth Stabilization.** Minority ion heating and current drive have both been demonstrated to stabilize the central sawtooth instability, consistent with the model that sawteeth are due to an internal  $m=1$  kink instability [Coppi (1976)]. Stabilization can take place either by adding core pressure due to cyclotron resonant accelerated minority ions [White (1998)] or by phasing the ion cyclotron range of frequencies antenna to launch a toroidally directed mode and thereby drive localized toroidal currents with the same ion cyclotron harmonic resonant wave, as demonstrated on JET.

Minority ion heating with FWs is a well established tokamak tool, and it has been used on DIII-D at the second harmonic of a hydrogen minority in a deuterium plasma. The ability to establish a well directed toroidal FW with the DIII-D four strap antennas also makes localized minority ion current drive possible. The resultant toroidal Doppler shift of the wave in the rest frame of a minority ion means that the resonant ion velocity is a function of radial location. This effect can produce a reversal of the driven current direction on a scale of a few centimeters. This allows localized control of the current density profile, which can reduce the gradient in current and add a stabilizing term for the internal kink.

The direct central electron current drive mechanisms of FWCD and ECCD can also be brought to bear by simply driving a reversed central current and maintain the central  $q$  value above unity so that no  $m=1, n=1$  surface exists within the plasma.

**Tearing Mode Stabilization.** Tearing modes can occur at rational  $q$  surfaces other than the  $1/1$  surface important for the sawtooth instability, and rf current drive physics can be brought to bear to stabilize or mitigate these instabilities. The most important are the lowest order rational surfaces, such as  $3/2, 2/1, 5/2, 3/1$  etc. These exist between the core and the edge. If the magnetic islands which result from the tearing modes remain isolated radially, then these modes are a concern for transport of energy [Antonsen (1986)]. If there is overlap radially, a major disruption can occur as the thermal energy is rapidly transported out of the plasma. It may be possible to do this with MCCD, but localization and control of the deposition location are major questions.

Tearing modes can be driven unstable by the localized gradient in the current density profile. Minority ion current drive again can be used to locally modify this gradient. Once a magnetic island is formed, increasing the current within the center magnetic island (O-point) of the islands tends to reduce the width of the island in the usual positive shear regime. Localized ECCD can be used to obtain an increase in the O-point current, with the current drive location selected by the magnetic resonance location. It may be possible to do this with MCCD, but localization and control of the deposition location are major questions.

The so-called neoclassical magnetic island is the unstable growth of a seed magnetic island due to the concomitant loss of bootstrap current within the island (O-point) due to the flattening of the pressure [Hegna (1993)]. The neoclassical tearing mode (NTM) is a limiting factor in many discharges in DIII-D and it is expected to limit the plasma pressure in ITER to a factor around 2 below its theoretical stable maximum. This lost O-point current can be replaced with ECCD [Sauter (1996), Hegna (1997)].

**Disruption Control.** A major disruption occurs when  $3/2$  and  $2/1$  magnetic islands can grow to sufficient amplitude to overlap spatially, connecting the otherwise well confined, high energy density core with the exterior region of the plasma. ECCD is a natural choice to stabilize these modes by increasing the O-point current density [Hoshino (1993)]. The short timescale from island initiation to overlap in some cases means that the external detection and control system must be fast, robust, and reliable. The DIII-D group is highly experienced in sophisticated control systems and this will be combined with the ECH expertise in this type of disruption control experiment.

**ELM Stabilization.** Controlling the frequency of the ELMs in H-mode discharges is advantageous for several reasons, and it has been demonstrated on DIII-D with the 60 GHz ECH system [Prater (1988)]. An ELM rapidly expels both energy and particles confined within the separatrix in the high confinement H-mode regime. ELMing is a relaxation oscillation which clamps the time averaged level of thermal energy and density. Too infrequent ELMs (“giant ELMs”) dump so much energy that the instantaneous power poses a serious problem for the divertor in ITER. The power from smaller, more frequent ELMs can be more readily removed. Another reason to control the ELM frequency is to tailor the edge density profile for considerations of bootstrap current. Before or between ELMs the edge H-mode density gradient is very large, leading to a relatively large bootstrap current at the edge. This edge current is generally undesirable for full current drive scenarios relying upon a significant fraction of bootstrap current and for stability of external kink modes. ELMs transiently reduce the edge density gradient by expelling particles from the interior. The time averaged edge density gradient in frequent ELM situations provides a better density profile for alignment of the bootstrap current with that required for steady-state equilibrium. Control of ELMs may also support control of the impurity content in the core.

The localized nature of ECH allows heating just inside, or outside, of the separatrix. Experiments on DIII-D showed that heating inside increases the ELM frequency, while heating outside reduces it. This is consistent with models which propose that ELMs are due to an edge ballooning instability driven by the pressure gradient. Inside heating causes the critical pressure gradient to be reached more rapidly during the ELMing cycle. Other models of ELMs postulate a tearing instability. The growth rate of these edge magnetic islands due to tearing would also be subject to localized ECCD.

#### References for Section 2.3.4

- Antonsen, T.M., and K. Yoshioka, *Phys. Fluids* **29**, 2235 (1986).  
Boozer, A.H., *J. Plasma Phys.* **35**, 133 (1986).  
Browning, P.K., et al., *Phys. Rev. Lett.* **68**, 1718 (1992).  
Coppi, B., et al., *Fiz. Plasmy* **2**, 961 (1976) [*Sov. J. Plasma Phys.* **2**, 533 (1976)].  
Darrow, D.S., et al., *Phys. Fluids B* **2**, 1415 (1990).  
Hegna, C.C., J.D. Callen, T.A. Gianakon, et al., *Plasma Physics and Controlled Fusion* **35**, 987 (1993).  
Hegna, C.C., and J.D. Callen, “On the stabilization of neoclassical modes using localized current drive or heating,” to be published (1997).

- Hoshino, K., in Proc. 10th Top. Conf. on Radio Frequency Power in Plasmas, Boston [American Institute of Physics, New York (1993)] p. 149.
- Itami, K., et al., Phys. Rev. Lett. **78**, 1267 (1997).
- Jarboe, T.R., et al., Phys. Rev. Lett. **51**, 39 (1983).
- Litaudon, X., et al., in Proc. 11th Top. Conf. on Radio Frequency Power in Plasmas, Palm Springs [American Institute of Physics, New York (1995)] p. 90.
- Lloyd, B., et al., Nucl. Fusion **31**, 2031 (1991).
- Majeski, R., C. K. Phillips, and J. R. Wilson, Phys. Rev. Lett. **73**, 2204 (1994).
- Majeski, R., et al., Phys. Rev. Lett. **76**, 764 (1996).
- Nelson, B.A., et al., Phys. Rev. Lett. **72**, 3666 (1994).
- Ono, M., et al., Phys. Rev. Lett. **59**, 2165 (1987).
- Ono, M., T.R. Jarboe, M.J. Schaffer et al., in Proc. 14th Conf. on Plasma Physics and Controlled Nuclear Fusion Research, Würzburg, [International Atomic Energy Agency, Vienna (1993)] Vol. 1, p. 693.
- Prater, R., et al., Proc. 12th Int. Conf. on Plasma Physics and Controlled Nuclear Fusion Research, Nice [International Atomic Energy Agency, Vienna (1988)] E-1-2.
- Petty, C.C., et al., in Proc. 12th Top. Conf. on Radio Frequency Power in Plasmas 1997, Savannah, (American Institute of Physics, New York,) in press; Prater, R., et al., in Proc. 16th Int. Conf. on Plasma Physics and Controlled Nuclear Fusion Research, October 1996, Montreal [International Atomic Energy Agency, Vienna, (1997)].
- Ram, A.K., in Proc. 11th Top. Conf. on Radio Frequency Power in Plasmas, Palm Springs [American Institute of Physics, New York (1995)] p. 269.
- Sauter, O., et al., to be published in Phys. Plasmas (1997).
- White, R.B., P.H. Rutherford, et al., Phys. Rev. Lett. **60**, 2038 (1988).

## 2.4. PATHWAYS TO THE FUTURE

*DIII-D will advance the scientific basis for many different paths to power-producing tokamak fusion concepts and can operate advanced tokamak scenarios that project along dimensionless parameter paths to attractive tokamak fusion systems.*

In constructing the scientific program for DIII-D, it is of interest to examine how DIII-D results can connect or project to tokamak systems that may be attractive next steps in fusion development. From a forward looking perspective, the designers of future tokamak devices, of course, rely heavily on results that have been and will be obtained on DIII-D. But it is also useful to back project from the design points of future tokamaks into the DIII-D parameter space in order to draw useful insights on the priority of various research elements and various parameter regimes accessible in DIII-D. In this section, we examine the connection of DIII-D research to four possible future directions for the tokamak program (Fig. 2.4-1):

1. ITER.
2. An advanced performance superconducting tokamak (as exemplified by ARIES-RS).
3. A compact, copper coil ignition experiment (as exemplified by CIT/BPX/IGNITOR).
4. A small spherical tokamak pilot plant.

We examine the implications of connecting DIII-D parameters to the parameters of these machines along dimensionless parameter scaling paths in order to locate the relevant region of parameter space in DIII-D. The basis of dimensionless parameter scaling is described in Appendix A. Each of these future paths for the tokamak program has specific implications for research elements in the DIII-D Program. We summarize all those research elements at the end of the discussion.

In general, we find that the research planned for DIII-D has a broad applicability to many possible future directions. Advances in confinement, stability, boundary physics, and current generation are generally useful to optimizing the tokamak in several directions.

### 2.4.1. THE PATH TO ITER

The ITER Project is nearing the end of the Engineering Design Activity so its parameter regimes and research needs are well established. ITER is, at present, the principal driver of understanding the ELMing

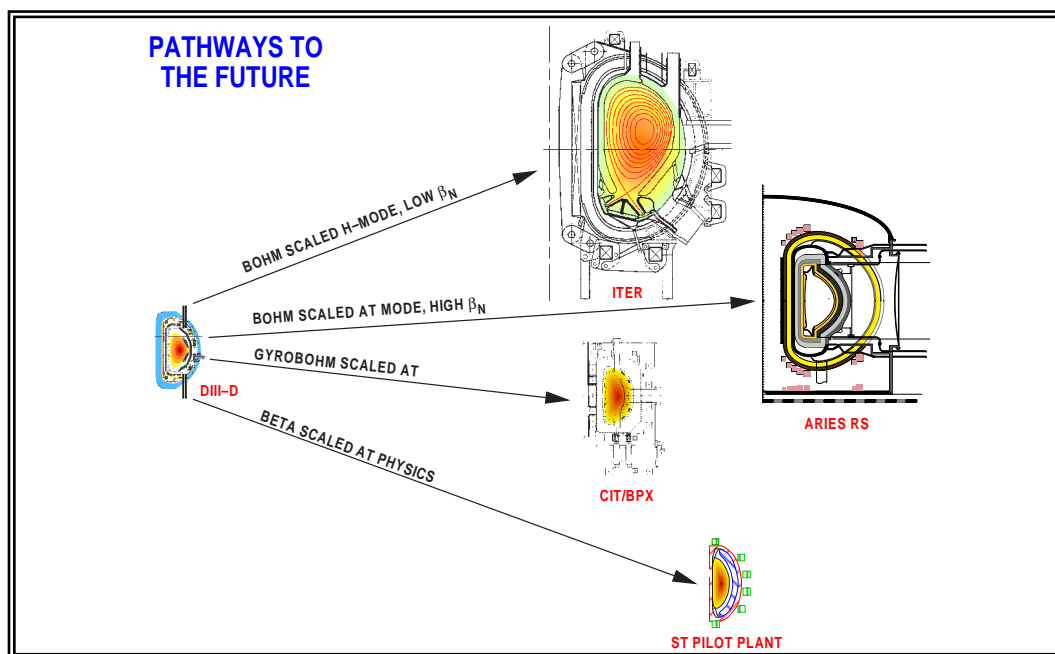


Fig. 2.4–1. DIII–D research connects to four possible tokamak program directions.

H–mode regime — its base operating regime. ITER is also, at present, evaluating the extent to which AT scenarios can be operated in ITER. For purposes of discussing and defining ITER’s research needs, it is useful to divide the plasma into three radial regions. The first region, the core plasma, is from the top of the H–mode pedestal inward. The second region is the H–mode shear layer, which comprises only a few centimeters just inside the separatrix in present machines. The third region is the SOL/divertor region from the separatrix to the divertor plate. In the plasma core region, it is considered that the dimensionless parameters of plasma physics  $\beta$ ,  $v_*$ ,  $q$ , and  $\rho_*$  will govern the plasma properties since neutrals have been almost completely attenuated in the H–mode shear layer. A subject of current debate is the extent to which a “stiff” transport model determines the entire core performance given the height of the pedestal on the inner side of the H–mode shear layer. The H–mode shear layer connects Regions 1 and 3 and provides boundary conditions for both. The physics of the H–mode shear layer must consider neutrals and so is unlikely to be described solely by the dimensionless parameters being used to make projections to ITER. Experimental and theoretical interest is currently focused on this shear layer. On its outer side, it sets the boundary conditions of power flow, density, and temperature for the SOL/divertor. The understanding of the important physics elements of the SOL/divertor problem has progressed to the point that the most important effects (classical parallel conduction, electron impact ionization, charge-exchange, impurity transport, noncoronal radiation calculations, recombination) are in 2–D divertor modeling codes and so the performance of the divertor plasma can be calculated given the upstream boundary conditions.

The scaling of core plasma parameters along dimensionless parameter paths from ITER to DIII–D has important implications on the overlap of core plasma and divertor research in DIII–D. In Table 2.4–1, we give ITER’s parameters in the leftmost column and parameters of DIII–D, JET, and

TABLE 2.4-1  
 $\rho_*$  SCALING FROM ITER TO VARIOUS TOKAMAKS

Quantity	Definition	Units	ITER	DIII-D	DIII-D	JET	Alcator C-Mod
$R_0$	Major radius	m	8.14	1.67	1.67	2.9	0.68
$a$	Minor radius	m	2.8	0.58	0.58	0.91	0.21
$A$	Aspect ratio		2.91	2.88	2.88	3.19	3.24
$\kappa$	Plasma elongation		1.6	1.6	1.6	1.7	1.6
$\delta$	Plasma triangularity		0.24	0.24	0.24	0.24	0.24
$B_0$	Toroidal field, on axis	T	5.70	2.07	0.98	1.71	4.04
$I_p$	Plasma current	MA	21.00	1.58	0.75	2.04	1.12
$T_i(0)$	Ion temperature	keV	18.00	5.42	3.30	5.54	6.03
$T_e(0)$	Electron temperature	keV	18.00	5.42	3.30	5.54	6.03
$n(0)$	Electron density	$\times 10^{20}/m^3$	1.10	0.48	0.18	0.32	1.65
$n/n_{GR}$	Ratio to Greenwald limit		1.17	0.29	0.23	0.37	0.19
$Z_{eff}$			1.80	1.80	1.80	1.60	1.40
$W$	Stored energy in plasma	MJ	1065.0	1.29	0.29	4.05	0.27
$P_{heat}$	Total heating power	MW	302.2	5.3	18.3	18.2	3.9
$P_{fusion}$	Fusion power	MW	1511.0	0.00	0.00	0.00	0.00
$\tau_E$	Energy confinement times		3.524	0.244	0.016	0.222	0.070
$P_{trans}$	Transport loss power	MW	175.3	4.0	13.7	13.7	3.1
$\tau_{E, trans}$	$\tau_E$ , transport only	s	6.076	0.314	0.020	0.240	0.072
$\tau_{E-93H}$	$\tau_E$ , transp ITER-93H		5.863	0.161	0.021	0.228	0.040
$H$	H factor over ITER-89P		2.638	2.505	0.600	1.242	2.706
<b>Dimensionless Parameters</b>							
$\beta_T$	Toroidal beta		0.027	0.028	0.028	0.029	0.029
$\beta_P$	Poloidal beta		0.70	0.73	0.73	0.81	0.76
$\beta_N$	Normalized beta	mT/MA	2.07	2.16	2.16	2.20	2.24
$q$	Safety factor		2.80	2.85	2.85	2.74	2.45
$\bar{\rho}_{*e}$	$\rho_* e$ at $\bar{T}_e$		$2.32 \times 10^{-05}$	$1.70 \times 10^{-04}$	$2.79 \times 10^{-04}$	$1.32 \times 10^{-04}$	$2.53 \times 10^{-04}$
$\bar{\rho}_{*i}$	$\rho_* i$ at $\bar{T}_i$		$9.88 \times 10^{-04}$	$7.21 \times 10^{-03}$	$1.19 \times 10^{-02}$	$5.63 \times 10^{-03}$	$1.08 \times 10^{-02}$
$\bar{v}_{*e}$	$v_* e$ at $\bar{T}_e$		$1.71 \times 10^{-02}$	$1.70 \times 10^{-02}$	$1.70 \times 10^{-02}$	$1.87 \times 10^{-02}$	$1.52 \times 10^{-02}$
$\bar{v}_{*i}$	$v_* i$ at $\bar{T}_i$		$1.21 \times 10^{-02}$	$1.20 \times 10^{-02}$	$1.20 \times 10^{-02}$	$1.32 \times 10^{-02}$	$1.07 \times 10^{-02}$
$\rho_*$ ratio				7.30	12	5.70	10.9
Alpha Factor	$\rho_*$ exponent			0	1.00	0.55	0.00
Confinement Scaling Type				Bohm	GyroBohm	Between	Bohm

Alcator C-Mod in the other columns. The parameters for today's machines are scaled from ITER varying only  $\rho_*$ , keeping all the other core dimensionless parameters constant. The first column for DIII-D is a full toroidal field scenario. It has a modest plasma current of 1.58 MA. The  $\beta$  and  $\beta_N$  and H factor values are not particularly challenging for DIII-D based on the AT discussion of Section 2.2. The third column is a projection to a discharge DIII-D which has already been operated as a "demonstration discharge" for ITER. It was at only 1 T field and 0.75 MA plasma current. An important conclusion here is that discharges that connect to ITER along a  $\rho_*$  path generally lie at reduced parameter regimes compared to DIII-D's capabilities. This conclusion is also true for JET and Alcator C-Mod.

The ITER plasma, like all future power system plasmas, has  $T_i = T_e$ , a condition unfavorable for ITG mode growth. DIII-D plasmas, in order to retain similarity in the dimensionless parameters  $T_i/T_e$ , must also have  $T_i = T_e$ ; this requires strong additional electron heating in DIII-D.

Confinement research on DIII-D in the ITER shape, the demonstration discharges, has shown that the scaling of ELMy H-mode is gyroBohm. The second column for DIII-D shows that a gyroBohm confinement projection back from ITER implies only a 0.020 s confinement time and 13.7 MW of heating power needed in DIII-D. In actual fact, the measured confinement time in this ITER demonstration discharge was 0.075 s and the power required to produce the plasma parameters listed was only about 4 MW. This illustrates that the gyroBohm scaling of confinement is actually too good for ITER. A gyroBohm projection in the forward direction from the measured confinement time in the DIII-D demonstration discharge in the second DIII-D column to ITER gives a 23 s confinement time [Petty (1995)]! The first column for DIII-D shows a much more reasonable match-up of ITER and DIII-D confinement and power levels using a Bohm confinement scaling. The column for JET gives plasma parameters between two demonstration discharges on JET. The confinement times and power levels come out about right if the confinement projection back from ITER is between Bohm and gyroBohm,  $\rho_*$ . A demonstration discharge planned for Alcator C-Mod back-projects most reasonable values of confinement time and power using a Bohm confinement scaling. The general conclusion is that present research in DIII-D and other tokamaks need only confirm that the confinement scaling is at least as good as Bohm scaling for ITER.

A most important point is that the density required in DIII-D plasmas that are dimensionally similar to ITER is less than 30% of the Greenwald limit density. The point is of general validity for today's tokamaks, as can be seen from the JET and Alcator C-Mod values of  $n/n_{GR}$ . This fact has important implications for the DIII-D Research Program. The studies of divertor detachment and density limits in DIII-D have all been done at densities above  $n/n_{GR} = 0.5$ . In Table 2.4-1, the densities for all the tokamaks listed lie below the densities for divertor detachment in those machines. The conclusion is that the parameter spaces of interest to ITER for core and divertor physics are *disjoint* in present day tokamaks. This conclusion can be softened substantially if one is allowed the freedom to change both  $\rho_*$  and  $v_*$  in connecting machines to ITER. If DIII-D and Alcator C-Mod are allowed to have  $v_* = 8$  times  $v_*$  in ITER, then scenarios can be constructed that provide an overlap of core confinement and detached divertor operation. These scenarios still are very collisionless plasmas,  $v_* \sim 0.1$ , and the argument for them is that the confinement properties of the core

are unlikely to change abruptly between  $v_* = 0.1$  and  $0.01$  (ITER). DIII-D has measured a weak dependence  $\chi \propto v_*$  in ELMing H-mode and no dependence  $v_*$  in L-mode. Some key parameters of such scenarios are given below (Table 2.4–2).

**TABLE 2.4–2**  
FROM ITER TO DIII-D AND ALCATOR C-MOD VARYING  $v_*$  AND  $\rho_*$

	ITER	DIII-D	Alcator C-Mod
$B_0$ (T)	5.7	2.0	5.9
$I_p$ (MA)	21.	1.53	1.62
$T_i(0)$ (keV)	18	2.6	3.9
$T_e(0)$ (keV)	18	2.6	3.9
$n_e(0)$ ( $10^{20} \text{ m}^{-3}$ )	1.1	0.9	5.4
$\bar{n} / n_{GR}$	1.17	0.58	0.42
$P_{\text{Transport}}$ (MW)	175	4.3	7.1
$\tau_E$ (s)	6	0.27	0.07
H	2.6	2.5	2.9
$\rho_{*i}$	$1 \times 10^{-3}$	$5 \times 10^{-3}$	$6 \times 10^{-3}$
$v_*$	0.012	0.096	0.086
$\rho_{\text{exponent}}$		0.5	0.5

While some compromise on  $v_*$  appears to allow overlap of core confinement and detached divertor studies, it is perfectly valid to study the basic physics elements of the divertor by using high density plasmas in DIII-D and equally valid and correct to study confinement properties of interest to ITER in lower density plasmas. It is not necessary to force these two lines of research to meet in DIII-D at one set of core plasma parameters. These two lines of research evidently do meet in ITER. There the density reaches the Greenwald limit and the calculations show the divertor does detach, even though the core plasma collisionality is still low. Density limit research in DIII-D, which has shown densities up to  $1.5 n_{GR}$  with H-mode confinement quality, is important to pursue to elucidate the basic physics mechanisms that limit the density. As is described in Section 2.3.3, the most restrictive density limiting phenomena originate in the divertor and the H-mode shear layer. The answer for what the density limit will be for ITER must be found in divertor calculations and the physics of the H-mode shear layer.

We provide in Table 2.4–3 a summary of our current views of the important research contributions from DIII-D that are useful to ITER.

**TABLE 2.4–3**  
**DIII-D CONTRIBUTIONS TO ITER**

Issue	DIII-D Contributions to ITER
Core Confinement	<ol style="list-style-type: none"> <li>1. Dimensionless scaling in ITER's shape and dimensionless parameter regime.</li> <li>2. Theoretical and experimental tests of the stiffness of various core plasma transport models.</li> <li>3. The physics of interior transport barriers and the role of plasma rotation.</li> </ol>
Core Stability	<ol style="list-style-type: none"> <li>1. Research on neoclassical tearing modes in the ITER shape at the ITER collisionality and assess the use of ECCD for stabilization.</li> <li>2. The interplay of plasma rotation and locked modes.</li> </ol>
H-mode Shear Layer	<ol style="list-style-type: none"> <li>1. Experiment and theory work on the structure of the shear layer (pedestal height, width of layer, local plasma parameters, effects of neutrals).</li> <li>2. Local parameter requirements and a theory for the L–H transition.</li> <li>3. Local requirements and a theory for avoiding the H–L transition (the density limit of most specific relevance to ITER).</li> <li>4. Compatibility of the edge transport barrier with high plasma mantle radiation.</li> </ol>
Density Limits	<ol style="list-style-type: none"> <li>1. Elucidation of the basic physical processes that limit the plasma density.</li> </ol>
Divertor Research	<ol style="list-style-type: none"> <li>1. Elucidate the basic physics mechanisms active in the SOL and divertor so they can be incorporated in codes.</li> <li>2. Find ways to increase divertor radiation at fixed upstream parameters (impurity enrichment, convective heat transport, noncoronal equilibrium radiation, non-Maxwellian effects, 2–D heat flow effects).</li> </ol>

## 2.4.2. THE PATH TO AN OPTIMIZED SUPERCONDUCTING TOKAMAK POWER SYSTEM

*DIII-D results, in the conventional aspect ratio range, provide a basis for minimal sized superconducting tokamak power systems like ARIES-RS. Key elements to demonstrate are confinement scaling at least as favorable as Bohm scaling, wall stabilization for high normalized beta, transformerless operation, and a radiative divertor compatible with the ARIES-RS collisionless core.*

Various authors [Galambos (1995)] have examined the extent to which the use of AT physics (high  $\beta_N$  and H) could be used to decrease the size of the superconducting tokamak. A result of those studies was that high values of  $\beta_N$  and H could bring the major radius of a superconducting tokamak down to 5 m. We have reproduced this result by constructing minimal sized superconducting tokamaks over a range of aspect ratio by considering all machines to run at our calculated wall stabilized  $\beta$  limit and allowing minimal inboard space for components consistent with key technological constraints.

The only inboard components considered are the superconducting toroidal coil and the blanket that is needed to protect it. A review of many superconducting tokamak designs indicates a reasonable blanket thickness allowance of 1.3 m. We consider growing the toroidal field (TF) coil from the axis of symmetry out (i.e., no hole in the doughnut), an impractical case but one which certainly gives a minimum sized overall system. Reviewing many superconducting coil designs, we found a reasonable value for the current density averaged over the winding and all associated coil structure was 18 MA/m<sup>2</sup>. We also constrain the systems to lie below a neutron wall loading of 5 MW/m<sup>2</sup>. At low aspect ratio (1.5, see Section 2.4.4 on the ST), the beta limits are sufficiently high that the neutron wall loading sets the device size and the toroidal coil is sufficiently small in radius that the stress limit of 16 T at the coil surface is not reached. As the aspect ratio is raised, the toroidal coil radius grows until it reaches 1.4 m (at aspect ratio 2.5) and the field at the surface of the coil is then 16 T. For aspect ratios larger than 2.5, the toroidal coil radius cannot grow, owing to the stress constraint, and so the plasma size shrinks against the fixed center column of the toroidal coil and the blanket. The dependence of the major radius versus aspect ratio that results is shown in Fig. 2.4–2. Although some machines with major radii less than 4 m appear at large aspect ratio, reference to Fig. 2.4–3 shows that these machines have rather low power output and neutron wall loading. They are not practical power plants and are large experiments, considering the fusion power of only 250 MW for a major radius just under 4 m. To make such systems more practical, one moves the toroidal coil outward, opening a “hole in the doughnut.” Then the ratio of the toroidal field at the magnetic axis to the (fixed at 16 T) toroidal field at the coil surface rises rapidly and the fusion power output rises like  $B^4$  and rises further because of the growing plasma volume. One increases the system size until a neutron wall loading of 3 MW/m<sup>2</sup> for all machines results. Major radii of some practical systems are shown in Fig. 2.4–3. By

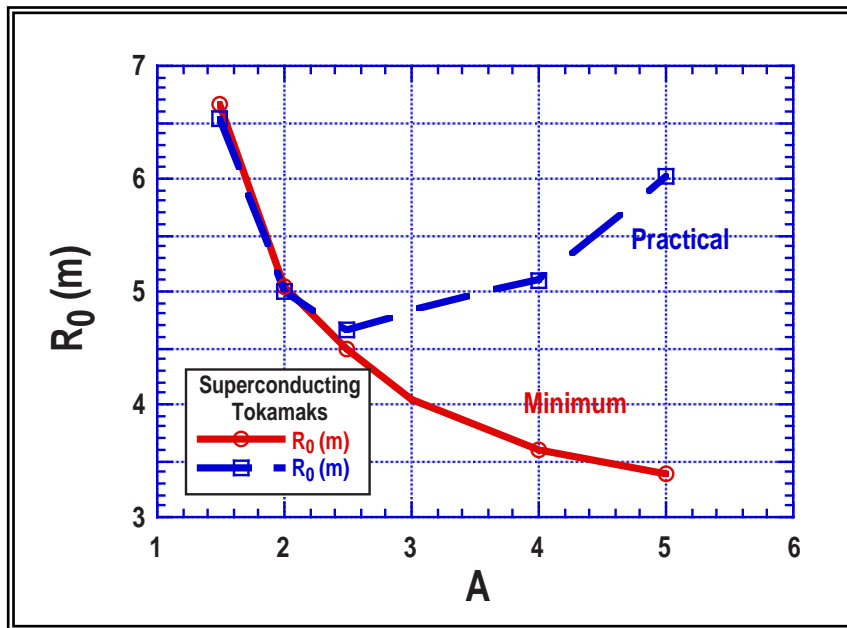


Fig. 2.4-2. The major radius of superconducting tokamaks is constrained by wall loading at low aspect ratio and by stress at high aspect ratio.

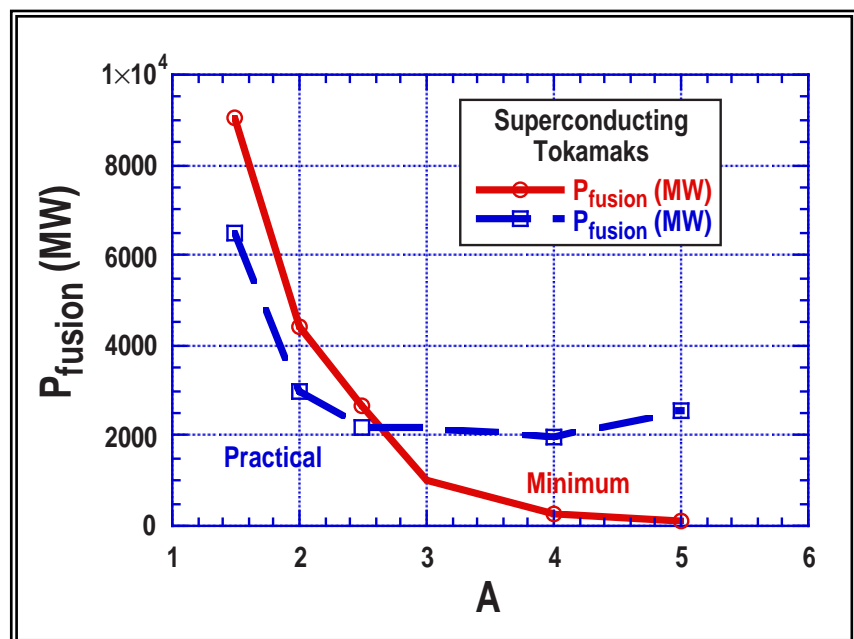


Fig. 2.4-3. High aspect ratio superconducting tokamaks have relatively low fusion power.

raising the major radius only from 3.5 to 5 m at aspect ratio 4, the fusion power rises from 250 to 2000 MW. However as can be seen from Fig. 2.4-3, there is a minimum major radius of 4.5 m. When more complete, practical design aspects are considered, the minimum major radius is over 5 m. The ARIES-RS design at a major radius of 5.5 m lies in this family of optimized superconducting tokamaks, minimal sized, and running near the beta limit.

In order to examine how this line of machine connects to DIII-D, we back projected from the aspect ratio 2.5 machine in this machine family, rather than ARIES-RS in order to avoid the complication of connecting the aspect ratio of 4 in ARIES-RS to the aspect ratio of 2.5 in DIII-D. In Table 2.4-4, we give in the leftmost column the parameters of the aspect ratio 2.5, minimum sized power plant. The first column for DIII-D is a back projection to DIII-D along a path varying only  $\rho_*$  that hits full toroidal field in DIII-D. Overall, these parameters match up well with the parameters of the DIII-D full field discharge scenario discussed in Section 2.2 although the plasma current and beta are a bit higher here. Using Bohm scaling, the heating power required is about what is proposed in the DIII-D scenario. The value of  $\beta_N$  implied is 5.5 and the H factor is about 4. A reasonable reduced field scenario is also constructed in the second DIII-D column using Bohm transport scaling. The use of gyroBohm scaling has the same difficulty encountered for ITER; the projected confinement in DIII-D must be much poorer than will be obtained. Turned around, a gyroBohm projection of confinement from DIII-D's primary scenario would give excess confinement time in the optimized, superconducting tokamaks. We conclude the discharge scenarios described for DIII-D in Section 2.2 are well positioned as a scaling point toward the line of optimized, superconducting tokamak machines.

As the ARIES-RS study in particular exemplifies, the physics that underlies the desired values of  $\beta_N$  and H contains even more elements of commonality with the DIII-D Research Program than just the match-up of parameters. The high values of  $\beta_N$  can only result from a successful outcome to the wall stabilization studies in DIII-D and other experiments. High values of  $\beta_N$  also require the NCS or at least WCS safety factor profiles envisioned in ARIES-RS and broad pressure profiles in elongated plasmas. The transport barriers formed by the  $E \times B$  shear stabilization of turbulence are needed to obtain the high confinement performance. Current drive for steady-state and current profile control using rf is required. Indeed, ARIES-RS is designed without an OH transformer, although since these machines have a "hole in the doughnut," it is somewhat optional whether a transformer is installed or not (as opposed to the ST case in which the transformer is impossible). Nevertheless, in the interests of simplifying the tokamak system, the ARIES-RS transformerless design motivates the research thrust toward transformerless operation on DIII-D.

TABLE 2.4–4  
 $\rho_*$  SCALING FROM AN OPTIMIZED SUPERCONDUCTING POWER PLANT TO DIII-D

Quantity	Definition	Units	A 2.5 Reactor	DIII-D	DIII-D	DIII-D
$R_0$	Major radius	m	4.67	1.67	1.67	1.67
$a$	Minor radius	m	1.87	0.67	0.67	0.67
$A$	Aspect ratio		2.50	2.49	2.49	2.49
$\kappa$	Plasma elongation		2.0	2.0	2.0	2.0
$\delta$	Plasma triangularity		0.6	0.6	0.6	0.6
$B_0$	Toroidal field, on axis	T	4.58	1.92	1.12	1.12
$I_p$	Plasma current	MA	14.35	2.15	1.26	1.26
$T_i(0)$	Ion temperature	keV	25.00	9.94	6.96	6.96
$T_e(0)$	Electron temperature	keV	25.00	9.94	6.96	6.96
$n(0)$	Electron density	$\times 10^{20}/m^3$	1.55	0.68	0.34	0.34
$\bar{n}/n_{GR}$	Ratio to Greenwald limit		0.95	0.36	0.30	0.30
$Z_{eff}$			1.80	1.80	1.80	1.80
$W$	Stored energy in plasma	MJ	711.0	5.98	2.05	2.05
$P_{heat}$	Total heating power	MW	362.4	17.3	7.1	42.6
$P_{fusion}$	Fusion power	MW	1727.0	0.00	0.00	0.00
$\tau_E$	Energy confinement time	s	1.962	0.345	0.289	0.048
$P_{trans}$	Transport loss power	MW	217.4	13.0	5.3	31.9
$\tau_{E, trans}$	$\tau_E$ , transport only	s	3.271	0.442	0.370	0.062
$\tau_{E-93H}$	$\tau_E$ , transp ITER–93H		1.363	0.115	0.089	0.027
$H$	Ratio to ITER–89P		4.589	4.355	3.810	1.555
<b>Dimensionless Parameters</b>						
$\beta_T$	Toroidal beta		0.088	0.092	0.092	0.092
$\beta_P$	Poloidal beta		1.96	2.05	2.05	2.05
$\beta_N$	Normalized beta	mT/MA	5.26	5.49	5.49	5.49
$q$	Safety factor		4.64	4.75	4.75	4.75
$\bar{\rho}_{*e}$	$\rho_* e$ at $\bar{T}_e$		$5.59 \times 10^{-05}$	$2.35 \times 10^{-04}$	$3.35 \times 10^{-04}$	$3.35 \times 10^{-04}$
$\bar{\rho}_{*i}$	$\rho_* i$ at $\bar{T}_i$		$2.38 \times 10^{-03}$	$9.98 \times 10^{-03}$	$1.43 \times 10^{-02}$	$1.43 \times 10^{-02}$
$\bar{v}_{*e}$	$v_* e$ at $\bar{T}_e$		$5.77 \times 10^{-03}$	$5.88 \times 10^{-03}$	$5.88 \times 10^{-03}$	$5.88 \times 10^{-03}$
$\bar{v}_{*i}$	$v_* i$ at $\bar{T}_i$		$4.08 \times 10^{-03}$	$4.16 \times 10^{-03}$	$4.16 \times 10^{-03}$	$4.16 \times 10^{-03}$
$\rho_*$ ratio				4.20	6.00	6.00
Alpha factor	$\rho_*$ exponent			0.00	0.00	1.00
Confinement scaling type				Bohm	Bohm	GyroBohm

The ARIES–RS design also points to critical features of the DIII–D divertor research. Like ITER, ARIES–RS back projects to densities that are less than 40% of the Greenwald limit in DIII–D. However, the ARIES–RS study provides motivation for the DIII–D Program to seek to find a detached, radiating divertor in this low density regime. As is typical of higher beta, higher power density designs, ARIES–RS has about twice the P/R index for divertor power loading as ITER. Since the machine is smaller overall, the power per unit surface area in the divertor becomes quite extreme in the standard model of divertor physics. The response of the ARIES team to this challenge points to the battleground of conflicting issues for the H–mode shear layer and divertor that DIII–D will address. To lower the power that needs to be handled in the divertor, it would of course be advantageous to use more core radiation. But increased core radiation may conflict with the desire for high confinement quality. In the ARIES–RS design, there was a bootstrap deficit near the edge calling for current drive. The efficiency of that current drive is severely compromised by adding  $Z_{\text{eff}}$  to the plasma edge region. ARIES–RS chose to escape from these conflicts by placing more burden on the divertor physics, calling for divertor impurity enrichment of 8 to radiate the power mainly in the divertor. Clearly, the ARIES–RS study calls for the full range of Advanced Divertor physics that DIII–D will investigate to obtain more highly radiative, detached plasmas at lower upstream densities. Success along this line may lie in the ability to couple a highly radiative, detached divertor in DIII–D with the primary core plasma scenario described in Section 2.2. The Advanced Core and Advanced Divertor Program thrusts in DIII–D may, in fact, meet in a common discharge parameter set, providing not only the physics basis elements for the optimized superconducting tokamak path, but also a demonstration of the integration of these elements.

We provide in Table 2.4–5 a summary of our current views of the important research contributions from DIII–D that support the line to the optimized, superconducting tokamak.

**TABLE 2.4–5**  
**DIII-D CONTRIBUTIONS TO THE SUPERCONDUCTING TOKAMAK PATH**

Issue	DIII-D Contributions to the Superconducting Tokamak Path
Core Confinement	<ol style="list-style-type: none"> <li>1. Dimensionless scaling of advanced confinement regimes, especially the negative central shear regime.</li> <li>2. Theoretical and experimental tests of the stiffness of various core plasma transport models.</li> <li>3. The physics of interior transport barriers and the role of plasma rotation.</li> </ol>
Core Stability	<ol style="list-style-type: none"> <li>1. The role of wall stabilization in allowing higher beta and high, well-aligned, edge bootstrap fractions.</li> <li>2. Profile optimization for higher <math>\beta_N</math>.</li> <li>3. Research of neoclassical tearing modes at low collisionality.</li> </ol>
H-mode Shear Layer	<ol style="list-style-type: none"> <li>1. Allowable edge pressure gradients for stability and possible second stable edge access.</li> <li>2. Allowable plasma mantle radiation consistent with the required plasma edge confinement quality and collisionality.</li> <li>3. An understanding of how the separatrix density is determined (crucial to a highly radiating divertor).</li> </ol>
Divertor Research	<ol style="list-style-type: none"> <li>1. Elucidate the basic physics mechanisms active in the SOL and divertor so they can be incorporated in codes.</li> <li>2. Find ways to increase divertor radiation at fixed upstream parameters (impurity enrichment, convective heat transport, noncoronal equilibrium radiation, non-Maxwellian effects, 2-D heat flow effects).</li> </ol>
Transformerless Operation	<ol style="list-style-type: none"> <li>1. Develop means of initiating and ramping up the plasma current without an OH transformer.</li> <li>2. Develop the physics basis for ECCD, FWCD, and high bootstrap fraction steady-state plasma sustainment.</li> </ol>

### 2.4.3. THE PATH TO A COMPACT IGNITION EXPERIMENT

*GyroBohm confinement scaling from DIII-D projects to a small sized ignition experiment in the DIII-D aspect ratio range.*

In our analyses of ITER and the optimized, superconducting tokamak, we found that a gyroBohm confinement scaling from DIII-D gave results too favorable to be used. The projected transport powers are insufficient to carry out the alpha power. The only use of gyroBohm scaling that we can see is to enable copious core plasma radiation (approaching 100%) to provide the loss channel for the alpha heat. The interesting question that arises is if gyroBohm scaling (which is observed in ELMing H-mode) could be relied on for other modes as well — what tokamak kind of device would be implied? The answer to that question is a compact, high field, copper TF coil ignition experiment.

In Table 2.4–6, we give the results of forward projecting the high performance discharge scenario from DIII-D along a path varying only  $\rho_*$  to such machines. The second column shows the gyroBohm scaling implies a machine somewhat smaller than DIII-D (major radius only 1.33 m) but with a toroidal field of 7.1 T and very high density. This compact machine uses  $\beta_N = 4.4$  and  $H = 3.5$  to produce 320 MW of fusion power. Bohm scaling gives a major radius in the 2 to 3 m range. At an aspect ratio of 2.5 and such high toroidal fields, these machines have insufficient room on the inboard side for a superconducting toroidal coil and full blanket; they would be copper TF coil ignition experiments. However, there is room for an OH transformer for these pulsed experiments.

This path of machine is rather precisely the path between the CIT device and the Burning Plasma Experiment (BPX) device. The original CIT device or IGNITOR was about the parameters of our gyroBohm projected machine. With more conservative confinement scaling (Bohm), the larger major radius BPX device results. The reader can find an almost identical discussion to the one we have just given about confinement projections from DIII-D to BPX in the BPX final report [BPX Team (1992)]. This machine line generally supports higher density, higher collisionality plasma physics. Since the research support needed for this machine line has been so extensively analyzed previously, we give in Table 2.4–7 only a brief summary of specific research issues for DIII-D that are raised by this machine line.

TABLE 2.4–6  
 $\rho_*$  SCALING FROM DIII–D TO A COMPACT IGNITION EXPERIMENT

Quantity	Definition	Units	DIII–D	gB Scaled	Bohm Scaled
$R_0$	Major radius	m	1.69	1.33	2.15
$a$	Minor radius	m	0.60	0.47	0.76
$A$	Aspect ratio		2.82	2.82	2.82
$\kappa$	Plasma elongation		2.10	2.10	2.10
$\delta$	Plasma triangularity		0.75	0.75	0.75
$B_0$	Toroidal field, on axis	T	2.10	7.10	6.30
$I_p$	Plasma current	MA	2.20	5.80	8.40
$\bar{T}_i$	Average $T_i$	keV	5.00	10.40	11.30
$\bar{T}_e$	Average $T_e$	keV	5.00	10.40	11.30
$\bar{n}_e$	Average $n_e$	$\times 10^{20}/m^3$	0.90	4.90	3.60
$\bar{n}/n_{GR}$	Ratio to Greenwald Limit		0.46	0.59	0.78
$Z_{eff}$			1.80	1.80	1.80
$W$	Stored energy in plasma	MJ	4.90	27.00	91.00
$P_{heat}$	Total heating power	MW	19.50	65.00	169.00
$P_{fusion}$	Fusion power (50:50 DT)	MW	5.10	326.00	847.00
$\tau_E$	Energy confinement time	s	0.25	0.41	0.54
$P_{trans}$	Transport loss power	MW	19.50	65.00	169.00
$\tau_{E, Trans}$	$\tau_E$ , transport only	s	0.25	0.41	0.54
$\tau_E$ 93H	$\tau_E$ , transp ITER–93H		0.13	0.23	0.38
$H$	Ratio to ITER–89P		3.11	3.48	2.74
<b>Dimensionless Parameters</b>					
$\beta_T$	Toroidal beta		0.077	0.077	0.077
$\beta_P$	Poloidal beta		3.35	3.35	3.35
$\beta_N$	Normalized beta	mT/MA	4.39	4.39	4.39
$q$	Safety factor		5.42	5.42	5.42
$\bar{\rho}_{*i}$	$\rho_*$ i at $\bar{T}_i$		$1.10 \times 10^{-02}$	$7.00 \times 10^{-03}$	$5.00 \times 10^{-03}$
$\bar{v}_{*i}$	$v_*$ i at $\bar{T}_i$		$1.20 \times 10^{-02}$	$1.20 \times 10^{-02}$	$1.20 \times 10^{-02}$
$\rho_*$ ratio				0.61	0.44
Alpha factor	$\rho_*$ exponent			1.00	0.00
Confinement scaling type				GyroBohm	Bohm

TABLE 2.4–7  
DIII-D CONTRIBUTIONS TO THE COMPACT IGNITION PATH

Issue	DIII-D Contributions to the Compact Ignition Path
Core Confinement	<ol style="list-style-type: none"> <li>1. Assurance of gyroBohm scaling of AT regimes.</li> <li>2. The physics of interior transport barriers and the role of plasma rotation at high magnetic field and density.</li> </ol>
Core Stability	<ol style="list-style-type: none"> <li>1. Wall stabilization for high <math>\beta_N</math> using current profiles that are not fully resistively relaxed.</li> </ol>
H-mode Shear Layer	<ol style="list-style-type: none"> <li>1. L–H transition requirements at high magnetic field and density.</li> <li>2. Local requirements and a theory for avoiding the H–L transition.</li> </ol>
Density Limits	<ol style="list-style-type: none"> <li>1. Elucidation of the basic physical processes that limit the plasma density.</li> </ol>
Divertor Research	<ol style="list-style-type: none"> <li>1. Steady-state solutions are not required.</li> </ol>

#### 2.4.4. THE PATH TO THE SPHERICAL TOKAMAK PILOT PLANT

*DIII–D research projects to a spherical tokamak power system along a Beta scaling path. DIII–D can provide a basis for wall stabilization for high beta, transformerless operation, and the radiating mantle power exhaust solution.*

The spherical tokamak may offer a path to a small fusion power system for a low cost next step in the program. The spherical tokamak achieves small size by discarding inner bore components. The low aspect ratio allows there to be no blanket on the inner wall and yet still have a tritium breeding ratio above 1. Without an inner wall blanket, there cannot be superconducting coils or insulated coils. Hence, the OH coil must disappear from the system and the toroidal coil must be copper with a single turn centerpost. A minimal shield would be provided with its thickness based on the economics of the power dissipation, the replacement time, and/or the waste disposal criteria for the centerpost. With the high beta values predicted for the ST ( $\beta_T \sim 50\%$  with 100% bootstrap current), we have been able to project [Stambaugh (1996)] a fusion development path along the spherical tokamak (ST) line and beginning with a pilot plant (defined as electric power break-even at the site boundary) only about the size of the present DIII–D tokamak (Fig. 2.4–4).

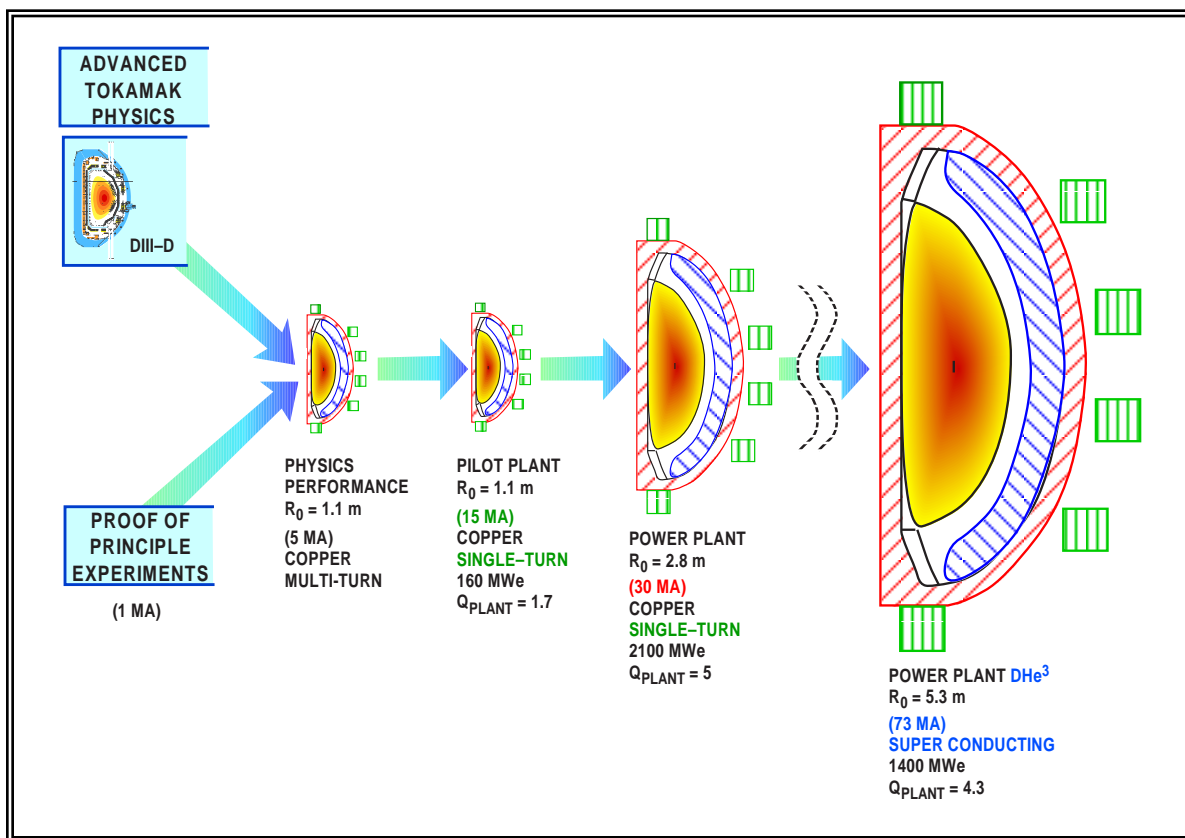


Fig. 2.4-4. DIII-D research projects to a spherical tokamak power system.

The ST pilot plant or power plant essentially transplants all the AT physics from DIII-D into low aspect ratio, where those physics elements are expressed more dramatically than at aspect ratio 2.5. Wall stabilization is the key to obtaining  $\beta_N$  greater than 3 at any aspect ratio. The broad pressure profiles called for in DIII-D for high  $\beta_N$  become almost flat out to the plasma edge in the ST high beta equilibria. The hollow current profiles sought in DIII-D become extremely hollow in the ST with most of the plasma current concentrated near the outer midplane edge of the plasma. One difference between the ST and DIII-D is that despite the very hollow current profiles, the  $q$  profiles remain monotonic in the ST with  $q_0 \sim 4$ , corresponding to the WCS regime. With the wall stabilization and profile control physics being sought in DIII-D, the ST is predicted to support  $\beta_N$  values in the range 8 to 10 and  $\beta_T \sim 50\%$  with 100% bootstrap current. These results optimize in the elongation range 3 to 4 in the ST, which is much beyond the elongation that can be investigated in DIII-D. Neoclassical tearing mode physics is also important in the ST owing to the high beta. Such modes are predicted to be stable owing to the large central  $q$  and to the unusually large value the stabilizing Glasser term acquires at low aspect ratio.

The turbulence suppression by sheared  $E \times B$  flow is vital to the ST obtaining the high values of confinement enhancement that are needed. Owing to the high plasma pressure and low toroidal field in the ST, the diamagnetic term in the turbulence shearing rate  $\omega_{E \times B}$  becomes very large. In high beta ST equilibria,

we find  $\omega_{E \times B}$  in the range 3 to 30 MHz whereas values of 100 kHz suffice to produce transport barriers with residual neoclassical transport in present tokamaks. We have performed 1-D transport studies for the ST which incorporate a full calculation of local  $\omega_{E \times B}$  and suppress the anomalous transport where  $\omega_{E \times B}$  exceeds the turbulence decorrelation rate  $\Delta\omega_T$ . We find that with some reduction in  $\Delta\omega_T$  to 60 kHz (from 100 kHz at  $A = 2.5$ ), we get sufficiently good transport barriers to support  $\beta_T \sim 50\%$ . The maximum growth rate  $\gamma$  of turbulent modes is often used as an upper bound to  $\Delta\omega_T$  and Rewoldt [Rewoldt (1996)] has predicted such reductions in  $\gamma$  at low aspect ratio. The experimental and theoretical work in DIII-D on determining the dependence of  $\gamma$  and/or  $\Delta\omega_T$  on local plasma parameters such as the magnetic shear and temperature and density gradient scale lengths will be important in determining the quality and radial location of transport barriers in the ST.

The ST line also motivates strongly the Advanced Divertor and radiative mantle research in DIII-D. The ST can use the most advanced results from the divertor research in DIII-D to achieve the highest possible radiation in the divertor, but even then, most of the power must be radiated from a core plasma mantle. With most of the current flow near the outer midplane edge of the plasma and that current coming from a fully aligned bootstrap current profile, the conflict we discussed above for ARIES-RS between mantle radiation and a collisionless plasma edge becomes even more acute in the ST. Moreover, owing to the absence of inboard PF coils, the ST will probably require an inboard limited plasma in which to work out the conflict between the collisionless, possible second stable H-mode edge and the mantle radiation. This research line in DIII-D presently springs from the encouraging results from the TEXTOR RI-mode (and from TFTR recently obtaining RI-mode) but its ultimate use is probably in the ST.

Since an OH transformer cannot be installed in an ST, the research to establish full transformerless operation is mandatory. It appears that DIII-D is well suited to undertake this new research thrust. Plasma initiation using only outer PF coils or coaxial helicity injection is being investigated, with ECH assisting for either preionization or current drive. Experiments on current ramp-up by bootstrap overdrive (bootstrap fractions over 100%) with assist from ECCD and FWCD are planned. The effort to ramp-up the current noninductively is a particular driver of the long pulse capability in DIII-D; it takes 5 to 10 s time scales for the back EMF to decay away. The key physics issue here is the stability of neoclassical tearing modes as the current is ramped up, an issue more difficult for DIII-D than the ST, as discussed above. Of course, steady-state sustainment of the current and the AT profiles has long been and continues to be an aim of the DIII-D Research Program.

Because the aspect ratio of the ST is so different from DIII-D, it is difficult to construct a dimensionless parameter connection. However, we have done so and the results have some surprising implications. We have taken the view that the higher aspect ratio DIII-D plasma simulates the core of the lower aspect ratio ST plasma. We match up dimensionless parameters on a flux surface that has the same local inverse aspect ratio  $\epsilon$  in the ST and DIII-D. We chose the flux surface with local  $\epsilon = 0.3$  which gives  $r/a = 0.4$  in the ST and 0.75 in DIII-D. The local plasma parameters can then be scaled to give the same or scaled local  $\beta$ ,  $v_*$ , and  $\rho_*$ . The safety factor profile is chosen to be the same over the entire range of overlap of

the two machines in local  $\epsilon$ . The  $q$  profile in the ST must be continued out to the edge, which results in the edge  $q$  being substantially different between the ST and DIII-D, but the DIII-D plasma is matched to the core of the ST plasma in this way. Table 2.4–8 shows an ST pilot plant in the first column and various projections to DIII-D in the other three columns. The ST pilot plant chosen was rather sub-optimal since we had to choose a low elongation of 2 to match up to DIII-D. Unlike the other machines discussed above that are connected to DIII-D mainly along a varying  $\rho_*$  path, the ST is connected to DIII-D along a varying  $\beta$  path with the ratio of  $\beta$  (DIII-D/ST) in the range 0.15 to 0.2. It was also necessary to vary  $\rho_*$  a bit with the ratio of  $\rho_*$  (DIII-D/ST) = 1.6 to 2. For the transport power and confinement time scaling, no dependence on aspect ratio or  $\beta$  was assumed and either a Bohm or gyroBohm assumption was made for the small  $\rho_*$  extrapolation. The parameters called for in DIII-D lie within the range of the DIII-D plan. AT core performance,  $\beta_N \sim 3.5$  to 4.5 and  $H \sim 2.5$  to 3.5, is called for but at lower edge  $q$  than scenarios for the higher aspect ratio machines discussed above. Surprisingly, the densities called for are still less than 40% of the Greenwald limit.

We provide in Table 2.4–9 a summary of the important research contributions that can be made by DIII-D in support of the ST path.

#### 2.4.5. RESEARCH IMPLICATIONS FOR DIII-D FROM A LOOK AT FUTURE TOKAMAK POSSIBILITIES

Our examination of the issues raised for DIII-D research by possible future tokamak initiatives and how to connect DIII-D's parameter regime to the regimes of these future machines has shown substantial overlap in both DIII-D's achievable parameters and in the research aims and goals of the DIII-D Program. One overall surprising result is that for *all* four future paths discussed above, the dimensionally similar plasma in DIII-D has a low density, less than 50% of the Greenwald density limit. While it is advantageous from the viewpoint of current drive efficiency to position DIII-D's core plasma studies in this very collisionless regime, it places great demands on the divertor program to develop advanced physics techniques to achieve radiative, detached divertors under conditions of high power flux and low plasma density. We have also found motivation for study of radiating plasma mantle scenarios, with all the attendant conflicts that must be worked out with the edge bootstrap requirements and the properties of the H-mode shear layer. We must also utilize strong additional electron heating to make  $T_e = T_i$  in DIII-D. Many challenging research tasks lie ahead.

TABLE 2.4-8  
 $\beta$  SCALING FROM AN ST PILOT PLANT TO DIII-D

Quantity	Definition	Units	Source	DIII-D	DIII-D	DIII-D
$R_0$	Major radius	m	1.4	1.67	1.67	1.67
$a$	Minor radius	m	1.0	0.67	0.67	0.67
$A$	Aspect ratio		1.40	2.49	2.49	2.49
$\kappa$	Plasma elongation		2.2	2.2	2.2	2.2
$\delta$	Plasma triangularity		0.4	0.4	0.4	0.4
$B_0$	Toroidal field, on axis	T	2.48	1.45	1.45	1.12
$I_p$	Plasma current	MA	10.50	2.01	2.01	1.63
$T_i(0)$	Ion temperature	keV	15.00	6.92	6.92	6.39
$T_e(0)$	Electron temperature	keV	15.00	6.92	6.92	6.39
$n(0)$	Electron density	$\times 10^{20}/m^3$	2.76	0.42	0.42	0.36
$\bar{n}/n_{GR}$	Ratio to Greenwald limit		0.66	0.24	0.24	0.25
$Z_{eff}$			1.00	1.00	1.00	1.00
$W$	Stored energy in plasma	MJ	80.0	3.02	3.02	2.38
$P_{heat}$	Total heating power	MW	98.2	4.1	6.5	7.7
$P_{fusion}$	Fusion power	MW	437.0	0.00	0.00	0.00
$\tau_E$	Energy confinement time	s	0.816	0.743	0.464	0.309
$P_{trans}$	Transport loss power	MW	73.6	3.0	4.9	5.8
$\tau_{E, trans}$	$\tau_E$ , transport only	s	1.087	0.725	0.453	0.302
$\tau_{E-93H}$	$\tau_E$ , transp ITER-93H		0.211	0.252	0.184	0.117
$H$	Ratio to ITER-89P		6.771	3.517	2.781	2.505
<b>Dimensionless Parameters</b>						
$\beta_T$	Toroidal beta		0.359	0.074	0.074	0.098
$\beta_P$	Poloidal beta		1.46	1.26	1.26	1.52
$\beta_N$	Normalized beta	mT/MA	8.48	3.56	3.56	4.52
$\beta$ ratio			1.00	0.15	0.15	0.20
Alpha beta	Beta exponent		0.00	0.00	0.00	0.00
$q$	Safety factor		5.56	3.81	3.81	3.81
$\bar{\rho}_{*e}$	$\rho_* e$ at $\bar{T}_e$		$1.49 \times 10^{-04}$	$2.59 \times 10^{-04}$	$2.59 \times 10^{-04}$	$3.23 \times 10^{-04}$
$\bar{\rho}_{*i}$	$\rho_* i$ at $\bar{T}_i$		$6.36 \times 10^{-03}$	$1.10 \times 10^{-02}$	$1.10 \times 10^{-02}$	$1.37 \times 10^{-02}$
$\bar{v}_{*e}$	$v_* e$ at $\bar{T}_e$		$2.39 \times 10^{-03}$	$3.33 \times 10^{-03}$	$3.33 \times 10^{-03}$	$3.33 \times 10^{-03}$
$\bar{v}_{*i}$	$v_* i$ at $\bar{T}_i$		$1.69 \times 10^{-03}$	$2.35 \times 10^{-03}$	$2.35 \times 10^{-03}$	$2.35 \times 10^{-03}$
$\rho_*$ ratio				1.60	1.60	2.00
Alpha $\rho$	$\rho_*$ exponent			0.00	1.00	1.00
Confinement Scaling Type				Bohm	GyroBohm	GyroBohm

**TABLE 2.4–9**  
**DIII–D CONTRIBUTIONS TO THE ST PATH**

Issue	DIII–D Contributions to the ST Path
Core Confinement	<ol style="list-style-type: none"> <li>1. Dimensionless scaling, especially beta scaling, of advanced confinement regimes, especially the WCS regime.</li> <li>2. The physics of interior transport barriers, especially the role of <math>E \times B</math> shear.</li> <li>3. Experimental and theoretical work on the connection of the turbulence decorrelation rate to local plasma parameters.</li> </ol>
Core Stability	<ol style="list-style-type: none"> <li>1. The role of wall stabilization in allowing higher beta and high, well aligned, edge bootstrap fractions.</li> <li>2. WCS <math>q</math> profiles, low edge <math>q</math> values, and very broad pressure profiles.</li> <li>3. Research on neoclassical tearing modes, especially the Glasser term.</li> </ol>
H–mode Shear Layer	<ol style="list-style-type: none"> <li>1. Allowable edge pressure gradients for stability and possible second stable edge access using inner wall limiter plasmas.</li> <li>2. Allowable plasma mantle radiation consistent with the required plasma edge confinement quality, collisionality, and bootstrap current alignment.</li> </ol>
Divertor Research	<ol style="list-style-type: none"> <li>1. Find ways to increase divertor radiation at fixed upstream parameters (impurity enrichment, convective heat transport, noncoronal equilibrium radiation, non-Maxwellian effects, 2–D heat flow effects).</li> <li>2. Develop the radiating plasma mantle solution to power exhaust.</li> </ol>
Transformerless Operation	<ol style="list-style-type: none"> <li>1. Develop means of initiating and ramping up the plasma current without an OH transformer.</li> <li>2. Develop the physics basis for ECCD, FWCD, and high bootstrap fraction steady-state plasma sustainment.</li> </ol>

In Table 2.4–10, we give an overall recapitulation of the research issues that are raised by looking toward various future tokamak possibilities and an indicator to which machine path the issue primarily applies.

### References for Section 2.4

- Petty, C.M., Luce, T.C. et al., *Phys. Plasmas* 2, 2342 (1995).
- BPX Team, *Fusion Technology* 21, 1081 (1992).
- Galambos, J.D., et al., *Nucl. Fusion* 35, 551 (1995).
- Stambaugh, R.D., et al., “The Spherical Tokamak Path to Fusion Power,” General Atomics Report GA-A22226, submitted to *Fusion Technologies* (1996).
- Rewoldt, G., et al., *Phys. Plasmas* 3 1667 (1996).
- Najmabadi, F., and the ARIES team “Overview of ARIES–RS Tokamak Fusion Power Plant,” in *Proc. 4th Int. Symp. on Fusion Nuclear Technology, Tokyo (1997)*.to be published.

**TABLE 2.4–10**  
**DIII–D CONTRIBUTIONS TO FUTURE TOKAMAK PATHS**  
 (IT = ITER, RS = ARIES–RS, IG = IGNITION, ST = SPHERICAL TOKAMAK)

Issue	DIII–D Contributions to Future Tokamak Paths	Applies To			
		IT	RS	IG	ST
Core Confinement	1. Dimensionless scaling with $\beta$ , $v_*$ , $q$ , and $\rho_*$ of advanced confinement regimes: <ul style="list-style-type: none"> <li>• In ITER's shape and regime.</li> <li>• In the NCS regime.</li> <li>• In the WCS regime.</li> </ul>	✓	✓	✓	✓
	2. Theoretical and experimental tests of the stiffness of various core plasma transport models.	✓	✓	✓	✓
	3. The physics of interior transport barriers, the role of E×B shear and rotation.	✓	✓	✓	✓
	4. Experimental and theoretical work on the connection of the turbulence decorrelation rate to local plasma parameters.	✓	✓	✓	✓
Core Stability	1. The role of wall stabilization in allowing higher beta and high, well-aligned, edge bootstrap fractions.		✓		✓
	2. Profile optimization for high $\beta_N$ .		✓	✓	✓
	3. WCS $q$ profiles, low edge $q$ values, and very broad pressure profiles.				✓
	4. Research on neoclassical tearing modes at low collisionality, especially the Glasser term, and the use of ECCD for stabilization.	✓	✓	✓	✓
H–mode Shear Layer	1. Experiment and theory work on the structure of the shear layer (pedestal height, width of layer, local plasma parameters, effects of neutrals).	✓	✓	✓	✓
	2. Local parameter requirements and a theory for the L–H transition.	✓	✓	✓	✓
	3. Local requirements and a theory for avoiding the H–L transition.	✓	✓	✓	✓
	4. Allowable plasma mantle radiation consistent with the required plasma edge confinement quality, collisionality, and bootstrap current alignment.		✓		✓
	5. Allowable edge pressure gradients for stability and possible second stable edge access using inner wall limiter plasmas.				✓
	6. An understanding of how the separatrix density is determined.	✓	✓	✓	✓
Density Limits	1. Elucidation of the basic physical processes that limit plasma density.	✓	✓	✓	✓
Divertor Research	1. Elucidate the basic physics mechanisms active in the SOL and divertor so they can be incorporated in codes.	✓	✓	✓	✓
	2. Find ways to increase divertor radiation at fixed upstream parameters (impurity enrichment, convective heat transport, noncoronal equilibrium radiation, non-Maxwellian effects, 2–D heat flow effects).	✓	✓	✓	✓
	3. Develop the radiating plasma mantle solution to power exhaust.		✓		✓
Transformerless Operation	1. Develop means of initiating and ramping up the plasma current without an OH transformer.		✓		✓
	2. Develop the physics basis for ECCD, FWCD, and high bootstrap fraction steady-state plasma sustainment.	✓	✓		✓

## 2.5. THE DIII-D NATIONAL FUSION FACILITY — STATUS AND UPGRADES

### OVERVIEW OF CURRENT CAPABILITIES

DIII-D National Fusion Facility provides the capability to carry out a wide range of the-art tokamak experiments. At the heart of the facility is the DIII-D tokamak, which is capable of operating at plasma currents up to 3.0 MA with a magnetic field of 2.2 T. The DIII-D tokamak is renowned for its research in highly noncircular limiter and divertor plasma configurations. Substantial plasma heating and current drive capability is available from 20 MW (delivered) of neutral beam heating, 6 MW (source) of ICRF power and 2 MW (source) of ECRF power (3 MW at end of FY98). The DIII-D diagnostics set provides over 50 diagnostic systems capable of providing definitive measurements of plasma parameters in the core, edge, and boundary regions of the plasma. Control of the tokamak, heating systems, and auxiliaries is managed through a set of interconnected computers.

Operation of the DIII-D facility is the responsibility of GA, who provides the core operational engineering and technical staff, along with the appropriate infrastructure to organize the effort. Many collaborators in the DIII-D Program participate in operational activities including, in particular, the design, installation, and operation of diagnostics and plasma systems such as rf heating, pellet injection, etc. GA is responsible for coordinating and focusing these efforts, ensuring safety, and maintaining appropriate levels of quality.

The DIII-D facility provides over 100,000 sq. ft. of floor space on a ten acre site dedicated to support the activities of the DIII-D Program and its collaborators (Fig. 2.5-1). The DIII-D tokamak is located at the heart of the facility (Fig. 2.5-2) with the many support systems, utilities, and diagnostics arrayed around it.

In the years 1998 and preceding, the DIII-D facility operated for research from 8:30 a.m. to 5:00 p.m. with technical staff arriving up to two hours earlier to prepare and stay afterward for shutdown. Research operations have been carried out on a five-day-a-week basis for three weeks of operation followed by two weeks of maintenance, calibration, and testing. In addition, longer shutdowns are sometimes needed for major maintenance tasks. Typically one longer period is set aside each year for new installations and major refurbishments. In recent years, the number of operating weeks has been limited by funding (8 weeks in FY97 and 13 weeks in FY98 compared to up to 27 weeks earlier). The number of operating hours per year could readily be increased by a factor of two or more with appropriate funds.

The tokamak is housed within the machine hall, which provides access control during operations and provides radiation shielding to allow deuterium to be used as fuel in the tokamak. Within the machine hall, the tokamak is surrounded by heating systems, most notably the large neutral beam lines, diagnostic systems, and other auxiliary systems.

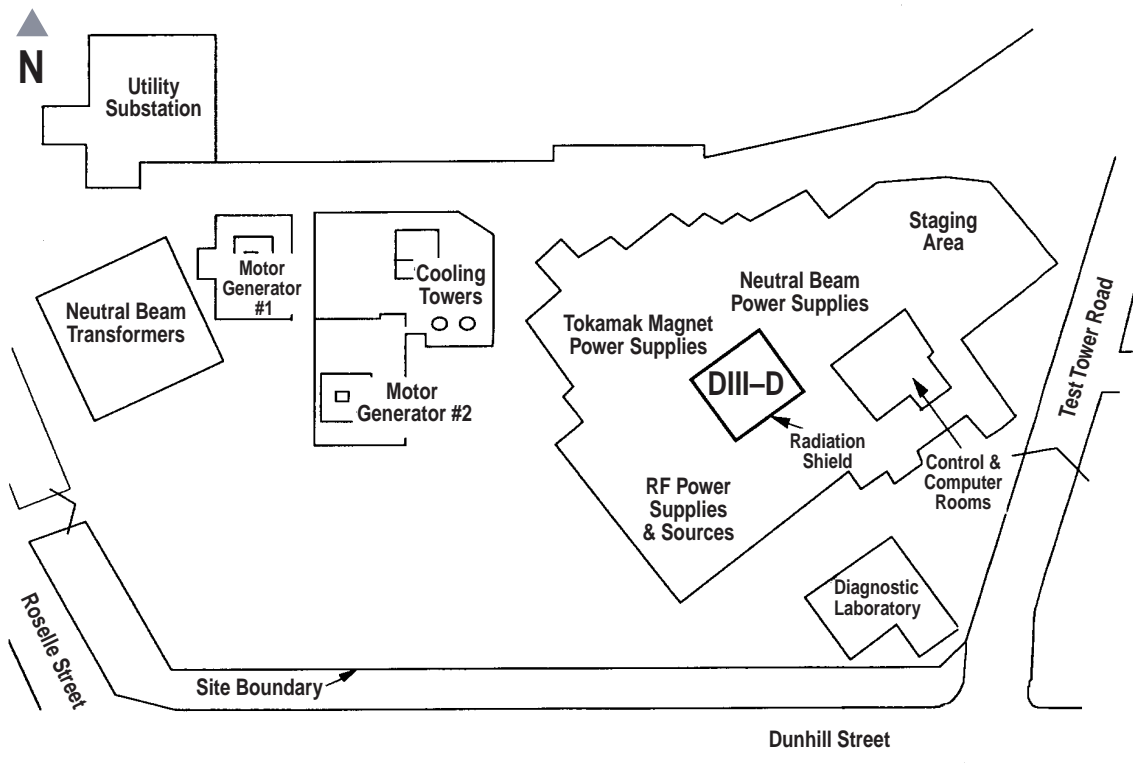


Fig. 2.5-1. The DIII-D tokamak facility spans a half city block.

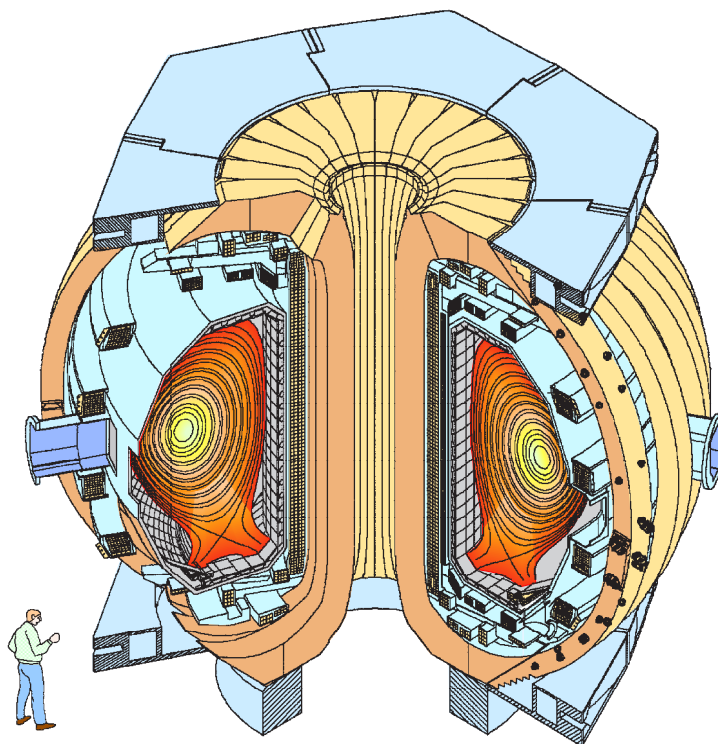
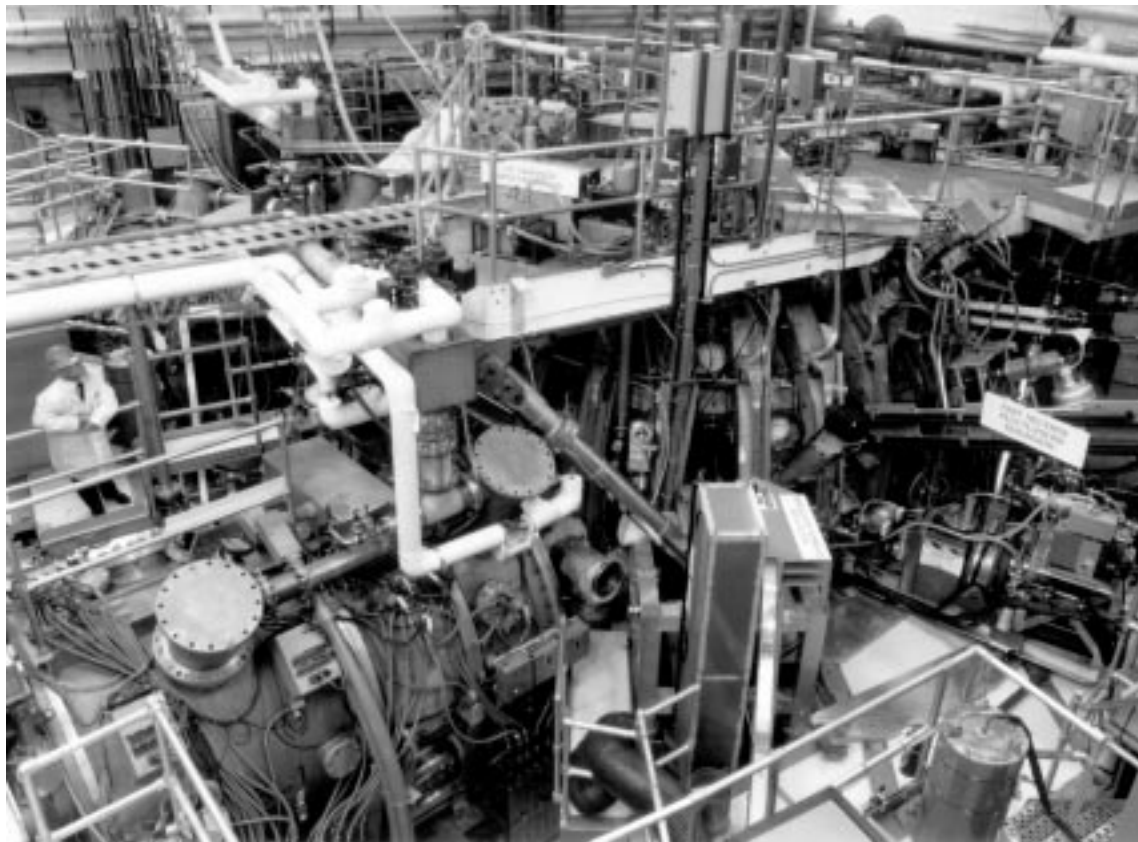


Fig. 2.5-2. The heart of the facility is the DIII-D tokamak with its many support systems, utilities and diagnostics.

The DIII-D tokamak uses conventional water-cooled coils to provide the magnetic field configuration. The coil systems are designed to operate in a pulsed mode with the joule heat stored in the coil mass during the discharge and removed in the ten minute interval between discharges. They routinely operate at full 2.2 T toroidal field and at 2 MA plasma current for a discharge flat-top duration of 5 s (Fig. 2.5–3). This can be readily extended to 10 s with modest upgrades of the coil system connections, feeds, and power supplies. Operation for longer duration at lower field and plasma current is also possible. The DIII-D coil configuration is noteworthy for its 18 independently controlled poloidal field shaping coils, each powered by an independent current regulator. These coils shape the highly noncircular plasma cross sections which are typical of the DIII-D Research Program. Lastly, there is a set of six 5 m<sup>2</sup> picture frame coils mounted in a belt around the midplane which correct the residual error fields due to anomalies in the magnetic field configuration.

A graphite first wall covers the entire interior plasma facing surface of the vacuum vessel (Fig. 2.5–4). Graphite is an effective choice because it has low atomic mass so that sputtered graphite entering the plasma has little impact, it has good thermo-mechanical properties in contact with the hot plasma, and it has good thermal conductivity. Graphite tiles are directly mounted to the chamber wall to provide cooling in the period between discharges. The first wall is conditioned for operation by first baking and outgassing under vacuum at 350°C. The wall is then coated with a fine layer of boron (boronization) which serves largely to getter oxygen in the vessel. Finally, helium glow discharge cleaning is used in the interval between discharges to clean and degas the wall surfaces before the next discharge.

Also, located at the top and bottom of the plasma chamber, are baffled cryopump systems designed to pump away excess neutral gas at the edge of the separatrix flux surface of divertor plasmas. The upper and lower divertor cryopumps are illustrated in Fig. 2.5–5. These pumps operate at liquid helium temperatures and actively pump both the plasma fuel gas and all volatile impurities during the discharge. They also have the capability of substantially lowering the plasma density. The cryopump at the bottom of the plasma chamber is optimized to pump the edge of single-null divertor discharges with low triangularity prototypical of ITER. The pump at the top of the chamber is optimized for pumping at the edge of the upper null of highly triangular double-null divertor discharges. Each cryo-pump has a capability of 40,000 l/s. The D<sub>2</sub> is defrosted from the pumps during the helium glow between discharges and the pumps are fully defrosted and outgassed during nonoperational periods.

Substantial auxiliary heating is provided to heat the tokamak discharges to the temperatures needed to achieve the conditions appropriate for efficient fusion reactions and to facilitate driving currents in the plasma. The capabilities of these heating systems are summarized in Table 2.5–1. The neutral beam systems are the workhorse of day-to-day operation. They are routinely available on demand to provide heating at their design levels. They have also become an important source for a number of diagnostics including ion temperature, current profile, and turbulence. The ICRF system is fully operational and experiments are underway to refine techniques to couple the power to the plasma. The 110 GHz ECH system has been commissioned and has been used in plasma experiments.

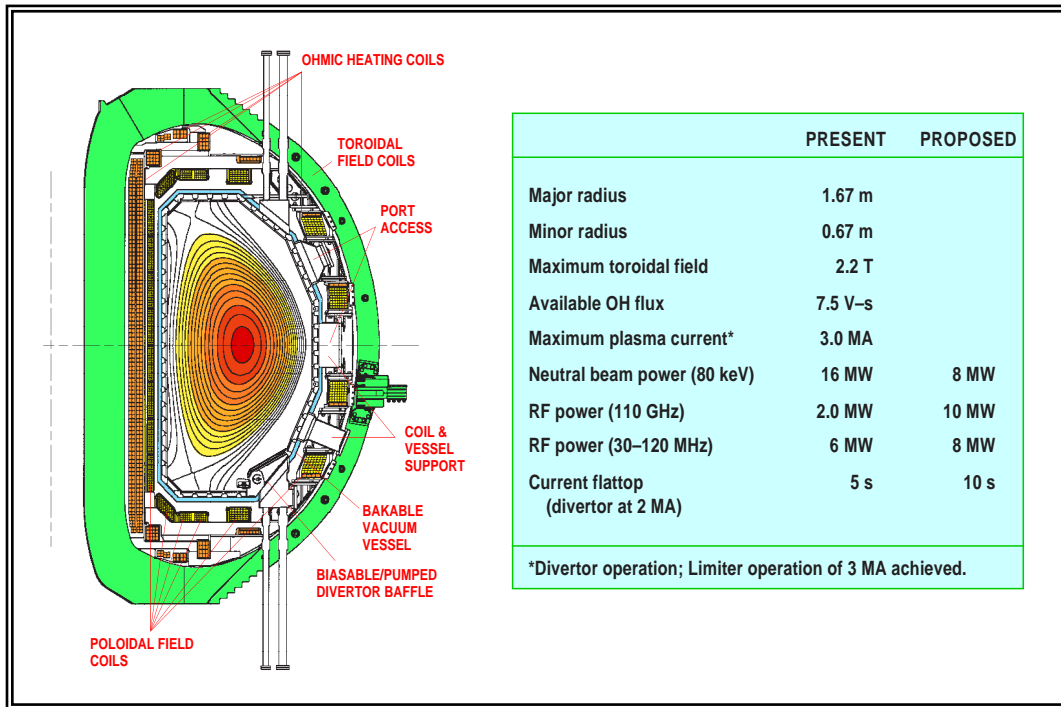


Fig. 2.5-3. DIII-D capabilities allow a wide range of research and technology issues to be addressed.

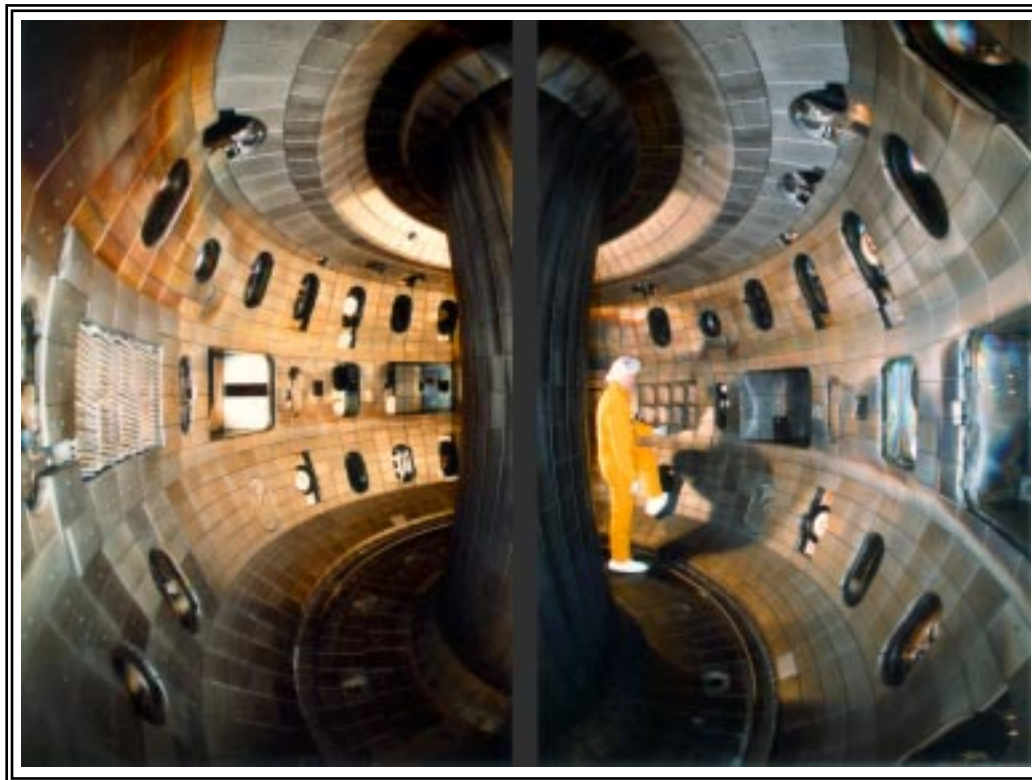


Fig. 2.5-4. The entire DIII-D first wall is graphite.

An ensemble of more than 50 diagnostics is used to characterize DIII-D plasmas. These diagnostics provide a set of data unparalleled anywhere in the world. Measurements of core, edge, and boundary parameters allow the scientists to analyze the key facets of plasma behavior. They typically provide measurements of the spatial distribution of plasma parameters continuously throughout the discharge duration.

An extensive array of computer systems is used to operate the tokamak and auxiliary systems, collect the data, and carry out the analysis (Fig. 2.5–6). These computers are interlinked in a network that effectively applies these resources to the needs of the program. The tokamak control computer provides for control and monitoring of the entire operating cycle. Critical safety limitations are applied with hardwired systems. The heating systems are separately controlled. The acquisition and archiving of data is controlled by another computer that serves as the hub of a large network of computers, both at GA and off-site, used to provide storage and analysis of data. In addition, an array of computers is used to operate, manage, and analyze the data for the diagnostics.

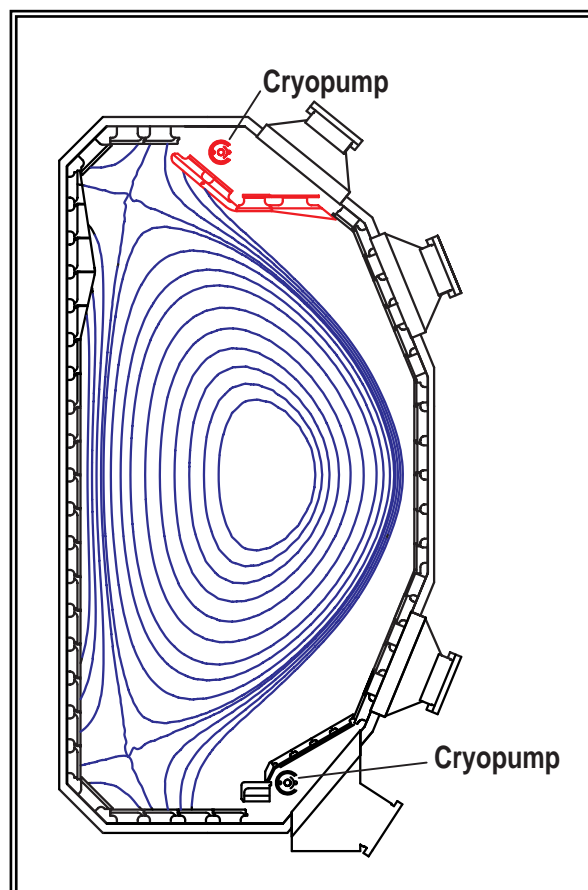


Fig. 2.5–5. The upper divertor cryopump is optimized to pump highly triangular double-null divertor discharges.

TABLE 2.5–1  
POWER TO PLASMA OF AUXILIARY HEATING SYSTEMS (JUNE 1997)

System		$P_{\max}$ (MW)	Duration (s)	P (5 s) (MW)	P (10 s) (MW)
Neutral beams	LBL 80 kV	20	3	16	8
ICH	ABB 30–55 MHz*	2.8	20	2.8	2.8
	FMIT 30–60 MHz	1.4	$\geq 10$	1.4	1.4
ECH (110 GHz)	Gycom gyrotron	0.75	2	0.30	0.15
	CPI gyrotron	0.80	0.8	0.28	0.24

\*The rf power must be decreased above this frequency (to 20% at 120 MHz).

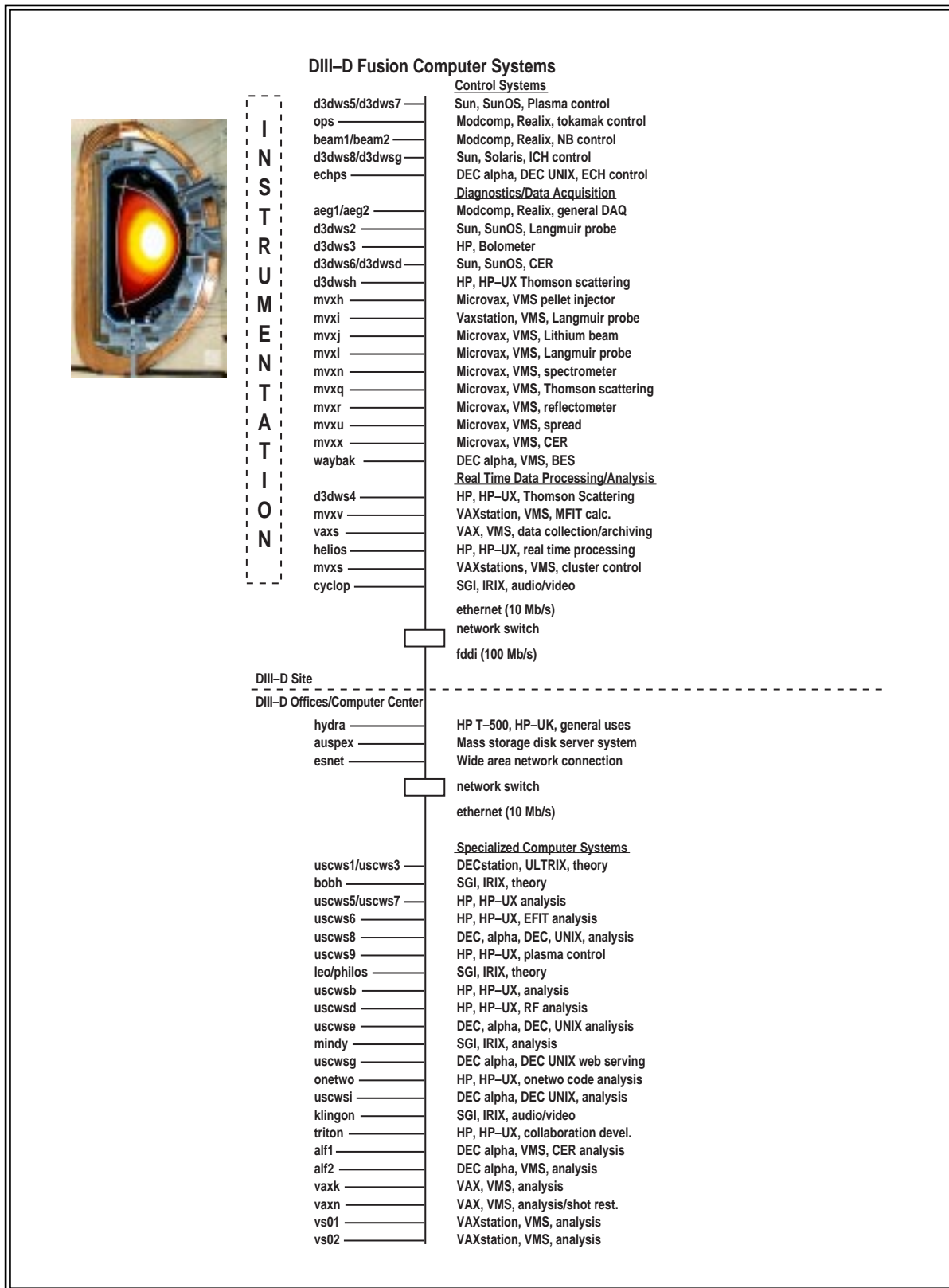


Fig. 2.5-6. An extensive array of computer systems operates the tokamak and collects and analyzes the data.

The plasma control system provides state-of-the-art high speed digital control of the plasma cross-sectional shape (magnetic configuration) and key plasma profile parameters. This system uses multiple input multiple output control technology that allows the wide range of plasma shapes studied in the DIII-D Program to be routinely operated on a shot to shot basis. Recently the implementation of isoflux control has provided realtime control of the plasma boundary using realtime calculation of the MHD equilibrium to evaluate the plasma configuration. The system has the capability for integrated control of the plasma profile parameters using diagnostic measurements as inputs. The system also serves as a platform for the seamless addition of control functions for other parameters such as the plasma density, total energy, or coupling to the ICRF antenna.

The gas puff system and pellet injector provide for control of the plasma fueling. The gas system provides a completely programmable source of a diverse range of gases to initiate the discharge and fuel it from the edge during the pulse. The pellet injector provides fueling deeper into the plasma by injecting high velocity pellets of frozen fuel gas from the plasma edge. The injector is capable of delivering a continuous stream of pellets during a discharge.

A substantial number of more utilitarian systems are necessary to operate the facility. Prime power for the auxiliary heating systems is taken from the local utility power mains. The power for the coil systems is supplied by one of two flywheel energy storage motor generators (525 MVA and 260 MVA). These generators are spun up to full energy between discharges and then the energy is drawn out during the 10 s of the discharge. The coils are powered by a set of phase controlled power supplies. In the case of the plasma shaping coils, there is a series switching current regulator in series with each. The auxiliary heating systems are powered by 12 high voltage power supplies each typically capable of 6 MW of power.

A 150 l/h helium liquifier provides the cryogenic helium needed to support operation of the neutral beamlines, ECH magnets, pellet injector, and divertor cryopumps. A substantial water conditioning system supplies the high pressure, high purity water needed to cool the coils and other systems.

Operation of the tokamak with deuterium fuel results in significant neutron production. These neutrons create a need for radiation monitoring and control. The radiation shield forming the wall and roof of the machine hall reduces the radiation levels sufficiently to allow the facility to be operated with acceptable exposure to the public and workers. Radiation levels at the site boundary are limited to 40 mRem/yr by agreement with the DOE. Radiation levels for staff are limited to 5000 mRem/yr by the NRC and internally to 400 mRem/qtr. The facility is operated within the ALARA principles in order to keep radiation doses as low as reasonably achievable. The quarterly site radiation levels are summarized in Fig. 2.5–7.

The radiation shielding of the DIII-D facility is adequate to carry out the proposed plans. Presently the radiation dose at the site boundary for the typical shift-week of operation is 0.5 mRem. Thus, the facility can be operated for roughly 80 shift-weeks at the present level without exceeding our DOE guideline. In this plan, we propose to increase the total power available by increasing the rf power and the pulse duration. The additional power, if used in addition to the beam power, will increase the radiation levels albeit not to

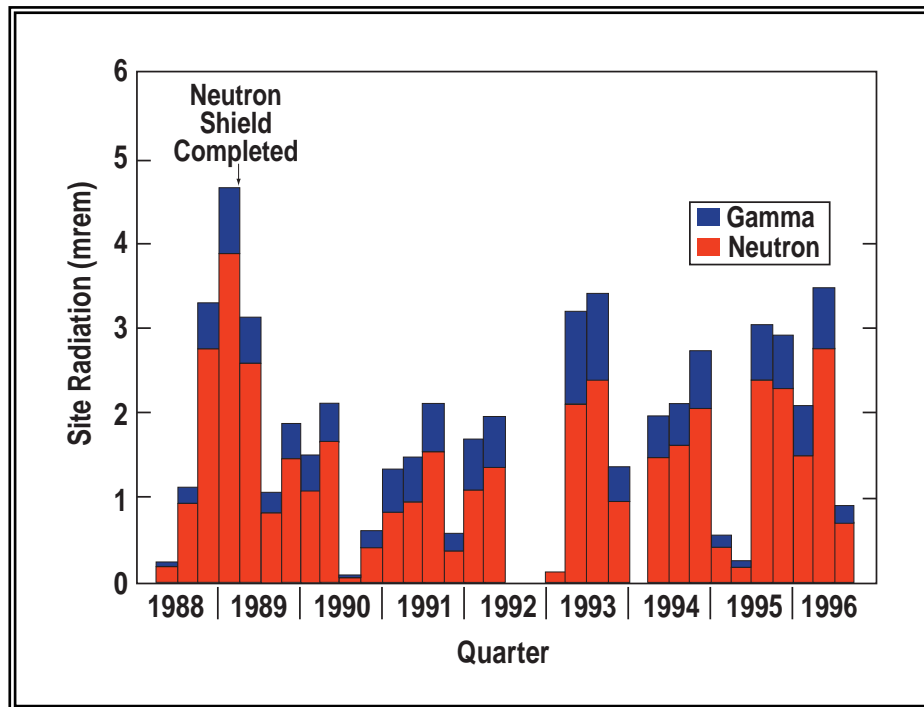


Fig. 2.5–7. Quarterly boundary radiation levels show the site is maintained well below the 40 mrem operating limit.

as high a level as if the increase was in neutral beam power since there are no beam-thermal contributions to the dose for rf heating. The increase in pulse length will also increase the radiation from a given discharge. However, the present plan is to apply the 16 MW 5 s neutral beams serially so that the maximum beam power is 8 MW for 10 s. The rf is anticipated to be capable of 10 s operation. Lastly, it should be noted that with long pulse operation, the repetition rate will likely decrease somewhat, lowering the total dose during a given day.

## OVERVIEW OF THE DIII-D FACILITY UPGRADES, IMPROVEMENTS, AND REFURBISHMENTS

Development and evolution of the capabilities of the DIII-D facility has been the key to the success of the DIII-D Program in the past, and continued development of the facility is necessary if the research program is going to address the emerging scientific issues of the future. Not surprisingly, development of the facility is expected to proceed along a number of fronts in order to meet the scientific challenges of the program. The facility development consists of:

- Major baseline upgrades (capital projects that have been costed as upgrades in the Volume IV, Cost Proposal).
  - Contingency upgrade options (projects not costed in Volume IV, Cost Proposal).
- Facility improvements and refurbishments (activities costed as part of Tokamak Research in Volume IV, Cost Proposal).

These activities would take place over the duration of the proposed five-year period. The presently proposed timeline for baseline upgrades and contingency options is shown in Fig. 2.5–8.

The proposed development of the facility has been refined from ideas developed within the DIII–D National Program and new ideas from the DIII–D Program staff, both GA and collaborator. The proposals presented here were further refined from inputs presented at a workshop held at GA in February 1997.

Upgrades to the tokamak would provide longer pulse lengths and provide new heating, divertor, and fueling systems. The development of the ECH and ICRF will include increasing power and improving antennas to carry out the advanced tokamak program. Development of the divertor configuration will provide continued understanding and refinement of the divertor. Various magnet systems will be upgraded to allow a 10 second pulse length. Similarly, the data acquisition and analysis computer systems will continually evolve to support the evolution of the increasing diagnostics and analysis capability. The diagnostics systems will evolve with the understanding of the tokamak in order to provide the essential measurements to further physics understanding. Progress on the control of the plasma has gone hand-in-hand with improved confinement and stability and further progress will be required to achieve the goals of the research program.

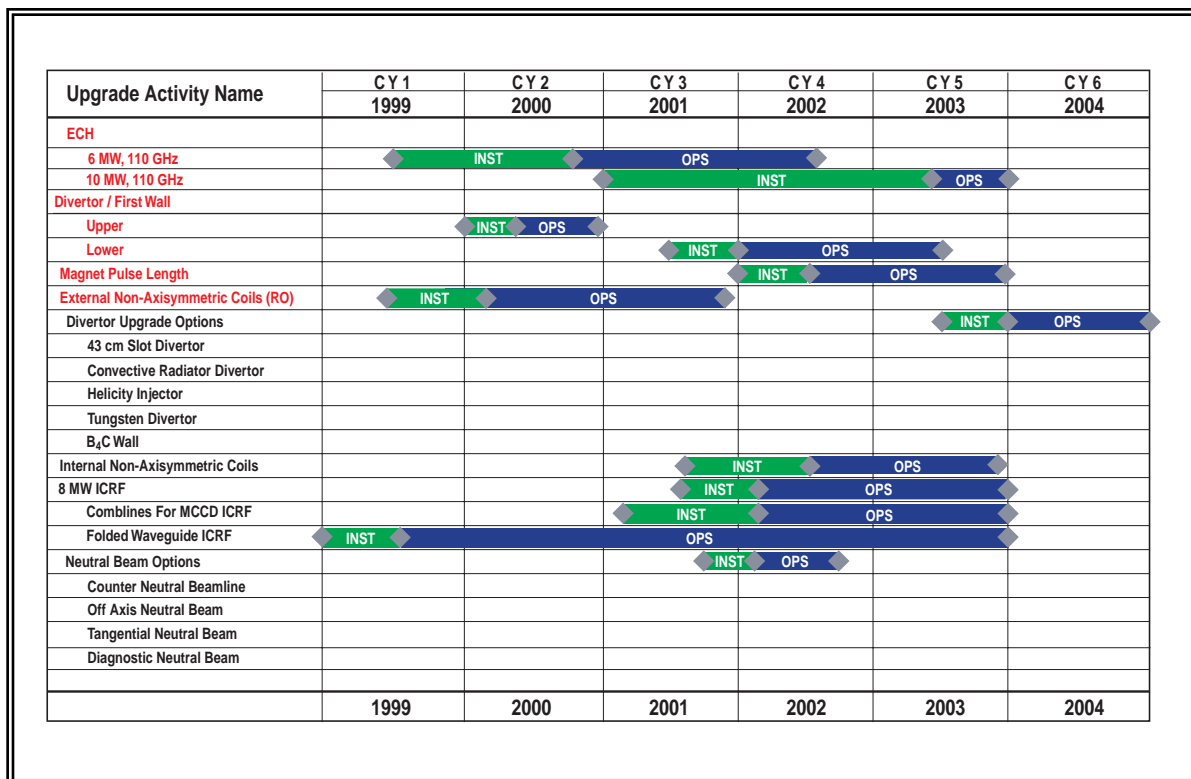


Fig. 2.5–8. Proposed facility development incorporates ideas from GA, collaborators and the February, 1998 workshop.

**Electron Cyclotron Heating and Current Drive.** The 110 GHz electron cyclotron heating and current drive power will be increased first to 6 MW and then 10 MW for 10 s pulse lengths. This will require the initial installation of an additional three (followed eventually by another four) gyrotrons and the associated power equipment. In order to attain our goals, gyrotrons capable of 10 s operation will be procured. The launchers at the tokamak must be upgraded to 10 s operation and additional launchers installed. The upgrades to all of the heating systems are summarized in Table 2.5–2.

**TABLE 2.5–2**  
**POWER CAPABILITY OF HEATING SYSTEMS AFTER PROPOSED UPGRADES ARE COMPLETE**

System	Power (MW)	
	5 s	10 s
Neutral beams	16	8
ECH	10	10
ICRF	8	8

**Divertor Systems.** The evolution of the in-vessel divertor systems has been key to understanding and improvement of the divertor configuration. The proposed work begins with the completion of the present Radiative Divertor Program. First the private flux baffle and cryopump for the upper null will be installed. Then the lower divertor hardware will be installed, completing the Radiative Divertor Program.

Following this, several optional steps might be envisioned to optimize the configuration by modest changes in the details of the divertor region, including perhaps another major revision, the convection divertor. We will also pursue the understanding and development of effective divertor materials for ITER or other devices.

**Magnet Pulse Length Upgrade.** Upgrading the present nominal pulse length of 5 s at full field to 10 s is modest to implement because much of the capability is already built into the coil systems and power supplies. This upgrade would provide a more suitable discharge length for carrying out experiments to modify and control the plasma profiles. It would also allow more secondary experiments to be carried out during the longer discharge. The upgrade consists largely of increasing the capability of the busswork for the coils. The plasma heating would be provided by a combination of the neutral beam systems run in two groups serially for 8 MW of power and the ECH and ICRF systems which will have been separately upgraded to meet these capabilities. Owing to the reduced total power level of the heating systems and the more efficient use of the thermal capacity of the first wall and vessel, the vessel thermal capacity is adequate. The diagnostics can be upgraded to these longer pulse lengths with conventional extensions of their local memory.

**Computer and Data Systems.** The data acquisition system will require continuous upgrades to meet the demands of new and improved diagnostics and more sophisticated analysis techniques. The machine control and neutral beam heating computers have been recently upgraded and will likely serve, with minor modifications, through this plan period. The data acquisition systems are already at their capacity and upgrades of CPU, storage, and CAMAC interface systems will be expanded. The network connections within GA and to the user community will be upgraded to 100 Mb/s. Further integration of remote users into the DIII-D Program will require the development of specialized tools to facilitate further interaction with the database and on site scientists. This will also include increased ability to operate DIII-D from remote sites (already demonstrated from LLNL).

In order to improve the effectiveness of the DIII-D Program, and to better facilitate the participation of our collaborators, a new database and database management system for access to and analysis of shot data is being developed for the DIII-D Program and it is anticipated that this activity will continue. This activity will include a comprehensive common database, improved access to the database, a modern database management code, user friendly codes for analysis and visualization of the data, and the development of a set of common interlinked tools.

**Diagnostics.** The diagnostic systems on DIII-D are presently the best in the world. However it will be necessary to continue to develop the diagnostic system to provide the capability to address emerging research issues, and to support the changes in other hardware systems either by modifying systems to function following changes in the vessel configuration or to provide new capability to address the issues posed by the new hardware. The installation of the lower radiative divertor components will necessitate the reconfiguration of a number of diagnostics to move their field of view inward.

The DiMES diagnostic will be expanded to additional locations to provide greater understanding of materials at the plasma edge. This would be followed by the installation of more suitable materials in the divertor region (possibly tungsten) and the use of more suitable coated tiles in the main chamber (possibly B<sub>4</sub>C or Si doped graphite).

A number of diagnostics modifications will also be undertaken to improve the diagnosis of the core plasma. New diagnostics will be implemented to better understand electron transport and turbulence. These include measurements of small scale turbulence, magnetic field fluctuations, and temperature fluctuations. A Thomson Scattering System to measure the central electron temperature will complement the present detailed measurements of the outer three-fourths of the plasma. 3-D equilibrium reconstruction will provide a means of reconstructing the magnetic configuration without the present limitation of the assumption of axisymmetry. A new diagnostic is proposed to measure the current profile at high densities where present techniques become ineffective. This would benefit both DIII-D and ITER. Lastly, we propose to implement a new technique to enhance the performance of beam emission spectroscopy diagnostics by using an auxiliary laser to pump the observed atomic transition.

**Tokamak Systems.** Other tokamak systems can also be improved to better meet the needs of the program. Improved pellet fueling systems would provide more effective fueling of the torus. Plasma control system development will focus on developing feedback control systems for the plasma profiles as part of the existing state-of-the-art plasma control architecture. Nonaxisymmetric coil configurations are proposed for both outside and inside the vessel to stabilize destructive plasma instabilities and to affect the plasma edge. A specialized liquid jet or pellet system to ameliorate the undesirable energy fluxes following a disruption could be developed (option).

**Ion Cyclotron Heating (Option).** The ion cyclotron heating system may be upgraded from 6 to 8 MW (source) by the addition of an upgraded FMIT transmitter from PPPL. To accommodate this power and to provide long pulse capability, the least capable antenna in the machine would be replaced with a folded wave-guide launcher previously developed at ORNL. It is also proposed to investigate the installation of combline antennas on the interior wall of the vacuum vessel to provide mode conversion current drive.

**Neutral Beams for Rotation Control and Diagnostics (Option).** No major upgrading of the neutral beam capability is planned, but it is proposed (option) that one beam line be rotated to the counter-injection position so that it could be used in conjunction with the remaining three co-injecting beam lines to better understand and vary the momentum injected into the plasma and to control the rotation of the plasma in particular. This change would require a major modification of the beam line structure and the systems in the surrounding area.

## 2.5.1. ELECTRON CYCLOTRON HEATING AND CURRENT DRIVE SYSTEMS UPGRADE

Work presented in Sections 2.2 (Advanced Tokamak Program), 2.3.1 (Confinement Science and Transport Barrier Control), and 2.3.4 (Science of Plasma Current Generation and Heating) shows that 6 MW and possibly up to 10 MW of source ECH power will be required to achieve the science goals of the DIII-D Program. Detailed computer modeling shows that this power can drive sufficient current off-axis, when combined with bootstrap current, to generate steady-state current profiles which are consistent with advanced tokamak performance at densities suitable for effective heat removal. This section describes the hardware upgrades needed to carry out this program.

**2.5.1.1. PRESENT STATUS OF ECH SYSTEMS.** At present, we have two 110 GHz gyrotrons operating at a nominal 1 MW (source) power level. The first gyrotron is made by Gycom in Russia. It has an edge-cooled window of boron nitride which limits the pulse length to 2.0 s at a power level of 1 MW. It has achieved power levels of 960 kW for 2.0 s pulses in tests in Russia. The other gyrotron is made by CPI (formerly Varian). It has a face-cooled window of sapphire which limits the power to 1 MW for 0.8 s or 0.5 MW for 2 s. Both vendors indicate their designs are cw compatible except the window. These gyrotrons have injected power into DIII-D through the transmission system, and the beam patterns and locations generated in the vacuum vessel correspond approximately to those expected from the theory of Gaussian beam propagation and from vacuum ray tracing using a 3D computer model. A third 1 MW gyrotron is expected from CPI in late 1998.

The transmission system for these gyrotrons is evacuated corrugated waveguide of diameter 31.75 mm propagating the  $HE_{11}$  hybrid mode. Presently there are four launchers on the DIII-D tokamak, each capable of launching 1 MW of ECH power. Each launcher comprises a 60.3 mm diameter corrugated waveguide launcher, a fixed focusing mirror located about 30 mm from the termination of the waveguide, and a steerable flat mirror that can be pivoted poloidally so the rf beam can be aimed at any elevation between the plasma center and the upper edge. They are tilted off-normal by 19 deg in the toroidal direction so that the rf beam is launched in a manner which will drive toroidal plasma co-current near the cyclotron resonance. The steering in the toroidal direction can be changed, but only during a vent of the vacuum vessel. The present mirrors are tilted 19 deg in the toroidal direction in order to generate co-current drive.

Power supplies for the gyrotrons are modified neutral beam supplies. A single neutral beam power supply has sufficient power to support the operation of two 1 MW gyrotrons. However, Gycom gyrotrons operate near 72 kV and CPI gyrotrons operate near 80 kV, so gyrotrons of mixed brands cannot be operated by a single supply. At present, we use a modified MFTF neutral beam supply for the Gycom gyrotron and a modified DIII-D Universal Voltronics Corporation (UVC) neutral beam supply for the CPI gyrotron.

**2.5.1.2. UPGRADE TO 10 MW OF ECH POWER (BASELINE).** The upgrades to the ECH system during the next five-year period will be based upon the designs developed and tested on the three 1 MW 110 GHz ECH systems being installed presently. Upgrades to 6 MW, and subsequently to 10 MW if the physics necessitates more power, have been considered. The final system is designed to achieve a pulse length of 10 s, for which development of a suitable gyrotron by one of the major gyrotron developers (CPI, Gycom, Thomson, or Toshiba/JAERI) is a key issue. A detailed description follows of what would be added or changed to support an upgrade to 6 MW and 10 MW.

**ECH Power Supplies.** At present, two more MFTF power supplies are available on site. The transformer/rectifier systems have been placed on concrete pads in the DIII-D switchyard but not yet connected to the incoming power lines or to the DIII-D building. To support the 6 MW ECH system the existing modulator/regulator needs to be repackaged to fit into a room  $10 \times 21$  ft and the other two mod/regs would also need to be similarly condensed. There is no technical problem in doing so, but significant work is required. To go to 10 MW, two more MFTF power supplies will have to be obtained from LLNL and installed.

A new underground duct bank will have to be installed to bring the high voltage conductors from the transformers to the DIII-D building. Also if pulses longer than a few seconds are needed, the ac power substation will need to be expanded.

**Gyrotron System.** A gyrotron system consists of the gyrotron, the superconducting magnet, the high voltage oil tank which houses the high voltage feed, filament power supply, diagnostics, protective circuits, the water cooling manifold and instrumentation, the collector coil and power supply, and the transmission line interface unit. For both the upgrade from 3 to 6 MW and 6 to 10 MW, most of this equipment will be new and will have to be either procured or manufactured, but in general it will be identical to the equipment already in use. In addition to the hardware for each gyrotron system, a support structure and other auxiliary equipment will be needed.

Considerable gyrotron development is needed to make this task successful. The present gyrotrons do not have windows that allow them to operate at full power for more than a second or two and they have not been demonstrated in 10 s operation. Several promising window concepts are being developed at various laboratories around the world, including variants of the 'distributed' window developed at GA, and a promising concept utilizing an edge-cooled diamond disc. Progress on windows made of polycrystalline diamond has been spectacular over the last year. The diamond discs are made by a variant of chemical vapor deposition, and diamond windows of diameter up to 5 in. and thickness 0.080 in. have been made. Diamond discs have now been tested which have extremely low absorption and high thermal conductivity. High power tests of a CPI gyrotron with a diamond window is expected at DIII-D in late 1998.

**Transmission Line.** Two new transmission lines, plus some additional components, will be needed for the 6 MW system, and an additional four transmission lines will be needed for the 10 MW systems. They will be identical to the present corrugated evacuated waveguide which transmit the  $HE_{11}$  mode.

**ECH Launcher.** For the upgrade to 6 MW (10 MW), two (six) new launchers will need to be built and installed. For 10 s operation, the mirrors on the present launchers as well as any new launchers will need to be actively cooled. Through an SBIR contract with Thermacore, a water cooled mirror using "porous metal" heat removal technology is being developed with anticipated validation on DIII-D in a few years. If this work is successful, then this technology could be adapted to future ECH launchers. It is also anticipated that at least one of the launchers will rotate with a moderately fast slew rate ( $>100$  deg/s) in the poloidal plane so that magnetic islands or active MHD zones can be tracked as the plasma evolves with time.

## 2.5.2. DIVERTOR SYSTEM UPGRADES

### 2.5.2.1. PRESENT STATUS OF DIVERTOR AND FIRST WALL.

DIII-D presently has a comprehensive carbon first wall and divertor targets to protect the vacuum vessel in areas of high heat fluxes and to limit high  $Z$  impurities in the plasma (Fig. 2.5–9). The first wall is a robust system, operating for ten years without failures, providing maximum experimental time. The wall consists of inertially cooled graphite tiles, absorbing energy during a discharge then releasing it to the water cooled vessel wall through a compliant heat transfer interface in the ten minutes between discharges. A wide range of plasma configurations can be run including single-null divertors with either upper or lower null, highly shaped double-null divertors, and limiter discharges on any of the surfaces. The tile design provides cavities between the vacuum vessel wall and the tiles for diagnostics, protecting them and their signal cables from large heat fluxes.

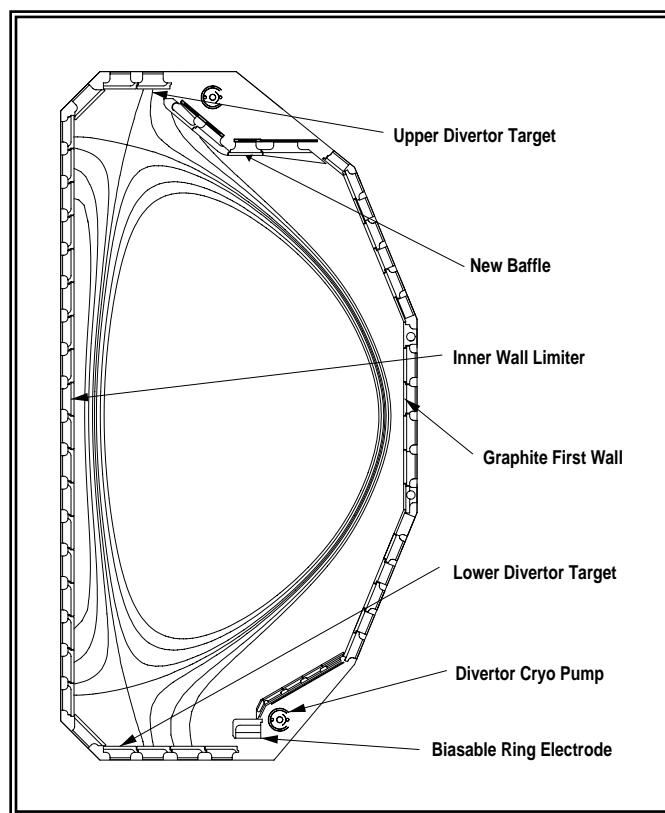


Fig. 2.5–9. The carbon first wall and divertor targets protect the vacuum vessel and limit high- $Z$  impurities.

A toroidally continuous baffle with cryopump in the lower divertor region has been in use for several years. Divertor characterization experiments have been successful using the extensive lower diagnostic set to benchmark many computer plasma models. Low triangularity plasmas are routinely pumped by placing the separatrix at the aperture of the divertor plenum to provide density and particle control with 40,000 l/s pumping speed. An integrated biasable ring electrode has allowed the study of the effects of electric fields on the neutral pressure in the baffle, as well as evaluated novel noninductive startup techniques.

The upper divertor target area was modified in the beginning of FY97 with the installation of the first phase of the Radiative Divertor. This hardware included a toroidally continuous baffle and cryopump similar to the existing lower system in the bottom except the aperture to the pumping plenum is at a smaller minor radius, allowing pumping and particle control high performance, high triangularity discharges. The structure is comprised of water-cooled Inconel 625 panels with graphite tiles mounted to the surface. The cryopump is of a design similar to the proven lower pump. The pump provides pumping speeds of nearly 40,000 l/s for the high performance discharges.

**2.5.2.2 RADIATIVE DIVERTOR PROGRAM (BASELINE).** DIII-D experiments have shown that high triangularity and particle control are necessary ingredients for high performance discharges. The Radiative Divertor is a major element of the DIII-D Program to provide particle control for high performance AT operation, and carry out ITER divertor physics research to develop methods of reducing the heat flux at the divertor target without impacting the core confinement. The RDP includes the installation of divertor structures and cryopumps to permit this new research to be carried out (Fig. 2.5–10). The first phase installation, the upper outer cryopump and baffle, was completed in February 1997 and we are currently engaged in an experimental campaign utilizing the new hardware. In parallel, we are working on the detailed engineering design of the second phase hardware. When completed, the RDP will allow for pumping of all four strike points of a double-null high triangularity plasma. The installation of the Radiative Divertor components impacts a number of diagnostics and effective use of the hardware requires the installation of a number of new diagnostics. These are discussed in the diagnostics section.

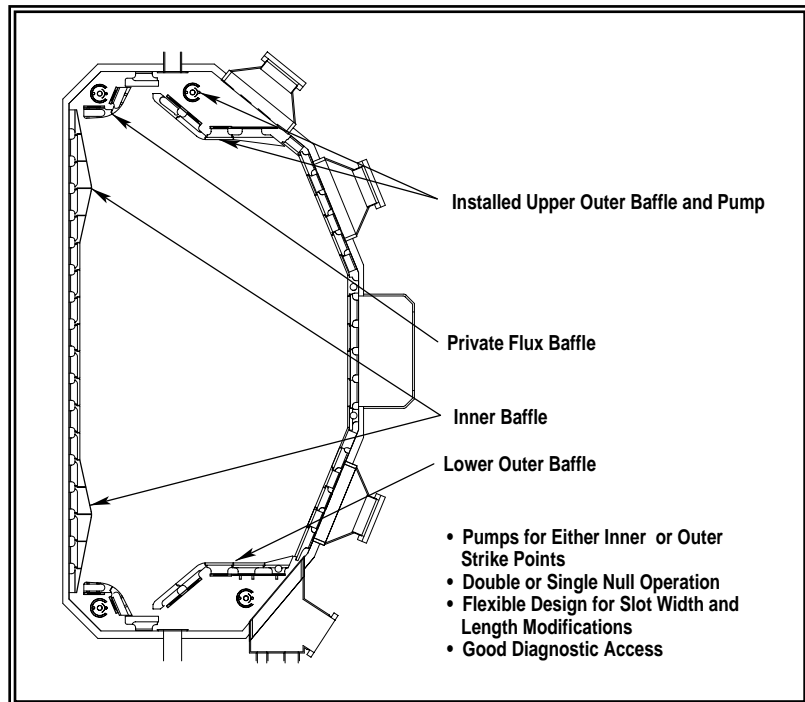


Fig. 2.5–10. The planned completion of the Radiative Divertor installation includes the lower baffle and the private flux baffles together with new tiles making up the inner baffles.

The Radiative Divertor baffles have been designed to be very flexible, as the height and width of the slots can easily be varied. This will allow us to both optimize the configuration based on experimental results and benchmark computer models with various configurations. The initial installation was designed for a slot width of 1.5 cm and a length of 23 cm based on the values from the combined UEDGE and DEGAS models for optimum reduction of the core ionization. The modeling indicates that if the slot is made narrower, the core ionization increases because the slot becomes a recycling source that is close to the plasma core. If the slot is made wider, neutrals can leak around the plasma and enter the core at the mid-plane. In the present design, the nominal slot can be changed by about 3.5 cm by adding thicker or thinner graphite tiles. We estimate that this can be accomplished in about three weeks of total down-time on DIII-D. The length of the slot can be increased from 23 cm to 43 cm by lengthening the supports for the tiles and adding a vertical baffle structure. We can also make a “gasbox” type of divertor by leaving the structure below the baffle open in the 43 cm slot case. It is envisioned that a height change could be done each year

during the major DIII-D maintenance period. We plan to change slot widths and slot lengths guided by the data, so that the important quantities can be determined and results evaluated.

As part of the effort to advance the development of low activation materials for fusion use, we had planned to manufacture the water cooled panels for the upper private flux baffle using vanadium alloy. It was the goal of the program to demonstrate not only the manufacture of vanadium alloy components, but also to operate them within DIII-D to demonstrate their compatibility with the tokamak environment. The research and development of the manufacturing methods has been ongoing for the last two years at GA in collaboration with the DOE Fusion Materials Program. In preparation for the project, the world's largest heat of vanadium alloy has been produced (1200 kg) and converted into sheet and rod. Regrettably, this program is presently unfunded.

### 2.5.2.3. FUTURE DIVERTOR AND FIRST WALL (OPTIONS)

**Expanded Erosion System Capabilities.** Initial results from the DiMES experiments have extended the understanding of divertor surface materials erosion and transport in tokamaks. These results have helped to quantify the possible erosion rate, re-deposited distribution and the corresponding tritium inventory of graphite for the ITER divertor design. The DiMES team has generated data on the net erosion rate and re-distribution of C, Be, W, V and Mo coating materials, which have been used for the assessment of selecting suitable divertor coating material for advanced reactor designs. However, further parametric results will be needed to confirm the present data which is limited to the lower divertor. It is also necessary to extend the database to cover the upper divertor, the first wall and different plasma operating scenarios. Based on these observations, and in coordination with the installation of the RDP divertors, we propose to add two DiMES sample changers to DIII-D. This will expand the DiMES program capability over the present DiMES changer in the lower divertor.

At its present location, the lower DiMES changer (DiMES-L) will be shadowed by the lower RDP outboard baffle plate when it is installed. However, DiMES-L can still be used to monitor material deposition within the divertor plenum and to provide information on material transport from seed materials introduced from the other two proposed DiMES locations. With modification, DiMES-L can be made to extend its vertical delivery and to insert a sample with its plasma facing surface parallel to the slanted surface of the RDP outboard baffle, but the sample will not be exposed to the plasma strike point.

We propose to construct an upper sample changer (DiMES-U) to DIII-D in order to maintain the capability of exposing material samples to the plasma strike point. This might be accomplished by the insertion of a material sample radially to the top outboard strike point of high triangularity discharges in DIII-D. This will allow continued study of material surface erosion at the plasma strike point under different scenarios of plasma operation, including ELMs and disruptions.

It is also proposed that a third sample changer be installed at the mid-plane of DIII-D (DiMES-MP). By taking advantage of the increased available space, DiMES-MP will be designed to provide better

instrumentation of the sample and characterization of the surrounding edge plasma. In order to maintain temperature control, the sample surface will be heated.

DiMES-MP can also function as a user facility. Enhanced collaboration is possible by focusing on the development of new plasma diagnostics and in-situ measurements techniques for erosion and material recycling of the first wall material. With three sample changers in place, a more comprehensive knowledge of SOL material transport, including the region behind the divertor baffle can be obtained. Suggestions for advanced diagnostics are: quartz film deposition monitor, optical diagnostics (colorimetry, interferometry, and ellipsometry) for in-situ coating deposition measurements, solid-state hydrogen sensors for the measurement of incident particle flux and/or energy, and laser or neutral beam desorption diagnostics for the determination of deposited film composition. (The last approach will need laboratory development.)

**Tungsten Divertor Surface Options.** The purpose of this option is to investigate the behavior of tungsten surfaces in the divertor region. The DIII-D Program would continue to emphasize plasma performance issues while providing increased effort on first wall studies. This test would be reactor relevant and also relevant to the ITER Program. For both ITER and future systems, tungsten will provide both a *low erosion divertor material* and a *material that is resistant to neutron irradiation*. It is of significant importance to demonstrate that tungsten can be retained in the divertor region and be kept from migrating into the main plasma chamber where it may raise the core radiation to untenable levels. Preparation could begin at the end of this plan period.

High-Z divertor experiments have been conducted in both Alcator C-Mod and ASDEX Upgrade. On both devices, both high and low core impurity radiation conditions have been observed, depending on details of the operating mode. C-Mod has a deep slot configuration with an all molybdenum wall. ASDEX Upgrade uses tungsten coated graphite tiles in a high recycling baffled outer divertor. The area where tungsten would be used in the DIII-D divertor is shown in Fig. 2.5-11; the inner and outer divertor target plates are coated, as well as the central baffle. The strike points could be either carbon or tungsten.

This test would investigate the behavior of: tungsten divertor walls, compare carbon or tungsten strike zones, and evaluate the use of mixed wall materials. They would address the issues of: plasma operation with

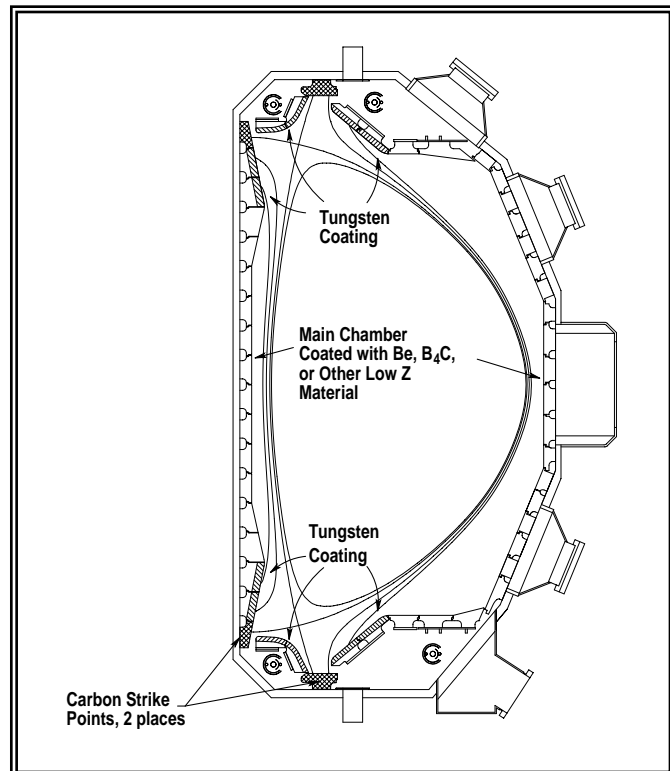


Fig. 2.5-11. Divertor and first wall surface options will be tested on DIII-D.

tungsten divertor walls, mixed material wall conditioning, wall material erosion and migration, and surface property changes of wall materials.

Bulk tungsten will not be used due to its weight and cost. Tungsten coated graphite tiles will be developed based upon the recent experience of ASDEX Upgrade. Since the erosion rates of tungsten are expected to be very low, relatively thin coatings ( $<50 \mu$ ) are suitable. High heat flux and disruption simulation tests will be conducted in collaboration with SNL prior to installation. Suitable surface diagnostics and analysis tools will be developed in coordination with the DiMES Program on DIII-D.

**Alternate Wall Materials in the Main Plasma Chamber (Options).** The purpose of this option is to select and then use fusion power plant relevant wall materials for the DIII-D main plasma chamber. The DIII-D Program would continue to emphasize plasma performance issues while providing increased effort on first wall studies. This test would be reactor relevant and also relevant to the ITER Program. Important considerations are low activation and minimum impact on core plasma dilution and radiation. Materials under consideration are beryllium, vanadium,  $B_4C$ , and silicon doped or SiC conversions.

A series of experiments will be conducted to determine an appropriate material for use in DIII-D. These experiments will both determine the best first surface material and develop methods of applying these materials. High heat flux and disruption simulation testing of candidate materials will be carried out and the exposure of candidate materials in the DIII-D chamber will be studied by replacing existing tiles with special ones or through use of the DiMES facility.

Bulk materials or coatings will be prepared externally to the DIII-D vessel. Various methods of constructing the first wall tiles would be investigated and tested. Bulk beryllium, bulk boronized graphite, or CFC could be used. It is most likely that a relatively thin coating of selected material will be applied to either cleaned and refurbished DIII-D graphite tiles or that new tiles will be machined from appropriate materials.

The area where alternate materials would be used in the first wall of the DIII-D main chamber is shown in Fig. 2.5–11.

- Mixed wall materials, when taken in conjunction with the tungsten divertor.
- Possibility of self-reconstructing coatings during confinement discharges.

Operational issues to be addressed include:

- Plasma operation with reduced carbon influx.
- Mixed material wall conditioning with the proposed tungsten divertor.
- Wall material migration.
- Surface property changes of wall materials.

### 2.5.3. MAGNET PULSE LENGTH UPGRADE (BASELINE)

Extending the pulse length of the DIII-D tokamak from 5 to 10 s for a 2 Mega-amp (MA) plasma at full field requires only minor modifications to the tokamak and additional auxiliary heating required to study the current profile control. The additional heating requirements will be treated in a separate section. In the following paragraphs, the modifications required to the coil systems, the power supplies, primary power, cooling system, and radiation limitation will be discussed. The conclusion is that the interconnecting busswork between the bundles of the toroidal field coil, upgrade of the poloidal field shaping coil regulators (choppers), and an upgrade of the cables on the patch panel and the cables connecting the motor generator to the dc power supplies are the only changes needed to upgrade the tokamak to 10 s plasmas. One dc power supply will be required for the poloidal field coils.

**Coil Systems.** Once this upgrade is completed, the joule capability of the toroidal field coil and power supply are well matched to the poloidal field system for plasma currents of about 2 MA. The toroidal field coil is capable of 10 s operation at 2.1 T and longer pulse length at lower fields limited only by the joule heating of the coil (Fig. 2.5–12). However the use of this coil is thermally limited by the interconnecting busswork that runs along the midplane of the machine on the outside of the coil and the free-wheeling diodes. This limits the pulse length to 5 s at full field, whereas the coil turns and the feed from the power supply have the capability of supporting 10 s operation at full toroidal field of 2.1 Tesla on axis. Thus only the interconnecting busswork and diode need to be upgraded for the toroidal coil to support a 10 s plasma.

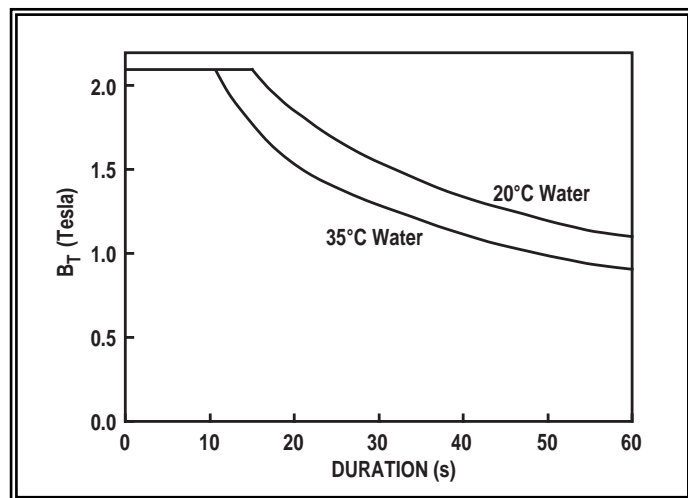


Fig. 2.5–12. The toroidal field coil is capable of 10 s and longer pulse operation with the completion of the proposed upgrade.

The Ohmic heating coil was put back into its original configuration during the fall of 1997. The reconfigured circuit delivers 7.5 volt-seconds (V-s) of flux. About 5.0 V-s are required to breakdown the plasma and ramp the current to 2 MA. Thus 2.5 V-s are available for sustaining the plasma current during flat-top. With auxiliary heating of about 10 MW it is possible to heat the plasma sufficiently to lower the plasma resistance to  $0.125 \mu\Omega$ . Thus a one-turn voltage of 0.25 V can drive a 2 MA plasma for 10 s with the available volt-seconds. The use of rf and neutral beam current drive (along with bootstrap current) will further reduce the flux requirement. Thus no upgrade of the Ohmic heating coil is required to support 10 s pulse length.

All the field-shaping coils have sufficient thermal capability to support 2 MA plasmas for 10 s. However, some of the interconnecting cables will have to be upgraded.

**Power Supplies.** The toroidal field power supply is capable of powering the coil for all of these scenarios. The Ohmic heating power supply has far more capability than the Ohmic heating coil. The field-shaping coil current regulators (choppers) need to be upgraded. The varistors in the X-choppers need to be replaced, whereas all the other components can support 10 s operation. In the HX-choppers only the grid resistors need to be replaced.

**Primary Power.** For long pulses, the coil power supplies are powered from the motor generator (MG2), from which 2.25 GJ can be extracted. About 1.6 GJ are required for the coil power supplies for a 10 s plasma. Thus the MG has sufficient extractable energy. The cables connecting the MG2 to the power supplies need to be upgraded.

The auxiliary heating systems, the neutral beams, ICH, and ECH, are powered from a 138/12.47 kV transformer, which is rated at 9.4 MVA continuous and 84 MVA for 1 s. With the anticipated additional rf power, a second transformer will have to be installed.

**Cooling System.** The 2.25 GJ capacity of the motor generator limits the joule heat deposited in the coil and power supplies during a shot and it is assumed that a maximum of 20 MW of auxiliary power can be injected into the plasma. This means that for five shots per hour a total of 12.25 GJ or an average of 3.4 MW of heat will have to be removed from the tokamak, its coil systems and power supplies. The capacity is 4.2 MW, so no upgrade is required.

**Reversing Switches for Toroidal and the Ohmic Heating Circuits.** It is often necessary to change the direction of the toroidal field or of the plasma current. This is currently done by moving busswork and is labor intensive. It is therefore not done as often as would provide maximum benefit to the research program, nor can it be done during a day, where it would allow one to compare data with opposite toroidal field or plasma current with the same vacuum conditions. By installing switches in the two circuits to reverse the polarity of the power supply, one would be able to do the change over in a matter of minutes versus hours currently. For both the toroidal and the Ohmic heating circuit, two double pole switches would have to be installed. The two switches would be required to carry 150 kA continuously.

## 2.5.4. IMPROVEMENTS TO THE DIII-D TOKAMAK (COMPLETED AS PART OF TOKAMAK RESEARCH)

**2.5.4.1. NONAXISYMMETRIC COIL SYSTEMS.** The installation of nonaxisymmetric coils systems to apply resonant magnetic perturbations to the plasma in DIII-D is required to carry out a wide range of important experiments. There are five principal applications which have been identified: toroidal alfvén eigenmodes (TAE)/beta driven alfvén eigenmodes (BAE) mode studies, RWM active control, plasma rotation control, active control of resistive MHD internal modes, and ergodization of the plasma edge. The required perturbations span a range in frequency from several hundred kilohertz for the study of TAE and BAE modes to dc for the generation of an ergodic magnetic structure in the plasma edge and a range in toroidal mode number from  $n=4$  to 8 for TAE/BAE studies to  $n=1$  for plasma rotation and internal mode control.

The DIII-D vacuum vessel wall time constant, which is a few ms, divides the approaches proposed into two distinct groups. Applications which require the frequency of the applied magnetic perturbations to be below 100 Hz can be external to the vacuum vessel. These include control of the RWM which grows on the time scale of magnetic soak field through of the vacuum vessel wall and ergodization of the plasma edge. Applications which require the frequency of the applied magnetic perturbations to exceed a few hundred hertz will require a coil set internal to the vacuum vessel. These include TAE/BAE mode studies, plasma rotation control, and active control of resistive MHD internal modes. The requirements on the design of nonaxisymmetric coil systems discussed above are summarized in Table 2.5-3.

**TABLE 2.5-3**  
**SUMMARY OF THE FIVE AREAS OF RESEARCH INTO NONAXISYMMETRIC MAGNETIC PHENOMENA AND HOW THEY WOULD BE ADDRESSED BY THE PROPOSED EXTERNAL AND INTERNAL COIL SYSTEMS**

Application	Coil Location	Applied Frequency	Ampere-Turns	Toroidal Mode	Poloidal Mode	Current Channels
RWM Control	External (C-coil+)	dc to 100 Hz	5-10 kA	1	2-4	9
RWM Control	External (vessel)*	dc to 100 Hz	5-10 kA	1-3	2-4	25
RWM Control	Internal	dc to 100 Hz	2-5 kA	1-5	2-6	50
TAE/BAE Studies	Internal	40-500 kHz	5	4-8	6-16	1
Rotation Control	Internal	dc to 10 kHz	5-10 kA	1	2-4	2-6
Feedback Control	Internal	dc to 10 kHz	5-10 kA	1	2-4	2-6
Ergodic Edge	Internal	dc	10 kA	2	7-9	1
Ergodic Edge	External	dc	15 kA	3 and 5	9 and 15	1

\*These two options can only be achieved with a more specialized coil system to be developed later in this task.

**Preconceptual Design of Basic External Nonaxisymmetric Coil Sets.** The existing C-coil consists of six coils each 60 deg wide toroidally and extending about  $\pm 25$  deg about the midplane at the radial location of the TF coil set. This coil set could provide reasonable control with respect to toroidal spatial resolution for an  $n=1$  RWM, but its capability to match the poloidal mode structure is poor. Since we expect the dominant RWM to be  $3/2$  and  $4/1$ , a much improved match to the expected mode structure on the outer vacuum vessel wall could be obtained by adding additional coils above and below the existing C-coil each with the same 60 deg toroidal width as shown schematically in Fig. 2.5–13. Because the C-coil is relatively far from the plasma, only  $2/1$  and  $3/1$  helicities can be generated with significant amplitude at the plasma edge while the relative amplitude of the  $4/1$  component is an order of magnitude smaller. Providing some overlap with the existing C-coil may increase the relative  $4/1$  component and optimization studies need to be carried out.

Improved resolution of the poloidal and toroidal mode structure can be obtained if a network of response coils could be mounted on the vacuum vessel allowing finer spatial resolution. A nearly complete coverage  $n=5$  coil set combined with a sparse  $n=3$  set could provide improved RWM control together with improved control of ergodic layer generation.

**Preconceptual Design of an Internal Coil Set (Option).** To obtain better control of the RWM, if experiments carried out in the next few years indicate that  $n>1$  resistive wall modes are important for setting the ultimate  $\beta$  limit of AT plasmas, coils as well as the conducting structure would need to be placed closer to the plasma than the present DIII-D vacuum vessel allows. This requires consideration of the installation of an internal conducting wall and control coil network. The installation of such a structure and high resolution internal coil network would be incompatible with the high-frequency internal coil set proposed in the following section and would also affect the basic operation of DIII-D depending on the time constant chosen for the internal stabilizing wall, and hence would be an option for installation late in the five-year research program.

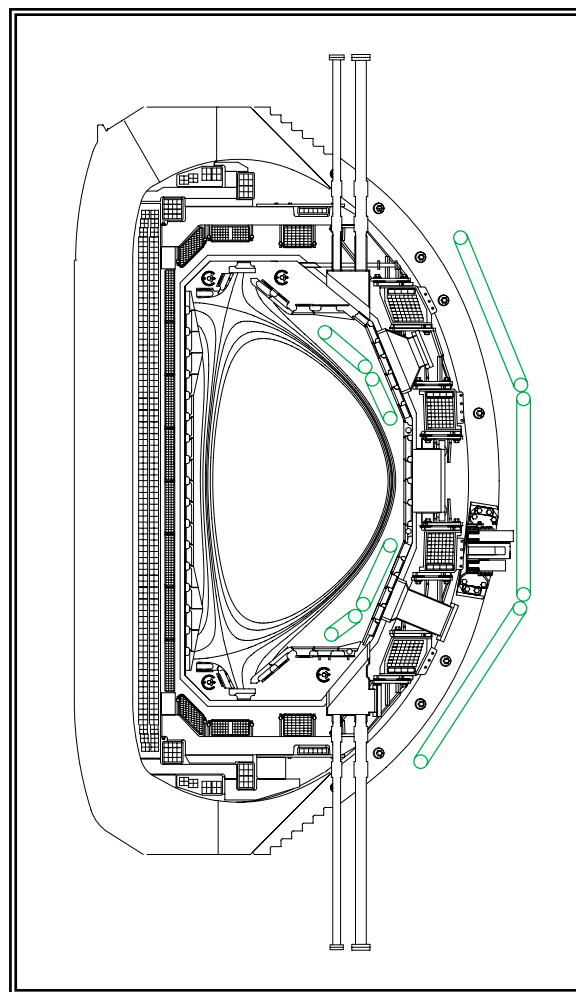


Fig. 2.5–13. Additional coils would give an improved match to the outer vacuum vessel wall mode structure.

To reduce the cost and complexity of these systems, we seek to combine as many of the capabilities as possible into one internal and one external coil set. The internal coil set might consist of four coils groups each 45 deg wide and spaced 90 deg apart to allow generation of  $n=1, 2,$  and 4 modes depending on relative phasing of the coil set drive and could address the four of the five applications areas including TAE/BAE mode studies, plasma rotation control, active control of resistive MHD internal modes, and creation of an edge ergodic layer. Each group would consist of two coils above and two symmetrically below the midplane starting just above and below the neutral beam ports, respectively, as shown in Fig. 2.5–13. These coils could be constructed as single-turn, carbon armored plate coils (about 10 cm wide) whose central toroidal locations could be chosen to be rotated relative to the 16-fold port symmetry of DIII–D to minimize diagnostic interference and avoid crossing the NBI ports.

**n=1 Connection.** Upper and lower coil groups are connected to add and are 180 deg out of phase with each other. This allows two-phase drive with peak amplitudes in the 2/1, 3/1, and 4/1 helicities required for plasma rotation and tearing mode active control.

**n=2 Connection.** Upper and lower coil groups connected 180 deg out of phase. This allows generation of dominant helicities of 7/2, 8/2, and 9/2 with a dc power supply for ergodic layer formation in the plasma edge. Further work is needed in design refinement to reduce the level of 3/2, 4/2, and 5/2 helicities which could interfere with modes in the plasma core.

**n=4 Connection.** Upper and lower coil groups are connected to add and are also in phase with each other. This produces dominant helicities of 3/4, 4/4, and 5/4 as well as 7/4, 8/4, and 9/4 which are needed for the high frequency, low current excitation studies of TAE/BAE modes.

**2.5.4.2. PELLET FUELING (TOKAMAK RESEARCH).** The DIII–D facility is equipped with a versatile cryogenic pellet injection system for shallow and deep plasma core fueling that is capable of simultaneous operation with three independent repeating gas guns. In its present configuration [1.8 mm, 2.7 mm (2) at a repetition rate 10 Hz], particle throughput is well matched to the DIII–D divertor pumping capability allowing DIII–D to investigate advanced particle control schemes. To date, this injector has been used to deliver (1) deuterium pellets at high throughput for transport and density limit studies and (2) high  $Z$  “killer pellets” (neon, methane, argon, etc.) for investigating ways to induce a fast current quench during vertical displacement events. A separate lithium pellet injector is also available for edge plasma modification and wall conditioning.

Several straightforward modifications/additions to the present injector system are proposed to support the DIII–D Advanced Tokamak Program and the long pulse upgrade. These include:

1. Reconfiguration to allow for both high field and low field side and top launch.
2. Installation of three higher volume extruders which would allow 10 s pulse operation (up from 3 s) at present or slightly higher throughputs. In addition, the data acquisition system will be

upgraded to accommodate the longer pulse operation and a Roots blower will be incorporated in the injection line vacuum system to cope with the higher gas load.

3. Fabrication of a new chambering mechanism to convert one of the present 2.7 mm guns to 1.8 mm. This will result in a two fold increase in the delivery rate (up to 20 Hz) during simultaneous operation of two guns. This is required to increase the throughput to allow higher density operation under shallow fueling conditions (the smaller pellets have less range and lower mass content than the 2.7 mm guns).
4. An addition to one existing gun of a repeating two stage light gas driver for higher speed operation (for deeper or advanced fueling scenarios). An injector similar to that used on DIII-D has been operated at ORNL in collaboration with ENEA/Frascati) at 2.5 km/s and 1 Hz after such a modification. The higher velocity capability will provide DIII-D with the option of exploring deep fueling for control of the density profile shape.
5. In addition to the above proposed modifications to the present injector system, a new low cost in situ condensation type injector is proposed which would serve as a dedicated injector for disruption mitigation studies. A two-shot injector is envisioned that would be capable of deuterium, high Z and mixed gas operation. The addition of this system would free up the existing injector for fueling studies.

#### 2.5.4.3. THE PROFILE CONTROL SYSTEM INITIATIVE (TOKAMAK RESEARCH)

**Motivation.** Elongated divertor tokamaks, and those implementing advanced tokamak scenarios in particular, require feedback control of the discharge parameters in order to optimize performance and reproducibility. The DIII-D tokamak presently utilizes detailed control of the discharge shape, plasma density, and total current on a routine basis and specialized control, such as for total stored energy, radiation, or rf loading resistance, is added for some experiments.

In discharges with a high performance core, the local discharge parameter profiles become more important. The local pressure gradient can easily approach MHD stability limits. The pressure profile is strongly influenced by the input power profile and the thermal transport profile. The thermal transport is influenced by the electric field profile and thus by the rotation profile, momentum input and, through ion force balance, by the pressure profile. Stability and transport are both influenced by the current profile and the current profile is partially determined by the pressure profile. Thus, the tokamak core can be viewed as part of a complex feedback loop that must be controlled in order to optimize the discharge performance.

Feedback control involves using diagnostic measurements to calculate discharge parameter profiles, comparison to the required profiles, and use of actuators to change the profiles to correct any error. In order to improve the ability to control the DIII-D discharge parameter profiles, both new actuators and improvements in the plasma control system are required. New actuators such as ECH, rf power, nonaxisymmetric

coils, and counter-injection neutral beam are described elsewhere. Here we describe the approach for improving the plasma control system.

**Implementation.** With the present DIII-D Plasma Control System (PCS) we have demonstrated the use of multiple digital processors to acquire and process diagnostic data and provide commands to the tokamak systems such as power supplies, gas valves, neutral beams, and rf transmitters. The algorithms used for evaluation of the diagnostic data include a real-time equilibrium reconstruction technique. The present system has been used primarily to control global parameters such as discharge shape.

To improve the system to give it the capability for profile control we will expand its computing and data acquisition capacity. Hardware will be installed to allow real-time acquisition of ion temperature and electron temperature and density profile data from the CER, Thomson scattering, and ECE diagnostics. The system presently acquires data from 16 MSE channels; this will be expanded to acquire all 35 MSE channels. These new data will be the basis for determining pressure, current, and electric field profiles in real time.

Improved, more computationally intensive algorithms will be required for parameter profile calculations. The basis will be the present real-time EFIT algorithm which implements a subset of the functions in the standard EFIT code used for off-line analysis. The capability to include the profile diagnostic data in the equilibrium reconstruction will be added to the real-time algorithm.

This more capable real-time equilibrium reconstruction algorithm will require a significant increase in the computing capacity of the plasma control system. The present control system uses digital processors which were state-of-the-art in 1990. The continual rapid increase in the speed of commercially available microprocessors has resulted in processors that will make possible the required improvements in the real-time equilibrium reconstruction algorithm. It appears that processors, approximately 50 times faster than those presently used in the PCS, are available. We plan to modify the present architecture of the PCS so that it will be possible to easily incorporate the latest high speed processors as they become available, and as demands of the real-time algorithms evolve.

Expanded capability to implement control algorithms must be accompanied by new capability to modify plasma parameters with the available actuators. Development of control algorithms will parallel the development in the physics research program of the understanding of how to modify the tokamak parameter profiles to achieve the desired performance. Modeling codes such as CORSICA will be used to both understand the tokamak physics and to develop and model control algorithms. These off-line tools will be used in combination with the real-time data acquisition and computation hardware to provide the required profile control capability.

## 2.5.5. DIAGNOSTIC SYSTEMS (TOKAMAK RESEARCH)

**2.5.5.1. PRESENT STATUS OF DIAGNOSTIC SYSTEMS.** The DIII-D plasma diagnostic set is made up of more than 50 instruments built and operated by the DIII-D National Program. This ensemble of instruments is the most complete of any tokamak in the world and routinely produces the high quality data required to fuel the DIII-D Scientific Research Program. The DIII-D diagnostics set includes extensive divertor and edge measurement capability, plasma core profile measurements of density, temperature and plasma current and a large suite of fluctuation diagnostics. A complete list of the diagnostic systems installed on DIII-D and the measurements that they make is shown in Table 2.5–4.

**2.5.5.2. DIAGNOSTIC SYSTEM UPGRADES.** There are additions and upgrades to the diagnostics that will have a large pay-back in terms of the scientific output of the DIII-D Research Program. These additions are motivated by new areas of research requiring either new measurement capability or changes in the DIII-D machine hardware, or in some limited number of cases such as the core Thomson scattering diagnostic, to fill in gaps in our existing measurement capability. In addition to the diagnostic improvements described in this section, we expect to implement other unforeseen diagnostics or improvements during the five-year span of this plan.

**Radiative Divertor Diagnostics.** Our strategy for diagnosing the divertor region in DIII-D is to concentrate most of our resources in the lower divertor. There is a large investment in the diagnostic systems already installed in the lower divertor and maintaining that extensive capability is a prime consideration in our planning. Consequently, a limited number of diagnostics will be installed for use on the upper RDP. During the installation of the upper, inner portion of the RDP in fall of 1999, a minimal set of diagnostics listed in Table 2.5–5 will be installed with the aim of measurements to control the diverted plasma shape and pumping speed. Later in the five-year plan, the lower divertor will be replaced with an RDP structure. In order to maintain the measurement capability in that region, significant diagnostic modifications will be required. A list of those changes is shown in Table 2.5–6. The new configuration does not lend itself to the use of Thomson scattering for electron temperature measurements. Thus, the present divertor Thomson System will be used to benchmark a variety of spectroscopic techniques for diagnosing local plasma parameters; these techniques include: (1) determination of  $n_e$  from Stark broadening transitions arising from high  $n$  levels, (2) determination of  $T_e$  from line ratios, and (3) discrimination of ionizing plasmas from recombining ones by means of Balmer series line ratios in deuterium. Maturation of these techniques is essential for reliable diagnosis of plasma parameters in the slot divertor. The spectroscopic techniques listed above are the same ones on which ITER will most likely rely as a consequence of the difficulties its high neutron flux imposes on line-of-sight diagnostics. RF reflectometry or interferometry and a new insertion path for the fast reciprocating probe are additional measures under consideration for help in replacing the loss of the Thomson scattering data in the divertor. An essential part of the plan will be a large software effort to automate the analysis of data from the spectroscopic diagnostics above, so that processed information will be available to the whole scientific staff for a large number of discharges and discharge times, as is the case with DIII-D's sophisticated Thomson Scattering Systems. The development of a reliable spectroscopic determination of critical plasma parameters in the divertor will be a major program element.

**TABLE 2.5-4**  
**DIAGNOSTIC SYSTEMS INSTALLED ON DIII-D**

<b>Electron Temperature and Density</b>	
Multipulse Thomson scattering	8 lasers, 40 radial points
ECE Fourier transform spectrometer	Horizontal midplane profiles
ECE radiometer	Horizontal midplane
Multichannel vibration compensated (infrared) interferometer	3 vertical chords, 1 radial chord
Microwave reflectometer	Midplane edge profiles
<b>Ion Temperature and Velocity</b>	
Charge exchange recombination spectroscopy	16 vertical channels; 16 horizontal channels; 3 mm edge resolution
<b>Core Impurity Concentration</b>	
VUV survey spectrometer (SPRED dual range)	Radial midplane view
Visible Bremsstrahlung array	Radial profile at midplane, 16 channels
<b>Radiated Power</b>	
Bolometer arrays	2 poloidal arrays, 48 channels each
<b>Divertor Diagnostics</b>	
Visible spectrometer	7 channels
VUV survey spectrometer (SPRED)	Vertical view along outer divertor leg
Tangential TV (visible)	2-D image of lower divertor
Tangential TV (VUV)	2-D image of lower divertor
Infrared cameras	5 cameras
Graphite foil bolometers	12 locations
Fast neutral pressure gauges	4 locations in divertors
Penning gauges	Under divertor baffle
Baratron gauge	Under divertor baffle
Langmuir probes	18 radially across lower floor, 2 upper divertor throat
Moveable Langmuir probe	Scannable through lower divertor outer leg
Tile current monitors	Radial and toroidal arrays
Reflectometer	Vertical view through X-point
<b>Magnetic Properties</b>	
Rogowski loops	3 toroidal locations
Voltage loops	41 poloidal locations and 30 saddle loops
$B_\theta$ loops	2 × 29 in poloidal arrays
Diamagnetic loops	9 toroidal locations
<b>Plasma Edge/Wall</b>	
Plasma TV	4 cameras, radial view, rf antennae
IR camera	Inside wall and coiling views
Visible filter scopes	16 locations
Moveable Langmuir probe	Scannable across outer midplane

TABLE 2.5–4 (CONTINUED)

<b>Fluctuations/Wave Activities</b>	
Microwave reflectometers	2 radial systems
Far infrared scattering	Radial view
Infrared scattering	Vertical view
Mirnov coils	Toroidal, poloidal, and radial arrays
Li beam injector	Radial beam with 16 channel tangential viewing channels
X-ray imaging system	100 channels, 5 arrays
RF probes	10 probes in poloidal array, 10 probes in toroidal array, 1 launch antenna
<b>Fast Ion Diagnostics</b>	
Neutral particle analyzer	Scannable horizontal view, 3 vertical views
Fast neutron scintillation counters	2 radial channels
Fusion products probe	1 new midplane probe
<b>Plasma Current Profiles</b>	
Motional Stark polarimeter	35 channels, 2 radial arrays
Nonthermal Electron Distribution	
Soft x-ray pulse height spectrometer	1 scannable radial view
ECE Michelson spectrometer	1 vertical view
<b>Miscellaneous</b>	
Neutron detectors	3 toroidal locations
Hard x-ray monitors	2 toroidal locations
Synchrotron (IR) radiation detector	2 tangential chords on midplane
Torus pressure gauges	
Residual gas analyzer	

TABLE 2.5–5  
UPPER DIVERTOR DIAGNOSTIC ADDITIONS

<b>Diagnostic</b>	<b>Institution</b>	<b>Comment</b>
Power loss measurements		
Under-baffle, 4-ch bolo arrays	LLNL	Copy lower
Reflectometer or interferometer	UCLA	New or copy of lower
Partial pressure in plenums with fast pressure gauges	ORNL/GA	New diagnostic
Magnetic probes on the baffles	PPPL/GA	

TABLE 2.5–6  
LOWER DIVERTOR DIAGNOSTIC MODIFICATIONS

Diagnostic	Institution	Comment
Power loss measurements		
Vertical IR TVs	LLNL	Re-aim
Foil bolometers	GA	New
Under-baffle, 4-ch bolo arrays	LLNL, GA	New
Filtered line monitors ( $D_{\alpha}$ , etc.)	ORNL	Re-aim
Fast pressure gauges (inner and outer plenums, private flux)	ORNL	3 new (out of 5 total)
Magnetic probes on baffles	GA	New in lower
Fixed Langmuir probes	SNL, UCSD	Rebuild probe tips, upper and lower
Tangential TV imaging, visible	LLNL	Relocate
Vertical TV camera, visible	GA	Re-aim
EUV SPRED (10-160 nm)	LLNL, PPPL	Re-aim
Visible survey spectrometer	ORNL, GA	New fibers, upper
High resolution, visible spectrometer	ORNL, GA	
Vertical viewchords		New fibers, upper
Toroidal viewchords (for flow velocity)		Relocate
RF reflectometers (3 ch)	UCLA	New
Multilayer mirror spec.	JHU	New

**Plasma Control Diagnostics.** The AT Program relies to a large extent on the ability to control the pressure, current and  $E_r$  profiles. The diagnostics required to generate control signals for this task largely exist on DIII-D, however there are improvements to those diagnostics that are needed to fully implement the Plasma Control Program. The temperature and density profiles generated from the Thomson scattering diagnostic can be used for real-time plasma control with some changes to the Thomson scattering data acquisition system. The biggest improvement in the diagnostic systems in the area of plasma control is an upgrade to the MSE diagnostic to generate real-time  $E_r$  profiles, and to permit accurate real-time identification of the current profile in the presence of large radial electric fields typical in AT discharges.

When viewing a co- and counter-injected neutral beam simultaneously with two separate MSE systems the radial electric field  $E_r$  can be determined with good spatial and temporal resolution. The  $E_r$  field can easily be extracted from the raw MSE pitch angle data and could be used as a real-time feedback signal for control of  $E_r$ . In the present DIII-D system, all beams are co-injected, however, a direct measurement of  $E_r$  is achieved using the original tangential viewing array combined with a new radial viewing array of a single beam line. The addition of a counter-beam on DIII-D and use of a simultaneous view of co- and counter-beamlines would produce superior spatial resolution compared to the combined radial

and tangential view of a single beamline (10 to 25 cm). The simultaneous view also provides the maximum sensitivity of the measurement to  $E_r$ .

The direct measurement of  $E_r$  is demonstrated in Fig. 2.5–14 for a recent discharge using the new MSE system. In Fig. 2.5–14(c), the effective vertical field (assuming  $E_r = 0$ ) is plotted for a tangential chord (solid line) and a radial chord (dashed line) at a radius of  $R \sim 2$  m. If  $E_r$  were zero, then these two curves would track one another. The separation of the two curves during the ELM-free period from 2 to 2.25 s is an indication of the buildup of radial electric field.  $E_r$  is calculated directly from the MSE measurements as shown in Fig. 2.5–14(d). The temporal evolution of  $E_r$  follows closely the time evolution of the plasma toroidal rotation in Fig. 2.5–14(e) obtained from charge-exchange measurements of carbon impurities. The maximum time response of the MSE  $E_r$  measurement is 1 ms with an RMS noise resolution of  $\sim 7$  kV/m. The curve in Fig. 2.5–14(c) was generated using a 5 ms sliding boxcar average giving somewhat better resolution. Possible systematic errors in  $E_r$  due to spatial averaging in the radial chords and calibration are a factor of 2–3 larger than uncertainties due to noise.

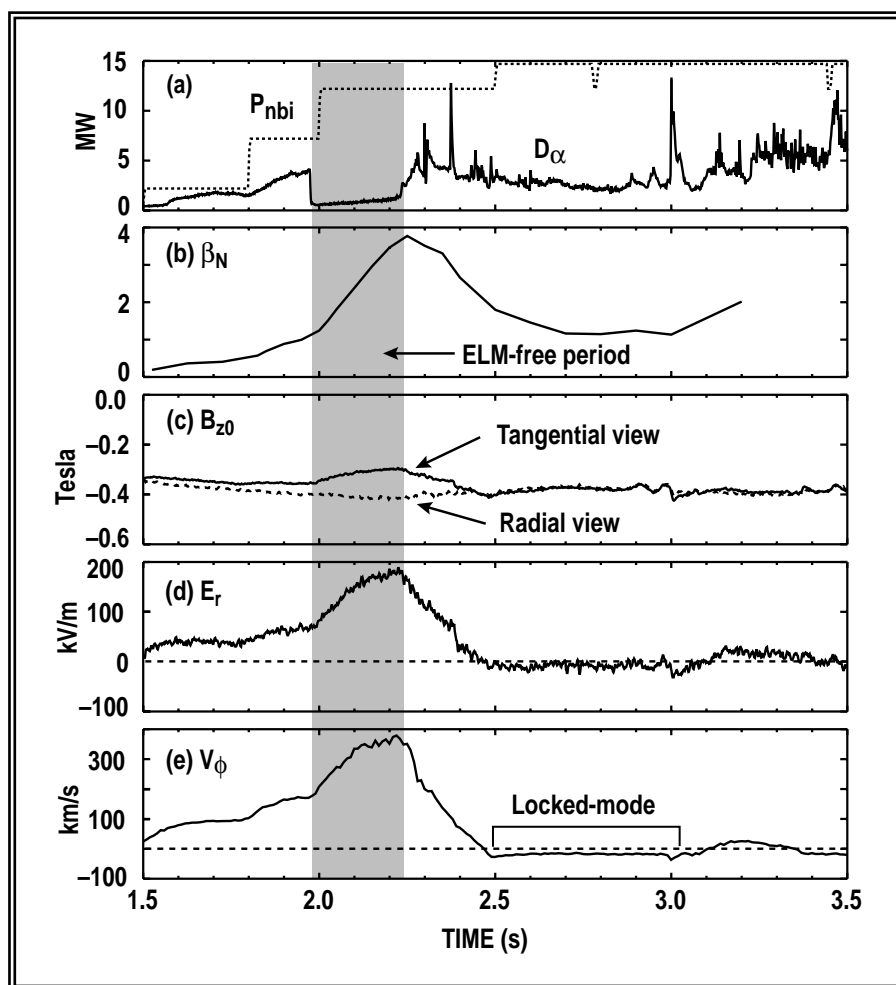


Fig. 2.5–14. The new MSE system features a tangential and radial view of a single beam line.

The use of MSE for measuring the radial electric field has been demonstrated; using this technique for a real-time feedback measurement of  $E_r$  could be accomplished by adding the new MSE channels to the plasma control system data acquisition system. The addition of the counter neutral beam and the MSE channels to view the counter neutral beam would substantially improve the spatial resolution of the  $E_r$  measurement and the current profile when a large  $E_r$  is present.

**Electron Transport Diagnostics.** The physics role and need for electron transport diagnostics is described in Section 2.3.1, but, in brief, the remaining challenge in understanding core turbulence and transport in fusion plasmas is determining what mechanisms are responsible for anomalous electron transport and how electron transport can be controlled. In order to address this electron transport issue, new diagnostic measurement capabilities are required. At present, only relatively low wavenumber (long wavelength) density turbulence is measured in the core of DIII-D, using far infrared (FIR) scattering, beta emission spectroscopy diagnostic (BES), and reflectometer systems. However, several other mechanisms such as short wavelength turbulence, or magnetic turbulence may be responsible for the anomalous electron transport. To further understand these possible transport mechanisms we will expand the turbulence diagnostic coverage as follows:

- Search for and measure electron mode turbulence using a scattering system specifically modified for the purpose. Theoretically predicted electron mode turbulence (such as  $\eta_e$  modes) have wavelength 20–60 times shorter than that responsible for ion transport.
- Measure core magnetic turbulence using a cross-polarization scattering system, as on Tore Supra, or using enhanced scattering at the upper hybrid layer as proposed by Russian and Dutch groups.
- Measure core electron temperature fluctuations using a correlation ECE radiometer system. Temperature fluctuations are directly related to heat transport, while density fluctuations are more directly related to particle transport.
- Improve the central density fluctuations measurements by upgrading the phase contrast imaging diagnostic by adding a central viewing set of sightlines.

It should be noted that in addition to their role in the search for electron transport mechanisms, these diagnostics will also generally enhance our physics measurement capability. For example, a magnetic turbulence diagnostic will allow us to address the long unresolved issue of the relative importance of electrostatic and magnetic turbulence in core transport. More detailed descriptions of the three new diagnostics follow.

**Study of Small-Scale Turbulence Via Scattering.** Turbulent structures with wavelengths approaching the ion gyroradius can be measured using coherent scattering, but are far too small for core turbulence measurement techniques based on multiple point correlation analysis. Therefore, we propose to reconfigure the current FIR scattering system (which currently probes larger structure turbulence at small scattering angles) to allow short wavelength density fluctuations to be detected. A number of technical issues such as

the specific scattering geometry optimum for use in DIII-D, effects of  $E \times B$  convection and Doppler shifts, and wavenumber resolution must be solved in a developmental effort. The availability of an existing collective scattering system on DIII-D offers a cost-effective opportunity to resolve this issue.

**Magnetic Field Fluctuation Measurements.** Recent work on Tore Supra, using mode conversion scattering, has suggested that such fluctuations may prove important in explaining the anomalous electron channel. However, many concerns continue to exist related to the diagnostic technique of cross polarization scattering in a fusion plasma and the specifics of the Tore Supra work. It is anticipated that these will be resolved during the proposed plan period, and that installation of a magnetic field fluctuation diagnostic on DIII-D will take place in around three years. Such a system will require an inside launch and an outside receive capability, a combination which does not currently exist on DIII-D. The major developmental issue will, therefore, initially focus on establishing such a launch/receive arrangement and determining the details of antenna design and associated plasma facing components. The feasibility of applying a second magnetic scattering technique utilizing enhanced scattering from the upper hybrid layer will also be evaluated.

**Measurement of Turbulent Temperature Fluctuations.** Electron temperature fluctuations can be measured using correlation electron cyclotron emission (ECE) radiometer systems. However, the field of view of the current ECE system utilized for electron temperature measurements is not suitable for fluctuation studies as the wavenumber sensitivity is too limited. Consequently, for fluctuation measurements a new optimized antenna system is required so as to obtain the desired wavenumber sensitivity. Installation of a new optimized system on DIII-D should be complete within the year, as well as development of the required data acquisition and software analysis routines.

It is anticipated that diagnostic development aspects of this work will be supported through the UCLA Advanced Diagnostic Development Program, in addition to DIII-D Program support.

**Central Thomson Scattering.** The multipoint, multilaser Thomson Scattering System that currently operates on DIII-D has been a critical diagnostic for the Research Program on DIII-D. The detailed temperature and density profiles routinely produced by the Thomson scattering diagnostic are essential to the scientific progress of the Research Program on DIII-D. The Thomson scattering diagnostic uses a vertical laser beam path. Due to vertical port locations the laser beam does not pass through the center of most discharges and typically provides data from about 0.25 of the minor radius outward. The Central Thomson Upgrade will allow Thomson scattering measurements to be extended from  $R = 194$  cm to the magnetic axis at  $R = 165$  cm covering the center of essentially all of the discharges made in DIII-D. This extension is critical for such diverse areas as: (1) core transport analysis and stability in pressure peaked discharges, (2) modeling of current profile evolution and  $q_0$  control algorithms, (3) modeling of high performance discharges, and (4) high density experiments.

**3-D Equilibrium Reconstructions.** MHD instabilities play a major role in limiting plasma performance and in catastrophic disruptions. Both theory and simulations suggest that the degradation of the plasma

performance and plasma disruptions are due to the growth of magnetic islands driven by these MHD instabilities. The development of a systematic technique, and tools to experimentally reconstruct the magnetic island structures, is crucial to improve the understanding and subsequent control of these instabilities. 2-D equilibrium reconstructions have been extremely useful in the studies of instabilities, however many of the catastrophic instabilities driven by static error fields, mode locking, or a resistive wall are nonrotating or rotate slowly and do not lend themselves to 2-D analysis. This task is to extend the 2-D reconstruction to 3-D reconstructions by modeling the distortions of the magnetic surfaces and growth of magnetic islands in three dimensions using an extended set of toroidally displaced diagnostic measurements. The task consists of two main elements: (1) construction of the extended set of diagnostics, and (2) the code development required to produce the 3-D reconstructions. The code development is an extension of the EFIT 2-D reconstruction currently used on DIII-D.

The diagnostic requirements center around making measurements of poloidal and toroidal distortion of the magnetic surfaces both at the surface of the plasma and internal to the plasma. Many instabilities of interest have low toroidal mode numbers ( $2/1, 3/2$ ) and this allows us to reduce the requirements on the toroidal resolution of the diagnostics. There are four diagnostics that can play an important role in providing this information: magnetics, ECE, x-ray arrays and MSE. A limited number of additional poloidal arrays at new toroidal locations of each of these diagnostics can be used to reconstruct the  $2/1, 3/2$  and possible higher distortions in the plasma. Other diagnostics that will be considered are a tangential viewing x-ray system for improved resolution of high  $m, n$  modes and improved spatial resolution BES.

The magnetic diagnostics can play by far the most important role due to the relative ease of installing large numbers of sensors. The addition of four poloidal arrays of 24 measurements (12  $B_\theta$  and 12  $B_r$ ) each separated by 90 deg poloidally would allow the reconstruction of modes up to  $n=3$  and  $m=7$ . The ECE and x-ray arrays would provide internal measurements of  $T_e$  and x-ray emission (x-ray emission is a function of impurity concentrations, electron density and temperature). If we assume that these parameters are constant on flux surfaces, then the measurements can be used to determine the internal magnetic structure. An additional toroidally displaced ECE system will be installed and the existing toroidal array of x-ray detectors could be upgraded with additional detectors. Finally, assuming the addition of the counter neutral beam injector a new MSE diagnostic could be installed giving information on distortions in the current profile.

**Current Profile Measurements at High Densities.** The MSE System is a very effective tool for current profile measurements at moderate densities. However, in DIII-D at densities approaching  $1.5 \times 10^{14} \text{ cm}^{-3}$ , strong attenuation of the diagnostic neutral beam makes measurement of current profile in the inner half of the plasma impractical. In ITER, because of the larger size of the device, this problem can be even more severe unless high intensity neutral beams with energies  $>500 \text{ keV}$  are developed. We propose to develop a new current profile diagnostic system that uses a sub-millimeter laser instead of a neutral beam for probing the plasma. The new concept is based on the well known Fizeau effect and uses a new interferometer concept which is the key for making this measurement possible.

The system measures the line integral of current density, in contrast to the MSE which measures the poloidal component of the magnetic field. This system is therefore, most sensitive near the magnetic axis of the plasmas. For the DIII-D applications, the proposed system would be complementary to the existing MSE System. For future devices, a complete profile system based on this concept could conceivably be installed. We propose a two-phase development plan for the system. In the first phase, we would design and install a single channel system. Once the behavior of the system is well documented, we would proceed to the second phase where we would install an array of four to five channels to unfold the current profile in the inner half of the plasma.

The Fizeau effect is a well-known phenomenon causing a small phase shift of an electromagnetic wave traveling through a moving dielectric medium. This phase shift is of the order of  $V_D/c$  of the normal phase for a stationary medium, where  $V_D$  is the drift speed of the medium and  $c$  is the velocity of light in vacuum.

A practical problem with the measurement of the current density dependent term is its small value compared to the phase shift for a stationary medium, since small changes in geometry or plasma density result in far more phase shift than that due to plasma motion. As a result in tokamaks with standard interferometers, measurement of the first order term is impractical. This difficulty is overcome with the interferometer arrangement shown in Fig. 2.5–15. In the arrangement shown the reciprocity theorem guarantees perfect cancellation of the zero order term, while the contribution due to the motion of the medium is doubled.

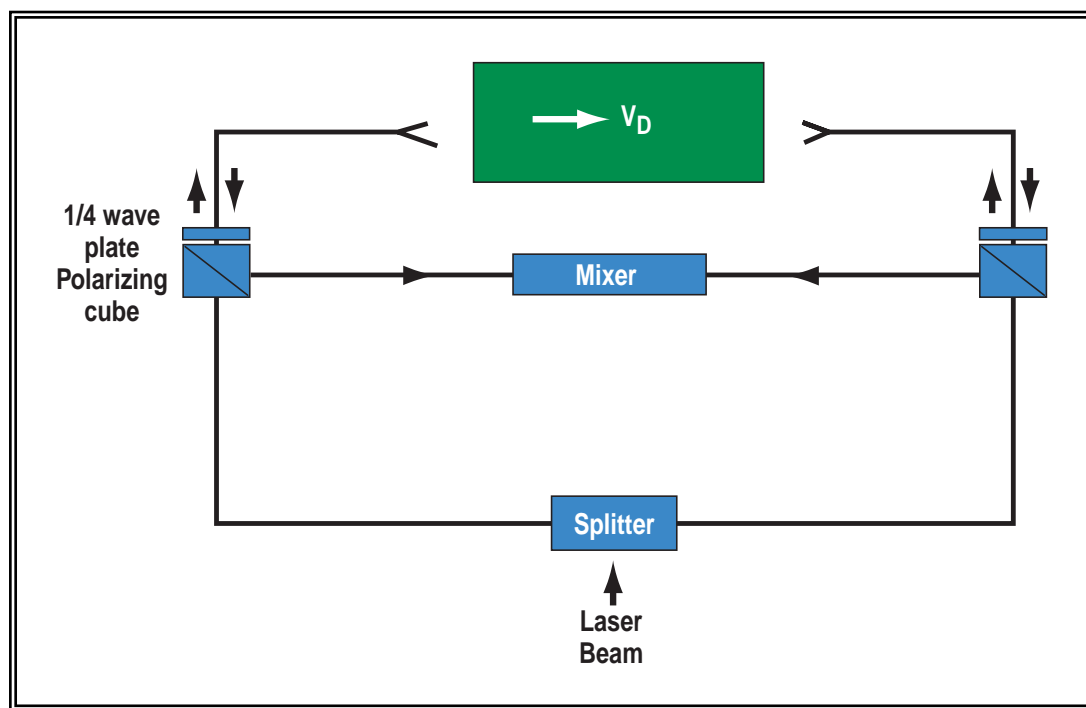


Fig. 2.5–15. New interferometer concept overcomes the difficulty with measurement of the first order term.

**Laser Pumping to Improve Beam Emission Spectroscopy Diagnostics.** Two key diagnostics on DIII-D would be significantly improved by using laser pumping to affect the population of the  $n=3$  level in the neutrals injected by the neutral beam injectors. The BES could achieve an improvement in signal to noise by about a factor of six through this technique, shortening the minimum time resolution by the same factor. Data analysis for the CER System could be greatly eased by using the same laser pumping to modulate the charge exchange signal. These improvements in the diagnostics would be beneficial in the study of plasma transport processes.

The basic idea of using laser pumping to improve the BES signal was invented by Fonck at the University of Wisconsin. The fundamental concept uses a laser, tuned to the 656.3 nm transition between the  $n=2$  and  $n=3$  levels of deuterium to illuminate the region being examined and thus increase the population of the  $n=3$  state. The signal that the BES System detects is due to spontaneous emission from  $n=3$  to  $n=2$ . At readily achievable laser intensities, it is possible to saturate the transition, making the population of the  $n=3$  and  $n=2$  states equal. Since the  $n=2$  state population in the absence of the laser is significantly larger than the  $n=3$  state population, this results in an appreciable enhancement of the BES signal. A proof of principle test of this technique is being pursued as part of the work that the University of Wisconsin collaborators is doing at DIII-D. If it is successful, further development would be required to apply this technique to all the BES channels.

BES is a key diagnostic for measuring density fluctuations in the plasma. The time resolution of this measurement at present is typically hundreds of milliseconds at present, owing to insufficient signal. Even so, significant changes in plasma turbulence have been measured. However, other diagnostics, for example FIR scattering, suggest that the turbulence can change even faster. (FIR scattering has excellent time resolution but poor spatial resolution.) If this laser pumping scheme is successful, the minimum time resolution for the BES System could be decreased by about a factor of six, which would be quite significant.

The CER System is used for a number of measurements on DIII-D: ion temperature, poloidal and toroidal rotation, impurity density, and radial electric field. Analysis of the data is difficult owing to the complexity of the spectra. One way to greatly simplify the analysis is to modulate the charge exchange signal and subtract the spectra taken with the modulation off from the spectra taken with the modulation on. Such modulation of the signal has been done, for example, by modulating the neutral beams. However, because of equipment limitations, such modulation tends to be slow (50 to 100 Hz) and it is frequently the case that the plasma changes during this time. This makes time slice subtraction ineffective, since the interfering lines in the spectra have also changed. In cases where the subtraction is successful, analysis of the resulting CER spectrum is trivial, because it consists of a single Gaussian peak. Laser pumping would allow much more rapid modulation, decreasing the plasma changes occurring between the CER measurement and the background measurement thus improving the effectiveness of the background subtraction.

By using laser pumping of the population of the higher  $n$  levels of the deuterium in the neutral beam, the charge exchange signal can also be modulated, since the cross sections increase rapidly with  $n$  level. In the case of the CER measurement, either resonant pumping of the  $n=2$  to  $n=3$  transition or photo ionization of the levels with  $n=2$  and greater could be used to effect the modulation. In the one case, the charge exchange signal would increase, in the second it would decrease. Since the photo ionization technique affects more levels, it would probably have the larger amplitude; however, it may require significantly greater laser power. We intend to assess both techniques and develop the best.

**Diagnostic Neutral Beam.** There are three diagnostics which could be significantly improved by a diagnostic neutral beam. The MSE diagnostic measures the field line pitch angle from which the plasma current profile is calculated and the radial electric field  $E_r$  in the plasma. A diagnostic neutral beam directed counter to the plasma current would significantly improve the real-time  $E_r$  measurement and the plasma current profile measurement. The CER System is used to measure ion temperature, poloidal and toroidal rotation, impurity density, and  $E_r$ . A diagnostic beam, capable of being operated at a higher beam modulation rate and higher beam power density with a smaller diameter beam, would increase the CER signal and improve spatial resolution. The improvement in signal to noise ratio is of particular importance at the core of the plasma where beam attenuation now limits the accuracy of the measurement. The BES diagnostic would benefit from a diagnostic beam with higher power density to improve time resolution, and its measurement might, based on theoretical estimates, be improved by use of a helium diagnostic neutral beam.

**The Impact of the Long Pulse Upgrade on Diagnostics.** The ten second current flattop planned for DIII-D during the Five-Year Plan period will primarily affect the various diagnostics data acquisition systems. The changes and additions to the Data Acquisition Systems are straightforward. Some diagnostics will require additional digital memory, or new digitizers and/or computers to fully take advantage of the longer plasma pulse.

## 2.5.6. CONTROL, DATA ACQUISITION AND ANALYSIS SYSTEMS (TOKAMAK RESEARCH)

The DIII-D tokamak is a national and international fusion research facility. The extraction of data from the experiment, the production of results through data analysis, and the dissemination of information to national and international researchers involves computer systems and programming at all levels. This section outlines what is needed in the area of computer systems, programming, and user support in order to effectively accomplish the goals of the experimental facility and the researchers over the next five years.

These system requirements are divided into two broad areas: (1) hardware systems (including CAMAC, CPUs, networks, storage systems) and associated system software needs; and (2) analysis software (including databases, user interfaces, analysis/visualization codes).

### 2.5.6.1. HARDWARE SYSTEMS: STATUS, FUTURE NEEDS, AND UPGRADES

**General Considerations.** One of the significant aspects of DIII-D is the production of large quantities of data. In FY96, 430 GB of raw data were acquired, with the largest single shot being 190 MB. The data rate is expected to increase about 40%/year due to participation of more collaborators, more diagnostics, more operation and longer pulses. Based on past history, it is expected that within five years the size of a shot will be 400-500 MB, and that over the course of the next five years, 4-5 TB of raw data will be acquired. The ability to handle and analyze these quantities of data will require order of magnitude increases in the capabilities of the computer hardware supporting the experiment. History also indicates that new hardware will be available to help meet this challenge.

Another significant aspect of the DIII-D Program is that as a national facility, the number of collaborators on-site and at remote sites are expected to increase considerably. This, in turn, will create large increases in the demand for network bandwidth. Currently most of the networking within the DIII-D site is Ethernet operating at a rate of 10 Mb/s. In order to handle the increased networking over the next five years, the network must be upgraded to a minimum of 100 Mb/s.

Historically, there was a clear division between the real-time experimental systems used for data collection and the systems for general users and long term data analysis. The modern networked distributed environment of computers has completely blurred this division. Even the general purpose computers have become necessary to the running of the experiment, as well as later data analysis. An even further blurring of functional division is in the desktop computer area. Systems once used only for word processing and spreadsheets are now being used for data analysis and collection. The computer systems will, however, be divided for purposes of this discussion into those systems directly tied to experimental control and data acquisition, and those systems used for analyzing data from the experiment.

**Control and Data Acquisition Systems.** The computer systems required for running and diagnosing DIII-D can be divided into: (1) the tokamak control system, (2) neutral beam control systems, (3) the

plasma control system, (4) general purpose data acquisition systems, and (5) data acquisition systems for specific diagnostics. Over the past three years, items 1–3 have been upgraded to modern UNIX platforms, and near-term upgrades are not anticipated. Further development of the plasma control system is discussed in another section.

The general purpose data acquisition system with one CAMAC highway has been expanded with a second CAMAC highway to accelerate data acquisition. Still it is clear that with the ever increasing quantities of data, a second data acquisition system will soon need to be added. This could be either a clone of the existing system or possibly a new system altogether. Two systems with two CAMAC highways each should be sufficient for the next five years.

Data is also collected from a number of diagnostics; e.g., pellet injector, Langmuir probe, lithium beam, Thomson scattering, FIR, SPRED, CER, plasma control system, ICH, and others. New diagnostics will lead to more data handling, new computer systems, accompanying data acquisition hardware, and additional programming personnel.

**Systems for General Users and Data Acquisition.** The general purpose computers of the User Service Center currently used for shot retrieval and data analysis (both real-time and long term), will require considerable upgrades over the next five years. As the number of users increases and the size and complexity of codes increases, more computing power is needed to do analysis. The main central processing unit (CPU) server is frequently saturated during operations. Higher performance CPUs currently exist which can be dropped into place with little impact on operations, and memory can also be doubled from 0.5 GB to 1 GB. Of particular importance is magnetic disk storage for user space, raw shot data space, and calculated results. Storage needs are anticipated to increase an order of magnitude over the next five years.

The shot data space is of particular concern, since the number of shots on-line goes down as the size of the shot goes up. At the same time as the number of physicists increases, there is a desire for more shots on-line. Shot servers based around inexpensive CPUs and disks are being considered. The shot restore system can be augmented through the use of a rewritable optical jukebox storage system. Given the large quantities of data involved, this system should hold 0.5 to 1 TB of data and have expansion capabilities. This jukebox is intended as a large near-line storage facility to migrate the storage of data from the existing VAXS computer to the data servers computer systems.

Of paramount importance to the analysis of DIII-D data is the purchase and implementation of a new commercial database system. In recent years, there has been a proliferation of “private” databases within the DIII-D Program where only a few people know how to access each database. This often leads to an overlap in functions and results, as well as leading to inefficient usage of disk space and scientific staff time. A new database system would provide a flexible, easy to use mechanism for creating databases with standard tools for maintenance and client access from various CPUs. Since this system will contain the bulk of calculated results, the server system will also require a large amount of disk storage (~100 GB) for various types of databases. Section 2.5.6.2 contains further information on the structure of the database.

A number of UNIX workstations of various types are in use for specific purposes (although they may have a number of users). Additional specific workstations will be added as the need arises. One such system would be dedicated to theoretical modeling.

Although the DIII-D Program has mostly moved away from VMS based systems, there is still a need for such a system. The current system will be replaced by one DEC Alpha-VMS System.

**Desktop Computing.** Desktop capability used to mean just word processors, spread sheets, e-mail, and a few other miscellaneous office-type activities. However, desktop computers have become very powerful processors in their own right. They are now more and more being used to do analysis work that only a few years ago would have been done on mainframes and high performance workstations. It is important to begin making use of their capabilities and this power on the desktop. A more integrated environment will need to be developed that can handle Macintoshes (primarily used today), PCs with Windows 95 (more and more desired by the staff), and Windows NT (which is becoming more common in other environments).

**Networking.** It is the network that ties all the computer systems together. As stated previously, an order of magnitude increase in bandwidth just within the DIII-D environment over the next five years will be necessary. Upgrades to higher bandwidth must be coordinated with the GA facility. Another factor not previously mentioned driving the network needs is the increased usage of the World Wide Web, both for internal use, as well as external. The Web will increasingly be used for the dissemination of information about the DIII-D Program for both publication of results and real-time interactions.

**Five-Year Scenario.** The following is a proposed schedule for the next five years.

#### *YEAR 0*

- Add second CAMAC highway for increased data acquisition throughput.
- Add computer system for database server and begin implementation of new database system.
- Begin implementation of shot server/archival system.

#### *YEAR 1*

- Upgrade memory, disk storage, and CPU power of general CPU servers.
- Begin further integration of desktop computers into the "data" environment.

#### *YEAR 2*

- Complete upgrade of network.
- Expand shot server storage and database server storage.
- Add second general data acquisition system to handle more data.

*YEAR 3*

- Upgrade CPU servers again.

*YEAR 4*

- Evaluate control and neutral beam systems for potential upgrades.
- Add second highway to second data acquisition system.

*YEAR 5*

- Begin upgrades of control/beam systems if necessary.

**2.5.6.2. THE DATA ANALYSIS UPGRADE INITIATIVE.** With the decline of magnetic fusion funding, the U.S. Fusion Program is left with fewer experimental facilities. DIII-D and Alcator C-Mod are the two major operating U.S. tokamaks that will be relied upon to produce data and scientific understanding essential for the improvement of the tokamak concept. They have become national user facilities, serving researchers from many institutions, both on-site and off-site. To facilitate this national mode of operation, modernization of the computing environment is needed to provide the ability for remote participation and a distributed data analysis and modeling capability. This requires the following features to be added:

- A common I/O file standard to facilitate data transfer.
- A modern, commercially available data warehousing software to archive and retrieve a variety of data.
- User-friendly tools for code invocation, data visualization, and data transfer.
- Programmable environment for code coupling and continuous improvement of comprehensive simulation capability.

Our upgrade initiative will focus on developing the above capabilities in three major areas: improving access to data, overhauling the DIII-D database, and developing data analysis tools.

**Improve Access to Data.** This is an immediate issue. The problem has been that restoring shot files from tape to disk for analysis can take more than 24 hours if the system is busy, and that the lifetime for keeping a shot on disk is short. The problem of short lifetime on disk has been alleviated by the doubling of disk capacity, and beginning to implement a system for restoring only portions of shots, since usually only a small portion of the shot data is wanted. Section 2.5.6.1 discussed further upgrades for making shot data more available.

**Overhaul the DIII-D Database.** The present “public” database was designed over ten years ago. Many of its functionalities are antiquated, difficult to use, and may even be inappropriate. This led to a significant decline in archived data in this database. Furthermore, it uses S1032 software which is only available on the

VAXes, whereas the trend for computer hardware upgrade is towards UNIX platforms. It is recognized, however, that an easily accessible, comprehensive “public” database is essential to enhance the productivity of the entire DIII-D Group. Hence, the redesign of the DIII-D database is an urgent task that requires immediate attention. Based on needs at present and in the foreseeable future, it appears that a layered structure is most suitable with interconnectivity among layers.

1. The first layer is a broad, but shallow database containing basic information from essentially all DIII-D discharges. This will facilitate surveys and searches of past experiments to find what has been done, to determine trends, to select shots for detailed analysis, and to plan new experiments. It should include a descriptive set of parameters for a discharge, all control room analysis information, and a small number of time slices from each shot to provide some information about time history. Data entry would be automatic and stored in the main computer.

*Proposed upgrade*

- Centralize and automate all control room analysis.
  - Revamp the existing database concept and add desirable functions.
2. The second layer consists of processed (blessed) data, kinetic EFIT, profile data divertor, fluctuations and some analyzed transport data. Such data may be stored in distributed computer platforms, but we need to keep a directory on them and develop the tools to view and extract information.

*Proposed upgrade*

- Design and implement a directory and associated tools.
  - Improve ease of data entry and add comment capability.
  - Where possible automate (or speed up) data reduction procedures for CER, Thomson, magnetics, divertor, etc.
  - Further automate kinetic EFIT and 4D (data display code).
  - Work towards a common format for data entry and examination (self-describing files).
3. The third layer contains highly analyzed, publication quality data. This will serve for publication, for unrestricted outside distribution, and for testing models. All the supporting data files would be included.

*Proposed upgrade*

- Improve ease of data entry and add comment capability.
- Web-based access to this level of data.
- Develop software or protocol for viewing and downloading data.

**Develop Tools for Data Search, Entry/Retrieval, Visualization and Analysis.** The implementation of a new database has to be done in combination with the development of modern tools to facilitate the above functions. We need to improve the user-friendliness of a suite of commonly used analysis codes and physics

modeling codes. We also need to develop remote access for off-site collaborators to analyze DIII-D data with this suite of codes, or their own codes, and to make entry to the DIII-D database.

*Proposed upgrade:*

- Improve tools and procedures for entry and examination of data, and for invocation of codes.
- Develop a common interface for on-site and remote access.
- Assemble a common library of basic tools and routines for getting diagnostic data, mapping and postprocessing calculations.
- Retrofit heavily used analysis and physics application codes to improve connectivity and ease of use. These codes include EFIT, 4D, CER, ONETWO, stability codes, and divertor codes. Collaborator codes may be added.

**2.5.6.3. DISTRIBUTED SITE OPERATION.** Research in fusion energy science continues to involve several collaborative efforts that are national and international in scope. LLNL and GA have pioneered the development of concepts that allow researchers at distant locations to more fully participate in fusion research. These efforts currently support a limited amount of off-site participation in the DIII-D Program, and serve as a prototype for potential future application to ITER remote operations.

Recent modifications to the DIII-D controls and data acquisition system hardware and software have enhanced capabilities for remote access to the experimental facility. Existing network bandwidth supports significant levels of activity in areas critical to remote participation: exchange of newly acquired data and processed results on a time scale comparable to the acquisition rate, ability to operate hardware systems from a remote station, and capability for interactive communications among geographically separated researchers. Local network upgrades acting in concert with ESnet T3 wide area connections allow near real-time transfer of information among researchers and computer systems at the DIII-D and remote sites. Internet-based video conference technology provides views of the control room, and is used to broadcast the morning preoperations meeting and selected meetings critical to the DIII-D Program.

The DIII-D Program is implementing additional technologies and capabilities to support remote use of the facility and facilitate off-site involvement in the U.S. Fusion Science Program. As capability has expanded to include remote control of more complex instrumentation, such as tokamak shape and heating systems, secure access becomes a more critical issue. System modifications are required to increase user authentication security and for authorization to services and hardware during distributed operations. Integration of audio capabilities with operations, additional audio and video channels, and the use of shared computer displays, applications and electronic notebooks will promote more efficient, interactive collaborations. Extending the use of internet audio/video to a wider range of meetings and applications and the use of web technology will provide a means for rapid dissemination of information, thus expanding the physics base for collaborations and enhancing the role of DIII-D as a national facility.

## 2.5.7. FAST WAVE ICRF SYSTEMS (OPTION)

The upgrades for the systems in the ICRF, which are planned for this plan period, will leverage on the existing ICRF equipment. The primary objectives of the upgrades are to increase the pulse length capability of antennas used for fast wave injection on DIII-D, and to increase the power available for heating electrons. Electron heating, as described in previous sections, is useful for enhancing the bootstrap current, improving the current drive efficiency for fast wave or electron cyclotron waves or neutral injection, and for many applications such as effective electron heating during the current ramp to generate plasma configurations with negative magnetic shear. The heating and current drive depends on Landau damping and transit time magnetic pumping, so the heating does not require a resonant magnetic field.

**2.5.7.1. PRESENT STATUS OF FAST WAVE SYSTEMS.** We have three ICRF power sources. A modified FMIT System has a power of 2 MW for at least 10 s over the frequency range 30 to 60 MHz. Two ABB transmitters have rf power of 2 MW for at least 10 s over the range 30 to 55 MHz with power falling off to 0.4 MW at 120 MHz. The FMIT power is coupled to an uncooled four strap antenna which is limited to a 2 s pulse length. The ABB transmitters are connected to water-cooled four strap antennas which can operate for 10 s.

A transmission line configuration more tolerant to variations in plasma-antenna loading is being installed, which is based upon a traveling wave concept. This configuration uses a less efficient coupling factor between the antenna strap and the plasma, which results in a lower perturbation back at the transmitter for any change in plasma edge condition. However, the loss in coupling efficiency is recovered by recirculating the uncoupled power back to the antenna using a resonant ring loop.

**2.5.7.2. UPGRADE TO 8 MW (OPTION).** The water-cooled antenna discussed above can support 4 MW per antenna, so combining both ABB transmitters onto one antenna can free up an antenna. An additional unmodified FMIT transmitter exists at DIII-D and can be upgraded to 2 MW at a fixed frequency of 80 MHz for modest cost. This modification could be performed by PPPL under the DIII-D collaboration, with GA responsible for site modification and installation. In addition, a folded waveguide (FWG) launcher capable of 10 s operation, which was originally built for PBX/TFTR, will be modified for DIII-D by ORNL at modest cost. This unit will be installed and operated at 58 MHz using the existing FMIT unit.

The FWG is presently configured with a flexible feed and a vacuum valve at the vessel interface. This allows for the removal and rotation from fast wave configuration to ion-Bernstein wave, without having to vent the tokamak. However, this assembly is too long to fit on the midplane work platform. Therefore, the option of changing configuration without a vent will be abandoned, and the FWG will be repackaged with a shorter vacuum feed section and no torus isolation valve. A short stroke bellows at the vessel interface will be maintained to allow for some adjustment between the antenna and the outer wall tiles. All of the mechanical rework of the FWG antenna will be carried out by ORNL. The primary work for GA is to make the port available (relocate or remove the UCLA Reflectometer) and to hook up the transmission

line.

Operation at lower frequency, 20–35 MHz, for minority heating or mode conversion current drive will require replacement of the straps on the water-cooled antennas or installation of a combline antenna. Since the existing antennas were of modular construction, this replacement can be accomplished easily. If a frequency below 32 MHz is desired, modification or replacement of the existing transmitter would be required.

There are two options for using a combline antenna to launch fast waves for mode conversion current drive with the physics benefits and disadvantages delineated in Section 2.1.3.4. These two options are a combline antenna either on the inside wall of the DIII-D vacuum vessel, or on the outside wall of the vessel. In general, each combline will need multiple current straps approximately 7.5 cm wide, 1 cm thick, spaced every 15 cm, and 120 cm long. For long pulse operation, the straps would need to be water-cooled and would have similar construction as the water-cooled current straps in the existing antennas. The Faraday shield would not be water-cooled, but would be mounted on water-cooled backing plates. A 12-to 15-strap combline antenna would mount on the inner wall, within the 5.4 cm envelope used by the graphite armor, and would span a 100 to 120-deg midplane sector of the vacuum vessel.

Mounting a combline antenna on the outer wall has different challenges. The straps must be longer and the (175 cm) length of the current straps will not fit in the space between the  $R\pm 1$  ports. In order to reduce the length, additional capacitance at the ends of each strap will have to be included. This can be in the form of lumped capacitance such as vacuum capacitors, or it can be achieved by complex designs of the ends of the current straps. Also the length of the combline will be limited to the space between the 270 deg port and the 300 deg port, since this is the only midplane space available.

## 2.5.8. NEUTRAL BEAM HEATING SYSTEMS

**2.5.8.1. PRESENT STATUS OF THE NBI SYSTEMS.** The DIII-D Neutral Beam Systems consist of four beamlines, and each beamline has two positive ion sources in parallel, focused through a common drift duct. These neutral beam systems were designed for 5 s deuterium beam operation at beam energy of 80 keV with 16 MW of total injected neutral beam power from eight sources. They routinely operate at this level. Improvements in operational technique and in system hardware have led to the routine operation in deuterium at beam power level of 20 MW for 3.5 s. Successful testing and operation of three ion sources at 93 keV deuterium beam energy also leads to the possibility of enhancing system capability to 28 MW. Control and data acquisition computers have recently been upgraded, along with several instrumentation and control systems to improve system functionality, availability, and reliability.

**2.5.8.2. COUNTER BEAMLINE FOR TOROIDAL ROTATION CONTROL (OPTION).** The primary physics base for a counter neutral beamline derives from the need to be able to dynamically influence the plasma rotation during plasma discharges with significant neutral beam heating power. With the present beam configuration on DIII-D, we can have either all co- or, by reversing the plasma current, all counter injection. This means that there is always a one-to-one connection between the heat and particles deposited by the beams and the torque that they produce. A dedicated counter neutral beamline would allow us to break this connection, so that the toroidal rotation could be independently varied.

The existing neutral beamline and tokamak structure does not allow converting from co-injection to counter-injection easily. Rotating the existing beamline counter-clockwise by 39 deg about the injection point will result in a counter-injection symmetric image to the co-injection beamline. Figure 2.5–16 shows the top view drawing of the beamlines and other major DIII-D equipment and diagnostics. Based on the scope of work and costs, the 330 deg beamline is the best candidate for converting to counter-injection beamline. The major tasks include relocating the entire beamline including ion source housing and its stand, rebuilding the beamline drift duct, relocating two machine hall staircases and elevator, and relocating several diagnostics such as CER, MSE, SPRED, and magnetics.

**2.5.8.3. REALIGNMENT OF A BEAM FOR OFF-AXIS INJECTION (OPTION).** We have considered off-axis injection of beams for off-axis neutral beam current drive to control of  $q$  profiles and reduction of central particle fueling from beams. However, the existing toroidal coil makes access to the plasma chamber at a more tangential angle very difficult. Another option for off-axis beam injection is to mask half of the beam (50% beam power) at the ion source between the arc chamber and the accelerator. This will produce a beam with its center almost 30 cm off axis but will reduce the injected power. Injecting beams further away from the axis will require modification of the port on the tokamak vessel and relocation of the toroidal magnetic field coils. We concluded not to consider off-axis injection further.

**2.5.8.4. TANGENTIAL LOW ENERGY BEAM (OPTION).** The physics motivations for a tangential low energy beam injector are: (1) shallow, but nonedge particle fueling dominated by energetic particles, (2) tangential

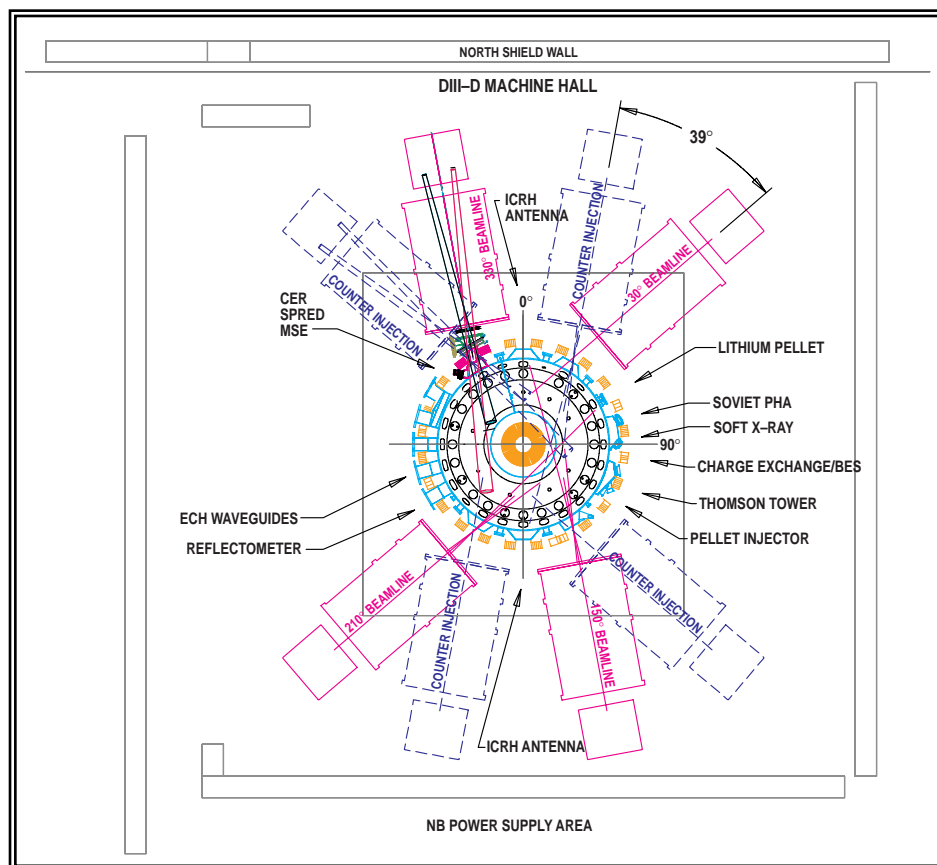


Fig. 2.5–16. Several possible beamline rotation options would allow counter-injection.

edge momentum input to stabilize the resistive wall mode and locked mode, and (3) tangential edge momentum input to develop large  $E \times B$  shear for good confinement. All of these have direct relevance to ITER. The required beam energy and total beam power are 10 to 20 keV and 5 to 10 MW, respectively.

Since for the present beamlines beam power is proportional to (beam energy)<sup>5/2</sup>, very little power is delivered when the beam energy is lowered to 20 keV. Deuterium beam power from a DIII-D ion source will be only about 80 kW at a beam energy of 20 keV, a sharp drop from the 2.5 MW from 80 keV beams. Unless a new class of extreme high perveance (ten times or more than existing sources) ion source is developed, the low energy beam is not a viable option.

**2.5.8.5. DIAGNOSTIC NEUTRAL BEAM (OPTION).** An attractive diagnostic neutral beam should have the following specifications: beam energy between 80 keV or higher, beam cross-sectional area about one-third of the DIII-D beams, beam power density a factor of 2 to 10 higher than the present beam, beam optics comparable to present beams, beam pulse length extended to 10 to 20 s, beam modulation rate as high as 500 Hz with relatively low duty cycles (i.e., low average power), and capable of being operated in helium for long pulse.

Existing neutral beam ion source technology is capable of producing an ion source which will satisfy the above specifications, except the beam power density (present DIII-D ion sources have higher beam power density compared to ion sources employed at other fusion research institutes). Ion source operational techniques for high frequency beam modulation would need to be developed, but it is achievable. In addition to the cost of developing such an ion source, additional cost will be incurred in building the power supply system and the beamline. It is anticipated that many components such as the bending magnets, stripping cell, and gas pumping requirement would be similar to the existing beamlines and thus the beamline will be a substantial undertaking.

## 2.5.9. OTHER UPGRADE OPTIONS

**2.5.9.1. LIQUID JET/KILLER PELLETS SYSTEM (OPTION).** Recent results from DIII-D disruption mitigation experiments indicate that both the high heat flux to the divertor and the large forces due to halo currents during disruptions can be significantly reduced by the use of high-Z impurity pellet injection, often referred to as “killer” pellets. However, the use of these pellets has been shown on DIII-D and other devices to result in the production of runaway electrons. Modeling for ITER indicates that high-Z pellet injection can produce runaway currents up to 15 MA with energies in excess of 10 MeV. To achieve disruption mitigation without the runaway production, it has been proposed to inject a high velocity liquid helium (LHe) jet that would both cool the plasma and raise the density sufficiently to prevent the runaway production. GA has proposed to the ITER and Technology Division of OFES a program to design, build, and install a pulsed liquid helium jet injector on DIII-D, and then to carry out experimental studies of this new plasma termination and disruption mitigation concept. Since the jet is expected to isobarically cool the plasma below 100 eV, this will be followed by the injection of a higher Z impurity pellet to radiate away the thermal and magnetic energy.

Although the technology exists for making continuous high-speed liquid jets in atmospheric conditions, the pulsed mode is a new variant. In addition, initial studies show that for a 20 times increase in the electron density in DIII-D, the jet velocity required for penetration to the magnetic axis is nearly 800 m/s, more than four times the LHe sound speed in the jet of 180 m/s, requiring the development of a new nozzle design.

GA proposes to do liquid jet development and subsequent experiments in collaboration with INEL and ORNL. Simultaneous with this development, vacuum propagation issues will be addressed in a collaborative study conducted at INEL. The liquid jet would be installed on a horizontal midplane port on the DIII-D in order to minimize the distance the jet must traverse in vacuum and to reduce the path length to the plasma core. The existing high time resolution diagnostic set used for present disruption experiments would be augmented with a Kodak Motion Analyzer. This fast framing camera would allow investigation of both the vacuum propagation and the penetration of the jet into the plasma.

While the cryogenic liquid helium jet/killer pellet concept is presently the most developed concept, simulations show that the use of a liquid jet pentaborane or hexaborane is very promising. These low-Z room temperature liquids present the possibility of significantly reducing the system complexity. This would eliminate the cryogenic system and possibly avoid the need for the additional pellet system since the boron would provide the radiation required to dissipate the plasma energy. Presently, the safe handling and manufacturing these liquids present significant obstacles and will need to be addressed in order to pursue this option.

**2.5.9.2. COMPACT TOROID FUELING (OPTION).** Compact toroids are an effective means of depositing fuel in the core of a tokamak without disruptive instabilities. Recent Spheromak-like Compact Toroid (SCT) injection experiments by CCFM/CFFTP on the TdeV tokamak with the CTF injector have demonstrated

core plasma fueling with an accelerated SCT is possible with a low level of impurities. Recent increases in CT density and velocity have been achieved experimentally on RACE at LLNL and continued with the progress achieved on MARAUDER at Air Force Phillips Laboratory. UC Davis has shown repetitive operation using a passively-switched SCT injector that can produce SCTs with sufficient lifetime to transverse a 1.5 m coaxial accelerator followed by 1.5 m of open drift tube resulting in the fueling of a tokamak discharge. The fast gas valve, which initializes the SCT formation, has been demonstrated to be reliable and the saturable cores which provided the necessary time delay between the formation and acceleration sections performed faultlessly for a 1000 consecutive SCTs at a rate of 0.2 Hz.

We propose to monitor the progress of CT fueling in present experiments and in JT-60U. If results and the needs of the U.S. Fusion Program warrant it, we would perform a preliminary study to define the size, velocity, and repetition rate of an injector for DIII-D, with each CT supplying about 10% of the particle content of the confined plasma. Cost will be estimated during the study. As an example of the approximate size of the injector, Fig. 2.5-17 shows a LLNL RACE-scale device.

The study would include both physics analysis of the plasma response, a conceptual design of the injector, and diagnostics to investigate the physics of the CT reconnection and plasma deposition processes. Additional diagnostics could include a direct-to-digital holographic interferometry technique recently developed at ORNL to determine spatially resolved density profiles in the CT/plasma interaction region. Development work will be required to determine how best to operate the system at high repetition rate. This work will involve electrode cooling, coating materials, and pulsed capacitor bank switching design.

### 2.5.9.3. TOROIDAL FIELD UPGRADE (OPTION)

**Operation at 3.4 T Toroidal Field.** Operation at higher toroidal field would allow higher plasma energies, higher density, higher temperature plasma conditions, and perhaps more efficient rf heating. DIII-D was originally designed to allow operation at 3.4 T following the addition of substantial load reacting components. Such an upgrade would be timely and costly so is considered only as an option beyond the timeframe of this plan.

After the long pulse upgrade of the toroidal field system, the joule capability of the coil and power supply are well matched (2.2 T for 10 s). Similarly, the joule heating

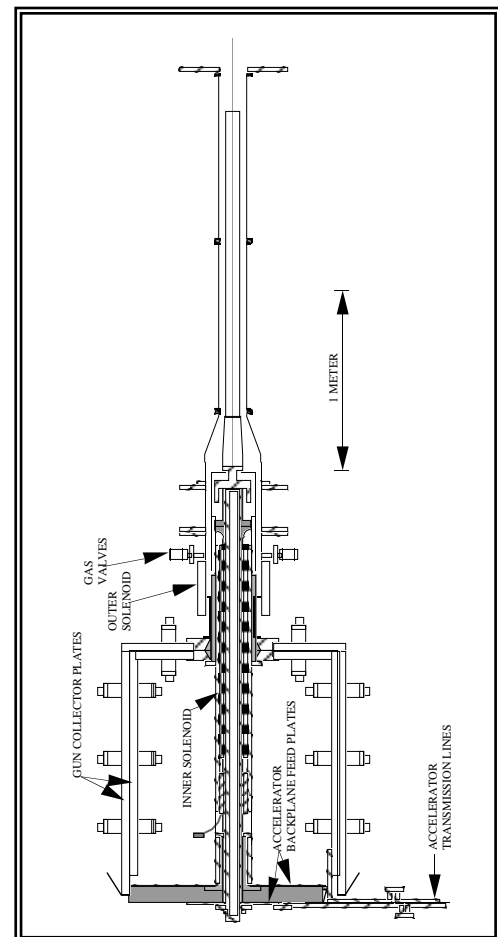


Fig. 2.5-17. The LANL RACE compact toroidal injector is of the size needed for DIII-D.

limited flat-top pulse length available at 3.4 T is 1.8 s. When the current is increased by 50% the heating increases by 2.25. The total heating pulse duration includes ramp up and ramp down and at high field, these become a substantial burden.

Operation of DIII-D at 3.4 T requires a number of upgrades to existing systems. Assuming that the long pulse upgrade is completed, these include:

- Apply clamping caps to the top and bottom of the centerpost with tensioning rods in between (see Fig. 2.5–18).
- Relocate all of the utilities and diagnostics in the way of the new components.
- Install dynamic control for the existing radial prestress system at the top and bottom of the machine.
- Install five additional power supply modules.

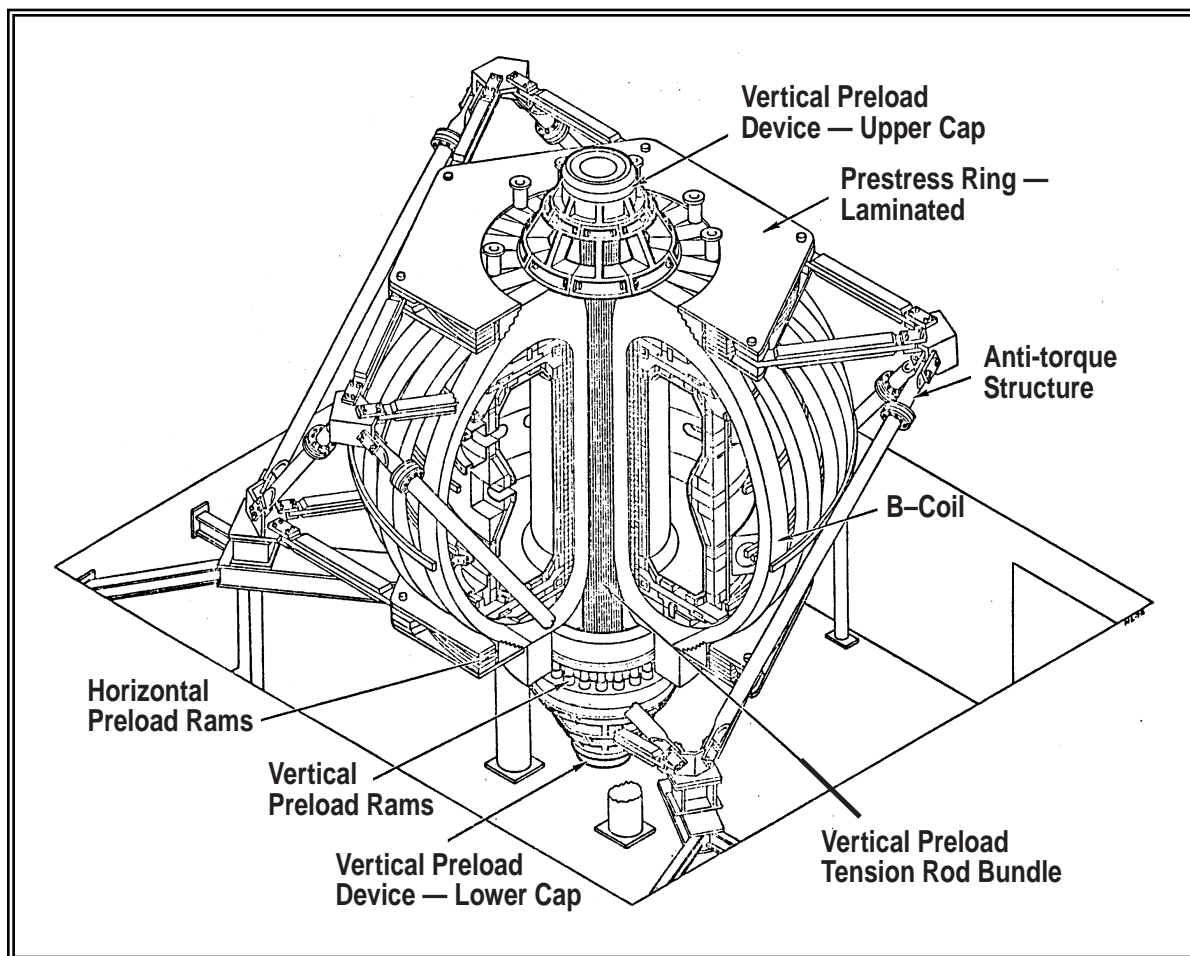


Fig. 2.5–18. Operation of DIII-D at 3.4 T requires upgrades such as the application of clamping caps to the top and bottom of the centerpost with tensioning rods in between.

- Install ac feeds for the additional modules.
- Increase in the number of feed points at the toroidal field coil to three — requires adding one and moving at least one.
- Add a new free-wheeling diode and upgrade existing free-wheeling diode sets to operate at higher currents.
- Install one new TF coil bus from power supply to new feedpoint.
- Operate two MGs in parallel which requires additional high voltage busswork and safety items in the yard.

A second option might be considered to increase the voltage and current of the existing modules, but only use two feed points. This doesn't change power supply costs, but requires us to operate with 50% higher voltage on the coil and all of the existing busswork (up from 1100 V).

In addition, there will be a limitation on the Ohmic heating coil current. Since the maximum current in the off-coil is limited by the force on its current feed and the force is proportional to field, the Ohmic heating coil current and thus the V-s capability will be reduced to two-thirds of its present value.

These changes will be expensive to implement. Not only is the directly associated cost high, but the space for those upgrades located close to the machine has been given up to other systems, including water manifolds and the like at the bottom of the machine. Considerable additional cost would be incurred to move these systems.

## 2.6. THE DIII-D NATIONAL FUSION PROGRAM

The DIII-D National Program evolved from the Doublet III device, which was wholly constructed and initially operated by GA in 1978. During that first year of Doublet III operation, a major collaboration was established with the JAERI. JAERI subsequently invested \$80M (FY98 money) in the DIII-D facility and was provided half the run time in the period 1978–1984. This early major collaboration set the program on the course that has led to the present National Team. When Doublet III was converted into the DIII-D tokamak in 1986, an expansion of collaborations was sought as a goal of the new DIII-D Program. With the DOE, GA developed major collaborations with Lawrence Livermore National Laboratory (LLNL), Oak Ridge National Laboratory (ORNL), Princeton Plasma Physics Laboratory (PPPL), Sandia National Laboratory (SNL), and the Universities of California at Los Angeles (UCLA) and San Diego (UCSD). In addition, many other institutions (Table 2.6–1) collaborate on DIII-D. These collaborations carry out the integrated DIII-D Program mission. Presently, about two-thirds of the research physics staff is from the national and international collaborating institutions. GA provides most of the operations support.

**TABLE 2.6–1**  
**DIII-D PROGRAM COLLABORATORS**

<b>National Laboratories</b>	<b>Universities</b>	<b>International Laboratories</b>
ANL	Cal Tech	Academia Sinica (China)
INEL	Columbia U.	Cadarache (France)
LANL	Hampton U.	CCFM (Canada)
LLNL	Johns Hopkins U.	Culham (England)
ORNL	Lehigh	FOM (Netherlands)
PNL	MIT	Frascati (Italy)
PPPL	Moscow State U.	Ioffe (Russia)
SNLA	RPI	IPP (Germany)
SNLL	U. Maryland	JAERI (Japan)
	U. Texas	JET (EC)
	U. Toronto (Canada)	KAIST (Korea)
<u>Industry Collabs</u>	U. Washington	Keldysh Inst. (Russia)
CompX	U. Wisconsin	KFA (Germany)
CPI (Varian)	UCB	Kurchatov (Russia)
GA	UCI	Lausanne (Switzerland)
Gycom	UCLA	NIFS (Japan)
Orincon	UCSD	Troitsk (Russia)
		Tsukuba U. (Japan)
		Southwestern Inst. (China)

### 2.6.1. NATIONAL LEADERSHIP ROLE

A key responsibility of the DIII-D Program Plan for the period 1999–2003 is for the DIII-D Program to provide a National Program leadership role in the area of its mission: optimization of the tokamak approach to fusion energy. As illustrated in Fig. 2.6–1, DIII-D research is implemented by using the DIII-D facility and the DIII-D National Research team with its collaborations and outreach. The responsibility of the DIII-D National Team extends beyond the conduct of the DIII-D Research Program using the DIII-D facility. The outreach required is in six directions illustrated schematically in Fig. 2.6–1:

1. The DIII-D Program will identify the critical theoretical effort needed for the mission and will seek to obtain that effort from the broader Theory Program.
2. The DIII-D Program will be pro-active in identifying experimental research from other domestic programs, especially closely coordinated collaborations with Alcator C-Mod and smaller university experiments such as HBT-EP and LCT-2, which support the DIII-D mission and will form

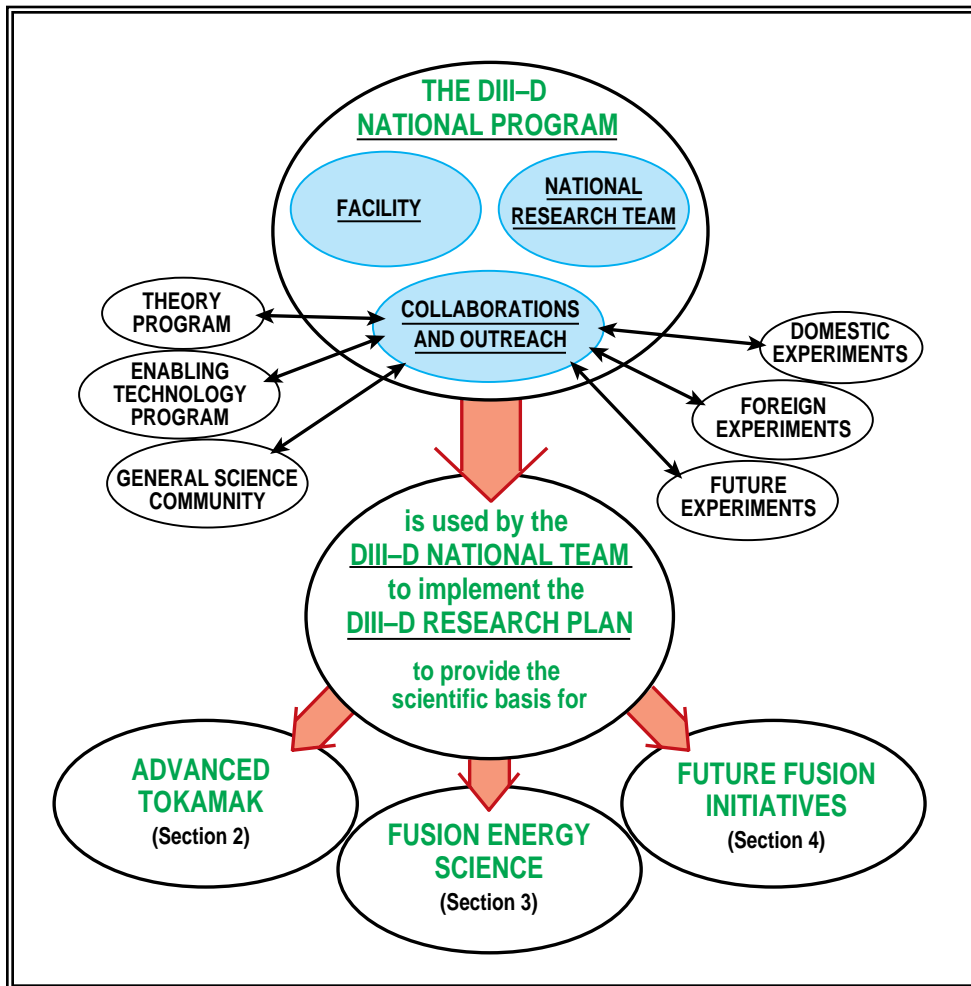


Fig. 2.6–1. The DIII-D Program advances fusion energy science and improves the tokamak

linkages to assist those experiments to succeed and to obtain timely input of their results into the DIII-D Program.

3. The DIII-D Program will continue its active program of collaboration with foreign experiments to assist their progress with DIII-D results and to obtain their input into the DIII-D research directions.
4. The DIII-D Program will continue to strengthen its coupling to the design teams for future devices to assure timely and accurate input of the important research results from DIII-D into the planning for future facilities.
5. The DIII-D Program will help advance and will benefit enabling technology programs.
6. The DIII-D Team will communicate the excitement and progress of fusion energy science to the general science community and the public.

## 2.6.2. COLLABORATIONS AND OUTREACH

The DIII-D Program itself is a multi-institution collaboration (see Table 2.6–1). In addition, the DIII-D Program extends collaborations and outreach to national and international facilities and organizations to carry out the scientific research called for in the DIII-D Program objectives. Figure 2.6–2 illustrates the tokamak facilities with which DIII-D carries out its main collaborations. Indicated are key areas of collaborative research. This DIII-D collaborative research spans a wide range of activities.

**2.6.2.1. DIII-D RESEARCH AND THE U.S. THEORY PROGRAM.** The DIII-D research has provided, and will continue to provide, key data for testing theories. Both the GA theory staff and experimental research staff are committed to helping collaborators in the U.S. Theory Program with access to the data. We give some specific recent examples.

In the confinement and transport area, DIII-D has provided almost half the discharges in the ITER profile database used by modelers as a standardized test bed for theoretical transport models. DIII-D has been in the forefront providing data on transport barrier formation particularly with high-quality profile data on toroidal rotation and electric field shear at the L/H mode transition and the NCS core transition. This data should help isolate the dominant mechanism for barrier formation:  $E \times B$  shear or alpha-stabilization. DIII-D has launched a program to do ECH pulse modulation studies specifically designed to test the leading ITG transport models to determine if they can be clearly delineated from models without a critical temperature gradient. DIII-D has provided an enormous wealth of archival point data on L/H power threshold scaling and global confinement time scaling. Perhaps, most importantly, DIII-D has long taken a lead role in dimensionless variable scaling studies which attempt to isolate the dependence on the key theoretical variables, like the relative gyroradius, and to establish by collaborative comparative experiments with JET and C-Mod that only plasma physics variables determine confinement scaling.

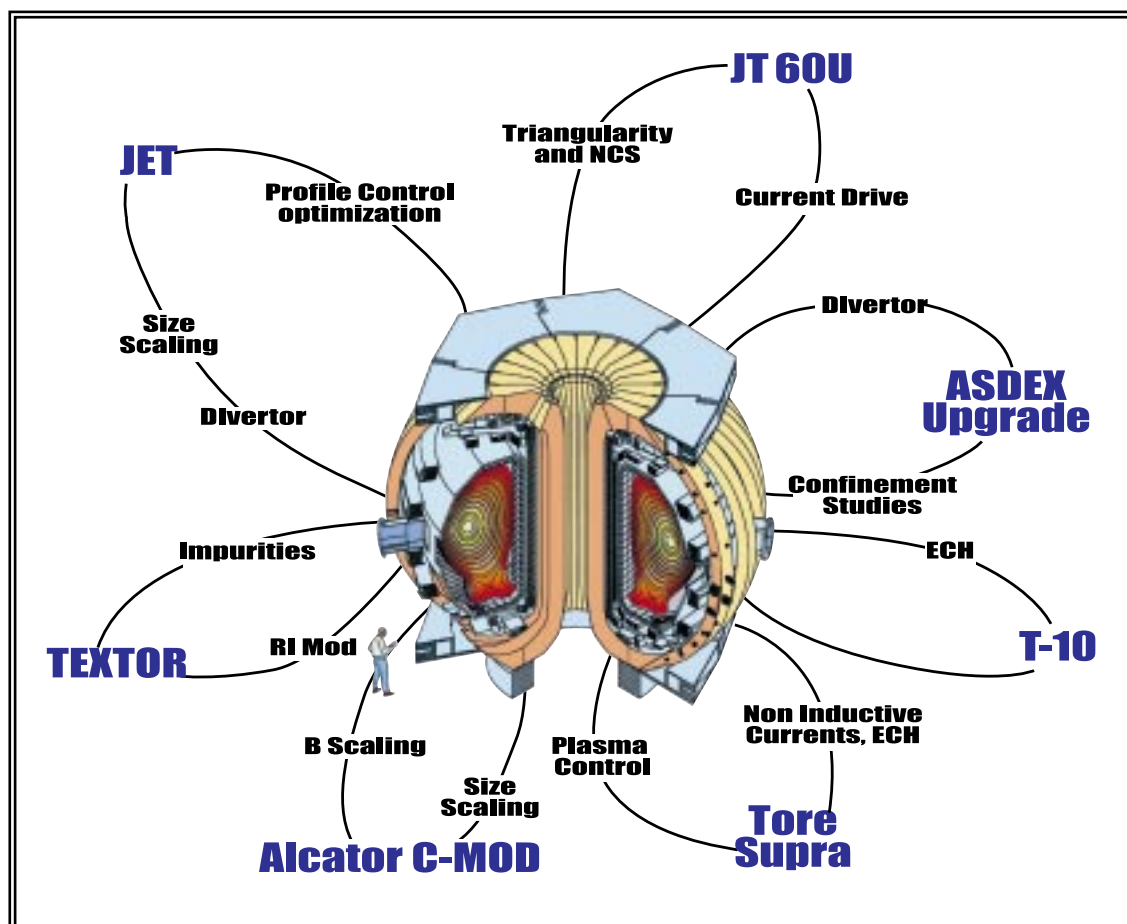


Fig. 2.6–2. DIII-D collaborates with the world's premier tokamak facilities.

Recently there has been a focus on organizing the H–mode pedestal data to test the theoretical idea that the pedestal beta may be limited to the product of the MHD critical beta gradient and the poloidal gyroradius; a critical issue for ITER. Another critical issue for ITER in the MHD stability area is the possibly unfavorable low collisionality scaling of the maximum beta from neoclassical tearing modes. DIII–D has provided the main source of data and inspiration to a strong U.S./European theoretical effort on neoclassical tearing mode physics. There was significant input from the theorists suggesting that if broad pressure profiles could be induced by controlling the L/H transition, the beta limit in DIII–D NCS discharges could be increased. This led to a record gain ( $Q_{DT} = 0.3$ ) in fusion performance. The high beta NCS shots are currently being used as a test bed for nonlinear MHD code simulations to resolve resistive interchange mode physics. Similarly, DIII–D has provided well diagnosed profiles for validating competing models of resistive wall mode stabilization and has contributed to the theoretical understanding of fast particle driven TAE mode physics, as well as disruption phenomena such as halo current and runaway electron generation.

In the radio frequency heating area, DIII–D has been the leading testbed for rf current drive theories, both for fast wave and electron cyclotron wave. Of special note is the validation of the favorable temperature scaling in current drive efficiency, which was predicted previously in Fokker-Planck studies. DIII–D

has also provided measured power deposition profiles, which were compared against calculations from ray-tracing and full-wave codes, confirming the validity of wave absorption physics. Theory has suggested using mode conversion at the ion cyclotron frequency range to drive off-axis current. DIII-D plans to test this in the near future. The existence of bootstrap currents is one of the major theoretical contributions to fusion research. With its capability to measure the parallel inductive electric field profile, DIII-D was the first to carry out the direct confirmation of bootstrap current. This success has led to the idea of transformerless operation using bootstrap current ramp-up.

A unique element of the DIII-D Program is the close involvement of theorists in the planning, execution, and analysis of experiments. Theorists have a representation in the Research Planning Committee. They participate in the preparation of experimental mini-proposals and have even been session leaders of some experiments. Up to now, collaborating theorists interested in accessing DIII-D data to test their models have to work through a GA scientist who can point the way to relevant data. In the next five years we plan to upgrade our data analysis capabilities using modern computing tools to allow much easier access to data, and provide the framework for coupling of physics application codes to the DIII-D experiment. This will make theory participation on DIII-D even more productive.

**2.6.2.2. LINKAGES OF DIII-D TO OTHER U.S. EXPERIMENTS.** To serve more fully as a National Fusion Program focal point, the DIII-D Program has established and will seek to expand linkages to other magnetic confinement experiments in the U.S. Fusion Program. These linkages are seen as a two way street. Other experiments can supply early tests of concepts and supporting information that might be utilized in later stages of the DIII-D Program. The DIII-D Program, representing a large collaboration of institutions, will seek to assist linked programs to succeed in their research endeavors. We describe below some of the on-going linkages.

**ALCATOR C-Mod** is the other major tokamak facility in the U.S. Program. Located at MIT, it complements the research on the DIII-D tokamak with its high toroidal magnetic field and accompanying high density operating capability. Because of the high field, ALCATOR C-Mod is better able than DIII-D to pursue Lower Hybrid current drive for current profile control. The lower field in DIII-D makes it easier to use electron cyclotron current drive in DIII-D. Both machines have strong programs in divertor physics. An essentially unified national team in divertor modeling provides the theory and code support for divertor research in both programs. Because of the wide range in size and plasma parameters, DIII-D and Alcator C-Mod play important roles in the worldwide conduct of dimensionless scaling experiments with the larger JET and JT-60U tokamaks.

**High Beta Tokamak — Extended Pulse (HBT-EP)** is a small tokamak at Columbia University presently studying the issue of wall stabilization. The research is pursuing both the “smart shell” approach to making a resistive wall look superconducting and the use of nonaxisymmetric coils to force plasma rotation in the core plasma. The idea of forcing plasma rotation by rotating magnetic islands in the plasma with external coils (“magnetic stirring”) originated at GA by T. Jensen. That idea and the smart shell approach are best tested on a small experiment before implementation on a large machine like DIII-D. With a successful out-

come on HBT-EP, these ideas are proposed for implementation on DIII-D in the next five-year period. Columbia staff have played prominent roles in DIII-D high performance and stability experiments.

**LCT-2** is a large low magnetic field tokamak being built at UCLA. Its purpose is to explore the possibility of achieving classical confinement in tokamaks at very high beta with omnigenic magnetic surfaces with fast E×B plasma rotation. DIII-D high beta physicists have provided theoretical analysis of the LCT-2 plasma configuration.

**National Spherical Torus Experiment (NSTX)** is a medium sized tokamak being built at PPPL. It will be the proof-of-principle experiment for the spherical torus approach investigating, in depth, most of the important scientific issues for the ST. Consequently, the scientific basis it lays will be crucial to any possible future ST scale-up device in the DIII-D facility. NSTX is presently forming its national collaborative team. GA is a member of the NSTX Program Advisory Committee and six scientists from GA and DIII-D collaborators participate in the various NSTX working groups.

**PEGASUS** is a small ST experiment being constructed at the University of Wisconsin. It will be capable of an early demonstration of  $\beta_T$  in the range of 20% to 40% and of investigating high plasma elongation. Success in these research goals will provide stimulation for the DIII-D Program to move in the ST direction toward the end of the next five-year period. GA has provided design engineering and analysis help for the PEGASUS vacuum vessel, and has provided the port extensions in order to assist in a more rapid startup of this device. GA assistance in the equilibrium and stability area is also planned.

**Helicity Injected Tokamak (HIT)** is a small, low-aspect ratio tokamak at the University of Washington. It has shown the successful use of coaxial helicity injection (CHI) to start up a tokamak to the 250 kA level without using an OH transformer. GA has provided the EFIT code to Helicity Injection Tokamak (HIT) and assistance in analyzing the equilibria being produced using CHI. University of Washington and DIII-D scientists have collaborated on divertor biasing and CHI experiments on DIII-D. CHI is seen by the DIII-D Program as one element of the transformerless operation research thrust for DIII-D in the next five-year period. This research line supports either possible future spherical tokamak or spheromak devices in the DIII-D facility.

**Sustained Spheromak Experiment (SSPX)** is a spheromak experiment under construction at LLNL. Its basic mission is to show the possibility of good interior plasma confinement and magnetic surfaces for pulses approaching ten milliseconds shell time. Success in this experiment will be an important supporting element toward any future spheromak scale-up experiment in the DIII-D facility. GA has provided ideal MHD stability calculations using GATO in support of the design of SSPX. This support is being expanded and possible diagnostic collaborations are being discussed.

In addition to the above explicit program linkages, the DIII-D Research Program has many points of contact with alternate concept research.

**Stability Research.** Perhaps the most striking area of shared interest between the DIII-D Program and alternate concept research is wall stabilization. The primary reason for confidence that the wall stabilization techniques to be applied in DIII-D will be successful is that wall stabilization has been employed for many years as an essential element of operation of the reversed field pinch (RFP) and the spheromak. These devices employ conducting shells to evolve discharges through difficult regimes of rotational transform to their operating points. The wall stabilization physics is common to the tokamak, RFP, and spheromak. The “smart shell” approach being developed on DIII-D for stabilizing low- $n$  kinks for times longer than the shell time constant is likely a necessary development for other magnetic confinement approaches. Eventually, these alternate concept approaches will have to develop feedback approaches to stabilizing MHD modes, and these approaches will probably employ nonaxisymmetric coils in a topology; not much different than the approach taken for DIII-D.

The codes used and developed in the DIII-D Program for low- $n$  ideal kink analysis have proven fairly, easily adaptable to evaluating the stability of alternate concept configurations like the spheromak. Probably the field reversed configuration can also be treated. Tearing mode stability physics is shared by the tokamak and the RFP. The EFIT equilibrium code has been used for spheromak equilibrium calculations.

**Confinement.** The outstanding example of confinement physics developed on DIII-D that has proven to have a larger universality is the stabilization of turbulence by sheared  $E \times B$  flow. We believe that this single underlying mechanism is responsible for the transport barriers formed in DIII-D at the edge in H-mode, near the edge in VH-mode, and in the plasma interior in NCS mode. Transport reduction by sheared  $E \times B$  flow has been seen in all divertor tokamaks that have operated since 1982 and in all limiter tokamaks that have operated off an outside limiter, in a current-free stellarator (W7-AS), in a heliotron/torsatron (Heliotron E), in linear tandem mirror machines (HIEI and Gamma-10), and most recently in the RFP (MST). Consequently, we can conclude this principle of turbulence suppression is a basic property of magnetically confined plasmas discovered in a tokamak, but of general applicability as a pathway to improved confinement.

**Divertor Research.** The physics of the scrapeoff layer and the divertor in a tokamak is dominated by open field line physics, and so this physics is generally applicable to any magnetic confinement approach that bounds a closed field line system with an open field line edge (spheromak, FRC, stellarator) or the linear mirror machines. The fluid and Monte-Carlo codes for modeling the plasma fluid, neutral, and impurity transport in the tokamak SOL/divertor should be readily transferable to boundary plasma research on other magnetic confinement devices. These codes are reaching an advanced degree of sophistication with benchmarking on tokamak experiments. Presently, most alternate concepts are short pulse devices relying on inertial cooling of in-vessel plasma facing components. When these concepts progress to long pulse operation in which heat loads to surfaces become an issue, the SOL/divertor modeling codes developed in the Tokamak Program will be found close at hand.

**Current Drive and Steady State.** The various standard methods of noninductive current drive (NBCD, LHCD, ICCD, ECCD) developed in the Tokamak Program are not tokamak specific. Their physics depends mainly on the interaction of waves with target plasma distribution functions. Consequently, the development of the physics and technology of these current drive techniques can more or less be taken directly over into alternate concept devices. The principle challenge to date has been the rather high power levels required in the low temperature, high density regimes of most alternates. For that reason, the alternate concepts program has pursued various different current drive approaches more along the lines of Ohmic current drive. HICD derived from oscillating toroidal and poloidal fields has been proposed for the RFP ( $F-\theta$  pumping). A test of this approach with a null result was carried out in DIII-D some time ago. Helicity injection current drive from electrodes is the basic method of current drive in the spheromak. In the HIT device at the University of Washington, HICD has been successfully employed to start up a tokamak. DIII-D has made some investigations of HICD and intends to further develop the technique with a view to using it eventually for startup of spherical tokamaks and spheromaks.

**2.6.2.3. LINKAGES OF DIII-D TO U.S. PROGRAM STRUCTURES, TTF, ITER EXPERT GROUPS, AND SMALL BUSINESS INCENTIVE RESEARCH.** GA and DIII-D staff participate in the national conduct of the U.S. DOE Fusion Program. GA and DIII-D staff play leadership roles in assisting the DOE's Office of Fusion Energy Science in planning and executing the U.S. Fusion Research Program. Drs. David Baldwin and Tom Simonen, and other DIII-D personnel, have appeared before the President's Committee of Advisors for Science and Technology (PCAST) and other Congressional Committees to inform the government on the need for fusion energy and plasma science, and to document the progress in fusion research. DIII-D scientists and managers are active members in the committees and task forces which forge the direction of the U.S. fusion program. Dr. Tony Taylor is a member of the Fusion Energy Science Advisory Committee (FESAC). He and others have headed or served on various FESAC subcommittees and subpanels.

The Transport Task Force (TTF), which is now a joint U.S./European effort, was formed to address the special need for a coordinated effort to understand particle and energy transport in magnetized plasmas. DIII-D has two of the TTF group leaders, Dr. Rich Groebner heads the L-H Group and Dr. Ron Waltz heads the Transport Modeling Group. GA and DIII-D scientists have played an active role in the TTF. In addition to investigations in L-H transition physics and transport modeling, we have contributed to the understanding of how  $E \times B$  flow shear creates transport barriers, the study of heat pinches, transient transport, and the study of the heat transport in the separate ion and electron channels.

As part of the effort to satisfy the ITER physics research and development needs, the ITER Expert Groups were established. As described in an ITER Memorandum of Understanding (MOU), the principal activities in the ITER Physics Organization will occur via the seven Expert Groups, whose mandate is to identify ITER research needs within their area of expertise and to propose research programs, including suggestions for specific facilities, both to the separate Party programs and to the ITER Physics Committee. Dr. Simonen is a member of the ITER Physics Committee, Dr. Ron Stambaugh chairs the

Divertor Expert Group, Dr. Keith Burrell is a member of the Confinement and Transport Group, Dr. Jim DeBoo is a member of the Confinement Modeling and Database Group, Dr. Gary Porter, a DIII-D scientist from LLNL, is a member of the Divertor Modeling and Database Group, and Dr. Tony Taylor is a member of the Disruptions, Plasma Control, MHD Group. Many other DIII-D scientists have enthusiastically participated in these groups via extensive presentations, written contributions, database inputs, and participation at working sessions.

Support of fusion-related Small Business Incentive Research (SBIR) proposals and resulting contracts continues to be an element of the DIII-D Program and the GA fusion effort. Recently completed and currently on-going collaborations (Table 2.6-2) include DIII-D diagnostic development, DIII-D controls development, fusion technology development, and fusion device design. In CY97, endorsements and support were provided for eight new SBIR proposals to DOE.

**TABLE 2.6-2**  
**RECENT SBIR COLLABORATIONS WITH THE GA FUSION GROUP**

Company	Topic	Status
Creare	Helium-Cooled Divertors	Phase II complete
ORINCON	CER Spectrum Neural Net	Phase II complete
ORINCON	Neural Net Disruption Alarm	Phase II complete
InterScience	Data Acquisition & Processing System	Phase I on-going
IR&T	Interferometer/Densitometer Diagnostic	Phase II on-going
Surmet	Carbon-Carbon to Copper Joining	Phase II on-going
Thermacore	Helium Cooled Faraday Shield	Phase II on-going
TSI Research	Volumetric Neutron Source	Phase II on-going

**2.6.2.4. ROLE OF DIII-D IN THE INTERNATIONAL FUSION PROGRAM.** The DIII-D Program has played, and will continue to play, the lead role internationally in the AT thrust. The flexibility of the DIII-D device allows early testing of new approaches that can, if successful, later be implemented on the larger tokamaks such as JET and JT-60U. DIII-D scientists have participated in such experiments on foreign machines transferring techniques developed on DIII-D. Working with foreign tokamaks of various sizes, DIII-D has played a key role in developing the dimensionless parameter approach to the scale size dependence of plasma confinement. The path of developing AT approaches on DIII-D and confirming those approaches on the larger foreign tokamaks will provide the scientific basis for use of AT operating modes on future international or domestic next step machines.

For example, in developing the reversed or NCS regime for use on JET, a strong interaction of the JET and DIII-D research staff took place. JET scientists came to DIII-D and JET-shaped plasmas were operated in DIII-D. In those plasmas, the techniques for timing and application of neutral beam heating

were developed that allowed internal transport barrier regimes with negative central shear to be created. Later, about six DIII-D scientists went to JET and participated in the initial D-D experiments at JET in which NCS internal transport barrier plasmas were created in JET as preparation for the DT campaign. DIII-D personnel also participated in the DT campaign.

DIII-D and JAERI have had a long interactive history in AT studies, particularly around the issue of plasma shape, and specifically, triangularity. This interaction began early in the DIII-D Program with the discovery of the Type II or grassy ELM regime when high triangularity plasmas were operated in DIII-D. Stability analysis by JAERI scientists showed the edge of such plasmas was predicted to be in the second stability regime from which sprung today's intensive effort to understand the stability of the H-mode pedestal region. More recently, DIII-D scientists have first assisted in implementing on JT-60U the wall conditioning techniques developed on DIII-D for discharge optimization and, secondly, DIII-D scientists have assisted in developing on JT-60U plasma control approaches that allowed higher discharge triangularity. These higher triangularity discharges in JT-60U have better beta limit and ELM properties.

The EFIT equilibrium code has been exported from DIII-D to most tokamaks around the world, and has played a prominent role in the design and analysis of their AT experiments. The EFIT code was implemented on JT-60U by DIII-D scientists and used to analyze internal transport barrier discharges, as well as to deduce the radial profile of noninductively driven current in discharges that have not resistively relaxed to a new steady-state current profile. A similar use of EFIT has been made on Tore-Supra as part of a larger collaboration on advanced methods of plasma control. Experts in DIII-D's digital plasma control system have participated in work on Tore-Supra.

The shaping flexibility of DIII-D has enabled DIII-D to match the plasma shapes run in other tokamaks, e.g., JET, ASDEX Upgrade, Alcator C-Mod. This ability to run identical plasma shapes has enabled dimensionless parameter scaling studies of confinement to be carried out between DIII-D and these three tokamaks. The results have provided a more sound basis of projecting confinement to future devices, in particular, to ITER.

DIII-D began a detailed program of investigation of the effects of magnetic field errors on performance and, in particular, on plasma rotation. This work was expanded into collaborative work on the larger tokamak JET and the smaller tokamak COMPASS. The resulting three machine database has provided a scaling law that has been used to estimate error field problems on ITER. This collaborative work has continued onto the subject of neoclassical tearing modes which frequently appear in AT regimes.

The RI-mode is an AT mode first discovered on TEXTOR. Its prominent features are confinement of H-mode quality or better with densities above the Greenwald limit and a radiated power fraction approaching 100%. Because the diagnostic set on TEXTOR is limited, the TEXTOR group have initiated a collaboration on DIII-D on RI-mode plasmas. Because of the excellent edge diagnostics set on DIII-D, it is expected that a deeper understanding of the physics of the RI-mode might be obtained on DIII-D.

The role of DIII-D in developing the principle of  $E \times B$  shear suppression of turbulence as the reason for the confinement improvement in H-mode is well known. The detailed focus on the plasma edge made by DIII-D has motivated other tokamaks to mount new diagnostics focused on the plasma edge. The result has been a present intensive worldwide effort to understand the structure and physics properties of the H-mode shear layer. This work has high leverage on the overall performance of the tokamak because of the sensitive dependence of the overall confinement on the height of the H-mode pedestal; a dependence that results from “stiff” transport models for the core plasma predicted by theory.

**International Collaborations.** The DIII-D international collaboration program continues to provide a broad source of innovative ideas and opportunities which support the DIII-D Research Program. Throughout, the DIII-D Program has benefited from the activities in many foreign collaborating institutions.

The DIII-D Program is a major collaboration between the U.S. and Japan, and was implemented by DOE and JAERI. JAERI contributed substantial financial resources and manpower from 1979 to 1986. A U.S./Japan Doublet III Steering Committee meets annually to assess progress and review future plans.

Collaborations have been carried out with JET in England, ASDEX-Upgrade in Germany, Tore Supra in France, and JT-60U and JFT-2M in Japan through bi-lateral agreements. In addition to the benefits gained from DIII-D staff assignments in these and other laboratories, foreign scientists visiting DIII-D have made significant contributions to DIII-D Program goals. A summary of some of the recent major international collaborations by DIII-D staff members is given below.

**JET (England)** is the large European tokamak approximately twice the size and magnetic field strength of DIII-D. Our collaboration with JET is one of the largest of our international collaborations. Several DIII-D scientists from GA, LLNL, and ORNL collaborated at JET in a two-step exchange on NCS-type high performance tokamak discharges. First a series of experiments were performed on DIII-D with participation by JET scientists. Then DIII-D scientists participate in experiments at JET. In other experiments, DIII-D and JET scientists have carried out dimensionless scaling experiments to investigate fundamental confinement properties and to provide results to the ITER database. The results from this series of experiments were very successful. Ion temperatures of about 30 keV and electron temperatures of about 16 keV were obtained. These results represent some of the highest fusion parameters attained in deuterium plasmas on JET.

**Tore Supra (France).** The primary emphasis for our collaboration with Tore Supra has been ECH physics and technology, noninductive current drive, and plasma and current density profile control. The Tore Supra program includes electron cyclotron, fast wave, and lower hybrid heating and current drive research which complements the DIII-D electron cyclotron and fast wave heating and current drive research.

**ASDEX Upgrade (Germany).** The ASDEX/DIII-D collaborations are primarily in the area of Divertor research and RF. This includes impurity transport and heat transfer mechanisms involving Edge

Localized Modes and MARFEs. Research also includes H-mode confinement studies. RF collaboration includes ICRF and ECH.

**JAERI (Japan).** GA scientists participated in an exchange at JT-60U, working in the area of NCS, high confinement, and neutral beam current drive. The equilibrium reconstruction code, EFIT, was used to analyze JT-60U NCS configurations. A successful experiment using the GA-designed “Comblin” antenna was carried out on the JAERI JFT-2M tokamak. This antenna allows better coupling to the plasma over a wide range of plasma parameters. The highly successful JAERI/DIII-D cooperation continues. This collaborative program entails the long term participation of JAERI scientists in the DIII-D Fusion Research Program.

**Russia.** DIII-D maintains a broad collaboration program with several Russian Fusion Research Institutes. With the TRINITY lab at Troitsk, near Moscow, the main topics are: materials for plasma facing components, divertor spectroscopy, and the use of the Russian developed DINA code for modeling dynamic plasma behavior. With Kurchatov, collaborations were on ECH, electron temperature measurements using an x-ray spectrometer, and remote analysis of charge exchange recombination data. Funded by the Theory Grant, GA is contracting with Moscow State University to support Russian theorists to perform theoretical analyses of plasma physics problems of relevance to understanding the performance of DIII-D.

**China.** The main thrust of our exchanges with the Chinese Fusion Research Program has consisted of the long term participation of Chinese scientists in the DIII-D Program at the DIII-D site. These exchanges have concentrated in the area of the Thomson scattering diagnostic, the CER diagnostic, and ECH systems.

**2.6.2.5. ROLE OF DIII-D IN ENABLING TECHNOLOGIES, CONTRIBUTIONS AND NEEDS.** Progress in fusion has been closely coupled to advances in enabling technology. Future success requires continued development of new tools. DIII-D has identified several areas where progress in science can be enabled by the timely development of heating, fueling, wall conditioning, and plasma control technologies. Success in advanced tokamak studies to date has been achieved using transient controls. Further progress needs active control tools to maintain the desired profiles of current density and plasma pressure. DIII-D has identified fast wave heating and current drive for control of the central current drive, electron cyclotron heating and current drive for central and off-axis profile control, inside launch pellet injection for central fueling, divertor pumping for density control, coils for active nonaxisymmetric MHD mode control, and active real-time plasma control. Key needs in each technology area are outlined below.

**ECH Microwave Technology.** The key enabling technology requirement for the DIII-D Program is the development of reliable, long-pulse MW gyrotrons at 110 GHz. MW-level gyrotrons have been demonstrated, but vacuum windows have limited the pulse length. Long pulses are essential to control the current density profiles due to the noninductive response of the plasma. The recent development of diamond windows appears to offer the long sought solution, but it must be demonstrated on gyrotrons at high power.

Improved launchers to allow fast tracking for MHD mode control are required. Improved mode purity of the output mode and depressed collectors for improved efficiency are areas where work is needed.

**ICRF Fast Wave Technology.** Although the technology for ICRF/FW is relatively more mature, improvements in antenna design (comblines) and transmission line topography (TW) have been shown to improve the power handling capability and the tolerance to load changes due to plasma changes (L–H transitions, ELMs, etc.). Typically ICRF/FW experiments operate at only 50% to 75% of the installed power due to coupling difficulties. Further work is needed to capitalize on the comblines antenna and traveling wave configuration successes, along with efforts to understand the causes of breakdown in antennas. High power qualification of the existing folded waveguide antenna would enable an IBW capability on DIII–D for exploration of transport barrier control.

**Fueling and Particle Control.** In the particle control arena, divertor baffling and cryopumps have been demonstrated in DIII–D and particle injector technology is quite mature. These technologies are installed on DIII–D and will be optimized to demonstrate their effectiveness for high triangularity advanced tokamak discharges. Recent success with inside launch pellet injectors at ASDEX has stimulated an exploration on DIII–D, so the ability to direct pellets around a curved trajectory is a key technology for implementing this approach. A related technology need is liquid jets for disruption amelioration.

**Plasma Control.** A newly developing area is real-time plasma control. The active control of plasma profiles necessitates internal measurements with subsequent corrections applied by the heating, fueling, and current drive systems as required. This process requires rapid computing and control response. Active control is already employed in DIII–D and other tokamaks; for example, magnetic configuration control, and edge position control for rf heating. As more sophisticated control is implemented, new approaches may be required to provide the time response required.

**Materials.** DIII–D utilizes the expertise which exists in the fusion materials community for advice in the planned use of vanadium and tungsten in DIII–D.

**2.6.2.6. DIII–D CONTRIBUTIONS TO THE PLANNING OF FUTURE FUSION EXPERIMENTS.** DIII–D has a very versatile plasma shaping capability that allows it to study many confinement, transport, and stability issues related to the dependence on plasma shape parameters such as size, elongation, and triangularity. This same versatility allows DIII–D to carry out comparison experiments coordinated with other tokamaks which require the plasma shapes to be closely matched. Such experiments include the class of experiments referred to as dimensionless parameter scaling of global energy confinement and local transport coefficients. The proof-of-principal experiments for these type of experiments involved comparing plasmas with identical dimensionless parameters including aspect ratio, elongation, and triangularity to validate that the product  $B\tau$  remained constant. Successful experiments of this type were carried out with JET [Fig. 2.6–3(a)], C–Mod, and a special case of this type of experiment, with all dimensionless parameters and engineering parameters matched, was performed with ASDEX–Upgrade.

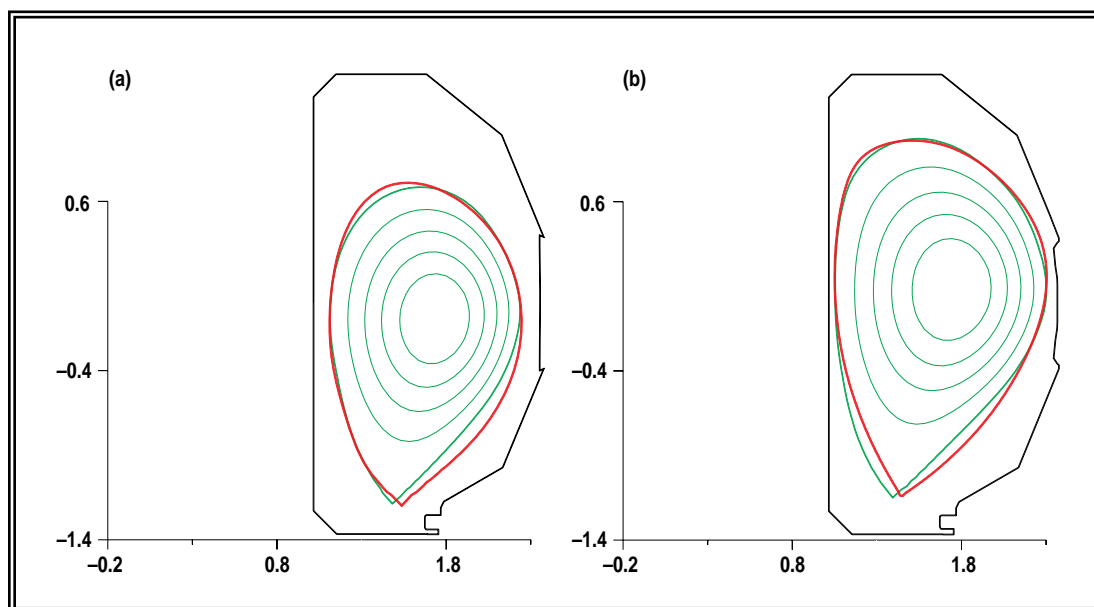


Fig. 2.6-3. The DIII-D tokamak is capable of producing plasma shapes of other tokamaks. Shown are (a) JET and (b) ITER.

Since today's tokamaks can match all dimensionless parameters envisioned for a fusion reactor with the exception of size, characterized by the normalized gyroradius  $\rho_*$ , recent dimensionless parameter experiments have primarily focused on determining the  $\rho_*$  scaling in order to determine how to scale results from current tokamaks to future devices such as ITER. Experiments of this type have been performed with JET in order to extend the range in  $\rho_*$  and have indicated gyro-Bohm-like transport for low  $q$  H-mode discharges, a regime in which ITER would like to operate. Other experiments of this type have been performed in DIII-D with the ITER plasma shape [Fig. 2.6-3(b)] itself. These so-called ITER demonstration discharges have been used to study critical ITER R&D issues such as dimensionless parameter scaling, stability, beta limit, and disruption issues, and the impact of ELMs on plasma edge parameters.

More experiments in these areas are required to further our understanding of basic transport and to better predict operation in ITER. One active area of current research in transport is the role of plasma flows from sheared rotation in improving energy transport. Future dimensionless parameter scaling experiments are needed where the plasma rotation profiles can be controlled so as to hold them fixed. Experiments, to date, have not addressed this issue. Another area of need, particularly for projections to ITER, is a model for the plasma edge. Output from such a model serves as boundary conditions needed as input to existing transport models for the plasma core. Further experiments with ITER demonstration discharges is required to develop models for plasma edge scaling. One key to all of these future experiments is versatility and flexibility in controlling the plasma shape, a particular asset on DIII-D.

The DIII-D tokamak has been one of the major contributors to the ITER Engineering Design Activity. One of the DIII-D scientific objectives is to "Advance understanding of fusion plasma physics

and contribute to the physics base of ITER through extensive experiment and theory iteration” in the following areas:

- MHD stability.
- Plasma turbulence and transport.
- Wave-particle interactions.
- Divertor boundary physics.

This objective is achieved through a close interaction with the ITER JCT and the ITER Home Team. Research topics, which have been identified as ITER Urgent Tasks, are given specific attention in the DIII-D experimental planning process. Examples of ITER Urgent Physics R&D topics which have been addressed in the past are as follows: confinement scaling in the ITER shape (ITER demonstration discharges), erosion studies of a graphite divertor target plate sample, radiative tests of a ITER relevant long divertor leg, and studies of beta stability limits in ITER shaped ELMing H-modes. In Table 2.6–3 are listed the components of the DIII-D 1997 plan which address the ITER Urgent Physics R&D issues.

Planned future research activities which will support ITER include: studies of disruption mitigation, radiative divertor research, continued additions to the ITER confinement database, and studies of the scaling and physics of the L-mode to H-mode transition.

In addition to experiments which directly address the ITER Urgent Physics R&D issues, the DIII-D Advanced Tokamak Program’s goal is to advance the understanding of tokamak transport and stability beyond the envelope of the present ITER design so that promising new directions can be taken for ITER or the fusion device which will be subsequent to ITER.

In addition to DIII-D Program support, the GA Fusion Group supports ITER by providing secondees to the JCT at all three sites, by carrying out U.S. ITER Industrial Consortium (USIIC) tasks, and by execution of DOE funded contracts. Table 2.6–4 summarizes these efforts.

#### **2.6.2.7. DIII-D PROGRAM SUPPORT TO THE GENERAL SCIENCE COMMUNITY**

**University Participation in DIII-D.** The active, on-site, participation of university scientists is an important part of the DIII-D Fusion Research Program. Throughout the years, many major universities have taken part in the DIII-D Program. This participation has added an important breadth to our research, and has provided a mechanism by which we have been able to quickly and cost-effectively involve scientists with unique, specific experience and capabilities in our efforts. The experience which they gain by working with a major fusion research facility, in turn, enhances their ability to contribute to their home university’s programs both in teaching and research.

**TABLE 2.6–3**  
**DIII-D 1997 EXPERIMENTS EMPHASIZED URGENT ITER PHYSICS R&D**

Research Area	ITER Issues (ITER R&D No.)	DIII-D Experiment
Plasma termination and halo currents	Halo current characterization and self-consistent eddy currents (1.3)	VDE and halo current physics
	Effects of massive deuterium injection (1.2)	Killer pellet and massive gas puff
	Runaway electron currents (1.14)	Runaway electron suppression
Divertor detachment and radiation loss physics	Effect of divertor detachment on confinement (2.2)	Energy flow in detached divertors
	SOL plasmas and impurity flows (2.4)	Helium plasma campaign Impurities in attached and detached divertor Impurity entrainment with puff and pump Radiation enhancement with puff and puff Impurities in attached and detached divertor
	Development of 2D fluid Monte Carlo divertor codes (2.22)	Impurity entrainment with puff and pump Divertor geometry and pumping campaign ELM/pedestal versus density and trian.
	Divertor geometry effects (2.20)	
	Divertor scalar, ELM, and edge/pedestal database (2.7, 4.9)	
Density limit physics	Physics of edge density limit, especially for H-mode plasmas. Role of H→L transition. (2.5)	Density limit studies
	Improvements in penetration and fueling efficiency resulting from inside pellet fueling	(next year)
Finite- $\beta$ effects	ITER D EMO discharges; role of rotation (6.1)	Rotation effect in dimensionless scaling Campaign: stability versus plasma shape
	ECH stabilization of neoclassical islands (1.4S)	ECCD stabilization of neoclassical tearing Campaign: stability versus plasma shape
	Tolerable ELMs (2.12)	ELM/pedestal versus density and trian.
H-mode power threshold	Coordinated size scaling experiments in different devices (3.1)	Grad-B drift effect on L–H threshold
		H-to-L threshold scalings Test L-H transition theories L-H trans. identity comp. with C-Mod
		Grad-B drift effect on L-H threshold H-to-L threshold scalings Test L-H transition theories
	Threshold database (4.2)	
H-mode core confinement	Nondimensional scaling experiments, effect of finite $\beta$ and flow shear (3.2)	High-beta H-mode scaling to ignition
	Global thermal database (4.1)	Rotation effect on dimensionless scaling $q$ scaling with fixed dimensionless parameter $q$ scaling with fixed dimensionless parameter
	Development of 1.5D local transport models; profile database (4.4)	

**TABLE 2.6-4**  
**GENERAL ATOMICS PROVIDES ITER SUPPORT IN ADDITION TO DIII-D PROGRAM SUPPORT**

Support Area	Support Arrangement	Status
RF Engineering	Garching JCT Secondee	Completed 2/95
Remote Maintenance	Naka JCT Secondee	Completed 12/96
Safety	Naka JCT Secondee	Completed 2/97
Design Integration	Three San Diego JCT Secondees	On-going
Physics Integration	Two San Diego JCT Secondees	On-going
Director of Engineering	San Diego JCT Secondee	On-going
Plant Systems Engineering	San Diego JCT Secondee	On-going
External Relations	San Diego JCT Secondee	On-going
Pumping and Fueling	Garching JCT Secondee	On-going
Cryogenic Systems	Naka JCT Secondee	On-going
Plasma and Field Control	Naka JCT Secondee	On-going
Superconducting Structures	Naka JCT Secondee	On-going
Divertor Design	USIIC Task through Raytheon	Completed 2/95
Blanket/Shield/First Wall Design	USIIC Task through Raytheon	Completed 2/95
ECRF System Costing	USIIC Task through Raytheon	Completed 6/95
ECH & Current Drive Modeling	USIIC Task through Raytheon	Completed 12/95
MHD Stability Analysis	USIIC Task through Raytheon	Completed 12/95
Power Supply Design	USIIC Task through Raytheon	Completed 12/96
Plasma Control	USIIC Task through Raytheon	On-going
Diagnostic Design	USIIC Task through Raytheon	On-going
Divertor Design	USIIC Task through Raytheon	On-going
ECRF Design	USIIC Task through Raytheon	On-going
First Wall/Blanket/Shield Design	Subcontract from MDA	Completed 11/96
Plasma Facing Components	Subcontract from MDA	On-going
Radiation Resistant Probes	DOE Contract	On-going

**Opportunities for Training Future Faculty and Postdoctoral Fellows.** GA and the DIII-D Program are active participants in postdoctoral training programs. We participate in the DOE-sponsored Fusion Energy Postdoctoral Research Program and the ORNL-sponsored Postdoctoral Research Associates Program, and also sponsor a GA Postdoctoral Research Associates Program. All of these programs are administered by the Oak Ridge Institute of Science and Engineering. The postdoctoral positions have durations which can vary from one to four years. To date, approximately ten recent Ph.D. graduates have participated in the DOE/GA experimental and theoretical fusion research under the sponsorship of these programs. Scientists holding postdoctoral fellowships from the universities, mentioned in the previous section, have also furthered their scientific training at the GA fusion facility.

**Opportunities for Training Ph.D. Students.** Almost all of the universities, which are participating in the DIII-D Program, use the facility as a training ground for graduate students. Approximately 20 students have performed research at the GA fusion facility, which has led to the award of an advanced degree. As an example, the University of California at Berkeley has awarded six Ph.D.s for work related to the GA DIII-D Program in recent years. Some students may be full-time at the DIII-D site designing, installing, and using diagnostic systems, or analyzing DIII-D data. Others may work at their home university writing computer codes or developing theories which explain plasma phenomena which are observed on DIII-D. Table 2.6–5 shows a list of recent Ph.D. candidate students who have worked on DIII-D.

GA is also actively involved in the National Undergraduate Fellowship Program in Plasma Physics and Fusion Engineering which is administered by the Science Education program of the Princeton Plasma Physics Laboratory. Each year, this program provides 25 summer internships to outstanding undergraduate students of U.S. colleges and universities. Typically, GA hosts about four students each summer. From the results of student evaluations, it is clear that GA has provided these students with a valuable learning experience.

**GA Educational Outreach Program.** The Fusion Group maintains an Education Outreach Program for middle and high school students throughout San Diego County. The program enables teachers and scientists to work together closely to produce effective educational materials on fusion science and technology for classroom use, and allows students unique opportunities to discuss science, engineering, and math topics with professional scientists and engineers. Key deliverables from previous work include workbooks, a curricular chapter on the electromagnetic spectrum, a poster for classroom display, a videotape on nuclear fusion energy production and DIII-D facility tours and tour stations. Workshops which cover the curricular materials are provided to teachers and educators to enhance their fusion knowledge base. Over the previous two years, more than 100 educators have attended our workshops, while others have used the materials as a basis for teaching a unit on nuclear fusion. Future work will include the production of an interactive CD-ROM on plasma science and fusion technology, expansion of the curriculum notebook to include activities on radiation, ICF, plasma, and fusion related engineering, and significant contributions to professional journals and classroom textbooks on plasma science and fusion technology. Classroom visits by scientists and engineers will also become part of the program.

A unique aspect of the Education Outreach Program is a three-hour DIII-D Tokamak Facility tour given to student groups. The tour is the culminating activity in the Educational Outreach Program. Students are given a brief overview of the on-going, worldwide efforts in harnessing nuclear fusion as an energy source and are then given a multistation tour of the facility. At the different stations, small groups of students participate in demonstrations and hands-on activities that cover general areas of science and technology. The stations are titled “Plasma—the 4th State of Matter,” “The Electromagnetic Spectrum,” “Engineering Analysis and CAD,” “Data Acquisition and Computers,” “Radiation, Radioactivity, and Risk Assessment,” “Inertial Confinement Fusion,” and “DIII-D Model and Experimental Hall.” At each station, scientists and engineers discuss topics and present demonstrations to reinforce the concepts presented. During the previous two years, more than 2000 students have toured the DIII-D facility.

**TABLE 2.6–5**  
**PAST AND PRESENT GRADUATE AND POST-DOCTORAL STUDENTS AT DIII-D**

Researcher	Affiliation	Topic
<u>Students</u>		
S. Coda	MIT	CO <sub>2</sub> phase image interferometer
W. Howl	UCSD	MHD reconstruction
R. Stockdale	Princeton U.	Perturbative transport experiments
T. La Hecka	UCLA	Microwave reflectometry
C. Rettig	UCLA	Microturbulence studies
K.W. Kim	UCLA	Fast density profiles reflectometry
J.H. Lee	UCLA	Fast wave studies
D. Hua	UCB	ITG modes and energy confinements
D. Finkenthal	UCB	He transport
Q. Nguyen	UCB	UEDGE development
B. Modi	UCB	Turbulence modeling
R. Gatto	UCB	Heat pinch modeling
J. Fitzpatrick	UCB	TAE mode analysis
M. Perry	Johns Hopkins	Impurity transport
A. Zwicker	Johns Hopkins	Multi-layer mirror spectrometer
S. Janz	U. Maryland	ECE diagnostic bolometers
D. Content	Johns Hopkins	Bolometers and visible bremsstrahlung
H. Duong	UCI	Fast ion bursts
G. Sager	U. Illinois	Data analysis program
Chuang Ren	U. Wisconsin	Plasma rotation and wall stabilization
E. Carolipio	UCI	TAE mode studies
<u>Postdoctorates</u>		
Ken Kupfer	ORISE	RF current drive
Jarad Squire	ORISE	X-ray diagnostic
Mickey Wade	ORISE	Helium transport
Rajesh Maingi	ORISE	Divertor physics
Jon Kinsey	GA/ORISE	Transport modeling
Max Austin	U. Maryland	ECE diagnostics
Dennis Whyte	CCFM/Canada	Divertor physics
P. Oshea	MIT	Phase contrast imaging
G. Garstka	U. Maryland	ECE diagnostics
R. Durst	U. Wisconsin	Beam emission spectroscopy
G. McKee	U. Wisconsin	Beam emission spectroscopy
T. Kurki-Suonio	UCB	Transport analysis
Alan Brizard	UCB	Transport analysis
R. Lehmer	UCSD	Divertor
A. Garafalo	Columbia U.	Wall stabilization

### 2.6.3. THE DIII-D NATIONAL TEAM

The DIII-D Research Program derives its strength from the diversity and capabilities of its national and international collaborating institutions and associated individuals. The DIII-D National Team consists of about 120 operating staff and 100 research scientists drawn from 9 U.S. National Laboratories, 19 foreign laboratories, 16 universities, and 5 industrial partnerships. The research staff ranges from undergraduates to senior scientists, with over 30 years experience in fusion energy science. The staff has been recognized for its outstanding research; the presently active staff contains 5 winners of the Excellence in Plasma Physics Award and 32 Fellows of the American Physical Society. In addition, suggestions for research and analysis of results are provided by many other institutions and individuals through normal channels, scientific publication, conferences, and individual interactions. The institutions, which are currently directly collaborating on DIII-D, are given in Table 2.6–1. Over the past decade, the fraction of collaborating physicists has increased from one-third to two-thirds of the total with the fraction of GA physicists decreasing from the two-thirds to one-third. Approximately half of the GA physics effort is associated with hardware building or operation, coordination, code building or maintenance, and similar service support activities which are organized in Tables 2.6–6 to 2.6–9 under the fusion science categories of stability, transport, wave particle interaction, and divertor and boundary physics. Many of these broad and extensive collaborations are carried out under the aegis of the ITER Physics Experts activity, which provide forums for international communication and coordination of tokamak research.

In addition to GA, there are six major collaborating institutions which have broad programmatic area responsibilities on multiple topics and may carry management responsibilities. These collaborators join with GA to form the Executive Committee to guide the programs strategic and near-term directions. The programmatic responsibilities of the major DIII-D collaborators are given in Table 2.6–10.

University collaborations are an essential feature of the National DIII-D Program. The roles of these university collaborations is indicated in Table 2.6–11. In addition, several other institutions have critical roles in the DIII-D Program is indicated in Table 2.6–12.

**2.6.3.1. INSTITUTIONAL STRENGTHS OF MAJOR PARTICIPANTS.** The major DIII-D Program participants bring unique institutional strengths to the DIII-D Program. This multi-institutional character facilitates coupling to core competencies at their home laboratories and universities to strengthen and provide a broader technical base for the DIII-D Program.

As an industry committed to fusion development, GA strives to contribute to the development of fusion energy while developing a supportive position through DIII-D that could allow participation in the eventual commercialization of fusion. Accordingly, GA endeavors to develop technological and engineering expertise in tokamak design and operation. Industry has unique capabilities and GA brings these to the DIII-D Fusion Program.

**TABLE 2.6–6**  
**DIII-D COLLABORATIONS RELATED TO STABILITY AND DISRUPTION PHYSICS**

Topic	DIII-D Contact	Collaborating Institution	Key Collaborator
Equilibrium reconstruction (EFIT)	L. Lao	JET	D. O'Brien
	L. Lao	JAERI/JT-60U	T. Fujita
	L. Lao	MIT/Alcator C-Mod	S. Wolfe
	L. Lao	Textor	P. duMortier
	L. Lao	Culham/START	L. Appel
	L. Lao	Culham/COMPASS-D	D. Gates
	L. Lao	KSTAR	B.J. Lee
	L. Lao	PPPL/NSTX	S. Sabbagh
	L. Lao	Univ. of Wisconsin/PEGASUS	S. Kruger
	L. Lao	ITER-Garching	E. Solano
Negative central shear plasmas	E. Strait	JET	C. Gormezano
	T. Taylor	JAERI/JT-60U	Y. Kamada
High $\ell_i$ stability	L. Lao	Columbia University	S. Sabbagh
Dependence of stability on plasma shape	T. Taylor	JAERI/JT-60U	Y. Kamada
TAE mode studies	W. Heidbrink	JET	A. Fasoli
Kinetic stability	L. Lao	PPPL	G. Rewoldt
	M. Chu	UC-Irvine	L. Chen
Gyro-kinetic simulations	L. Lao	Cyclone working group	K. Bolton
Stability of internal modes	L. Lao	PPPL	J. Manickam
Resistive stability	M. Chu	CRPP-Lausanne	A. Pletzer
	L. Lao	PPPL	D. Monticello, A. Reimann
	M. Chu	Chalmers University-Gothenburg	A. Bondeson
	R. Miller	IFS	F. Waelbroeck
Magnetic reconnection	R. La Haye	Univ. of Iowa	A. Bhattacharjee
Neoclassical tearing modes	R. La Haye	Univ. of Wisconsin	J. Callen
	R. La Haye	Culham	H. Wilson
	R. La Haye	CRPP-Lausanne	O. Sauter
	R. La Haye	MIT/Alcator C-Mod	S. Wolfe
	R. La Haye	Culham	H. Wilson
Peeling mode stability	R. La Haye	Moscow State Univ.	A. Popov
Nonlinear resistive MHD simulation	A. Turnbull	Keldysh Institute	S. Galkine
Resistive MHD code development	M. Chu	NIMROD group	D. Schnack, A. Glasser
Nonlinear resistive MHD code			
Realistic wall model for MHD stability	M. Chance	PPPL	R. Miller
MHD mode analysis	T. Taylor	Orincon Corp.	J.S. Kim
Magnetic error fields, locked modes	R. La Haye	HBT-EP/Columbia Univ.	G. Navratil
	R. La Haye	IFS	R. Fitzpatrick
	R. La Haye	Culham	T. Hender
	R. La Haye	JET	A. Santagiustina
	R. La Haye	Columbia University	G. Navratil
Active mode control	R. La Haye	IFS	R. Fitzpatrick
	R. La Haye	PPPL	M. Okabayashi
Wall stabilization	E. Strait	Columbia University	G. Navratil, A. Garofalo
Disruption database	A. Kellman	PPPL	A. Reimann
Runaway electrons	A. Kellman	UC-San Diego	S. Luckhardt
Disruption simulation	D. Humphreys	TRINITI	R. Khayrutdinov
Disruption analysis and visualization	E. Strait	TRINITI	I. Semenov
MSE measurements	B. Rice	ASDEX-U	R. Wolfe
	B. Rice	JET	N. Hawkes
	B. Rice	JAERI/JT-60U	T. Fujita

**TABLE 2.6–7**  
**DIII–D COLLABORATIONS RELATED TO TRANSPORT AND FLUCTUATIONS**

Topic	DIII–D Contact	Collaborating Institution	Key Collaborator
Reflectometry, FIR scattering	K. Burrell/	UCLA	E. Doyle <sup>(a)</sup>
ECE fluctuations	R. Groebner		C. Rettig <sup>(a)</sup>
L–H and core barrier physics			T. Rhodes <sup>(a)</sup>
Leader of UCLA effort; member of DIII–D Executive Committee			W.A. Peebles
Midplane and X–point Langmuir probes	K. Burrell/	UCSD	J. Boedo <sup>(a)</sup>
L–H transition physics	R. Groebner		R. Lehmer <sup>(a)</sup> R. Moyer <sup>(a)</sup>
Theory of transport barrier formation and fluctuation suppression	Many people		P. Diamond
Beam emission spectroscopy; transport barrier physics	K. Burrell	U. Wisc.	G. McKee <sup>(a)</sup> R. Fonck
Phase contrast imaging	K. Burrell	MIT	P. O’Shea <sup>(a)</sup>
Theory of E×B shear decorrelation	K. Burrell	PPPL	T.S. Hahm
Transport barrier physics, CER analysis	K. Burrell/ R. Groebner		E. Synakowski
Leader of working group on testing theory-based models	D. Schissel		E. Fredrickson <sup>(a)</sup>
Dimensionless scaling	T. Luce		S. Scott S. Batha D. Mikkelson
Neutral effect on L–H transition	R. Groebner/	ORNL	B. Carreras
Core transport barrier physics	K. Burrell		L. Owen
Helium and impurity particle transport	Many people		M. Wade <sup>(a)</sup>
Test of theory-based transport models	D. Schissel	U. Wisc.	M. Kissick J. Callen
Comparison of JT–60U and DIII–D core transport barriers	K. Burrell	JT–60U	Y. Koide
Dimensionless scaling	T. Luce/C. Petty	JET	G. Cordey B. Balet
Dimensionless scaling	T. Luce/C. Petty	MIT	M. Greenwald S. Wolfe
Dimensionless scaling	T. Luce	ITER–JCT	R. Perkins
Test of theory-based transport models	D. Schissel	U. Texas	R. Bravanec

<sup>(a)</sup>On-site personnel.

**TABLE 2.6-8**  
**RECENT COLLABORATIONS RELATED TO DIII-D WORK (FORMAL AND INFORMAL)**  
**IN THE WAVE/PARTICLE TOPICAL AREA**

Topic	DIII-D Contact	Collaborating Institution	Key Collaborator
ICRF, ECH	R. Prater	ORNL	M. Murakami, F. Jaeger
ICRF technology	J. deGrassie		F.W. Baity
ECH, ICRF	R.Prater, J. deGrassie	PPPL	S. Bernabei, J. Rogers, J. Hosea
ICRF technology	W. Cary		N. Greenough
ECE	R. Prater	U. Maryland	G. Garstka, R. Ellis
ECE	R. Prater	U. Texas	M. Austin, G. Cima
ICRF, ECH physics	R. Freeman	MIT	M. Porkolab
ECH technology	R. Freeman		R. Temkin
ICRF	R. Pinsker		Y. Takase
ECH	J. Lohr, R. Prater	FTU/ANEA	M. Zerbini
ECH	R. Prater	Tore Supra	G. Giruzzi
ECH	R. Callis	JT-60U	K.Takahashi, K. Kikuchi
FWCD, ICRF	R. Pinsker	LHD	R. Kumazawa
FWCD	C.Petty,R.Pinsker	JFT-2M	T. Ogawa
ICRF technology	J. deGrassie	Asdex-U	F.Wesner
ICRF technology	W. Cary		F. Braun
ECH modeling	Y.R. LinLiu	TdeV	G. Leclair
ECH	R. Prater		Y. Demers
CD physics	P. Politzer	U. Wisconsin	C. Forest
ECH technology	R. Callis		R. Vernon
NTM stabilization	Y.R. LinLiu		J. Callen, C. Hegna
ICRF physics	J. deGrassie	UCSD	T.K. Mau
ECH physics	J. Lohr	T-10	K. Razumova
X-ray diagnostic	J. Lohr		V. Trukhin
QED physics	T. Luce	LLNL	P. Biersdorfer
RF modeling	Y.R. LinLiu	TCV	O. Sauter
RF modeling	R. Prater	CompX	R. Harvey
ICRF fast ions	C. Petty	U.C. Irvine	B. Heidbrink
RF/transport	R. Pinsker	TTF	B. Carreras, J. Callen
ECCD, NTM stabilization	R. Prater, R. La Haye	ITER JCT	R. Perkins
ECH technology	R. Freeman	IAP	A. Litvak
ECH technology	D. Remsen	KFA	M. Thumm

**TABLE 2.6–9**  
**DIII-D COLLABORATIONS RELATED TO DIVERTOR AND BOUNDARY PHYSICS**

Topic	DIII-D Contact	Collaborating Institution	Key Collaborator
Divertor physics	R. Stambaugh	LLNL	S. Allen
Detached plasmas	T. Leonard	LLNL	M. Fenstermacher
Data acquisition	D. Schissel	LLNL	T. Casper
Heat flux	T. Leonard	LLNL	C. Lasnier
Theory	G. Staebler	LLNL	W. Nevins
Diagnostic engineering	R. Snider	LLNL	D. Nilson
Modeling	R. Stambaugh	LLNL	G. Porter
Modeling — UEDGE	M. Mahdavi	LLNL	M. Rensink
Modeling	P. West	Dickinson College	M. Wolfe
Theory	G. Staebler	LLNL	R. Cohen
Pellet injection	M.A. Mahdavi	ORNL	L. Baylor
Neutrals	G. Jackson	ORNL	R. Colchin
Neutral modeling	M.A. Mahdavi	ORNL	L. Owens
Impurity modeling	P. West	ORNL	J. Hogan
Helium	P. West	ORNL	D. Hillis
Spectroscopy	P. West	ORNL	R. Isler
Pellet injector	R. Snider	ORNL	T. Jernigan
Density limits	M.A. Mahdavi	ORNL	R. Maingi
Divertor physics	R. Stambaugh	ORNL	P. Mioduszewski
Impurity transport	P. West	ORNL	M. Wade
Spectroscopy	P. West	PPPL	A. Ramsey
Langmuir probes	M.A. Mahdavi	SNLA	J. Watkins
Surface physics	R. Stambaugh	SNLA	M. Ulrickson
Surface erosion	C. Wong	SNLL	R. Bastasz
Modeling	M.A. Mahdavi	INEL	D. Knoll
Langmuir probe	T. Leonard	UCSD	R. Lehmer
Turbulence	K. Burrell	UCSD	R. Moyer
Plasma flows	P. West	UCSD	J. Boedo
Surface erosion	C. Wong	UCSD	D. Whyte
Edge density	K. Burrell	UCLA	E. Doyle
Divertor physics	R. Stambaugh	MIT	B. Lipschultz
Modeling	G. Staebler	MIT	S. Krashenninikov
Recombination	T. Leonard	MIT	J. Terry
Spectroscopy	P. West	Hampton U.	N. Jaluka
Modeling	T. Evans	Hampton U.	A. Punjabi
Divertor bias	G. Staebler	Tsukuba U.	T. Tamano
Spectroscopy	N. Brooks	Troitsk	S. Tugarinov
Surface physics	P. West	Troitsk	I. Opimach
Materials	P. West	Troitsk	O. Buzhinski
Erosion	P. West	KFA	V. Phillips
ITER experts	R. Stambaugh	JET	G. Vlases
Divertor physics	R. Stambaugh	JET	G. Matthews
Bolometry	T. Leonard	JAERI	S. Konoshima
New divertors	R. Stambaugh	JAERI	N. Hosogane
ITER experts	R. Stambaugh	JAERI	M. Shimada
Closed divertor	T. Leonard	JAERI	S. Sakarai
IR measurements	T. Petrie	JAERI	K. Itami
ELMs	T. Leonard	IPP Garching	H. Bosch
ITER experts	R. Stambaugh	IPP Garching	J. Neuhauser
Modeling	M.A. Mahdavi	IPP Garching	R. Schneider
Tangential TV	P. West	CCFM	G. Pacher
Theory	G. Staebler	Tore Supra	Ph. Ghendrih
Modeling	P. West	U. Toronto	P. Stangeby

**TABLE 2.6–10**  
**PROGRAMMATIC RESPONSIBILITIES OF MAJOR DIII-D U.S. COLLABORATORS**

<p><b>LLNL</b></p> <ul style="list-style-type: none"> <li>• Lead role in edge and divertor physics, diagnostics, and modeling</li> <li>• Leads radiative divertor program</li> <li>• Active role in advanced tokamak with current profile measurement (MSE)</li> <li>• Operates remote experimental station</li> </ul> <p><b>ORNL</b></p> <ul style="list-style-type: none"> <li>• Leads helium transport studies</li> <li>• Leads pellet injection program</li> <li>• Active role in divertor program</li> <li>• Active role in AT with pellet and FWCD ICRF hardware and modeling</li> </ul> <p><b>UCLA</b></p> <ul style="list-style-type: none"> <li>• Leads fluctuation studies</li> <li>• Divertor diagnostics</li> </ul>	<p><b>PPPL</b></p> <ul style="list-style-type: none"> <li>• Disruption studies</li> <li>• Advanced tokamak studies</li> <li>• ICRF support and profile control studies</li> <li>• Diagnostics</li> <li>• Tokamak operations and data analysis software development</li> </ul> <p><b>UCSD</b></p> <ul style="list-style-type: none"> <li>• Active role in divertor program</li> <li>• Participates in disruption studies</li> <li>• L–H transition physics</li> </ul> <p><b>SNL</b></p> <ul style="list-style-type: none"> <li>• Active role in divertor program</li> <li>• Plasma wall characterization</li> </ul>
---	--

**TABLE 2.6–11**  
**PROGRAMMATIC ROLES OF DIII-D UNIVERSITY COLLABORATORS (1997)**

<p><b>Cal Tech</b></p> <ul style="list-style-type: none"> <li>• Microwave waveguide components</li> </ul> <p><b>Columbia U.</b></p> <ul style="list-style-type: none"> <li>• High beta NCS</li> <li>• Wall stabilization</li> </ul> <p><b>Hampton U.</b></p> <ul style="list-style-type: none"> <li>• UV Imaging Diagnostics</li> </ul> <p><b>Johns Hopkin U.</b></p> <ul style="list-style-type: none"> <li>• Spectroscopic diagnostic development</li> </ul> <p><b>Lehigh U.</b></p> <ul style="list-style-type: none"> <li>• Transport modeling</li> </ul> <p><b>MIT</b></p> <ul style="list-style-type: none"> <li>• Fast wave current drive experiments</li> <li>• Phase contrast imaging long wavelength fluctuation diagnostic</li> </ul> <p><b>Moscow State U.</b></p> <ul style="list-style-type: none"> <li>• MHD code development and modeling</li> </ul> <p><b>UC Berkeley</b></p> <ul style="list-style-type: none"> <li>• CORSICA transport modeling (LLNL)</li> </ul> <p><b>UC Irvine</b></p> <ul style="list-style-type: none"> <li>• Neutron and fusion reaction and charge exchange diagnostics</li> <li>• Fast ion confinement</li> </ul>	<p><b>UCLA</b></p> <ul style="list-style-type: none"> <li>• Fluctuation diagnostics and H–mode physics</li> <li>• Reflectometer density profile</li> <li>• Heterodyne ECE — <math>\tilde{T}_e</math></li> <li>• Divertor reflectometer</li> <li>• ICRF wave physics</li> </ul> <p><b>UCSD</b></p> <ul style="list-style-type: none"> <li>• Advanced divertor and fast edge probes</li> <li>• Disruption and PMI studies</li> <li>• H–mode physics</li> </ul> <p><b>U. Maryland</b></p> <ul style="list-style-type: none"> <li>• Vertical and horizontal ECE measurements</li> </ul> <p><b>U. Texas</b></p> <ul style="list-style-type: none"> <li>• Transport experiments and modeling</li> <li>• Fine spatial/temporal scale ECE temperature measurements</li> <li>• BES turbulence studies</li> </ul> <p><b>U. Washington</b></p> <ul style="list-style-type: none"> <li>• Divertor bias and helicity</li> </ul> <p><b>U. Wisconsin</b></p> <ul style="list-style-type: none"> <li>• Neoclassical MHD BES fluctuation diagnostic</li> <li>• Pegasus</li> <li>• MST</li> </ul>
--	---

**TABLE 2.6–12**  
**PROGRAMMATIC ROLES OF OTHER COLLABORATIONS**

<b>ANL</b>	<b>KFA (Germany)</b>
Divertor erosion	Plasma wall interaction studies
Vanadium materials properties	<b>Academia Sinica (China)</b>
<b>Cadarache (France)</b>	Scientist exchanges
Coordinated experiments with Tore Supra	<b>Kurchatov Institute (Russia)</b>
<b>CompX</b>	Hard x-ray diagnostic instrument
Fokker-Planck modeling	Transport theory
<b>CPI (Varian)</b>	<b>LANL</b>
Gyrotron operation	MHD and UEDGE theory and modeling
<b>Gycom</b>	<b>MIT</b>
Gyrotron operation	Coordinated experiments with C-Mod
<b>INEL</b>	<b>Orincon</b>
Reliability studies	Disruption neural net
<b>IPP (Germany)</b>	<b>PNL</b>
Coordinated experiments with ASDEX-U	Vanadium material properties
<b>JAERI (Japan)</b>	<b>PPPL</b>
Integrated physics and control of high performance steady state tokamaks	NSTX working groups
<b>JET (EU)</b>	KSTAR
Coordinated experiments with JET	<b>Southwestern Institute (China)</b>
<b>KAIST (Korea)</b>	Scientist exchanges
Divertor electron energy analyzer	<b>Troitsk (Russia)</b>
<b>Keldysh Institute (Russia)</b>	Disruption modeling
MHD modeling and disruption studies	<b>Tsukuba U. (Japan)</b>
	Soft x-ray diagnostic detectors

National laboratories strive to bring their multidisciplinary capabilities to bear on critical areas of fusion physics and enabling technologies with universities with fusion and plasma science expertise bring unique academic capabilities to bear on critical areas of fusion science to deepen the fusion knowledge base. DIII-D is an international class fusion facility, ideal for training students and postdoctoral researchers. As members of the DIII-D Program, collaborating institutions retain their institutional identity.

**General Atomics Institutional Strengths.** GA is one of the world's largest privately owned centers for research and development in diversified energy and defense projects, conducting its research and development on a 120-acre site in La Jolla, California. It is the primary developer of gas-cooled nuclear power reactor technology in the U.S. and carries out the world's largest and most successful Fusion Program in private industry. Other GA R&D includes aeronautic defense systems, accelerator systems, nuclear space power, and advanced materials. Jointly with the University of California, San Diego, GA operates the San Diego Supercomputer Center for NSF.

GA's fusion experience began in 1957 under private GA funding and funding from the Texas Atomic Energy Research Foundation. Since that time, GA has designed, built, and operated numerous experimental devices including pinches, multipoles, and the Doublet series of tokamaks. In recent years, emphasis of the GA Fusion Program has been the development of toroidal magnetic confinement systems. GA has designed and built a series of increasingly sophisticated fusion machines culminating in the present DIII-D. The GA Fusion Group has the personnel and equipment required for research and development in all forms of magnetically confined fusion, including the full range of disciplines and technologies applicable to the proposed DIII-D Fusion Research Program.

The GA DIII-D team has a proven track record in fusion engineering, operations, and physics. Areas of exceptional GA engineering strength include divertor, microwave, power conversion, plasma control, plasma diagnostics, and vacuum systems. GA has an experienced multidisciplinary team responsible for operation of the DIII-D facility which includes: (1) tokamak magnet and vacuum systems with associated power and cryogenic systems; (2) neutral beam, radio frequency and microwave plasma heating systems; (3) plasma diagnostic instrumentation construction and operation; and (4) data acquisition, storage, and retrieval. The GA physics team includes experimentalists, diagnosticians, and theorists with areas of strength including advanced tokamak physics, plasma control, physics high beta MHD physics, H-mode physics, transport analysis and modeling, divertor physics development, ECH and rf heating and current drive, theory, and diagnostic development. Collaborating institutions provide engineering operations and physics expertise in areas in which they have institutional strengths to complement those of GA.

The DIII-D National Facility is a self-contained and integrated plant designed to provide all the equipment and services necessary to operate the DIII-D tokamak. It includes a large building to house the DIII-D device, the control room, offices, support shops, and auxiliary equipment. There also is a diagnostic laboratory and other buildings. The hardware attached to this facility includes motor generators and utility power, power converters and regulators, computer control and data acquisition systems, vacuum systems, and cooling and cryogenic systems.

Since the beginning of its Fusion Program in 1957, GA has invested corporate funds in the development of theoretical and experimental understanding of fusion plasmas and the requisite fusion technologies. It is worth noting that GA invests over a million dollars annually of IR&D funds in fusion science and technology programs that benefit the U.S. Fusion Program and the proposed DIII-D Fusion Research Program.

**Sandia National Laboratories Institutional Strengths.** Sandia has served for more than 50 years as one of the major national defense R&D labs, starting in 1945 in Albuquerque, New Mexico, as part of the Manhattan Project, which built the first nuclear weapons. Today, Sandia has two primary facilities: one in Albuquerque and one in Livermore, California. Sandia employs about 7500 people, are funded primarily by the U.S. DOE, and work closely with many U.S. government and industry groups to make contributions to preserve the nation's security. Sandia constantly explores new opportunities to team with government, industry, and university partners in this mission.

The Energy and Environment Sector contributes effective science and engineering solutions that improve national energy security and the quality of our environment. Sandia's current responsibilities include energy research, applied energy (fossil energy and renewable energy), nuclear energy, nuclear waste management, and environmental programs. Sandia conducts many projects supported through DOE's Office of Energy Research that contribute to DOE's science and technology mission. These projects include established activities in the basic energy sciences such as materials science, chemical sciences, geosciences, scientific computing, and magnetic fusion energy.

The goal of Sandia's Magnetic Fusion Energy Program is to develop a technology base to support the design of in-vessel components that will perform satisfactorily in fusion plasma environments. To achieve this goal, Sandia studies the interactions of plasmas and materials, the behavior of materials and components exposed to high heat fluxes, and the interfaces of plasma and fusion reactor walls. The components developed by Sandia have been tested in tokamaks both in the U.S. and internationally. It has fabricated a full toroidal belt Advanced Limiter Test (ALT-II) system for the TEXTOR tokamak in Germany, and an actively cooled pump limiter on the Tore Supra tokamak in France that is capable of steady state operation at 30 MW/m<sup>2</sup>. Sandia also has extensive expertise and diagnostics for materials studies. Plasma edge studies using diagnostics designed for high heat flux are being conducted in the DIII-D tokamak to assess the plasma boundary layer. Models have been developed to predict plasma conditions and component behavior for the next generation of devices such as ITER.

**Princeton Plasma Physics Laboratory's Institutional Strengths.** The PPPL is a collaborative national center for plasma and fusion science, devoted to innovation and scientific understanding leading to an attractive energy source. An associated mission is to conduct frontier research on the physics of plasmas, exploit this research for diverse applications, and provide the highest quality education in plasma science.

PPPL is the only single purpose laboratory funded by the U.S. DOE for the development of magnetic confinement fusion and for research in the underlying discipline of plasma science. The laboratory has a highly skilled work force and extensive capabilities for the experimental and theoretical study of fusion plasmas, and for the integrated design, fabrication, and operation of experimental plasma facilities including magnets, power supplies, plasma heating, and diagnostics systems. Management by Princeton University provides the institutional framework for a broad laboratory based program of education in plasma physics and related science and technology.

The core competencies of the PPPL work force that enable the Laboratory to achieve its objectives are listed below under the categories of plasma science and technology, engineering, and education.

#### **Plasma Science and Technology**

- Experimental analysis of stability and confinement in fusion plasmas.
- Plasma theory for fusion and other applications.
- Computational physics and numerical simulation of plasma processes.

- Physics design of experimental plasma confinement facilities.
- Physics and technology of plasma heating and current-drive, especially involving radio-frequency techniques.
- Physics and technology of plasma diagnostics and instrumentation.
- Physics and technology of plasma applications to advance industrial technologies.

### Engineering

- Engineering design and analysis of experimental plasma confinement facilities including magnetics, neutronics, and thermal and structural analysis.
- Systems integration and construction management for experimental plasma confinement facilities.
- Operation of experimental plasma confinement facilities.
- Mechanical engineering, including structures, vacuum, cryogenic, and tritium systems.
- Computer engineering, including data-acquisition, instrumentation, and controls systems.
- Electrical/electronic/electro-optic engineering, including power conversion, diagnostic, and radio-frequency systems.
- Environmental, safety, and health aspects of the operation and decommissioning of activated experimental fusion devices, including tritium operations.

### Education

- Provision of faculty for an integrated program of courses and research supervision for graduate students in plasma physics and related science and technologies.
- Implementation of a broad, Laboratory-based program of science education for the community at large, including undergraduate and pre-college science students and science and mathematics teachers at all levels.

**University of California, Los Angeles' Institutional Strengths.** UCLA, where the internet was born, is one of the worlds most outstanding and diverse public universities, and has been a leader in plasma fusion research and development for over 30 years. In both experimental and theoretical research, UCLA has been a pioneer. For example, computer simulation of plasmas, plasma diagnosis in the far-infrared spectral region, Taylor discharge cleaning, and biased H-mode in tokamaks are just a few examples of the many outstanding contributions made by UCLA faculty, research staff, and students over the years. UCLA plays a major role within the DIII-D Program in the education of students in plasma physics, fusion science, and millimeter/FIR technology. Over the past nine years *four* outstanding UCLA Ph.D Theses have been generated through participation in the DIII-D Program. Two of the these directly led to Invited Talks for the *students* at the APS Plasma Physics Divisional Meetings.

UCLA's primary scientific contributions, to date, in the DIII-D National Program have been in the areas of unraveling the mysteries of anomalous transport and identifying the roles of microturbulence and ExB sheared turbulent flow. It has played the leading collaborative role in the investigation of microturbulence on DIII-D. To this end it has brought to DIII-D an unrivaled capability in the area of millimeter wave and far-infrared plasma diagnosis and technology. UCLA has developed, operated, and maintained millimeter-wave reflectometry and far-infrared scattering systems to determine turbulent correlation lengths, monitor the evolution of turbulence, determine electron density profiles, and monitor ICRF waves internal to the plasma. Systems have been developed for the boundary region, including the divertor, as well as deep into the core of high performance DIII-D plasmas.

The UCLA Advanced Diagnostic Development Group has a strong permanent presence at DIII-D, but is also affiliated with the Electrical Engineering Department and the Institute of Plasma and Fusion Research at UCLA. This affords close interaction with a number of outstanding UCLA faculty and research staff, including such pioneers as Frank Chen, John Dawson, Chan Joshi, Walter Gekelman, and Bob Taylor. Some of the facilities at UCLA that directly benefit the DIII-D National Facility are described below.

The **Tokamak Fusion Laboratory** directed by Dr. Robert Taylor. This laboratory currently houses the LCT-1 tokamak and a sector of the approved "Electric Tokamak" — the LCT-2 device. Drs. Taylor and Peebles have a long-standing record of collaboration and joint publications. This will continue and flourish within the planned LCT-2 Physics Program, which will be housed in a new Science and Technology Building at UCLA. The size ( $R \sim 5$  m,  $a \sim 1$  m) and flexibility will allow *low-cost*, advanced diagnostic development to be performed that is relevant to LCT-2, ITER and DIII-D.

The **Large Plasma Device** laboratory directed by Prof. Walter Gekelman (Physics Department). This large (10 m long, 50 cm diameter) magnetized, linear plasma device is housed within the Institute of Plasma & Fusion Research. Strong collaboration with the LAPD Group is ongoing and involves development of new diagnostic systems related, for example, to internal magnetic field measurement.

The **Center for High-Frequency Electronics** directed by Prof. Chan Joshi is within the Electrical Engineering Department. The Center is a state-of-the-art instrumentation facility that is available to members of the department. Millimeter-wave test equipment is available in a frequency range from 10 to 300 GHz. In addition, equipment can be borrowed from the center thereby allowing prototype experiments to be performed without requiring the purchase of expensive equipment. This has significantly enhanced the UCLA capabilities at DIII-D.

The **Nano-Electronics Laboratory** directed by Prof. E. Yablanovich is a state-of-the-art microelectronics facility primarily for graduate research. The facility supports research on the nanometer scale by providing access to clean rooms and to solid-state processing equipment. Access is based on a low monthly fee combined with hourly charges for specific equipment. Again this has leveraged UCLA's capabilities in development of new millimeter-wave diagnostic systems.

The **School of Engineering Machine Shop** under the direction of Steve Grubweiser has extensive capabilities. Electric discharge machining (EDM) allows for fabrication of various waveguide components such as waveguide tapers, corner cube mixers, spacers, etc. Computer controlled mills and lathes are utilized in the fabrication of dichroic lenses, quasi-optical lenses and mirrors and myriads of other components.

**University of California, San Diego's Institutional Strengths.** The UCSD Fusion Energy Research Program was founded in 1994 as an interdepartmental program within the School of Engineering with affiliates in the Department of Physics. The program is dedicated to research in the fusion energy sciences including plasma physics, boundary plasma flows and turbulence, plasma-materials interactions, fusion technology, and power plant design and engineering. Approximately forty faculty, researchers, and students are currently affiliated with the UCSD Fusion Program.

The Fusion Program is organized into three research divisions: (1) Experimental Programs including the on-campus PISCES plasma and materials experiments and the off campus collaboration programs with the DIII-D tokamak group and the TEXTOR tokamak experiment at KFA Karlsruhe; (2) Fusion Power Plant Studies including team leadership for a national program involving participation from several national laboratories, universities, and industrial partners; and (3) U.S. ITER Home Team, and UCSD site. ITER is an international effort to construct a long-pulse burning plasma experiment. The U.S. Home Team has a major role in the ITER technology R&D programs for the Central Solenoid Model Coil and the Divertor Cassette and supporting roles for other ITER R&D activities.

The Fusion Experimental Program facilities include on-campus PISCES A and B experiments which provide steady-state plasma simulation of the boundary regions of a fusion reactor, with maximum densities in the range of  $10^{19}$ – $10^{20}$  m<sup>-3</sup>. These facilities serve as a test bed for validating physical models of boundary plasma flows, turbulence, atomic processes, and sheath phenomena. These facilities are particularly useful in studies of plasma-materials interactions where steady-state particle and heat flux conditions comparable to ITER or reactor conditions are generated. These plasma-materials experiments are part of a coordinated international research program to investigate candidate materials for use in ITER including beryllium, tungsten and carbon materials.

USCD researchers and students carry out collaborative experiments in major large-scale off-campus fusion facilities. These include boundary and divertor plasma physics, fast reciprocating probe measurements of boundary plasmas and turbulence, materials, and disruption studies at the GA DIII-D tokamak, and boundary control and flow measurements on the Forschungszentrum Julich TEXTOR tokamak.

**Lawrence Livermore National Laboratory's Institutional Strengths.** LLNL is a multi-disciplinary institution with highly skilled physicists, engineers, and technical staff working in a matrix organization. LLNL has worked in magnet fusion since the early 1950s; starting with the mirror program and then moving to the MTX Tokamak program and presently the DIII-D collaboration. LLNL is currently starting a new spheromak experiment.

The LLNL Magnetic Fusion Energy Program has overall goals in tokamak improvement, alternate concept devices, and increased reliance on computational models. It has a separately-funded fusion theory division that looks at both analytical and computational models of a broad range of fusion topics. The UEDGE (edge) and CORSICA (core) computer models have been developed in this division. It also has called upon other strength areas within LLNL, including computational support (including LLNL hardware), atomic physics calculations and spectroscopic measurements, and optics design (from the laser program).

The LLNL collaboration uses a task-oriented approach, with direct funding from DOE. Yearly, it agrees on a set of useful tasks and these are implemented, budget permitting. The breadth of LLNL allows us to bring a “full service” collaboration to DIII-D. It has physicists, engineers, and technicians on-site in San Diego. (Over half of our staff are located in San Diego.) Difficult machining and assembly can be done at LLNL when necessary. It also has a computational staff that travel to San Diego as necessary, and has developed a Remote Experimental Environment. Experiments have been operated on the C-Mod tokamak at MIT and the DIII-D machine from LLNL. These are all experienced people who have a demonstrated history of diagnostics, analysis, and modeling of fusion plasmas.

LLNL has supplied a large number of diagnostic instruments to the DIII-D experiment, including: Motional Stark Analysis (arguably the best system in the world), Divertor Thomson Scattering (only system in the world), a 2-D Bolometer with tomographic reconstruction, 2-D visible measurements with tomographic reconstruction, infrared measurements of divertor and wall heat flux, and divertor ultraviolet spectroscopy (absolutely calibrated). It has used these instruments, along with the UEDGE model, to develop a physics picture of the divertor. LLNL is presently predicting the operation of future divertors for DIII-D with UEDGE. In the advanced tokamak area, it has used the MSE diagnostic to measure  $J(r)$  and  $E(r)$  in the plasma, and to model these measurements with the CORSICA model. LLNL is currently developing future operational scenarios for DIII-D with the planned machine upgrades.

In all, LLNL has used its strong institutional strengths, along with the particular strengths of the MFE staff to study important physics on fusion machines. The task-oriented style has allowed very close coupling with the needs of the DIII-D Program, and also allows LLNL to focus on key physics topics.

**Oak Ridge National Laboratory's Institutional Strengths.** ORNL is one of the largest multi-purpose national laboratories in the United States; it has a history of more than 50 years of broad-based R&D. Today, ORNL is managed for the DOE by the Lockheed Martin Corporation. ORNL's core competencies are characterized by an integration of physical, chemical, and materials sciences; biological, environmental, and social sciences; and computational sciences and informatics. A distinguishing strength of the national laboratories is the ability to integrate broad technical foundations to develop and sustain core competencies in support of national R&D goals. The ORNL core competencies relevant to the Fusion Program are: energy production and end-use technologies; advanced materials synthesis, processing, and characterization; neutron-based science and technology; computational science and advanced computing; and instrumentation, manufacturing, and control technology. The DOE's Office of Energy Research is the

largest single sponsor of research at ORNL. It supports programs in magnetic fusion energy, high-energy and nuclear physics, and biomedical and environmental research.

The ORNL Fusion Program is distinguished by the breadth of its components subprograms in physics, technology, and engineering, and by extensive collaboration, both nationally and internationally. ORNL's fusion experience began in 1957. Since then, ORNL has had an active Fusion Research Program with experimental devices such as tokamaks (ORMAK, ISX-A, and ISX-B), Stellarators (ATF), and mirrors (DCX and Elmo Bumpy Torus); plasma and fusion technology development (NBI, rf launchers, pellet injectors, superconducting magnets); neutron-interactive materials development (HFIR); atomic physics for fusion research, and fusion engineering and design (FEDC).

Presently, ORNL supports the goals of the national fusion research through topical programs in the following areas:

- Experimental and theoretical studies aimed at understanding the science of fusion plasmas.
- Development of plasma technologies for existing and future experiments (pellet injectors and rf launchers).
- Engineering design of fusion components and devices.
- The development of radiation-resistant and low-activation materials.

Fusion research at ORNL is carried out in several ORNL divisions (Fusion Energy, Physics, Metals and Ceramics) and is organized by the following program elements:

**Confinement.** Addressing toroidal confinement issues through collaborations on experimental devices in the areas of plasma boundary physics, pellet fueling, wave-plasma interactions, confinement and stability, and alternate concept development.

**Spherical Torus.** Exploring compact, stable low-field plasma configurations characterized by good confinement, high plasma beta levels, and a self-driven current fraction of the order unity.

**Theory.** Emphasizing understanding of plasma confinement in tokamaks and stellarators, and on the development of alternative toroidal confinement concepts.

**Atomic Physics.** Focusing on experimental and theoretical studies of inelastic collision processes involving atomic and molecular fusion plasma impurity ions.

**Plasma Technologies.** Developing and applying (1) advanced fueling systems for magnetic fusion with the long-range goal to develop ultra-long to steady state pellet injection systems for fusion devices; (2) rf systems for heating and current drive for present and future machines that are cost-effective and compatible with operation in fusion power plants.

**Materials Program.** Aiming at the development of structural materials, ceramic, and first-wall and high-heat-flux materials for fusion applications.

All elements of the ORNL Fusion Program have active collaborations on the major fusion facilities of the national and world fusion program, such as DIII-D, NSTX, JET, Tore Supra, ASDEX-Upgrade, and TEXTOR in Europe, as well as on LHD and JT-60U in Japan. The expertise gained in these collaborations constitutes a very cost-effective extension of the achievements within the U.S. Fusion Program and greatly contributes to the progress of our domestic fusion machines such as the DIII-D tokamak

## 2.6.4. DIII-D NATIONAL PROGRAM GOVERNANCE

**2.6.4.1. DIII-D NATIONAL PROGRAM GOVERNANCE STRUCTURE.** As the collaborations expanded, a system of governance has also developed. The primary governing body is the DEC, which advises the DIII-D program director on matters of program planning, direction, task priorities, and budgets. The committee is comprised of the DIII-D program director, division directors, and the program leaders from the major collaborating institutions selected by their respective Institutional Leadership. A multi-institutional Research Planning Committee develops and reviews the Annual Experimental Plan and reviews, approves, and schedules experiments. A DIII-D Advisory Committee consisting of technical experts from other national and international fusion programs provides advice at least annually to the DIII-D Program and Executive Committee on Experimental Plans and other major programmatic issues. This system of governance is working well. The plan for the period 1998–2003 envisions expanding the collaboration along its present lines.

The DIII-D Program management organization structure is illustrated in Fig. 2.6–4. The DIII-D Program is implemented through a line management organization structure which includes GA and collaborators. The program is implemented through four research divisions (Operations, Core Physics, Boundary Physics and Technology, and RF Physics and Technology), headed by division directors. The research divisions include GA employees and employees of other laboratories, universities, and industries. Coordinators (group leaders) and task leaders (responsible for specific tasks) are drawn from GA or collaborators. By mutual agreement, each collaborator is a member of one of the DIII-D divisions. On-going issues of institutional roles and relationships in the DIII-D Program are resolved between GA and collaborating Institutional Leadership. Program execution flows through the DIII-D Program management.

GA has contractual responsibility to the DOE for operation of the DIII-D, and DOE retains the final approval authority on all modifications to the machine that would affect its operations. The DIII-D program director is a GA employee. In carrying out its responsibility, GA strives to accommodate collaborators interests and concerns. Proposals for research on the device, modifications, or implementation are discussed by the DIII-D Executive Committee and approved by the DIII-D program director prior to presentation to the community or submittal to the DOE for approval.

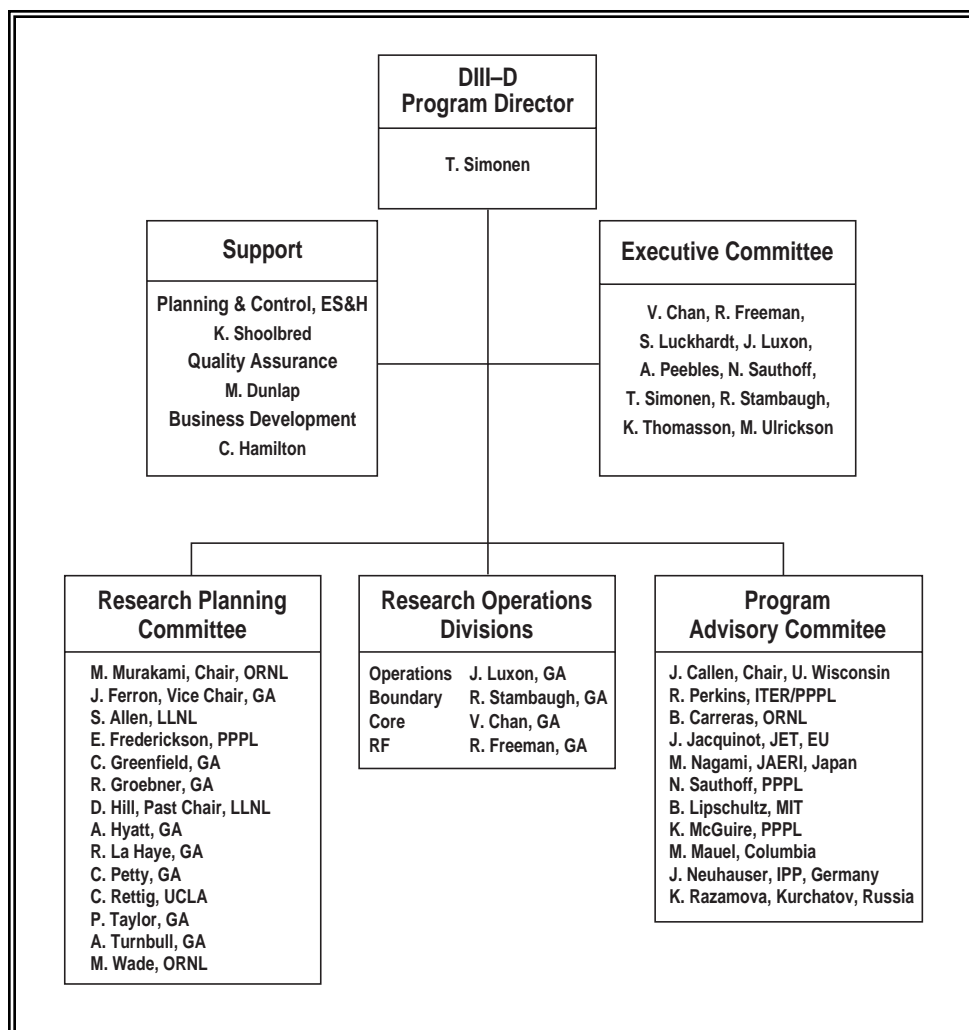


Fig. 2.6-4. The DIII-D program is implemented through a line management organization which includes collaborators and four GA research divisions (December 1997).

**The DIII-D Executive Committee.** The principal governing body is the DEC. It advises the DIII-D program director on matters of program planning, direction, task priorities, and budgets. It oversees the activities of the Research Planning Committee. It oversees major modifications to the core tokamak facility and auxiliary systems. Proposals for new collaborations are brought to the DEC for recommendation to the director. The committee is comprised of the DIII-D program director, division directors, and the program leaders from major collaborating institutions selected by their respective Institutional

Leadership. Members are appointed by the DIII-D director. The DEC provides advice to the DIII-D director on changes in its own membership. The current membership is:

**MEMBERSHIP OF THE DIII-D EXECUTIVE COMMITTEE  
DECEMBER 97**

Institution	Member
General Atomics	Tom Simonen Vincent Chan Dick Freeman Jim Luxon Ron Stambaugh
Lawrence Livermore National Laboratory	Keith Thomassen
Princeton Plasma Physics Laboratory	Ned Sauthoff
Oak Ridge National Laboratory	Peter Mioduszewski
Sandia National Laboratory	Mike Ulrickson
University of California at Los Angeles	Tony Peebles
University of California at San Diego	Stan Luckhardt

**The Research Planning Committee.** A DIII-D Research Planning Committee develops and reviews the Annual Experimental Plan, reviews and approves mini-proposals, and participates in scheduling experiments. The Research Planning Committee consists of DIII-D Program researchers from GA and collaborating institutions. The chairman is appointed by the DIII-D director upon the advice of the DIII-D Executive Committee and is also responsible for the weekly and daily scheduling and rescheduling of experiments.

**The DIII-D Advisory Committee.** A DIII-D Advisory Committee is selected by the GA senior vice president in consultation with the DIII-D program director and the Executive Committee. The committee consists of technical experts from other national and international fusion programs to provide external peer review of the DIII-D Program and Experimental Plans. Written comments are provided to the DIII-D director with copies to the DOE and Institutional Leadership. Each year, approximately one-third of the membership will be new. The committee meets in January or February and usually also in the summer.

#### 2.6.4.2. RESEARCH PROGRAM PLANNING

**The Long Range Plan.** The DIII-D Program operates with a Long Range Plan (typically five or more years), which is updated annually. Collaborating institutions participate in developing the strategy and implementation of these plans and setting priorities. This plan is reviewed by the Executive Committee, approved by the DIII-D director, assessed by the DIII-D Program Advisory Committee, and approved by DOE. It is the foundation for annual experiment plans and annual Field Work Proposals submitted to DOE.

**The Annual Experimental Planning Process.** The DIII–D Program operates with an Experimental Plan for each calendar year. Guidelines for the experimental plan are formulated by the DIII–D Executive Committee. The DIII–D Research Planning Committee (RPC) develops and reviews the Annual Experimental Plan. Topical Area Leaders are selected to collect research suggestions in their topical areas. Brainstorming sessions open to the entire research staff are held; proponents present their ideas. The topical area groups refine and collect those ideas. The RPC presents a strawman proposal of experiments to the DEC for ratification. After DEC approval, the RPC then reviews and approves the mini-proposals that implement that plan day-by-day and schedules the experiments. The plan is assessed by the DIII–D Advisory Committee. Progress and changes are tracked at Quarterly DOE Reviews.

**Mini-Proposals.** Mini-proposals are required before any experiment is performed. Mini-proposals are generated by DIII–D Program participant(s) or other sources. The mini-proposal is a brief description of the purpose, theoretical basis, background and consequences of the proposed experiments and specify required resources, shot plan, and hardware requirements. The mini-proposals are reviewed, approved, and prioritized by the Research Planning Committee. Typically, not all approved mini-proposals can be accommodated in the research schedule.

#### 2.6.4.3. MANAGEMENT OF THE COLLABORATIVE NATIONAL TEAM

**General Principles of Collaboration.** The following principles serve as guidelines for conducting institutional collaboration on the DIII–D Program:

1. Advancement of the DIII–D Program is held by all participating institutions to be essential for advancement of U.S. fusion energy science and to be in the interests of all DIII–D program participants.
2. Collaborators will accord high priority to their DIII–D commitments, both in the use of resources and in the assignment of personnel. GA will recognize that some collaborating personnel assigned to DIII–D activities may have additional responsibilities in their home programs.
3. In support of the DIII–D Program objectives, collaborators will be accorded lead responsibilities in defined areas and participation in other areas as spelled out in institutional MOU. “Lead responsibility” does not imply sole responsibility. In those areas where it does not hold a lead, a party may elect to retain a significant minority participation sufficient to develop and sustain expertise in the area. These lead or support roles will be based on consensus assessments of capability and party needs by the program leadership and the DIII–D Executive Committee. Individuals or groups which wish to collaborate on DIII–D should negotiate with the institution who has lead task responsibility. Cases of disagreement should be called to the attention of the director and Executive Committee. Institutions having lead responsibility for a task are not to delegate responsibility to another party without approval of the director.

4. GA will have sole responsibility for operating the DIII-D tokamak. If a collaborator has a lead role involving an auxiliary hardware system on DIII-D, they may undertake the responsibility to operate that system. The scope of the collaborators responsibility in design, construction, and operation of systems will be defined in the individual MOU between GA and collaborating institutions.
5. In order that the DIII-D Program accomplishes its programmatic objectives and the individual researchers have the opportunity to pursue rewarding research, it is generally expected the participants will spend roughly half of their time carrying out program-related support tasks (e.g., operating a diagnostic or acting as a physics operator) and spend the other half of their time pursuing an agreed-upon research program.
6. All data, raw or analyzed, will be considered the property of the DIII-D Program and will be accessible to others in the program. The rights of first authorship will be respected. It is expected that GA and collaborators operating diagnostics or doing specialized analysis will provide data into defined DIII-D databases on a routine basis and to other members of the program when requested.
7. Subject to DOE's technical data rights and patent rights, all data and results from the DIII-D Program will be freely shared and acknowledged between the collaborating parties. In general, all publications or reports must go through the standard GA DIII-D review cycle. However, in the case that the work reported on is principally done by collaborating personnel using collaborators equipment and codes, the publication or report may be submitted through the collaborating institution's review process. In such cases, a copy must be provided for timely courtesy review by the responsible DIII-D research area coordinator and division director. DIII-D division directors will make the determination of the appropriate review channel. Publications and reports will clearly identify that the work was done on the DIII-D tokamak and acknowledge DOE funding support.
8. DOE data and patent rights as specified in GA's contract with DOE will take precedence in all work done on or derived from DIII-D.
9. All GA data, which GA identifies as proprietary, will be protected by individual collaborators and collaborators' institutions.
10. Collaborating institutions are expected to participate in all DIII-D related DOE and community reviews.

**Institutional Agreements.** MOUs are written between GA and major collaborators. MOUs generally cover the historical background that has led to the collaboration, the institutional goals and requirements of both parties for participating in the collaboration, the principles and agreed upon procedures for the collaboration, and a definition of lead and participatory roles for the collaborator. The MOU is signed by the program leaders of GA and the collaborating institution. Presently, MOUs exist between GA and LLNL, UCLA, and ORNL.

**Project Approval Process.** Project Management Plans are developed for facility modifications or upgrades approved by the DEC. DIII-D participants, as well as outside technical specialists, may review project plans and provide advice. Progress, costs, and schedules for special projects are reported at DOE Quarterly Reviews. Both GA and collaborator DIII-D Program tasks will be summarized in common master schedules and milestones.

A manual describing the work procedures for DIII-D tasks and projects is available for all DIII-D personnel and collaborators. It describes a sequence of procedures (93:01 through 93:03) which establish a uniform approach to developing and maintaining new capabilities at DIII-D including designing, engineering, fabricating, installing, and maintaining hardware and equipment on the DIII-D tokamak or any of its related systems. Procedures are also included to guide the performance of work in the machine pit and within the facility. Procedure 93:01, "Initiation and Approval of DIII-D Project or Task Proposals," describes the process for gaining approval of new tasks at DIII-D. Procedure 93:02, "Implementation and Completion of DIII-D Projects and Tasks," and others following, cover the whole span of engineering development from the inception of an idea through the different approval cycles to the point where the product is operational.

A summary of these work procedures is available on the DIII-D Web site at <http://fusion.gat.com/DIII-D/infoguide>.

**Budget Planning.** Budgets for program tasks are generated by all tasks managers working with the DIII-D Planning and Control Group and submitted to the DIII-D program director for distribution to the Executive Committee and the DOE. Task priorities are set by the DIII-D program director in consultation with the DIII-D Executive Committee and in accordance with GA's contractual requirements with the DOE. Resource disbursements are made with input from collaborating DIII-D program leaders. The Executive Committee will also recommend on priorities of collaborators budgets. Disagreements will be arbitrated by DOE when they cannot be resolved by the Institutional Leadership.

**Reporting.** GA will submit all required plans and reports identified in its contract with the DOE. Each year, GA will prepare a "DIII-D Long Range Plan" that charts the major goals and milestones of the program. This plan will be developed with input from and consultation with major collaborators to ensure the program has a clear, consistent focus. This plan will be updated annually following DOE/OFE guidelines.

GA will also prepare a DIII-D Experimental Plan each year that details all planned experiments for that year including those to be performed by collaborators. It will be reviewed quarterly in conjunction with the DOE-OAK Quarterly Contract Review and updated as needed. The Plan will be prepared by the DIII-D Research Planning Committee, which includes representatives from the major collaborators as well as GA. Before submission to DOE for approval, it will be reviewed by the Executive Committee and approved by the director.

Technical program reports will be submitted quarterly as part of the DOE-OAK Quarterly Review or as needed. An Annual Technical Report and Final Contract Technical Report will also be submitted. An overall Management Plan will be submitted after contract award. At the beginning of the contract and on a quarterly basis thereafter, GA will submit management status and summary reports. Annually, GA will submit a milestone schedule plan, cost plan, and milestone schedule status report.

### 3. OTHER PERTINENT INFORMATION

#### 3.1. DEVELOPMENT PROCESS OF THE DIII-D FIVE-YEAR NATIONAL PROGRAM PLAN

The DIII-D Five-Year Program Plan was developed by the national collaborative team that operates, plans, and carries out research using the DIII-D facility.

A brainstorming session of the entire collaborative team was held in February 1997. Ideas were gathered for research elements and hardware elements of the DIII-D Five-Year Plan. The list of proposed elements was reviewed, prioritized, and edited by the DEC in March 1997. The DEC set up multi-institutional working groups to develop the proposed ideas in order to assess their technical merit and to estimate a cost. Reports from those working groups were the basis of writing the first draft of the DIII-D Five-Year Plan.

The draft plan was reviewed at the DIII-D National Summer Workshop in July 1997. Broad community input on the plan was obtained. In response to that input, many changes to the plan were made. Those changes are summarized in Table 3–1.

**TABLE 3–1  
CHANGES IN FIVE-YEAR PLAN  
SINCE JULY 1997  
(BASED ON JULY 1997 NATIONAL WORKSHOP)**

	Available Old Date	New Date
Delay 2 major installation periods by 6 months		Late (1999, 2001)
1. ECH Area		
Accelerate 6 MW by 6 months	2001	End 2000
Plan 10 MW system		End 2003
2. Fast Wave Area		
Delay 2 MW upgrade (to 8 MW total)	Mid 1999	Early 2002
Delay combline antenna for MCCD	Mid 1999	Early 2002

**CHANGES IN FIVE-YEAR PLAN  
SINCE JULY 1997  
(BASED ON SUMMER 1997 NATIONAL WORKSHOP) (CONT.)**

	Available Old Date	New Date
<b>3. Divertor Area</b>		
Delay full (lower) RDP	Early 1999	Early 2002
Complete upper private flux baffle	Early 1999	Early 2000
Vanadium program canceled	Early 1999	
Further divertor mod (e.g., 43 cm slot) not costed	2001	≥2004
<b>4. Non-Axisymmetric Coils</b>		
Plan for external coils	2002	Early 2002
Postpone internal coils		≥2004
<b>5. Counter Beamline</b>		
Delay	Early 2001	Early 2002
<b>6. Ten Second Pulse</b>		
Delay	Late 1999	Late 2003
<b>7. Diagnostics</b>		
Delay diagnostic		
Neutral beam	2002	≥2004
Central Thomson has a committed plan	Uncertain	1999
<b>8. Plasma Fueling</b>		
— Liquid jet for disruption mitigation		Proposed to I&T
— Compact toroid fueling		≥2004

The revised plan was reviewed in February 3–4, 1998, by the DIII-D Advisory Committee (DAC) with the following comments.

**“1. New 5-Year Plan**

The DAC compliments the DIII-D Team on the high quality and comprehensive DIII-D Five-Year Program Plan (GA-C22631, January 1998). The plan presents a well-conceived vision and strategy along with clear research goals and priorities on facility upgrades and improvements. The discussion of the fusion energy science in the DIII-D Program is particularly strong. The plan is placed in the context of DIII-D’s role in the national program and describes how DIII-D can be a strong contributor to various pathways of the future. In particular, the DAC endorses

the stated DIII-D Program Mission Goal: *To establish the scientific basis for the optimization of the tokamak approach to fusion energy production.*

The DAC notes that the plan appropriately describes the “upper envelope” of potential experimental programs and upgrades over the next five years. Achieving the stated goals and deliverables will depend, of course, on the availability of adequate annual funding and research progress.

The DAC offers three specific recommendations for further improving the plan:

- A. The role of DIII-D in the context of the overall international program on ATs should be expanded to more clearly describe DIII-D’s emphasis and role while acknowledging that a world-wide effort involving several tokamak experiments is needed to realize the promise of improved tokamak performance.
- B. The plan’s approach to the issue of disruptions, the mitigation of which is essential to the viability of the tokamak concept as a fusion energy source, should be given more visibility. The overall approach and philosophy to the disruption issue in ATs should be described as well as specific, proposed experiments.
- C. The anticipated contributions and connections of the DIII-D Research Program to general plasma science and alternate confinement research should be explicitly developed and brought out in the plan — to make clear the core role of DIII-D research in developing the science of high temperature plasmas that are toroidally magnetically confined.

The DAC also endorses the overall proposed facility upgrades (see next section for further discussion) with emphasis on providing up to 10 MW of ECH power by 2003, incorporating a double-null divertor by 2001 and providing wall stabilizing coils. While the DAC was not given a detailed specification of what the 3 (present level), 6 and 10 MW levels of ECH power could do, roughly speaking these levels correspond to perturbative, limited control, and full parameter ECH and ECCD experiments, respectively. The DAC particularly likes the approach of incorporating further experimental and modeling results in a staged approach to making key decisions, such as the anticipated decision to upgrade ECH to the 10 MW level in a couple of years — after 3 and some 6 MW experience is available.”

In response to the three specific recommendations for further improving the plan, we have taken the following actions:

**A. International Context of Advanced Tokamak Research on DIII-D**

1. Enlarged the discussion of this issue in Section 1.4, including reference to Chapter 4, Pathways to the Future, which contains an extensive discussion of how DIII-D results are and will be relevant to future major device steps in the national and international program.
2. Added to Section 6.2.4, Role of DIII-D in the International Fusion Program, an extensive discussion of international collaboration specifically on AT issues between DIII-D and foreign machines.

**B. Disruption Research**

1. Strengthened the discussion of DIII-D Disruption Studies in the subsection on Stability in Section 2.3.1.
2. Added a subsection on Disruption Avoidance and Mitigation to Section 2.3.2 Developing Tools and Techniques.
3. Strengthened Section 2.3.3 Theory Objectives.
4. Added emphasis to the introduction to Section 3.2 Stability Science.
5. Strengthened Section 3.2.5 Disruption Avoidance and Mitigation.

**C. General Science and Alternate Concepts Connections**

1. Strengthened Section 6.2.2 Linkages of DIII-D to Other U.S. Experiments, which contains a discussion of explicit linkages of the DIII-D Program to seven other U.S. experiments, including some alternates, by adding an additional discussion of scientific issues shared by DIII-D Research and Alternate Concept Research.
2. Strengthened Section 6.2.7 DIII-D Program Support to the General Science Community.”

## 3.2. HISTORY AND ACCOMPLISHMENTS OF THE DIII-D PROGRAM

*The DIII-D tokamak program at GA has made many major scientific contributions to the worldwide fusion effort. The DIII-D Program pioneered plasma shaping and profile control as a means of improving performance, leading to second stable high beta core plasmas in DIII-D. Confinement has improved, particularly in discharges with optimized magnetic shear, with the energy confinement time reaching four times that of the standard ITER-89P scaling. Pioneering programs in electron cyclotron and fast wave heating and current drive have made progress in developing and demonstrating the understanding necessary to sustain the conditions of optimized shear. New and effective divertor geometries were devised, leading to the divertor configurations widely used today and projected to ITER. The program continues to advance on a broad front, with major contributions in transport, stability, divertor physics, and in RF heating and current drive. The hallmark of the DIII-D Research Program is the integration of these science research topics into a program aimed at optimization of the AT.*

### 3.2.1. ORIGIN OF THE PROGRAM

The GA Tokamak Program has a history of creative concept development. The program began in 1968 with the Doublet I device, the first tokamak with a highly noncircular cross section, using solid copper walls to shape the plasma. Experiments on this device showed the doublet configuration to be magnetically and dynamically stable. These successes led in 1971 to the larger Doublet II device, also with solid copper walls. This device was reconfigured in 1974 to use external coils to replace the copper walls. The new device was named Doublet IIA, and it pioneered the use of external coils to shape a wide range of highly noncircular plasmas and maintain them in nondecaying magnetic configurations.

The success of these experiments led to construction of the Doublet III device, completed in 1978. In the first years of operation, it was the largest operating tokamak in the world and attained the highest current levels recorded at that time (2.2 MA). Experiments with a broad range of plasma configurations demonstrated the importance of elongation and shape control. Dee-shaped plasmas proved easiest to form and were projected to reach  $b$  values adequate for viable power plants. Diverted dee-shaped plasmas were also effective in achieving reduced impurity levels and enhanced confinement.

These successes led to the reconstruction of the Doublet III tokamak into a large dee-shaped cross section capable of a wide range of plasma shapes and divertor configurations. The device was renamed DIII-D in 1986. DIII-D rapidly reached currents of over 3 MA and achieved superior levels of confinement and  $b$ . Understanding of plasma stability, transport, divertor and current drive physics was developed.

The DIII-D Program has contributed outstanding results in most major areas of tokamak physics including: confinement, stability, boundary physics and technology, rf heating and current drive, and tokamak operations. This progress is typified by the evolution of the fusion triple product  $n\tau T$ . Over the last ten years, the performance has doubled every two years, reaching  $7 \times 10^{20}$  keV-s/m<sup>3</sup>. In the following sections, we summarize the scientific progress relative to our previous five-year plan.

### 3.2.2. ACCOMPLISHMENTS OF THE 1993 FIVE-YEAR DIII-D PLAN AND CONTEXT FOR THE 1998 FIVE-YEAR PLAN

**3.2.2.1. THE DIII-D 1993 PROGRAM MISSION.** The 1993 Mission of the DIII-D Tokamak Research Program was: *“to provide data needed by next-generation tokamaks such as the International Thermonuclear Experimental Reactor (ITER) and the Tokamak Physics Experiment (TPX) and to develop a conceptual physics blueprint for a commercially attractive electrical demonstration plant (DEMO) that would open a path to fusion power commercialization.”* In the intervening five years, the DIII-D Program has successfully carried out that mission within the context of the changing U.S. Fusion Energy Sciences Program.

DIII-D has been a major supplier of physics R&D data to the ITER Program and, before its cancellation, to the TPX Program. The TPX design incorporated a number of DIII-D features so the physics demonstration to the 10 s level now rests with DIII-D. Experiments for very long pulses remain to be carried by the Korean KSTAR and ITER superconducting tokamaks. While the U.S. fusion program strategy no longer calls for DEMO operation by 2025, the DIII-D Program develops the scientific basis for fusion energy through integrating fusion science elements in coherent scenarios aimed at improving the tokamak concept. We call this an AT Program. In this context, the 1998 DIII-D Program mission is *“to establish the scientific basis for the optimization of the tokamak approach to fusion energy production.”*

Fusion science and concept improvement are two of the elements of the new U.S. Fusion Program strategy, with international exploration of burning plasmas through ITER R&D being the third element. The DIII-D Program contributes to each of these three national strategic elements.

**3.2.2.2. ACCOMPLISHMENTS OF THE DIII-D 1993 OBJECTIVES AND GOALS.** The 1993 DIII-D Program objective was to *“carry out an integrated long-pulse demonstration of a well-confined high- $b$  plasma with noninductive current drive in an advanced plasma and divertor configuration.”* The quantitative goal was to sustain a 2 MA plasma with 5%  $b$  for 10 s. The accomplishment of these objectives required upgrades to the rf, microwave, divertor, and tokamak. These upgrades were only approximately 25% implemented during the past five years due to DOE funding limitations (see Table 3–2).

Lacking the needed upgrade capabilities, the quantitative goals were impossible to achieve. Nevertheless, with the existing capability, transient experiments were successfully carried out to investigate and advance understanding of a wide range of fusion science issues. Based on these experiment results, the 1998 plan will continue to implement:

- Complete the RDP top divertor upgrade in 1999 and complete modification of the bottom divertor in 2001.

**TABLE 3-2**  
**COMPARISON OF 1993 UPGRADE PLAN WITH ACTUAL UPGRADES IMPLEMENTED**

Upgrade	1993 Upgrade Plan		1998 Status		
	1993 Capability	Projected Projected 1998 Capability	Projected Expenditure (\$M)	Actual 1998 Capability	Actual Expenditures (\$M)
Radiative divertor	ADP	Double-null RDP	16.1	Single-null RDP	8.5
ECRF power	0	10 MW	28.2	2 MW	3.0
ICRF power	2 MW	8 MW	17.3	6 MW	9.7
10 s tokamak	2–5 s	10 s	<u>16.5</u>	2–5 s	<u>0.0</u>
Total (\$M)			78.1		21.2

- Two MW-level 110 GHz gyrotrons are now operational for 1–2 s pulses; a Gycom and a CPI (Varian) gyrotron. In addition, diamond windows have now been developed to extend the gyrotrons' pulse length to 10 s. By the end of 1998, we expect to have a 10 s gyrotron operational. In the next five-year period, we plan to increase the gyrotron power to 6–10 MW for off-axis current drive to accomplish the integrated program objectives.
- ICRF results, with three transmitters (6 MW system), indicates that the on-axis current drive efficiency increases at higher electron temperature as had been projected. A fourth transmitter, an available FMIT unit, will be modified by PPPL in the next five-year period.
- Upgrading the tokamak and auxiliary system pulse length to 10 s has not been initiated. This awaits completion of the ECRF and radiative divertor upgrades.

With completion of these upgrades, as well as active MHD and transport barrier control, in the next five-year period we expect to complete the original integrated AT Program objective. This integrated program will demonstrate and advance fusion science understanding of transport, stability, particle-wall interaction, and current drive. These previously implicit fusion science research topics are now explicit objectives in the new five-year plan.

**3.2.2.3. SCIENTIFIC ACCOMPLISHMENTS OF THE PAST FIVE YEARS.** The 1993 DIII-D Scientific Program was organized under two themes: AT and Divertor Development and Research Programs which were connected through an ultimate theme: Integrated AT Research.

**AT Research.** The 1993 AT Program Plan had three major research goals: “(1) to develop physics understanding of the formation and sustainment of AT configurations; (2) to establish experimental validation of the physics of active rf current drive and efficiency optimization; and (3) to combine these two to provide a demonstration of optimized, long-pulse AT operation with simultaneous improved confinement, enhanced stability, and fully noninductive current drive at high  $b$ .” These 1993 program goals were proposed to be accomplished through a number of studies to accomplish the objectives outlined in Table 3-3. Excellent progress was accomplished on all these objectives, except for the long pulse studies

requiring the future high power microwaves upgrade system. As characteristic of research, results of these studies opened unexpected new opportunities and deeper scientific questions to be investigated in the future. Overall, the scientific progress was more or less as envisioned while the ITER support was more than envisioned in 1993.

**TABLE 3–3**  
**AN ASSESSMENT OF PROGRESS ON THE 1993 ADVANCED TOKAMAK RESEARCH GOALS**

[A check (✓) indicates progress as anticipated, a minus (–) indicates less progress than anticipated, and a plus (+) indicates more progress than anticipated]

Goal	Progress
• Develop understanding of Advanced Tokamak regimes	✓
• Validate noninductive current drive (bootstrap utilized, fastwave to 0.3 MA, electron cyclotron by 1998)	✓
• Actively control, optimize, and demonstrate Advanced Tokamak regimes	
— Short pulse	✓
— Long pulse	–
• Stability and transport theory/experimental interaction	✓
• Disruption studies	✓
• Rotation effects with C-coil	✓
• Develop advanced (digital) plasma control	✓
• Provide ITER physics simulation	+

The first two goals were successfully addressed in the past five years of DIII-D research. The understanding of AT configurations was developed through experiments exploring the dependency of plasma stability and confinement on plasma shape and profiles. These studies utilized second stability regime experiments, NCS, and E×B shear flow improvements to confinement. Noninductive FWCD experiments supplemented by ECRF and bootstrap current were carried out. The efficiency of FWCD was found to approach the theoretically expected values which scale to attractive power plant scenarios when combined with optimized bootstrap current. During this five-year period, the need for off-axis electron cyclotron current drive to sustain NCS configurations arose and began to be rigorously pursued, albeit with the limited ECH upgrade capability mentioned earlier. The third, and ultimate objective, the goal to demonstrate long pulse AT operation at high beta awaits installation of additional ECH power for off-axis current drive. The availability of 6 to 10 MW of ECH power upgrade, together with completing the divertor and long-pulse upgrades, in the next five-year period will enable accomplishment of this integrated AT goal.

A major breakthrough of the past five-year research was the achievement of a neoclassical energy confinement in NCS plasma was one of five integrated AT scenarios proposed for investigation during the past five-year period (it was then dubbed the second stable core scenario with off-axis current drive and sheared plasma rotation). Although limited in our ability to actively control and sustain current profile, rotation, and plasma density, we, as well as other world tokamaks (JET, TFTR, Tore Supra, JT-60U),

have been able to establish transport barriers and achieve neoclassical levels of confinement. In the next five-year period, experiments to optimize and sustain NCS

**Divertor Development and Research.** The 1993 Divertor Development and Research Program was to develop and implement a divertor design that solves the “divertor problem.” Solving the divertor problem meant providing significant dispersal of plasma energy flow prior to it reaching the divertor surface to ease divertor heat removal and reduce surface erosion from excessively hot impinging plasma. The focus of these studies was to provide an ITER physics basis in coordination with other world tokamaks. The 1993 program was to be initially carried out with the lower advanced divertor and then with a radiative divertor upgrade. This program of experiments with divertor configuration modifications was to be supported by improved diagnostic measurements, modeling, and database benchmarking with other tokamaks. As indicated in Table 3–2, only partial implementation of the radiative divertor upgrade was realizable in the past five-year period due to severely constrained funding. Nevertheless, understanding and demonstrated achievements have exceeded those anticipated in 1993. This was accomplished with the help of a higher than planned effort in diagnostic and modeling improvements.

In 1993, the general idea of solving the divertor problem through radiation and recombination was being pursued. However, comprehensive understanding through experimental measurements and modeling was missing. DIII-D Thomson scattering measurements of low divertor electron temperatures and Alcator C-Mod spectroscopic measurements of atomic recombination have provided documentation of divertor physical processes which can now be modeled by divertor codes. Other world tokamaks have also provided key discoveries and confirmatory results. In the next five-year period, the divertor and AT research will be more closely coupled and integrated together.

The 1993 Divertor Development and Research Plan laid out expected levels of resolution of divertor issues and identified program goals to be pursued. The expected levels for resolution of divertor issues is reproduced in Table 3–4 with a check (3) by those issues which have been resolved during the past five years to the expected level. Six of the issues have been resolved to the expected level, although erosion mitigation was not investigated due to concentration on the other issues. Accomplishments of the Divertor Program goals and guidelines are indicated in Table 3–5. Overall, divertor science progress exceeded that envisioned due to better than expected experiment and theory understanding of divertor recombination physics. Implementation of the radiative divertor upgrade was less than envisioned (due to budgetary constraints, see Table 3–4). As a consequence the DIII-D ITER divertor physics support provided more physics understanding, but less than the desired information on the effects of changing divertor geometry and baffling.

**Integrated AT Research.** The aim of the 1993 DIII-D Program was to provide an integrated demonstration of the AT. With a limited 5 to 10-s pulse length, DIII-D is tackling the TPX mission. As described above, advances in confinement, stability, current drive, and divertor physics has been outstanding. The integration of these elements is now a key focus of our research.

- Using current profile control and plasma rotation to control transport rates.
- Using internal transport barriers to control pressure profiles to optimize beta.

**TABLE 3–4**  
**AN ASSESSMENT OF RESOLUTION OF 1993**  
**DIVERTOR RESEARCH PROGRAM FUNCTIONS/NEEDS ISSUES**  
**(D = DEMONSTRATED, I = INVESTIGATED)**

[A check (✓) indicates resolution at the expected level  
and a minus (–) indicates less progress than anticipated]

Issue	Divertor Development Phase	
	Advanced Divertor	Radiative Divertor
Power Dispersal	I ✓	D ✓
Density Control	D ✓	D ✓
Impurity Control	I ✓	D ✓
Helium Exhaust	D ✓	D ✓
Divertor Physics	I ✓	I ✓
Model Validation	I ✓	D ✓
Erosion Mitigation	I –	I –

**TABLE 3–5**  
**AN ASSESSMENT OF ACCOMPLISHMENTS OF 1993 DIVERTOR PROGRAM GOALS AND GUIDELINES**

[A check (✓) indicates that the goal or guideline was pursued and accomplished as  
expected and a minus (–) indicates less progress than anticipated]

1. Demonstrate radiative divertor power dispersal to lower the peak heat flux to ~1 MW/m <sup>2</sup> , from ITER levels of ~5 to 10 MW/m <sup>2</sup> .	✓
2. Implement divertor configuration consistent with the overall AT mission of DIII-D and the tokamak physics experiment (TPX).	✓
3. Provide research flexibility to settle the questions of single- versus double-null, pumping of the inner and outer divertor legs, and more detailed geometric issues.	✓
4. Implement the testing of AD concepts as part of the AT mission of DIII-D.	✓
5. Demonstrate density control in enhanced confinement regimes.	✓
6. Demonstrate impurity retention and entrainment in the divertor.	✓
7. Demonstrate sufficient helium exhaust for a reactor.	✓
8. Provide a validated model of divertor performance that can be used to design future machines.	✓
9. Show erosion reduction by power dispersal.	–
10. Engineer all divertor systems in all phases to be fully compatible with tokamak requirements, e.g., temperature ranges, thermal expansion and contraction, halo currents, disruption forces, arcing hazards, etc.	✓

- Using pressure profiles to optimally position bootstrap-driven currents for maximizing confinement and stability.
- Using divertor radiation and recombination to enable high core electron temperature for efficient current drive.

To quantify our progress, we use four measures. The first are commonly used normalized indicators:

- Plasma confinement quality measured by the H-mode quality factor,  $H = \tau_E/\tau_{ITER-89P}$ .
- Plasma stability measured by normalized beta,  $\beta_N = \beta/(I/aB)$ .
- Bootstrap current fraction,  $I_{BS}/I_P$ .
- Divertor power dispersal, the power reduction factor for power striking the divertor plates.

Integrated demonstration is then characterized by sustaining these four indicators for long durations. Table 3–6 provides a summary of the DIII–D Program progress over the past five-year period indicating that the program has moved from now standard H-mode tokamak performance toward those of an AT. The pulse length is limited by our inability, without off-axis EC current drive, to sustain the optimum NCS current profile. Independently (not simultaneously), DIII–D has achieved each of the AT parameter goals. This first measure of integrated performance represents major accomplishments given the limited upgrade capabilities available during this time period.

**TABLE 3–6**  
**INTEGRATED ADVANCED TOKAMAK**  
**PARAMETER GOALS AND ACHIEVEMENTS**

<b>Simultaneous Operation</b>			
	<b>1993 Status</b>	<b>1993 Target for 1998</b>	<b>1997 Achievement</b>
Confinement, H	2	4	3
Stability, $\beta_N$	2	6	4
Bootstrap Current fraction, $f_{BS}$	0.3	0.5	0.7
Divertor Power Dispersal factor	2	10	2
Pulse Length, s	10	1	1

A second measure of integrated performance is the fusion triple product;  $n_i t E_i$ . This product is composed of the central fusion fuel ion density, the global energy confinement time and the central fusion fuel ion temperature. Over the past five years, the DIII–D fusion triple product has increased four fold. This progress over the history of the DIII–D facility, shown in Fig. 3–1, is comparable to that of rapidly advancing activities such as the semiconductor computer industry. In the next five-year period, we do not intend extensive dedicated campaigns to push the triple product higher since these are very extreme hot ion conditions for a moderate size tokamak such as DIII–D. Instead, future research will concentrate on plasma regimes with near equal ion and electron temperature as characteristic of future fusion power plants.

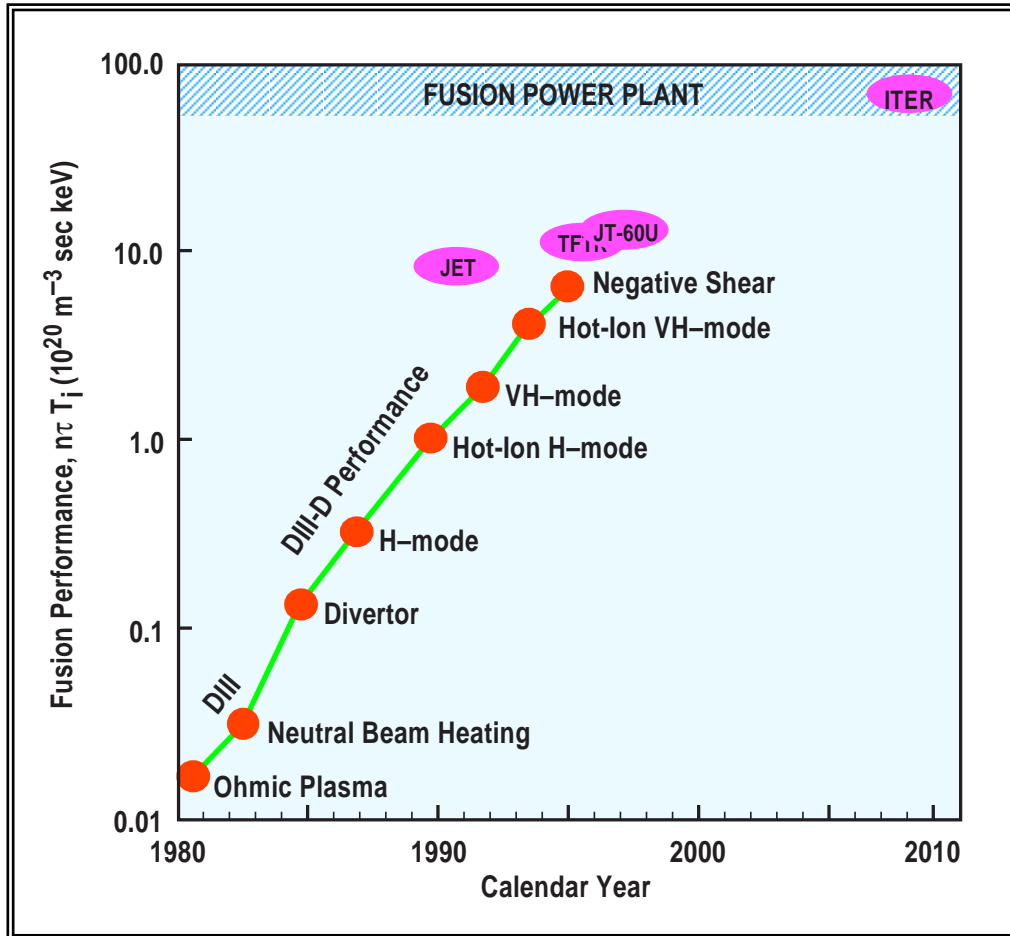


Fig. 3-1. Scientific progress: DIII-D fusion performance has doubled every two years.

A third measure of integrated fusion performance is by direct measurement of the fusion power produced normalized to the required plasma heating power. In the past five years, significant progress has been made through strongly shaped double-null plasmas, NCS plasma current profile, and broad plasma pressure profile. In this way, 28 kW of D–D fusion output power was produced in DIII–D with 18 MW of neutral beam input power. The D–D fusion gain was  $Q_{D-D} = 0.0015$ . For an optimum D–T fuel mixture, this is equivalent to a D–T fusion gain of  $Q_{DT}^{equiv} = 0.3$ . Compared to five years ago, this is an increase of a factor four.

### 3.2.3. DIII-D SCIENTIFIC PROGRESS AND ACCOMPLISHMENTS

**3.2.3.1. PLASMA STABILITY AND HIGH-BETA PHYSICS.** The DIII–D Program has made remarkable progress in understanding the nature of the  $\beta$  limit in tokamaks and in achieving higher values of the plasma  $\beta$ . Understanding of the stability of elongated discharges has led to operation with double-null discharges with high values of  $I/aB$  and the achievement of  $\beta = 13\%$ . The associated development of

detailed theoretical understanding, demonstrates that  $\beta$  values needed for power plant operation are credible and achievable. Accurate equilibrium calculations have demonstrated that regions of the plasma reach into the second-stable region. Understanding the role of the current profile in establishing  $\beta$  limits has led to the recognition that the limiting  $\beta$  value could be raised with properly optimized plasma profiles.

At high values of beta, self-driven neoclassical bootstrap currents become a significant contribution to the overall plasma current. This is beneficial for obtaining steady state discharges, but it can also lead to MHD instability. This coupling between the self-driven current and the plasma pressure, which establishes the stability limits, is referred to as neoclassical MHD. If finite size island structures form, the plasma pressure gradients flatten within the islands which causes the bootstrap current to weaken and the island to expand. This process has been shown to establish beta limits in plasmas in DIII-D and other tokamaks. Recent DIII-D experiments have compared this instability to theoretical models, and means of stabilizing the modes using localized currents driven by electron cyclotron current drive are being developed.

Important progress also has been made in understanding locked modes. These occur when rotating magnetic modes lock (to a stationary, local magnetic field asymmetry). This often leads to a disruption. Locked modes lead to limitation of the operating space. Particularly, they restrict operation with the low-density target plasmas that are crucial for obtaining efficient rf current drive and VH-mode confinement. Experimentally, it has been shown that an external perturbation can be added to the tokamak field configuration to minimize intrinsic local asymmetries and, thus, substantially increase the operating space.

**3.2.3.2. PLASMA CONFINEMENT PHYSICS.** Early operation of the DIII-D device led to the routine attainment of the high confinement regime, or H-mode. DIII-D H-mode results show a strong increase in energy confinement  $\tau_E$  with plasma current, consistent with worldwide tokamak results. DIII-D has made significant contributions toward understanding the physics of the transition from L-mode to H-mode. Improvements made in the DIII-D charge exchange recombination spectroscopy system provided important data on the change in the edge radial electric field across the transition. By measuring edge poloidal and toroidal rotation, temperature, and density of various plasma ions, our experimental data showed that the radial electric field changes just before the start of the transition, and that density fluctuations change right at the start of the transition in a localized layer where the radial electric field also changed. This is also the region where gradients of plasma density and temperature steepen after the transition indicating a decrease in local transport. Theory predicts that the increased shear in the  $E \times B$  drift velocity leads to this transport reduction. A similar effect explains the VH-mode, with a broader region of  $E \times B$  shear extending further into the plasma.

In the last several years, further confinement improvement has been obtained in the core of DIII-D plasmas by optimizing the magnetic and  $E \times B$  shear. The initial signs of the improvement were the creation of obvious core transport barriers in discharges where manipulation of the current density profile had resulted in suppression of sawteeth. Core barriers have been formed in discharges with both positive and negative magnetic shear. The key factor in all these plasmas appears to be the same  $E \times B$  decorrelation of turbulence that is operational in the plasma edge in H-mode and VH-mode. By optimizing the

plasma pressure profile with suitably timed L-to-H transitions, we have created plasmas where the whole discharge has low transport. For example, ion thermal diffusivity at or below the standard neoclassical level has been attained across the whole plasma. Such plasmas have a DIII-D record triple product  $n\tau T = 7 \times 10^{20} \text{ m}^{-3} \text{ s keV}$ . These discharges demonstrate that control of plasma current and pressure profiles can lead to significant confinement improvement over standard H-mode.

As part of the work on confinement improvement, a significant amount of work has been done on basic studies of local transport. These include assessment of local transport coefficients through power balance and perturbative approaches and comparison of coefficients for dimensionally similar discharges and off-axis heating experiments where the possible existence of a heat pinch term is indicated in experiments using either ECH or NBI. One of the key problems in thermal transport analysis is separation of the electron and ion thermal transport. The individual values are rendered uncertain by the uncertainty in the electron-ion power transfer term, which can depend on the difference of large numbers. The ability to separately heat the ions (with NBI) and the electron (with fast wave and ECH) has allowed us to reduce this uncertainty in discharges with combined heating because plasma can be made in which the uncertain power transfer term is actually a small component of the heat input to either species.

As part of the transport work, we have been actively involved in the ITER process, providing a significant amount of data to the ITER global confinement database. This has been combined with the data from tokamaks world wide to furnish means of predicting the confinement values in ITER. In addition, we have been one of the major players in the area of confinement investigations using nondimensional scaling. Indeed, it is probably only because of the careful nondimensional transport work done on DIII-D that this technique has been recognized as a reliable means of transport investigation. Because of DIII-D flexible shaping capabilities, we can match the plasma shape of other, less flexible machines, thus providing data for key tests of this technique.

In the past two years, so-called theory-based models of local transport have emerged, which have had some success in matching experimentally measured profiles from various machines. DIII-D experimentalist and theorists are actively involved in this work and DIII-D profile data makes up a significant part of the ITER profile database, which is being used to test these various theories. We are working with the whole transport community in testing and attempting to improve these models.

**3.2.3.3. BOUNDARY PHYSICS AND TECHNOLOGY.** DIII-D work in boundary physics and technology has concentrated on understanding and developing the divertor configuration, including the demonstration of long pulse discharges. Divertor configurations similar to those developed on DIII-D have become prototypical for next-generation tokamaks and stellarators, including ITER. Research on DIII-D has led to the development of the lower advanced divertor configuration and the upper high-triangularity divertor presently operational in DIII-D. Important work also has been done on vessel wall conditioning and the transport of impurities from the plasma edge.

Early studies of the heat loads to divertor targets led to the recognition that these loads can be strongly peaked and that the heat distribution can depend on the confinement mode (ohmic, L-mode, H-mode). These studies also quantified the differences between single-null and double-null discharges, and showed that the heat loads in double-null discharges could be maintained as essentially up/down symmetric. It was then demonstrated that the heat loads could be managed by sweeping the location of the divertor strike point across the target plate.

Results from DIII-D also show that by injection of gas at the plasma boundary, both peak and overall heat load to the divertor target plates can be reduced to one-fifth of the original value. Puffing of deuterium gas reduces the peak heat flux to the divertor tiles and at the same time —  $Z_{\text{eff}}$  is constant or slightly reduced. These results show that in DIII-D, gas puffing is a promising method of reducing heat load to the divertor. These results are an encouraging proof of principle of the radiative recombining divertor concept.

The desire to better optimize and control the divertor configuration and, in particular, demonstrate density control in divertor H-mode plasmas led to the conception and implementation of the advanced divertor configuration in conjunction with a team of collaborators from GA, LLNL, ORNL, SNL, and UCSD. This involved the installation of a cryogenic pump and a biasable ring near the divertor X-point to pump neutrals and to allow an electric field to be applied to the plasma in the divertor region. The application of a bias voltage to the ring electrode was shown to result in a further increase in the divertor pumping. An extensive set of diagnostics was added to the lower divertor including bolometric tomography, spectroscopy, and a divertor Thomson Scattering System. These new diagnostics showed that the divertor was cold, 1 to 2 eV indicating that plasma radiation, recombination, and convective power flow are dominant processes in the radiative divertor region.

Successive improvements in the wall condition of the DIII-D device have led to remarkable improvements in both confinement and impurity level. The DIII-D vacuum vessel was constructed with the capability to bake to nearly 400°C for the purposes of decontaminating the graphite vessel wall in preparation for plasma discharges. Boronization, the *in situ* coating of the vessel walls with a thin layer of boron, has resulted in a substantial improvement in discharge operation, especially with high current, high energy plasmas. Discharges of 3 MA achieved a plasma energy of 3.6 MJ,  $\langle\beta\rangle = 5.1\%$  at full toroidal field, thus fulfilling a long-standing DIII-D Program goal of reaching high  $\beta$  at full plasma parameters. Boronization resulted in the discovery of the VH-mode, a confinement regime substantially improved from those previously achieved with confinement.

The poloidal location of the advanced divertor is optimized for pumping low-triangularity single- or double-null divertors. As noted above, many of the AT scenarios involve high triangularity plasma shapes. We have recently installed the first phase of a double-null divertor configuration, the RDP, which consists of an upper baffle and cryopump for density control in high-triangularity plasma shapes. This hardware is currently operational, and we have demonstrated density control in high-triangularity upper single-null plasmas.

**3.2.3.4. RF HEATING AND CURRENT DRIVE PHYSICS.** DIII-D RF heating and current drive research has investigated the use of electron cyclotron waves and fast waves in the ion cyclotron range of frequencies to heat electrons and to drive plasma currents. ECH has the advantage of easy coupling of the power to the plasma with simple antenna structures and localized deposition of the power in the plasma. Initial ECH experiments on DIII-D utilized at a frequency of 60 GHz — the fundamental frequency at the maximum field of DIII-D. This system, while effective at localized heating of the plasma, was limited by the fact that coupling is cut off above relatively modest densities and that the unit size available for the power generation system (200 kW each) is prohibitively small for high power experiments. Recently, two 1 MW sources at 110 GHz have been installed for heating at the second harmonic in order to address both of these issues.

Experiments on DIII-D at 60 GHz have used all of the principal modes of ECH, including outside launch of the ordinary mode (O-mode) at the fundamental frequency, outside launch of the extraordinary mode (X-mode) at the fundamental and second harmonic, and inside launch of the fundamental X-mode. Propagation limits and absorption are well predicted by theory models. Central electron temperatures of 10 keV have been achieved with ECH. ECH provides the capability to increase the electron temperature closer to the ion temperature as will be the case eventually in burning plasmas. In addition to bulk heating, ECH has potential applications affecting confinement and stability. In DIII-D experiments, application of ECH has been shown to generate the H-mode of improved confinement, which is widely regarded as a test of the ability of a technique to heat without introducing significant levels of impurities; heating near the  $q = 1$  surface has suppressed sawteeth; and applying ECH with the resonance near the edge in H-mode discharges with substantial neutral beam heating has stabilized the Edge Localized Modes, leading to improved energy confinement.

In 1995, the 60 GHz ECH System was dismantled to enable the implementation of a new ECH System at 110 GHz. This system, at present, has two gyrotrons with nominal power of 1 MW each. The antennas are steerable mirrors to direct the power deposition at any minor radius along the resonance.

The ECH System is a key tool in performing critical experiments required for understanding and optimizing the tokamak concept. ECH is a unique heating technology in that the energy is coupled to the electrons in a localized spatial region of the plasma. This makes ECH a unique tool for studying transport through application of localized heat. In contrast to the predictions of standard techniques used to model energy transport in the tokamak, a series of careful experiments utilizing these capabilities revealed an anomalous inward flow of electron heat. Discovery of this heat pinch has stimulated new theoretical activity in the community which will hopefully be the key to unlock the puzzle of electron thermal transport.

ECCD experiments have been carried out at 110 GHz. Extensive data analysis and modeling showed that about 170 kA of current was driven by 1 MW of power and that this is consistent with predictions.

Fast waves are also useful for electron heating and current drive. The fast waves are launched from the low field side of the plasma with a toroidal velocity which is close to the thermal speed of the electrons. This results in moderately strong electron Landau damping and transit time magnetic pumping which heats

the electrons and drives current. Fast wave heating heats the high temperature center of the plasma preferentially. Good fast wave absorption requires high electron temperature and, thus, the Fast Wave Program is symbiotically linked to the ECH Program to achieve effective central heating and current drive. Strong central heating in discharges heated by neutral injection has also been observed. Pick-up loops on the vessel walls and reflectometer measurements are used to study wave propagation and absorption.

More recently, FWCD has been shown to be an effective method of electron heating and driving plasma current in the plasma core. The FWCD Program on DIII-D is a collaborative effort between GA and ORNL, which has provided a proof-of-principle demonstration of FWCD for application to DIII-D and other tokamaks. To avoid competing absorption mechanisms, such as absorption at ion cyclotron harmonics, we seek to maximize the single-pass absorption by first heating the electrons with ECH or neutral beam power.

FWCD experiments have led to record current drive by this means, about 290 kA. The magnitude of the driven current and its radial profile are in good agreement with theory. FWCD has been applied to discharges with NCS, where it has been effective at modifying the current profile and prolonging the duration of the negative shear phase. FWCD thus is a valuable tool, along with ECCD and NBCD, for controlling the shape of the current profile.

### 3.2.4. DIII-D OPERATIONS AND FACILITY IMPROVEMENTS

The DIII-D Research Program requires safe and reliable operation of the tokamak in new plasma configurations, refurbishing and improving the tokamak facility, and meeting the needs of expanding numbers of collaborators.

**3.2.4.1. OPERATIONS.** In 1993, we planned for 90 weeks of physics experiments over the five-year period based on a total funding of \$209M for operations. As seen in Table 3-7, 73 weeks of operation was achieved with \$179.4M funding. In order to maintain this relatively high operation level in the face of the facility fixed costs, it was necessary to defer refurbishments and normal procurements in FY96 and FY97. These postponements shifted additional obligations to the 1998 five-year period.

**TABLE 3-7**  
**COMPARISON OF 1993 PLAN AND ACTUAL**  
**GA FUNDING LEVELS AND OPERATIONS WEEKS**

	FY94	FY95	FY96	FY97	FY98	Total
Planned GA Funding (\$M)	40.7	38.3	38.6	42.3	49.1	209.0
Actual GA Funding (\$M)	38.2	39.0	34.0	30.7	37.5	179.4
Planned Weeks Operation	18	18	12	18	24	90
Actual Weeks Operation	11	19	16	9	18	73

**3.2.4.2. TOKAMAK FACILITY IMPROVEMENTS.** In addition to the major upgrades described in Section 3.2.3.2, the 1993 DIII-D Five-Year Plan envisioned implementation of a number of facility improvements listed in Table 3–8. The improvements were implemented, as envisioned, with the exception of the counter neutral beam included in the 1998 plan. Although the computer capability was increased, the improvements were inadequate to handle the unanticipated large increase in data, so aggressive effort was undertaken in FY98.

**TABLE 3–8**  
**FACILITY IMPROVEMENTS PLANNED AND IMPLEMENTED IN FY94–98**

Improvement	Status
Real time computer plasma control system	Operational (GA)
C-coil for magnetic error field correction	Operational (GA)
Pellet fueling	Operational (ORNL)
Operation of experiments from remote site	Demonstrated (LLNL)
Increased computer capability	Partially implemented (GA)
Counter neutral beams	Not implemented

**3.2.4.3. NEW DIAGNOSTICS.** New plasma diagnostics are needed to carry out the Research Program. The 1993 Five-Year Plan envisioned 25 new diagnostic instruments costing \$8.5M would be installed. As is usual, new physics discoveries and theories resulted in changes to the diagnostic implementation plan. However, as indicated in Table 3–9, 17 of the originally planned diagnostics will be operational in 1998. In addition, seven additional new diagnostic instruments, which were not envisioned in 1993, were also implemented. These are listed in Table 3–10. Thus, as planned, 25 new diagnostics were implemented with a total GA expenditure of \$8.5M; although 30% of the instruments were different than envisioned in 1993 due to advances in the physics program understanding.

**3.2.4.4. DATA ACQUISITION AND ANALYSIS.** In 1993, we anticipated that the data collected per shot would increase from 70 to 120 MBytes of data collected in 1998. Already in 1997, up to 220 MBytes is being collected on each shot. This larger amount of collected data is a result of increased sophistication of GA and collaborator diagnostic instruments, number of channels, and data collection rate. This increase in collected data has overloaded the computer and data retrieval systems. While the data acquisition and analysis computer systems have been somewhat improved, they are presently significantly under powered. Efforts are on-going to close this gap over the next few years with both new hardware and new data analysis software tools.

**TABLE 3-9**  
**AN ASSESSMENT OF THE 1993 FIVE-YEAR DIII-D**  
**NEW DIAGNOSTIC PLAN AND ACCOMPLISHMENTS**

---

**Current profile diagnostics**

Motional Stark effect edge upgrade (LLNL) — operational  
 X-ray spectrometer radial array (Russia) — only one channel operational  
 X-ray imaging — 1999  
 Additional magnetic probes (GA) — operational

**Fluctuation diagnostics**

Beam emission spectroscopy (edge and central) (U. Wis./GA) — operational  
 Improved microwave reflectometry, scattering (UCLA) — operational  
 Phase contrast imaging (MIT) — operational

**Core plasma diagnostics**

Charge exchange recombination upgrade (GA) — operational  
 Superheterodyne electron cyclotron emission (ORNL/U. Texas) — operational

**Disruption diagnostics**

Toroidal, Poloidal Thermocouple arrays  
 Fast infrared diode array — 1999

**Toroidal and poloidal asymmetries**

Infrared and visible TV cameras (LLNL) — operational  
 Upper divertor Langmuir probes and pressure gauges (GA, ORNL, SNL) — operational  
 Inner strike point pressure gauge (ORNL) — 1999

**Divertor impurity transport and radiation**

Multichannel divertor spectroscopy upgrade (GA) — operational  
 Fast impurity gas injector (impurity pellet) (ORNL) — operational  
 Normal incidence spectrometer (GA)  
 MLM spectrometer (JHU)  
 Divertor SPRED (LLNL) — operational

**Divertor erosion and redeposition**

Divertor real time interferometry

**Divertor ion and sheath physics**

Plasma ion mass spectrometer–PIMS (UCLA/SNL)  
 Divertor  $T_i$  diagnostic

**Basic scrapeoff layer parameters**

Reciprocating divertor probe (SNL/UCLA) — operational  
 Divertor reflectometer (UCLA) — operational  
 Divertor Thomson scattering (LLNL/GA) — operational

---

**TABLE 3–10**  
**NEW DIAGNOSTICS IMPLEMENTED ON DIII–D**  
**THAT WERE NOT ANTICIPATED IN THE 1993 FIVE-YEAR PLAN**

---

Core
Direct $E_r$ MSE (LLNL) — Operational
2D BES $T_e$ Fluctuation (U. Wisc.) — Operational
Disruption Tile Current Arrays (GA) — Operational
Divertor
EUV Spectroscopy (LLNL) — Operational
High Res. Bolometer (GA) — Operational
Flow Measurement (SNL) — Operational

---

### 3.2.5. TRANSITION TO A NATIONAL PROGRAM

During the past five-year period, DIII–D has become a true National Program. Already in 1993, DIII–D operated with national and international participation from 30 institutions. Now there are 50 institutions collaborating and now two-thirds of the DIII–D research physicists are from institutions other than GA.

DIII–D now has a Program Advisory Committee which meets regularly, and an Executive Committee composed of leaders of the major collaborating institutions. The program has unified technical and budget DOE quarterly reporting and reviews. Collaborators have chaired the 1996 and 1997 Research Planning Committees and collaborators now act in line management and project management roles. Needless to say, collaborators also lead experiment campaigns, are experiment session leaders, and represent the program at a wide range of meetings and other scientific forums. DIII–D has become even more of a national facility than was envisioned five years ago. This was due to a combination of a desire by the earlier collaborating institutions and due to a shrinkage in the number of other tokamak facilities as a result of the decline in fusion funding in FY96.